Habilitation Thesis

Novel Techniques for Mitigating the Flow Instabilities in Hydraulic Turbomachines and for Assessing Their Performance

Ilie-Alin BOSIOC,

PhD Associate Professor

Politehnica University Timișoara

Mechanical Machines, Equipment and Transportation Department

Research Centre for Engineering of Systems with Complex Fluids

2025

Contents

(A) ABSTRACT

The habilitation thesis summarizes my research activity carried out after the public defense of my PhD thesis entitled Swirling Flow Control in the Draft Tube Cone of Hydraulic Turbines, under the coordination of Prof.dr.eng. Romeo Susan-Resiga, at the Politehnica University Timișoara and the confirmation received from the Ministry of Education and Research (No. 4387/06.06.2011). The scientific, professional, and academic achievements included in the habilitation thesis cover the period from 2011 to 2025.

After completing my doctoral studies in 2011, I won, through national competition, a Postdoctoral research project PN-II-RU-PD-2011-3-0165 titled "Magneto-rheological device for rotational flow control", which was carried out between October 2011 and October 2013. The project was implemented at the Romanian Academy, Timișoara Branch, under the scientific supervision of Dr. Phys. Ladislau Vekas. Upon completion of the postdoctoral program, I applied for the position of Assistant Lecturer (fixed term) in 2013. I held this position for three years, and since February 2016 I have been employed as a permanent Assistant Lecturer. Beginning in March 2018, I was promoted to Lecturer, and as of September 2024, I hold the position of Associate Professor within the Department of Mechanical Equipment, Machinery and Transport at the Faculty of Mechanical Engineering. During this time, I have taught the practical (laboratory and seminar) components of the following courses: Fluid Mechanics, Fluid Mechanics and Hydraulic Machinery, and Measurement and Real-Time Monitoring of Hydraulic Parameters, addressed to students in the 2nd and 3rd years of the undergraduate program (first and second semesters), as well as to 1st-year Master's students. The courses I have taught are specific to the field of Mechanical Engineering and include Fluid Mechanics and Hydraulic Machinery, Turbomachinery, Hydraulic Turbines, Hydropower Plants and Pumping Stations, and Real-Time Measurement and Monitoring of Hydraulic Parameters. The considerable workload associated with teaching laboratories, seminars, and lectures has played a significant role in my development as an academic. Throughout my 14-year teaching career, I have supervised 22 undergraduate theses within the Hydraulic and Pneumatic Machines and Systems (MSHP) specialization and 15 Master's dissertations in the Hydrodynamics of Machines and Hydromechanical Systems (HMSH) program. Additionally, I have served as a member of the advisory committees for 9 PhD students. My didactic activity is reflected in 4 published books (covering both applications and theoretical courses), 5 book chapters, electronic teaching support materials available on the UPT Virtual Campus for all courses in my portfolio, as well as in the modernization or creation of 7 laboratory stands. I was also responsible for the accreditation of a new Master's program launched in 2024 within our department: Mechanical Systems for Ambient Energy Conversion and Transformation (SMART), which, starting with the academic year 2025–2026, will replace the former HMSH Master's program in our specialization.

With regard to research activity, starting in 2011, I have served as principal investigator or project director for five national projects and contracts. Additionally, I have been a team member on eleven other projects or contracts, in collaboration with both industrial partners and research institutions. The results of these research efforts are reflected in 60 scientific papers, in which I am listed as first author, corresponding author, or co-author, all indexed in Web of Science. In recent years, the expertise of the Hydraulic Machinery research group, of which I am a member, has been involved in a number of technical assistance and expert consultancy projects. I was actively involved in these projects as a member of the research teams, contributing to the commissioning of hydroelectric units, in-situ tests, model tests on hydraulic turbines, data analysis, and technical documentation assessment.

The professional and academic skills I have developed so far, both in teaching and scientific research, demonstrate my capacity to support the habilitation thesis in the field of Mechanical Engineering. The experience gained through teaching specialized courses, supervising bachelor's and master's theses, and engaging in national and international research projects provides a solid foundation for doctoral supervision. The main goal of this habilitation process is to obtain the status of PhD supervisor, to train and mentor young, motivated, and well-prepared researchers in the field of Mechanical Engineering. More specifically, I intend to focus on supervising doctoral theses in the specialization of Hydraulic Machinery, with particular emphasis on hydraulic turbines and centrifugal pumps, fields in which I possess confirmed expertise through scientific publications, experimental work, and interdisciplinary collaboration. I believe that training a new generation of researchers capable of addressing current challenges in the hydro-energy and industrial sectors is essential, and my contribution can bring added value both from a scientific and an educational perspective.

(A) REZUMAT

Teza de abilitare sintetizează activitatea mea de cercetare desfășurată după susținerea publică a tezei de doctorat cu titlul Controlul Curgerii cu Rotație în Difuzorul Conic al Turbinelor Hidraulice la Universitatea Politehnica Timișoara și primirea confirmării nr. 4387/06.06.2011 din partea Ministerului Educației și Cercetării. Realizările științifice, profesionale și academice incluse în teza de abilitare acoperă perioada 2011–2025.

După finalizarea studiilor doctorale în anul 2011, am câștigat prin competiție națională un proiect Post Doctoral PN-II-RU-PD-2011-3-0165 "Dispozitiv magneto-reologic pentru controlul curgerii cu rotație" care s-a desfășurat în perioada oct. 2011- oct. 2013. A fost un implementat în Academia – Română, Filiala Timișoara, având ca și consultant științific pe domnul Dr.fiz. Ladislau Vekas. După ce am finalizat studiile postdoctorale, mi-am depus candidatura pentru ocuparea postului de Asistent Universitar pe perioadă determinată in anul 2013. Am ocupat timp de 3 ani postul de Asistent Universitar pe perioadă determinată, iar din februarie 2016 sunt încadrat ca Asistent Universitar pe perioadă nedeterminată, începând cu Martie 2018 sunt Șef de Lucrări, iar din Septembrie 2024 sunt Conferențiar Universitar în cadrul Departamentului de Mașini Mecanice, Utilaje și Transporturi din cadrul Facultății de Mecanică. În această perioadă am susținut partea aplicativă la disciplinele Mecanica Fluidelor (seminar și laborator), Mecanica Fluidelor și Mașini Hidraulice (seminar și laborator), Măsurarea și monitorizarea în timp real a mărimilor hidraulice (laborator), discipline predate anul II, III semestrul I și II al ciclului de licență, anul I Master. Cursurile predate sunt in domeniul specific Ingineriei Mecanice: Mecanica Fluidelor și Mașini Hidraulice, Turbomașini, Turbine Hidraulice, Centrale Hidroelectrice și Stații de Pompare, Măsurarea și Monitorizarea Mărimilor Hidraulice în Timp Real. Acest volum mare de muncă pentru predarea laboratoarelor, seminariilor și a cursurilor a avut un rol important in dezvoltarea carierei de cadru didactic. Pe parcursul celor 14 ani de carieră didactică am coordonat 22 de studenți la lucrarea de licență în cadrul specializării de Mașini și Sisteme Hidraulice și Pneumatice (MSHP), 15 studenți la lucrarea de disertație din cadrul specializării de master Hidrodinamica Mașinilor și a Sistemelor Hidromecanice (HMSH) și am fost membru în comisiile de îndrumare a 9 doctoranzi. Activitatea didactică se regăsește în cele 4 cărți publicate pentru aplicații și curs, 5 capitole de carte, suport electronic disponibil pe Campusul Virtual UPT pentru toate cursurile din portofoliu, dar și 7 standuri modernizate sau noi realizate. Am fost responsabil de acreditarea noului master înființat in anul 2024 in cadrul departamentului: Sisteme Mecanice de Conversie și Transformare a Energiei Ambientale (SMART), iar începând cu anul universitar 2025-2026 înlocuiește vechiul master HMSH al specializării noastre.

Raportat la activitatea de cercetare, începând cu anul 2011 am fost responsabil sau director de proiect la 5 proiecte naționale și contracte, și am fost implicat în calitate de membru în echipă la 11 proiecte sau contracte atat cu mediul industrial dar și cu unitățile de cercetare. Rezultatele

cercetării sunt vizibile in cele 60 de lucrări în calitate de prim autor, autor corespondent sau coautor vizibile Web of Science.

In ultimii ani, expertiza colectivului de Mașini Hidraulice din care fac parte a fost implicată într-o serie de proiecte de asistență tehnică și expertiză. Am activat ca membru in echipa de cercetare al acestor proiecte și am fost implicat in porniri de unități hidroelectrice, teste in situ și teste pe model turbine hidraulice, analiză de date, expertiză documentație tehnică.

Abilitățile profesionale și academice dezvoltate până în prezent, atât în activitatea didactică, cât și în cea de cercetare științifică, reflectă capacitatea mea de a susține teza de abilitare în domeniul Ingineriei Mecanice. Experiența acumulată în predarea disciplinelor de specialitate, coordonarea lucrărilor de licență și disertație, precum și implicarea activă în proiecte de cercetare naționale și internaționale, constituie o bază solidă pentru activitatea de mentorat la nivel doctoral. Obiectivul principal al demersului de abilitare este acela de a obține calitatea de conducător de doctorat, în vederea formării și îndrumării unor cercetători tineri, motivați și bine pregătiți în domeniul Ingineriei Mecanice. În mod particular, intenționez să mă implic activ în coordonarea de teze doctorale în aria de specializare Mașini Hidraulice, cu accent pe subdomenii precum turbine hidraulice și pompe centrifuge, domenii în care dețin o expertiză confirmată prin publicații științifice, activitate experimentală și colaborări interdisciplinare. Consider că formarea unei noi generații de cercetători capabili să abordeze provocările actuale din sectorul hidroenergetic și industrial este esențială, iar contribuția mea poate aduce valoare adăugată atât din punct de vedere științific, cât și educațional.

(B) SCIENTIFIC AND PROFESIONAL ACHIEVEMENTS

(B-i) Professional Achievements

I defended my PhD thesis entitled "Swirling Flow Control in the Draft Tube Cone of Hydraulic Turbines", [1], in March 2011, under the scientific supervision of Prof. Dr. Eng. Romeo Susan-Resiga. The thesis followed the same research direction I had pursued since my bachelor's degree: the control of swirling flow in the draft tube cone of Francis turbines, a phenomenon commonly known as the helical vortex rope. The proposed solution involved axial water injection in the cone of the draft tube to mitigate the pressure fluctuations caused by off-design operation. This method was initially investigated through numerical simulations, which confirmed its potential, and was subsequently validated through experimental tests conducted on the laboratory test rig. Both computational and experimental results demonstrated the effectiveness of the method in significantly reducing pressure pulsations in the conical diffuser of the draft tube. This research drew interest from both the industrial sector and the academic community, with results disseminated through national and international conference presentations. The public defense of my doctoral thesis, attended by Hidroelectrica branch directors from across the country, highlighted the growing need to investigate and understand hydraulic turbine behavior under off-design operating conditions.

Immediately following the completion of my PhD, I successfully applied for a nationally funded postdoctoral research grant, winning a Postdoctoral Project PN-II-RU-PD-2011-3-0165, titled: "Magnetorheological Device for Swirling Flow Control". The project was carried out between October 2011 and October 2013. The host institution was the Romanian Academy – Timișoara Branch, and the scientific advisor was Dr. Phys. Ladislau Vékás. The goal of the project was to develop an innovative magnetorheological (MR) device designed to control the rotational speed of the free runner from the swirl generator, thus damping pressure pulsations in the draft tube cone of hydraulic turbines. This interdisciplinary research combined fluid mechanics and turbomachinery with materials science (magneto-rheological fluids), offering a novel approach to flow control in hydraulic turbomachinery, with potential applications for turbines operating in variable load regimes.

After completing my postdoctoral research, I applied for an academic position and was appointed as a Teaching Assistant on a fixed-term contract in 2013. I held this position for three years and, since February 2016, I have been employed as a permanent Teaching Assistant at the Faculty of Mechanics, Politehnica University Timișoara. During this period, I have been actively involved in both seminar and laboratory classes across several disciplines, including:

- Fluid Mechanics (seminar and laboratory – 2nd year, undergraduate)
- Fluid Mechanics and Hydraulic Machines (seminar and laboratory – 3rd year, undergraduate)
- Measurement and Real-Time Monitoring of Hydraulic Parameters (laboratory – 1st year,

master's level)

In March 2018, I was promoted as Lecturer in the same departments, and supplementary I was involved in the teaching courses:

- Hydraulic Turbines (course, laboratory and project – 4th year, undergraduate)
- Centrifugal Pumps (laboratory and project – 4th year, undergraduate)
- Measurement and Real-Time Monitoring of Hydraulic Parameters (course, laboratory – 1st year, master's level)

In September 2024, I was promoted to Associate Professor, and the curricula was improved with the following courses and applications:

- Hydroelectric power plants and pumping stations (course, laboratory – 1st year, master's level)
- Turbomachinery (laboratory – 1st year, master's level)

This substantial teaching load has played an important role in the development of my academic career, offering me the opportunity to refine my pedagogical approach, connect theoretical knowledge with practical skills, and mentor students at different levels of their education.

Within the Hydraulic Machinery Laboratory of the Faculty of Mechanics at Politehnica University Timișoara, I have continuously contributed to the development, modernization, and integration of advanced experimental infrastructure. These test rigs serve multiple academic purposes: they support bachelor's and master's thesis projects, enable cutting-edge doctoral research, and create opportunities for industrial collaboration. Moreover, they are essential for building experimental competence among students and young researchers and for strengthening our group's capacity to participate in national and international research initiatives. In parallel with teaching and mentoring activities, I have been actively engaged in the design, development, and modernization of experimental rigs within the Hydraulic Machinery Laboratory. These test rigs are used both in research projects and in student training. The main test rigs I have worked on are as follows:

- Experimental Test Rig for Magnetorheological Brake in Air and Water. Developed as part of the postdoctoral project "Magneto-Rheological Device for Decelerated Swirling Flow" (PN-II-RU-PD-2011-3-0165), finalized in 2013. This rig enables the study of MR fluids in brakes in both gaseous and liquid environments, with applications in flow control.
- Modernization of Swirling Flow Test Rig – Integration of Magnetorheological Brake for Rotating Blade System. The test rig was developed within the same postdoctoral project (PN-II-RU-PD-2011-3-0165), this upgrade involved the installation of a magnetorheological brake to control the speed of the free runner from the initial configuration of the test rig.
- Experimental Test Rig for Magnetorheological Clutch Systems. It was developed within the research project "Innovative Magnetorheological Device Solutions for Improving the

Performances of Centrifugal Pumps" (PN-II-RU-TE-2014-4-1089), finalized in 2016. This rig allows the testing of MR clutches for speed control with application in the centrifugal pums equipped with axial inducers.

- Experimental Micro Francis Turbine Test Rig. The test rig has been acquired using institutional resources from Politehnica University Timișoara (UPT) in 2020, this rig is designed to measure different operating regimes of a micro-scale Francis turbine, supporting student projects.
- Experimental Setup for Measuring Forces Generated by a Water Jet. The test rig was acquired with UPT support in 2021, this rig is dedicated to the study of impulse forces generated by a water jet. It allows basic investigations in hydraulic force measurement.
- Modernized Test Rig for Cavitation Testing in Centrifugal Pumps. Completed in 2021 with UPT funding, this upgraded rig enables the study of cavitation behaviour, an important topic in both industrial and academic contexts.
- Multifunctional Experimental Test Rig with ARMFIELD Recirculating Pump. Installed in 2022 as a result of a donation from ARMFIELD Fluid Technology, this test platform allows experiments in micro pumps used in the residential applications.

To support students enrolled in both bachelor's and master's programs, I have co-authored, together with colleagues from our research group, four academic books, page 144, [1] - [4] and five book chapters, page 144, [1] - [5], covering the disciplines we teach as part of the core mechanical and energy engineering curriculum. Since 2013, I have been actively involved in supporting students' practical training, particularly within the mandatory internship program for third-year students specializing in Mechanical Engineering. Each summer, I coordinated and supervised groups of 4 to 8 students during their internship activities, which take place within the Hydraulic Machinery Laboratory. The main areas of focus include experimental investigations on the swirling flow test rig, pump test rigs, and test rig involving magnetorheological fluid applications.

In addition to internship supervision, I have played an active role in promoting the academic programs offered by Politehnica University Timișoara, especially the Hydraulic and Pneumatic Machinery and Systems (MSHP) specialization, both locally and regionally. These activities have included: participating in visits to high schools to raise awareness of engineering study opportunities; hosting groups of high school students in the Hydraulic Machinery Laboratory for laboratory simple tests and interactive sessions; leading study visits for university students to relevant industrial and institutional sites, such as Iron Gates Hydropower Plant (Porțile de Fier I, II), Raul Mare Retezat, Aquatim, Colterm.

I have also actively supported the doctoral research activities of students under the supervision of Prof. Dr. Eng. Romeo Susan-Resiga, Prof. Dr. Eng. Liviu Anton, and Dr. Eng. Sebastian Muntean. This involvement included guidance and technical assistance that contributed to the

successful completion of several doctoral theses. Among the doctoral candidates I have supported are Dr. Eng. Constantin Tanasa, Dr. Eng. Ionel Drăghici, Dr. Eng. Raul Szakál. Also, I am member in PhD advisory committee for the following: PhD candidate Eng. Daniel Moș, PhD candidate Eng. Constantin Popescu, PhD candidate Eng. Sorin Constantin, PhD candidate: Greti Gherghe, PhD candidate: Eng. Ionut Rus, PhD candidate: Sorin Ioan Lupa, PhD candidate: Ionut Drula, PhD candidate: Dmytro Rozputniak.

I have consistently focused on improving the quality of teaching and mentoring, especially by updating applied course materials and adapting my communication and instructional strategies to better engage students. I actively seek and integrate feedback to ensure that the learning environment remains interactive, relevant, and aligned with students' professional needs. Throughout my 14-year teaching career, I have supervised 22 undergraduate theses within the Hydraulic and Pneumatic Machines and Systems (MSHP) specialization and 15 Master's dissertations in the Hydrodynamics of Machines and Hydromechanical Systems (HMSH) program. Additionally, I have served as a member of the advisory committees for 10 PhD students.

Moreover, in terms of the quality of research member of the Research Centre for Engineering Of Systems with Complex Fluids coordinated by Prof. Dr. Eng. Romeo Susan-Resiga, I have participated in presentations, and I contributed as a member of the organizing committee to national and international meetings, workshops and conferences, which are visible on page 155, [1] - [7].

My scientific activity includes multiple research stages and international collaborations, funded through competitive national and international grants, which have significantly contributed to the development of expertise in the field of fluid mechanics and hydraulic machinery, page 155, [1] - [4].

In 2024, I conducted a research stage at the Department of Fluid Mechanics and Hydraulic Machinery, University of Rijeka, Croatia, within the mobility project titled "Research stage for 3D reconstruction of hydraulic machinery", funded by UEFISCDI Romania (project code PN-IV-P2-2.2-MC-2024-0309). The work focused on developing an experimental framework for the 3D reconstruction of hydraulic turbines, with direct applications on numerical simulation and analysis.

Previously, in 2017, I undertook a research visit at HES-SO Valais-Wallis, Switzerland, within the project PN-III-P1-1.1-MC-2017-1620, also funded by UEFISCDI Romania. The research aimed at implementing an optical flow velocity measurement method using a high-speed camera, without the need for laser illumination, an important step toward non-invasive measurement techniques suitable for industrial setups.

In 2015, I received a Short Visit Grant from the Swiss National Science Foundation (SNSF), under project IZK0Z2_163500, and carried out scientific activities at HES-SO Valais-Wallis, Switzerland. The project focused on developing and validating a dynamic method for performance

assessment of hydraulic machines, with emphasis on transient regimes and pressure oscillations relevant to hydraulic machines applications.

Additionally, between 2010 and 2016, I was involved in an extended international collaboration with Chalmers University of Technology, Gothenburg, Sweden, within the Department of Applied Mechanics – Division of Fluid Dynamics. In partnership with renowned researchers (Prof. Håkan Nilsson, Dr. Ardalan Javadi, Dr. Olivier Petit), the research addressed numerical simulation of turbulent flows and experimental validation in hydraulic machinery. The collaboration resulted in multiple joint publications. An important result on this international collaboration is represented by swirl generator from our laboratory, with was imposed as a test case for numerical simulation community. The test case is available at: http://qnet-ercoftac.cfms.org.uk/w/index.php/AC6-14 - Swirling flow in a conical diffuser generated with rotor-stator interaction, 2016, Javadi A., Bosioc A.I., Nilsson H., Muntean S., Susan-Resiga R., test case for ERCOFTAC Knowledge Base Wiki Article.

These experiences have had a significant impact on my research directions and have strengthened international collaboration networks, facilitating further European research projects applications and partnerships. The list can be found below:

In recognition of these efforts, in December 2023, during the Politehnica University of Timișoara Gala, I was honored with the "Ioan de Sabata Award" for Excellence in Teaching and Mentorship, a distinction that reflects the commitment I have shown to student success and academic excellence.

(B-ii) Scientific Achievements

Since I defended the PhD thesis in 2011, I was involved continuously in the field of hydraulic machinery and flow control thru research projects and industry contracts.

A first project where I was involved as team member was the national research grant PN-II-ID-PCE-2012-4-0634, entitled "Self-induced instabilities of swirling flow in hydraulic turbines operating far from optimal regimes", coordinated by Prof. Dr. Eng. Romeo Susan-Resiga. As a member of the research team, I contributed to the project's objectives: developing an integrated methodology for the a priori quantitative estimation of swirling flows in hydraulic turbines. This predictive tool is essential for improving the preliminary design phase of turbine runners, especially for modern hydro units required to operate efficiently and safely over a wide range of discharges, often under off-design conditions where swirling flow instabilities become dominant. The research combined advanced numerical simulations with experimental validations.

In October 2015, I successfully obtained thru UEFISCDI Young Teams competition, the project PNII-RU-TE-2014-4-1089, titled "Innovative magneto-rheological device for improving the performance of centrifugal pumps – iRheoDev". This 2-year project focused on the mitigation of cavitation phenomena in storage centrifugal pumps by introducing an axial inducer with variable speed in front of the main pump runner. The rotational variable speed was achieved using a magneto-rheological (MR) fluid clutch, which allowed control of the axial inducer speed depending on the flow regime. The experimental setup developed in this project included a MR clutch and which was tested independently (in order to characterise the MR clutch) and on the pump test rig.

Continuing this path, in 2020, I obtained a second nationally funded Young Teams project (PN-III-P1-1.1-TE-2019-1594) entitled "Free Rotor for Swirling Flow Control at the Outlet of Hydraulic Turbines". The research explored passive control mechanisms for stabilizing swirling flows at the turbine exit by installing a freely rotating element that adjusts its speed depending by the flow from the draft tube cone. The freely rotor was tested experimentally in different configurations with the purpose of finding the optimum configuration. Within this project, I also promoted the young students, actively involving bachelor's graduates, master's students by performing measurements and presenting their work in that direction.

More recently, in 2025, I have successfully obtained, through a national competition organized by UEFISCDI, the winning Demonstration Experimental Project titled: "Energy-efficient Water Jet Control for Increasing the Flexibility in Operation of Hydro Turbines". This project reheats and further develops the concept of water jet injection at the inlet of the hydraulic turbine's draft tube cone, proposing a novel approach involving a radial-axial jet configuration. The main objective is to reduce the amount of water required for injection, thereby improving the overall energy efficiency of the turbine. In addition, the solution is designed to diminish flow instabilities that typically occur in the draft tube under partial load conditions, an issue that often limits operational

flexibility in hydro turbines. One of the key innovations of this project is to ensure that the jet control system is not only effective but also practical and accessible for implementation in existing hydropower plants, with minimal structural modifications. The project combines experimental validation with computational modelling, aiming to demonstrate the viability of this technology in real-world operational settings.

In recent years, the Hydraulic Machinery group from Politehnica University Timișoara, of which I am an active member, has also been engaged in several technical assistance and consulting projects with strong industrial relevance. These projects have provided high-impact solutions for the Romanian hydropower sector:

- BC/43/2025: Specialized technical assistance services for model testing of the turbines related to the investment objective ''Refurbishment of the Vidraru Hydropower Plant''.
- BC76/2022: Modernization of HA1 Slatina – Optimization of a combinatorial cam profile in terms of vibration and efficiency.
- BC26/2020: Expert advisory services in the international arbitration case ICC22482/MHM – Technical documentation analysis and participation in hearings.
- BC105/2021: Technical expertise for the arbitration case no. 8/2021 at the Court of International Commercial Arbitration, Romanian Chamber of Commerce.

The projects have coordinated by Prof. Dr. Eng. Romeo Susan-Resiga, and in these projects, I contributed as a technical expert in various phases including commissioning of hydropower units, on site testing, data acquisition and analysis, and review of technical documentation.

The list of the projects and contracts where I was involved in quality of responsible or team member are presented on page: 153, [1][2] in quality of Contract Director; 154[2] - [4] in quality of National research projects – Director; 154[1] - [4] in quality of Contracts member and 154 [1] - [6] in quality of member in National research projects.

All these research projects, technical assistance activities, and collaborations with both academic and industrial partners have led to a substantial body of scientific contributions. These results are reflected in a series of publications in internationally indexed journals, presentations at prestigious scientific conferences, as well as in authored and co-authored patents, books, and book chapters. Together, they demonstrate both the applied relevance and academic impact of the research activities carried out over the years. A synopsis of these results included in published materials, is presented in Table 1.

Table 1. Distribution on the categories of the published materials of the author starting with the year he obtained the PhD thesis.

Year	ISI Journals	ISI Conf. Proc.	BDI Journals	BDI Conf. Proc.	Books	Book chapters	Patents
2011	1						
2012	1						
2013	1	4					
2014	1	4	1				
2015	1	7					
2016	3	7	1			2	
2017	1	4	1		2		1
2018	1	2					
2019	1	6				2	2
2020	1						
2021	3	3		1	1		
2022				1			1
2023	1			1			1
2024	1	1			1		
2025	1			3			
TOTAL	**18**	**38**	**3**	**6**	**4**	**4**	**5**

The detailed list of the published materials can be found on the last chapter of the Habilitation Thesis, Annex with Scientific and Professional Achievements, on the following pages:

- ISI papers, page 147, [1]- [57];
- BDI papers, page 152, [1]- [9];
- Books, page 144, [1] - [4];
- Book chapters, page 144, [1] - [5];
- Patents, page 144, [1] - [5].

The results from the table above can be presented in a detailed graph with the evolution in time:

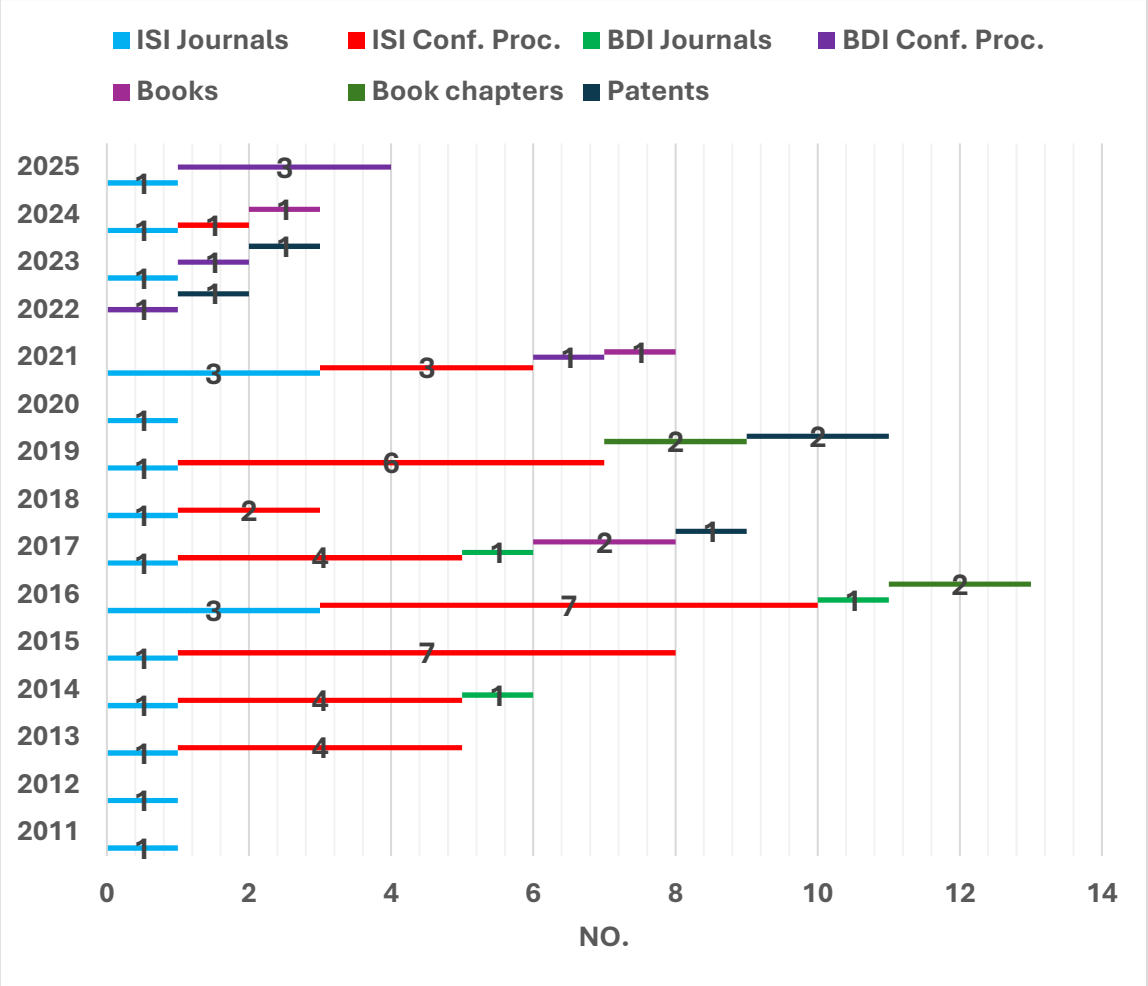

Figure 1. Evolution of the publications from the finishing of PhD Thesis (2011) up to this current year (2025).

The following pages present a comprehensive overview of the research output generated since 2011. These materials (journal papers, conference proceedings papers, books and chapter books and patents) represent the results of sustained and systematic investigations primarily in the field of turbomachinery, alongside parallel research activities in biomedical applications. I mention here Dr. Eng. Sandor Bernad, the initiator of the studies in biomedical applications and his group. The biomedical research line, conducted in parallel with my early turbomachinery studies, has yielded significant and conclusive findings supported by both numerical simulations and experimental validations.

(C) SCIENTIFIC DEVELOPMENTS

The developments to which I contributed through research projects and scientific papers led me to the realization of the following subchapters in the habilitation thesis:

C.1 Magneto-rheological fluids (MRF) and their applications in hydraulic machinery.

C.2 Control methods for diminishing the hydraulic instabilities in hydraulic turbines.

C.3 Control methods for diminishing the hydraulic instabilities in centrifugal pumps.

C.4 Advanced diagnostic and testing methods for pumps and turbines in energy applications.

Taking into account my professional development, the habilitation thesis begins with chapter C1. Magneto-rheological fluids (MRF) and their applications in hydraulic machinery, presenting results from the Post-Doctoral project conducted during 2011-2013 regarding the applications of magneto-rheological fluids in brakes used for speed control. The chapter continues with the detailing and analysis of a magneto-rheological fluid clutch, later developed for controlling the speed of the axial impeller used in large-capacity pumps with the purpose of reducing cavitation.

Chapter C2, Control methods for diminishing the hydraulic instabilities in hydraulic turbines, presents a series of passive and active solutions for controlling swirling flow in hydraulic turbines. The first part details a comprehensive experimental analysis of the rope vortex development and its control using a water jet, through velocity measurements with LDV, an investigation carried out after defending the doctoral thesis. The next subchapter presents the implementation of the magneto-rheological fluid brake on the swirling flow test rig, which increased the operating regimes of the test rig from part load to full load operation. The following two subchapters analyze two passive and active methods investigated both numerically and experimentally for reducing the effects of the vortex rope: a free runner mounted downstream of the main rotor and radial-axial water injection. Both methods demonstrated that the rope vortex in the conical diffuser of the suction tube can be reduced or even eliminated.

Chapter C3, Control methods for diminishing the hydraulic instabilities in centrifugal pumps, initially describes the experimental test rig for investigating large-capacity centrifugal pumps and the non-uniformity of flow at the pump inlet caused by a 90° elbow section at the inlet. The proposed solution for eliminating the non-uniformities and avoiding cavitation is presented in the following subchapter, which involves the use of an axial impeller mounted in front of the pump with variable speed. The impeller speed varied using the magneto-rheological fluid clutch described in chapter 1. Thus, by varying the impeller speed, the non-uniformities generated by the inlet elbow can be eliminated or controlled.

Chapter C4 presents the applied part of the thesis, namely dynamic tests conducted in the Hydraulic Machines Laboratory at HES-SO Valais-Wallis University, Switzerland, where during 07-

09.2015 I implemented the project Development and implementation of a dynamic method to measure the performances of hydraulic machines, project IZK0Z2_163500. The project was funded by the International Short Visit Grant, FNS Switzerland, coordinator Prof. Dr. Eng Munch-Alligne Cecile, and there I was able to perform tests on a model axial micro turbine and a pump used as a turbine (PaT). Efficiency tests were performed using a new method called the "sliding gate method," which allows a turbomachine to be tested much faster.

The final part of this thesis presents and discusses a comprehensive set of measurements conducted at the CHE Slatina hydroelectric power plant, located on the Olt River. The primary objective of these measurements was to determine an optimized combinatorial cam for integration into the automatic speed regulator (RAV) system, which governs the operation of the hydraulic turbine. The experimental testing was performed using the constant power method, in the absence of high-precision flow measurement equipment. Instead, the tests were based on controlled variations in the guide vane opening and the axial runner blade angles, while the electrical power of the generator was maintained constant. These investigations were carried out within the framework of the research contract titled "Modernizare HA1 Slatina – Determinarea unei came combinatorice optimizată din punct de vedere al vibrațiilor și randamentului" (Contract No. BC76, 2022), led by Prof. Dr. Eng. Romeo Susan-Resiga. As a member of the research team, I was actively involved in all phases of the project. This included assisting with the recommissioning and operational startup of the hydraulic turbine after a prolonged two-year period of inactivity. My responsibilities further encompassed conducting flow and vibration measurements, participating in detailed testing procedures for the determination of the combinatorial cam. Additionally, I contributed to the long-term monitoring and evaluation of the turbine's performance, specifically focusing on the correlation between guide vane and runner angle configurations and observed vibration levels, with the goal of refining the cam profile to meet both mechanical and efficiency-related optimization criteria.

(C-i) Magneto-Rheological Fluids (MRF) And Its Applications In Hydraulic Machinery

MRF description

Following the defence and awarding of the PhD degree, I had applied and won a postdoctoral research project funded by the Executive Unit for Financing Higher Education, Research, Development and Innovation (UEFISCDI). The project was hosted at the Romanian Academy – Timișoara Branch, under the scientific supervision of Dr. Phys. Ladislau-Nicolae Vékás, Director of the Center for Fundamental and Advanced Technical Research in Timișoara, within the Romanian Academy.

The focus of the postdoctoral project was on magneto-rheological (MR) fluids, with a specific objective to design and implement an MR brake aimed at expanding the operating regimes of a swirl generator previously developed during the doctoral research. The MR brake was intended to serve as an adaptive control mechanism for the speed of the runner in experimental setups, particularly those simulating draft tube flows in hydraulic turbines.

Magneto-rheological fluids are classified as smart materials, characterized by their ability to rapidly and reversibly change their rheological behaviour, primarily viscosity and yield stress, under the influence of an external magnetic field. This transformation, which occurs within milliseconds, is driven by the alignment of suspended ferrous particles, effectively transitioning the fluid from a free-flowing state to a semi solid structure. Such controllability enables real time modulation of damping forces, resistance, or torque in various mechanical systems.

Common industrial applications of MR fluids include automotive semi-active suspensions, vibration isolation systems in civil engineering, and adaptive clutches and brakes used in precision machinery. In the context of fluid mechanics and turbomachinery, MR fluids are increasingly applied in variable-speed control systems, particularly in centrifugal pumps and axial inducers, where they allow seamless torque transmission without the need for complex frequency converters.

The integration of MR brakes into swirl generators has proven especially valuable. These setups enable controlled studies of vortex rope formation, pressure fluctuations, and unsteady swirling flows, phenomena frequently encountered in the draft tubes of Francis turbines. By dynamically adjusting the braking torque through magnetic field, MR brakes provide a precise and non-invasive method for altering swirl intensity. The outcomes of these investigations formed the basis for the first and second chapters of the habitation thesis and are directly linked to the research project titled Magneto-rheological Device for Controlling Swirling Flow (Project ID: PD 32/2011, funding period: 2011–2013). This project marked the first successful implementation of MR fluid-based control systems in laboratory for speed control of the runner from the swirl generators in Romania.

Building on this foundation, further advancements were realized during the research project Innovative Magneto-Rheological Device for Enhancing the Performance of Centrifugal Pumps (Project ID: TE 62/2015, funding period: 2015–2017). In this phase, the MR clutch was applied to an axial inducer to operate at variable speed, allowing experimental investigations for efficiency and cavitation. The ability to modify the axial inducer speed with high precision provided enhanced flexibility by improving the pump cavitation.

These developments, detailed in the third chapter of the habitation thesis, highlight the potential of the magneto-rheological fluids, including both brakes and clutches, as compact, silent, and highly responsive alternatives to traditional electromechanical systems. Their integration into experimental rigs and further to industrial prototypes (if necessary) underlines their role in enabling smart, adaptive hydraulic systems capable of responding in real-time to operational demands.

Application of MRF in hydraulic turbines. Design and testing the MRF brake.

Magneto-rheological brakes (MRB) are one important research direction concerning these smart materials. Some of the advantages are convenient low-power control (through electrically generated magnetic field) and very good torque to weight ratio. The latter recommends them for applications where small devices able to generate high value of torque are needed, [2]. The electrical control possibility (the magnetic field can easily be electrically generated and controlled) is one very important advantage, [3]. According to [4], an electronically controlled brake is easier to adapt in any application by changing the software. Such a device ensures easier integration and what they call "new control features".

The basic property of magneto-rheological fluids is the ability to change viscosity in the presence of a magnetic field. The fast response makes them advantageous in interfacing electric signals and fluid power without the need of mechanical moving parts. Also, the MRF are designed to work at a high range of temperature (maximum 150 °C). The MRF were patented by [5], in the middle of twentieth century for a clutch application. Today MRF are used in a wide variety of applications such as dampers, shock absorbers, torque clutches or brakes. Typically, MRF are suspension of micron sized magnetic particles (iron) in a non-magnetic carrier fluid (hydrocarbon oil, silicone oil, water). When a magnetic field is applied the particles form a chain like structures aligned parallel to the applied magnetic field, [6].

A MRF brake was built for Laboratory of Hydraulic Machinery from Politehnica University Timisoara in order to slow down the speed and increase the operating regimes from the hydraulic machinery test rig [7]. For this purpose, a preliminary test rig was designed, developed and built in order to analyze in detail different brake models for other applications and to test different MR fluids available on the market as well as several MR fluids developed and characterized in our laboratory. This method was chosen considering the mechanical properties of the MR brake (easy to control,

small dimensions, adjustable). The test rig, Figure 2, consists of a variable speed drive motor, a torque detector, the MR brake and the control and acquisition system.

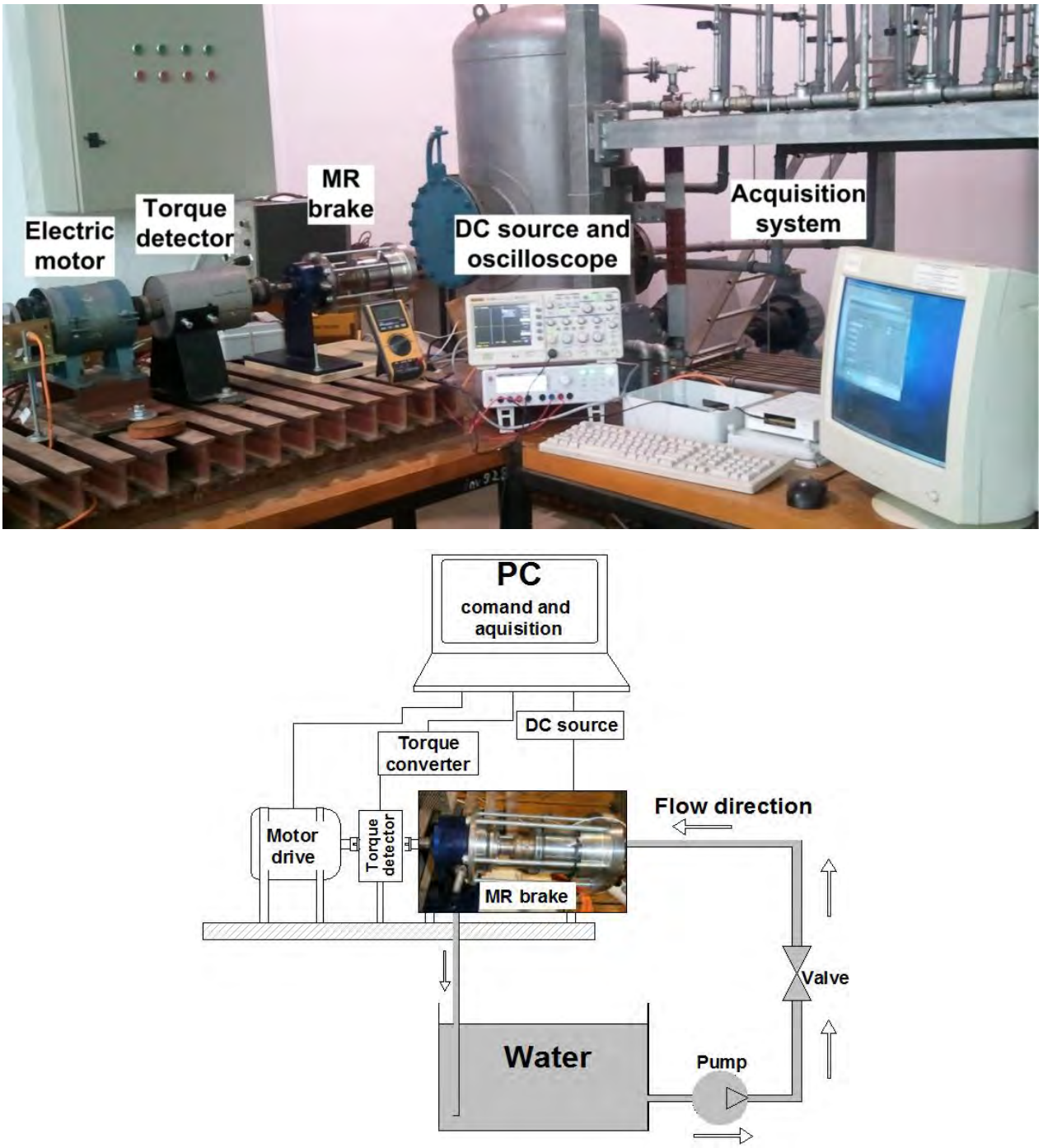

Figure 2. Experimental test rig for MRB applications, image from laboratory (up) and sketch of the test rig with main components and working principle.

The main characteristics and technical data about the brake system are presented in the table below:

Table 2. Main characteristics of the brake system

Component	Main characteristics
Motor drive	0-1000 rpm, 3 kW
Torque detector	0-9000 rpm, 20 Nm
MR brake	0-1000 rpm, design for air/water applications
Control/acquisition system	- 10 Hz acquisition frequency - maintain a constant speed independently by torque variation - has the possibility to acquire 4 temperatures inside/outside of the brake

The control and acquisition system sets the nominal speed of the electric motor and records the following data: (i) the torque value, (ii) electric motor speed, (iii) the voltage and current from the coil of brake or clutch and (iv) the brake temperature, respectively. The temperature is acquired on the outside wall or inside of the brake with ±1.5°C accuracy. Note that this investigation was carried out in air and water. In all measurements the temperature inside MRB close to the MR fluid was below threshold limit. A picture with our preliminary test rig for MR brake applications is presented in Figure 1.

The existing MRB, presented in Figure 3 is a bell shaped MRB, with an important advantage: it encapsulates two brakes by doubling the friction surface. The rotating part is the shaft and disc (bell shape). The magnetic circuit is a fixed part and is built using two pieces: the coil and the magnetic casing. To increase the torque of the MRB, the disc radius was increased as much as possible. The magnetic design of the coil ensures a radial magnetic field, to use the entire surface of contact where MR fluid is inserted. The entire magnetic circuit is built of magnetized iron.

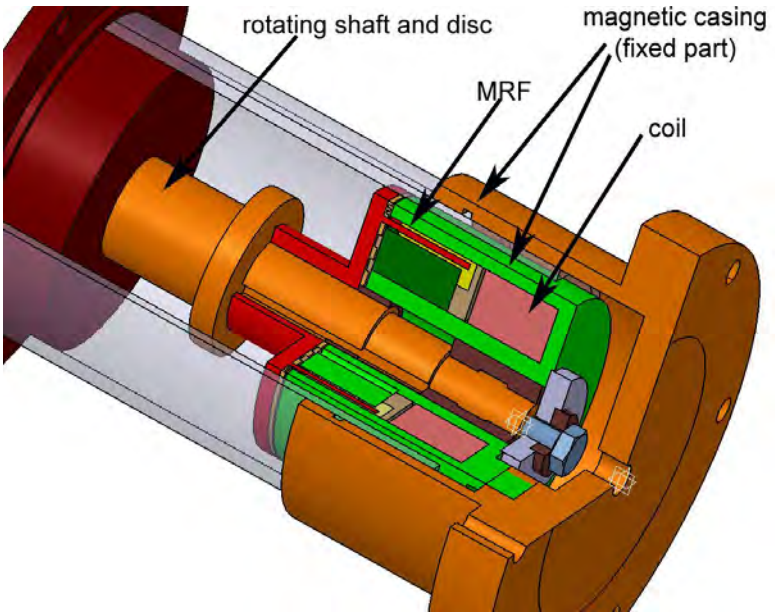

Figure 3. Sketch of the MRB existing in laboratory

The MR fluids used in the experiments are presented in Table 3:

MR fluid	Technical data	Producer
MRF 336 AG	Silicone oil with micro particles, density 3450 kg/m^3	Lord Corporation
SMR 5%	Mineral oil with micro particles, density 1230 kg/m^3	Lab. of Magnetic Fluids Romanian Academy-Timisoara Branch
SMR 15%	Mineral oil with micro particles, density 3880 kg/m^3	Lab. of Magnetic Fluids Romanian Academy-Timisoara Branch
SMR 25%	Mineral oil with micro particles, density 5700 kg/m^3	Lab. of Magnetic Fluids Romanian Academy-Timisoara Branch

The SMR 5%, SMR 15% and SMR 25%, have been produced in Laboratory of Magnetic Fluids, Romanian Academy-Timisoara Branch. The MR fluids have been especially designed for this type of application, the team from Timisoara having a long experience the preparation and characterization of this type of fluids, [8].

The control and acquisition program is presented in Figure 4.

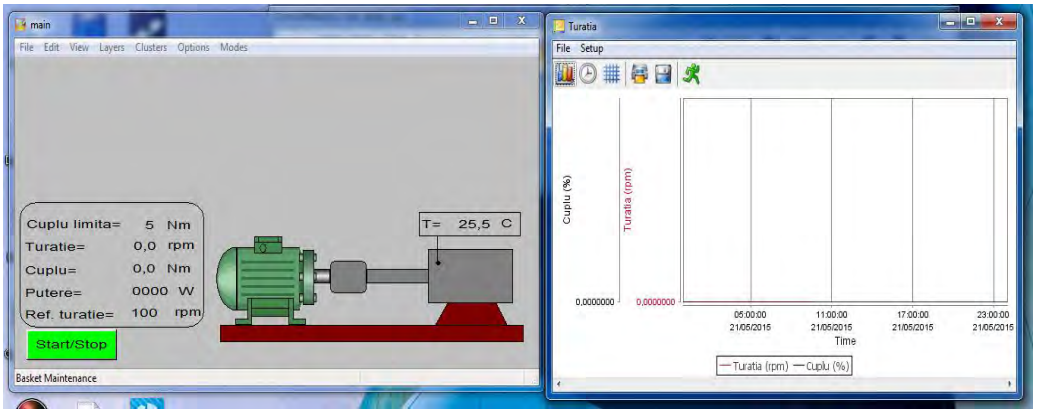

Figure 4. Control and acquisition program implemented on the MRB test rig.

The application allows setting the speed of the motor drive and a smooth start at speeds between 0 - 1000 rpm. Parallel the program allows monitoring the torque and the speed in real time. At the end of each measurement the acquired data can be saved in different formats.

The measurements have been performed in two environments: air and water. For each environment a speed was set between 300 and 1000 rpm with a step size of 100 rpm. At each speed the coil voltage was modified between 0 - 30 V with a step size of 1 V. For each voltage step size was registered: speed, torque, coil voltage, internal and external temperatures.

The first experimental investigations were presented for air measurements, see Figure 5. Have been tested all four MR fluids tested at speeds between 300 - 1000 rpm with a step size of 100 rpm.

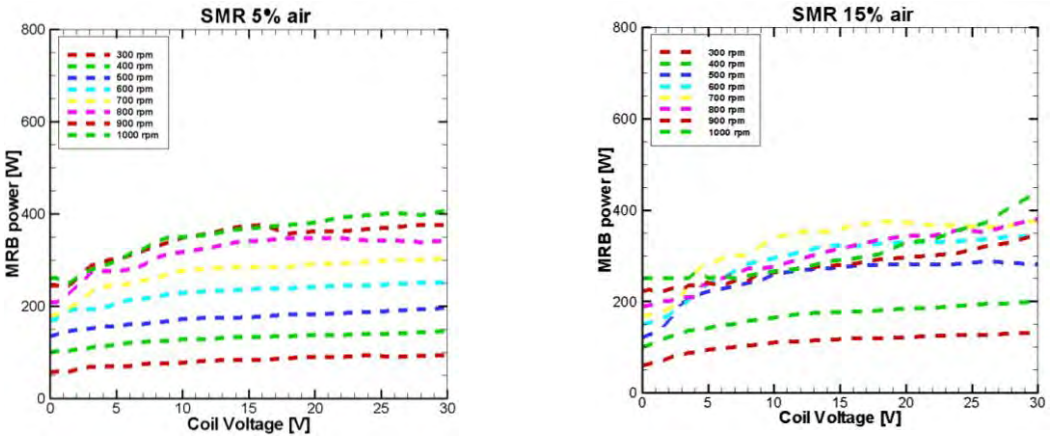

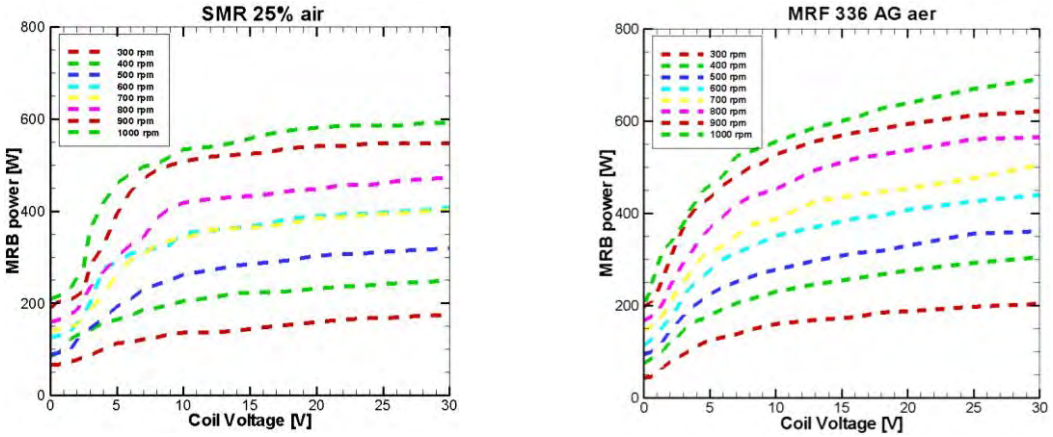

Figure 5. MRB power for different speeds and coil voltages in air

The same measurement configuration was repeated by mounting all MRB system in water, as presented in **Figure 6.**

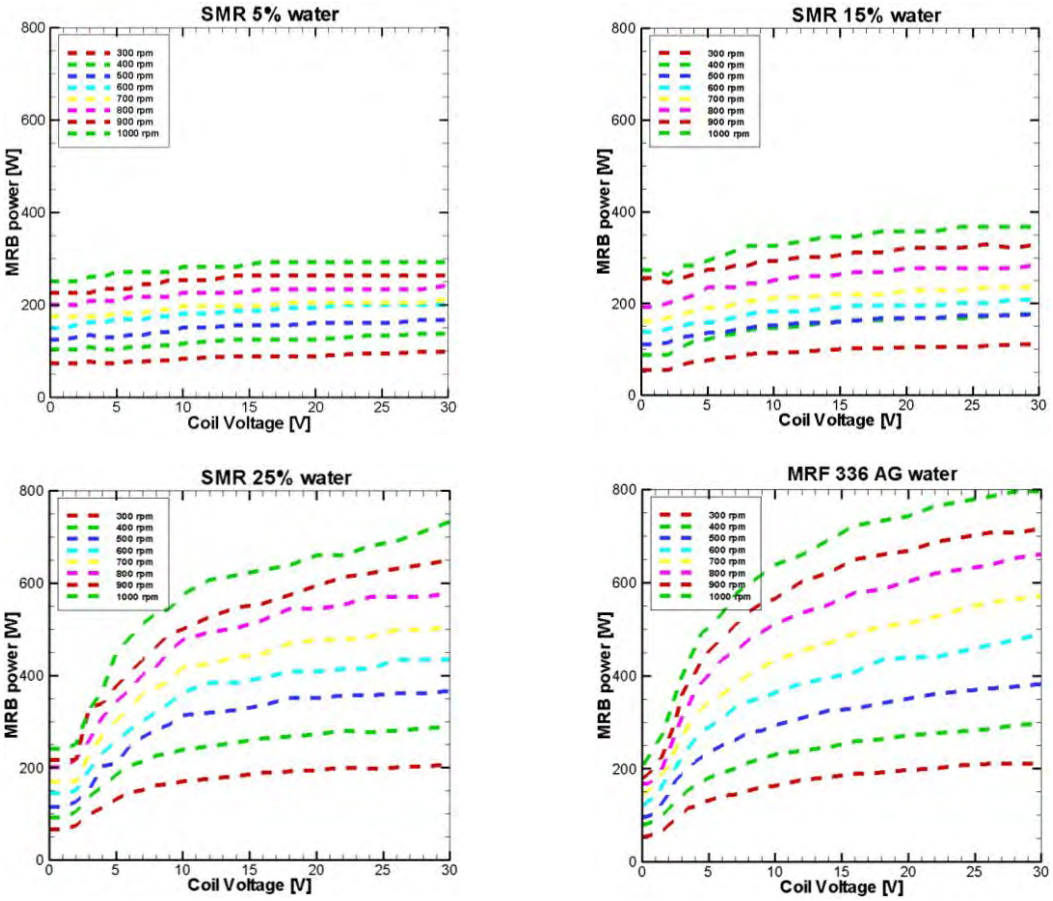

Figure 6. MRB power for different speeds and coil voltages in water

From the first evaluation of the MRB, in air and water it is observed that MRF 336 AG has the best performances. It generates a maximum power of 800 W when is used in water at the maximum coil voltage of 30 V. Even so, SMR 25% has the maximum brake power around 750 W, with 7% less.

The next analysis consists of an evaluation of the MRB at two voltages 10 V and 30 V for all MR fluids investigated in air and water.

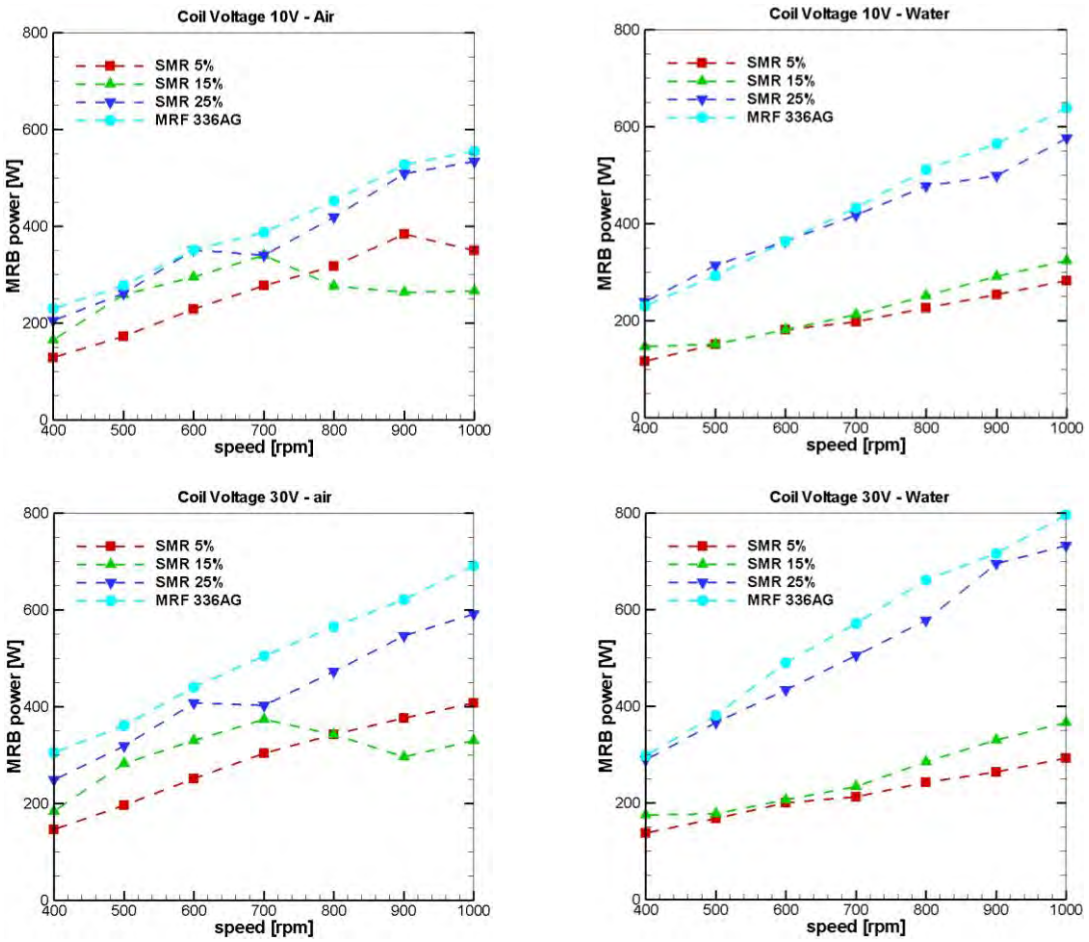

Figure 7. MRB power for two voltages of the coil (10V up, 30V down) for air (left) and water (right)

The evaluation presented in Figure 7 shows clearly the power generated by each type of MRF. SMR 5% and SMR 15%, even though they have different iron compositions, generate approximately the same power in the brake. Instead, SMR 25% generates approximately the same power as the commercial sample.

Keeping into account the fact that the final brake will operate in water, an important consideration is the washing of the MR fluid in time during the operation. Accordingly, Figure 8 present the recirculated water resulted at the end of the measurements. The visualization of the water shows that MRF 336 AG, even though it has good braking characteristics, is washed in time. The SMR 25% sample is not washed (at the same time as MRF 336 AG).

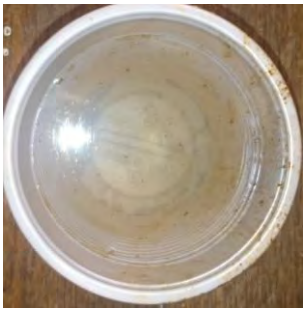

SMR 5%

SMR 15%

SMR 25%

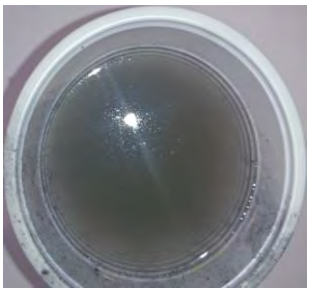

MRF 336 AG

Figure 8. Visualization of the recirculated water from hydraulic system at the end of water measurements

A last visualization consists in disassemble the MRB after each measurement and observe the amount of MR fluid left on the rotating disc. According with Figure 9, the amount of MR fluid is same as beginning for SMR 25%, while the MRF 336 AG is almost washed completely. As a result, even the MRF 336 AG has good braking characteristics; the washing phenomenon can remove completely the MR fluid from the brake.

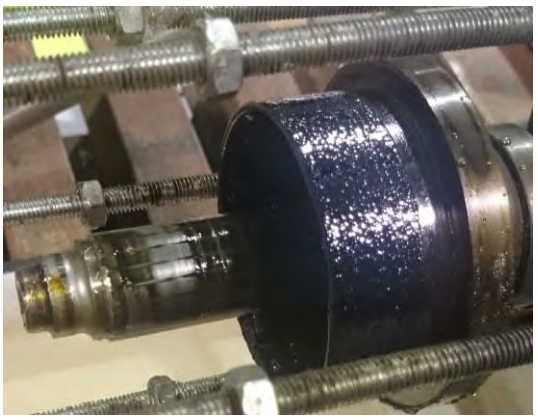

SMR 5%

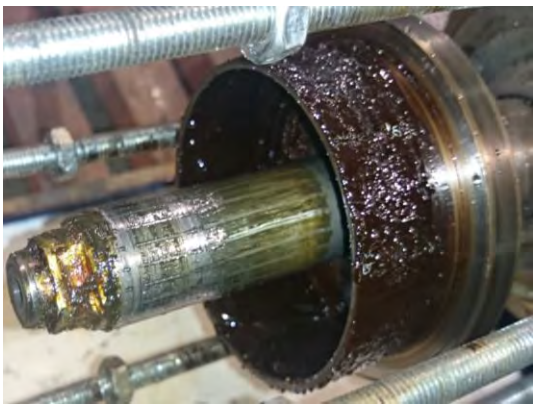

SMR 15%

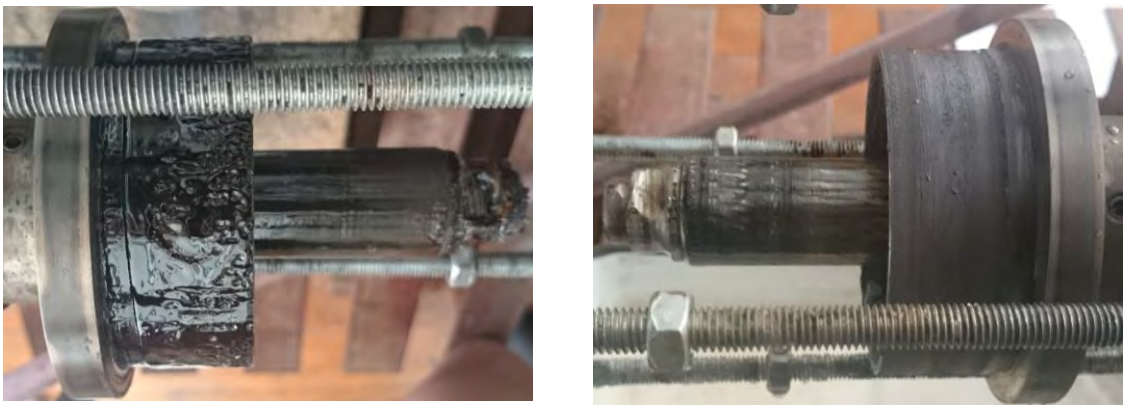

SMR 25% MRF 336 AG

Figure 9. Visualization of the MR fluids at the end of the water measurements on the rotating disc (bell disc)

A last analysis consists in analysis of external temperature for each MR fluid only for air measurements, see Figure 10. During the water measurements no cooling system was used. The external temperature at the MRB surface was same as ambient temperature from laboratory. The registered temperature corresponds to a complete measurement at 1000 rpm and varying the voltage between 0 - 30 V in a time interval of around 25 minutes.

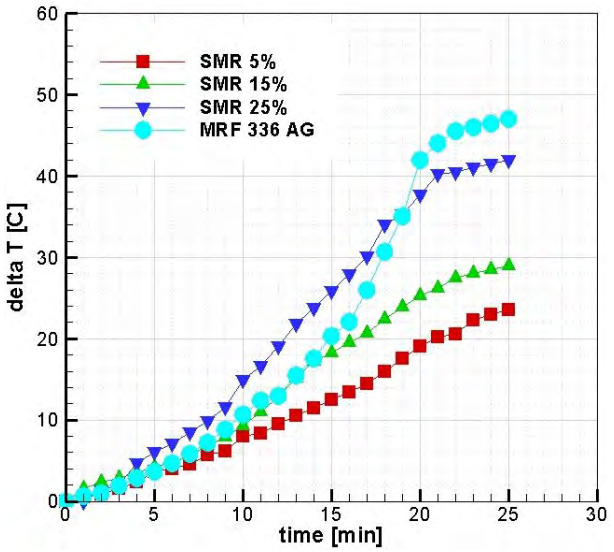

Figure 10. Temperature variation for each MR fluid during the tests

According with the variation of the temperature, see Figure 10, the maximum temperature is registered for MRF 336 AG. Even so, the maximum temperature does not reach the threshold temperature given by the producer.

The air and water measurements conclude that approximately similar braking characteristics are observed for MRF 336 AG and SMR 25%. The MRF 336 AG has 15% more braking power in air and with 7% more water. The major inconvenience of the MRF 336 AG represent the washing phenomenon when it is in contact with water. Instead, SMR 25% is more stable. The maximum temperature generated in

operation is 45C more than at the beginning of the measurement. The temperature is in normal working conditions for all MR fluids. For water operation, to increase the braking power, it can be produced a new MR fluid with a higher iron concentration.

Considering the temperature variation of the MRF, a numerical analysis of the temperature was performed in order to evaluate the parameters of the MRF brake. To investigate the influence of the viscosity of the MR fluid from the brake, first the numerical domain was reconstructed. The numerical domain corresponds to MR brake application based on the technical sketch from Fig. 2 (left). The main components of the MR brake consist in a rotating disc, the magnetic casing and the coil. The rotating disc is driven by the electric motor. In the present work the investigations were performed at 7 speeds between 900 rpm and 300 rpm. The magnetic casing and the coil are fixed parts. In the gap *h* between rotating disc and the magnetic casing is inserted the MR fluid. The rotating disc is located at a radius *r* by 0.035 mm from the symmetry axis of the MR brake. In order to slow down the speed, the magnetic casing and the coil were designed, so that magnetic field lines to close in the MR liquid. Since the MR fluid is located in the brake at a constant radius was possible to perform a 2D axi-symmetric computation.

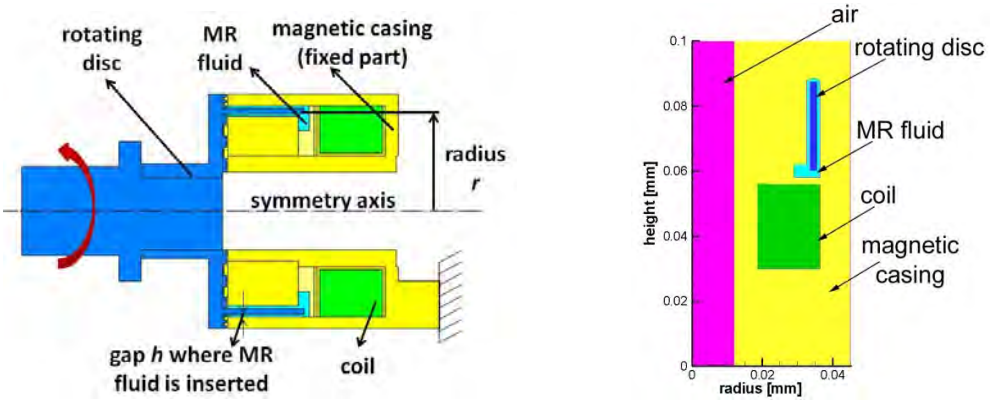

Figure 11. Sketch of the MR brake from the test rig (right) and 2D axi-symmetric computational domain for MR brake used in numerical simulation (left).

For numerical simulation of the MR brake is used a steady k-ε turbulence model. The numerical simulation uses the energy transfer equation and viscous heating was taken into account due to the high shear rate values for this fluid. The axi-symmetric flow model which is implemented in the FLUENT 6.3 code is used with the viscous heating model. A structured mesh with around 85000 cells is generated in order to compute the numerical solution for the temperature field. For numerical simulation, the exterior walls of the MR brake which are in contact with external air, was imposed as thermal condition the convection. For this condition was respected the heat coefficient for the air and the ambient temperature from laboratory. For each numerical domain (air, coil, rotating disc, magnetic casing) were selected the material properties corresponding to the test rig, while for the MR fluid domain were imposed the properties from Table 1. Note that for this evaluation no magnetic field was applied, the experiments and simulations were performed at the normal MR fluid viscosity (without magnetic field) which depends by the shear rate only.

Table 4. Properties of investigated MR fluid

Base fluid	Silicone oil
Operating temperature	-40°C ÷ 150°C
Density [kg/m^3]	3450
Viscosity [Pa s]	Between 0.05 and 0.2 according with shear rate measurements
Specific heat	0.65 J/g °C
Thermal conductivity	0.2 w/m °C

In the case of rotating disc domains were imposed the speeds presented in Table 5. The dynamic viscosity of MR fluid is selected in terms of shear rate associated to each case. Consequently, small values of dynamic viscosity were considered (0.05...0.2 Pa s) in these cases due to high peripheral speeds.

Table 5. Angular speeds for the rotating disc

Speed n [rpm]	Angular speed ω [rad/s]	Peripheral speed v' [m/s]	Shear rate γ [s^{-1}]	Dynamic viscosity η [Pa s]
300	31.42	1.0997	1010	0.2
400	41.86	1.4651	1465	0.18
500	52.35	1.8322	1832	0.155
600	62.83	2.1991	2199	0.115
700	73.30	2.5655	2565	0.09
800	87.90	3.0765	3076	0.07
900	94.24	3.2984	3298	0.05

The shear rate represents the ratio between peripheral speed v' and gap length h=0.001 m and was calculated with the following formula:

$$\gamma = \frac{v'}{h} = \frac{2 \cdot \pi \cdot n \cdot r}{60 \cdot h} \quad (1)$$

The dependency between shear rate and dynamic viscosity allow us to identify the corresponding viscosity for each operating point.

The temperature field for 7 cases was obtained based on axis-symmetric numerical simulation. The temperature color maps for smallest (300 rpm) and largest (900 rpm) speed values are plotted in **Figure 12**. In both cases it can be observed that the main heating source is associated with MR fluid viscosity. A maximum temperature value of 51.6 C is obtained inside of MR fluid at 300 rpm. In this case the rheological behavior of the MR fluid corresponds to the prescriptions delivered by producer. The maximum temperature value of 118 ^{o}C is reached inside of MR fluid at speed of 900 rpm. Also, this temperature is below to the threshold value provided by producer of 150 ^{o}C for this MR fluid. As a result, the rheological behavior of the MR fluid belongs to the prescriptions.

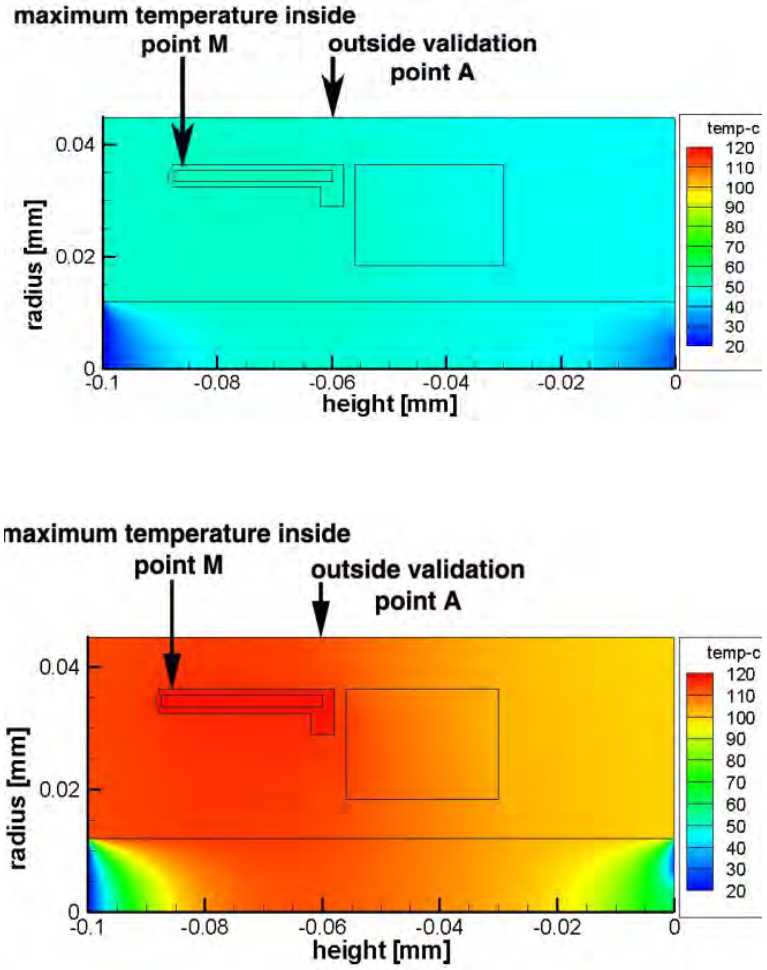

Figure 12. Temperature distribution for 300 rpm case (left) and 900 rpm case (right)

In order to validate the numerical model a qualitative comparison between numerical results and experimental data of the temperature field is provided in **Figure 13** (right). Consequently, on the surface of the MR brake a validation point A was chosen. It can be observed that there is a good

agreement between numerical results and experimental data in this validation point. However, the maximum temperature value is obtained inside the MR fluid **Figure 12**, properly was identified with this point and plotted in **Figure 13** (left).

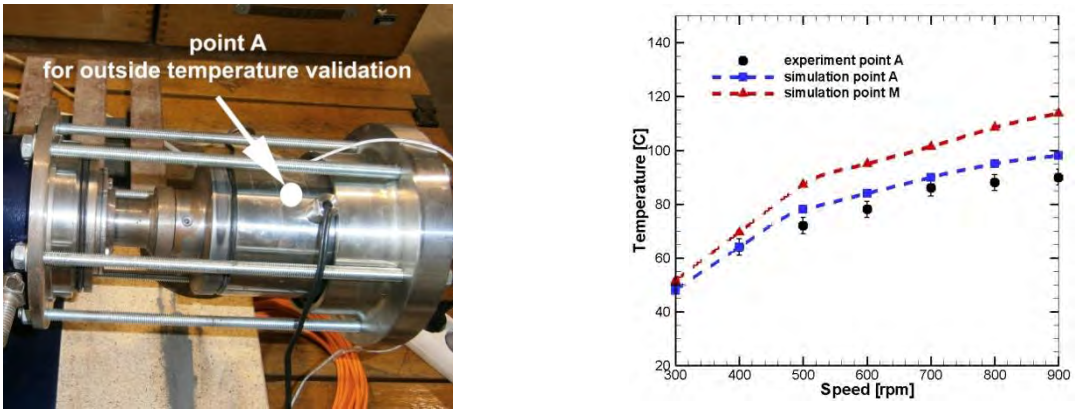

Figure 13. Location point for outside validation (right) and temperature validation on outside surface in point A, maximum temperature of MR fluid inside in point M (left).

As a result, is observed that inside the temperature of the MR fluid at small speeds is approximately the same as outside (300, 400, 500). When the speed is increasing (600, 700, 800, 900 rpm) the interior temperature is larger with 10% inside compared to the outside temperature. The numerical simulation was performed in order to compute the temperature field. All numerical investigations were performed considering zero magnetic field. A reference point A located on the outside wall of MR brake is selected to validate numerical results. A good agreement is obtained between numerical results against experimental data. The maximum temperature value was identified in the MR fluid (denoted point M) on the numerical map. The maximum temperature value of 118^{o}C corresponding to maximum speed (900 rpm) is below the threshold value of 150^{o}C for this MR fluid. The numerical results will be used to improve the magneto-rheological break operation/design.

Application of MRF in centrifugal pumps. Design and testing the MRF clutch.

Magneto-rheological clutches are one important research direction concerning these smart materials. Some of the advantages are convenient low-power control (through electrically generated magnetic field) and very strong torque to good weight ratio, [9], [10]. The latter recommends them for applications where small devices able to generate high value of torque are needed, [11]. The electrical control possibility (the magnetic field can easily be electrically generated and controlled) is one advantage, [5], [12]. Another advantage of MR clutches consists of variable torque transmission using a hybrid MR clutch with a permanent magnet and a coil for generating supplementary magnetic field, [13]. Accordingly, high torque transmissions can be obtained with negligible power consumption reduced size and absence of axial loads compared with conventional electromagnetic clutches.

This section presents the design details and testing results of a MR clutch. The main challenge in designing the MR clutch is the requirement of the application. The device is used for speed control of an axial rotor mounted in front of a centrifugal pump, [14], [15]. The numerical investigations have shown that slowing down the speed of the axial rotor, the minimum pressure is increased (the cavitational behavior is improved) and the flow field non-uniformity is diminished at the pump inlet.

A MR clutch was designed, built and installed in the Laboratory of Hydraulic Machinery from Politehnica University Timisoara in order to slow down the speed of an axial rotor mounted in front of a centrifugal pump, [14]. A new test rig was designed, developed and built to analyze in detail the behavior at variable speeds in order to test independently the performances of the MR clutch, [16]. Also, the test rig serves different MR fluids available on the market as well as several MR fluids developed and characterized in our laboratory, [17]. The method for slowing down the speed of axial rotor, was chosen taking into account the mechanical properties of the MR clutch (easy to control, small dimensions, adjustable parameters). The test rig presented in Figure 14 consists of a variable speed drive motor, a torque sensor, the MR clutch, temperature and speed sensors and the control system and the data acquisition program.

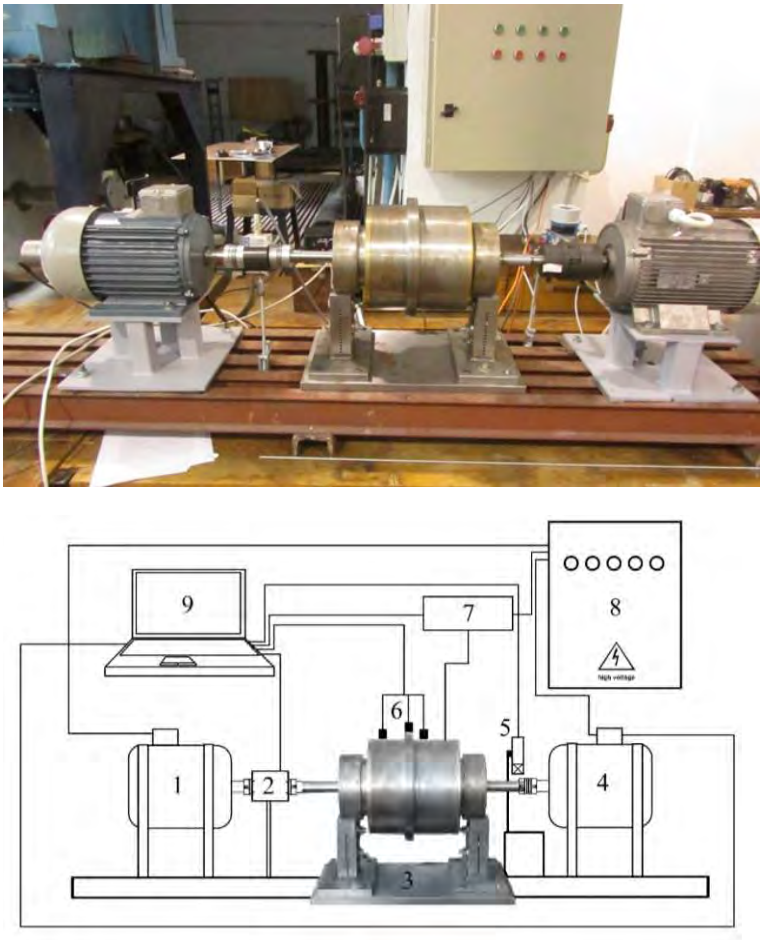

Figure 14. Test rig for MR clutch applications, image from laboratory (up) and sketch of the test rig with main components (down)

According to Figure 14, the main characteristics and technical data for the preliminary MR clutch test rig are presented below in Table 6:

Table 6. Main characteristics of the MR clutch test rig:

Number Item	Component	Main characteristics
1	high speed electrical motor	2500 rpm, 3 kW (fixed speed)
2	torque sensor	0-9000 rpm, ± 20 Nm
3	MR clutch	fixed speed (drive shaft): 2500 rpm variable speed (output shaft): 2500-2000 rpm
4	variable speed electrical motor	2500-2000 rpm, 3 kW (variable speed)
5	optical speed sensor	0-10000 rpm, ±0.5% accuracy

6	temperature sensors	2 temperature sensors: close to MR fluid (0-200 °C), on external surface (0-100 °C)
7	DC source	0-32 V, 0-10 A, programmable DC source
8	control/acquisition system	- 10 Hz acquisition frequency - maintain a constant speed independently by torque variation

The control system sets the speed of the variable electrical motor, and the data acquisition system records the following data: (i) the torque, (ii) the motor speed, (iii) the voltage and current from the coil of the clutch, (iv) the interior and exterior clutch temperature, respectively. The temperature is acquired on the external surface of the clutch while the inside point is located close to MR fluid with ±1.5°C accuracy. Note that this investigation was performed in air.

The designed and built MR clutch, presented in Figure 15, is a bell-shaped MR clutch, with an important advantage: it encapsulates two clutches by doubling the friction surface. The MR clutch has a drive shaft connected at the fixed speed electric motor and an output shaft connected at the variable speed electric motor, (Figure 15, up). It was designed in order to ensure the magnetic flux where the MR fluid is mounted (Figure 15, middle). Accordingly, the MR clutch was designed with two types of materials: magnetic and non-magnetic. The driving part (constant speed) is the shaft and disc (bell shape) at a constant speed of 2500 rpm (red colour). The magnetic circuit is mounted on the fixed part and the variable speed part is built using two pieces: the coil and the magnetic casing, respectively. The clutch radius was increased as much as possible to increase the torque of the MR clutch. The diameter of the clutch was limited at 0.25 m due to the geometrical constrains associated to the pump setup, where the MR clutch will be installed. The magnetic design of the coil ensures a radial magnetic field, in order to use the entire surface of contact where MR fluid is inserted. The entire magnetic circuit is built using magnetized iron.

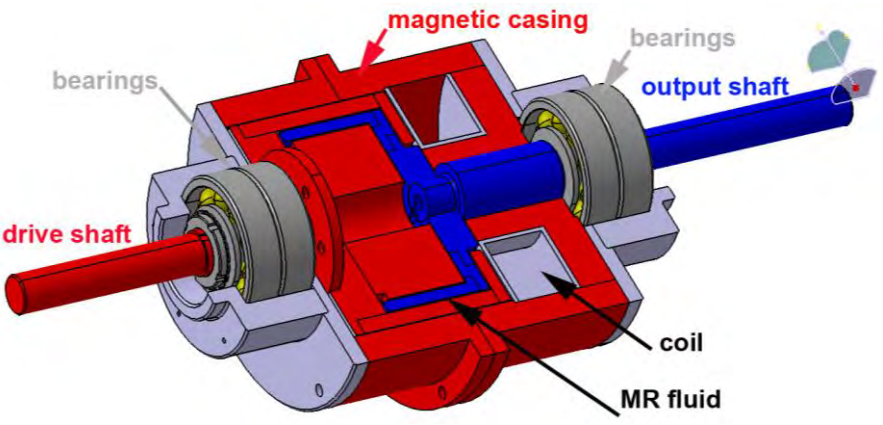

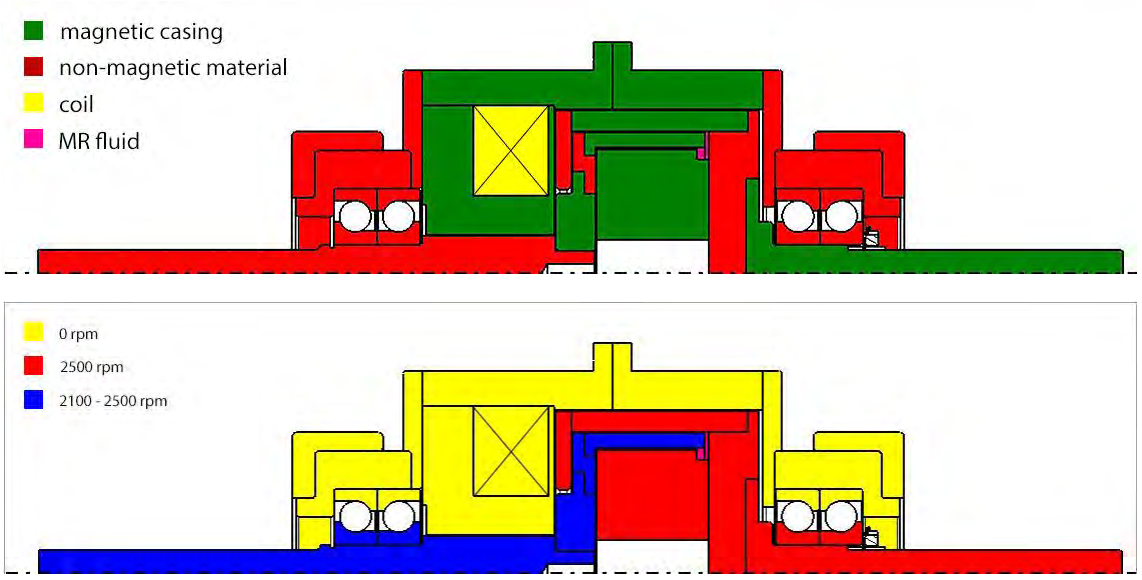

Figure 15. Sketch of the tested MR clutch considering the magnetic properties of the materials (middle) and the speed of each component of the device (down), [18].

A special attention has been paid to the magnetic circuit during design stage of the MR clutch. The coil is responsible for generating the magnetic flux density. It was designed a coil using a copper wire of Ø 0.35 mm, with 2000 turns, with a maximum current intensity of 1 A. The generated magnetic flux by the coil was directed through magnetic materials in the area where MR fluid is inserted on the clutch. At the end, the final geometrical configuration of the clutch was numerically analysed from magnetic point of view using the FEMM 4.2 programme available on http://www.femm.info/wiki/download, property of Aladdin Enterprises, Menlo Park, California, U.S.A. The results show that the magnetic flux density is directed on the magnetic casing of the clutch, with a maxim value of 1T close to the coil and lover values along to the magnetic circuit, see Figure 16. The 2D axial-symmetric plots of magnetic flux density along to the length where MR fluid is inserted shows a constant flux of 0.35 mT at maximum current intensity of 1 A. This result supports our choices performed at the design stage confirms the final geometrical configuration as well as the materials selected are appropriate.

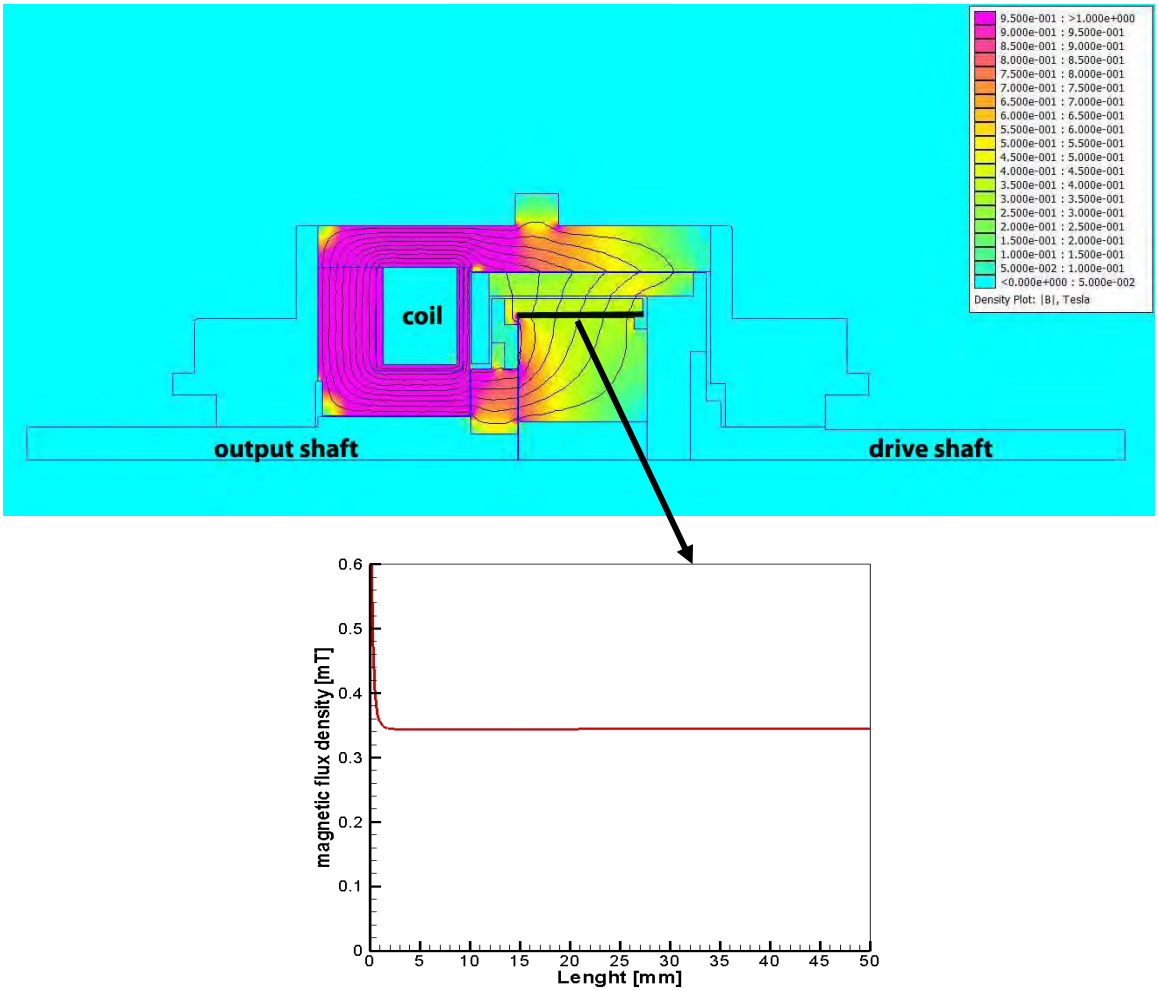

Figure 16. Magnetic flux density through designed MR clutch (up) and 2D axial-symmetric plot in the length of the clutch, where MR fluid is inserted (down).

The MR fluid used in the experiments is MRF 336 AG produced by the Lord Corporation. The MR fluid has two main components: silicone oil as carrier fluid together with iron micro particles. The main properties are presented in Table 7:

Table 7. Main properties of the MR fluid used for clutch application:

MR fluid	**336 AG**
Operating temperature	-40 °C ÷ 150 °C
Density [kg/m^3]	3450
Viscosity [Pa s]	Between 0.05 and 0.2 according with shear rate measurements
Specific heat	0.65 J/g °C
Thermal conductivity	0.2 w/m °C

It was chosen using this type of MR fluid due to high operating temperature (stable up to 150°C) and quite good behaviour in applications, [16].

The control system allows us to setup the speed of the variable motor with a smooth start. Parallel the program allows monitoring the torque and the speed in real time. At the end of each measurement the acquired data can be saved in different formats.

Table 8. The control and acquisition system characteristics:

Used platform	Control parameters	Acquired parameters
SCADA	Variable speed for electric motor	Torque – for variable and fixed speed motor
	Fixed speed for electric motor	Speed - for variable and fixed speed motor
	Variable voltage (applied at the coil clutch)	Temperature – on two points (close to the MR fluid and at the exterior wall of the clutch)
	Maximum torque (for safety precautions)	Power, voltage and current – applied at the coil

The measurements have been performed in air at environmental temperature of 22 °C. The setup for each measurement consists in a constant speed for high-speed electrical motor of 2500 rpm while the variable speed of the second (driven) electrical motor varies between 2450 and 2000 rpm with a step size decrement of 50 rpm. At each regime the coil voltage was modified between 0 and 30 V with a step size increment of 1 V. The measurement was performed considering a time period of 10 seconds with a frequency of acquisition of 10 Hz for each step size of 1 V. Accordingly, 100 samples is registered for each step from 0 to 30V. All investigated regimes are presented in next table:

Table 9. Investigated regimes:

Regime	Fixed speed motor (drive shaft)	Variable speed motor (output shaft)	DC source voltage
Δn 50	2500 rpm	2450 rpm	0 ... 30 V, step size 1 V
Δn 100	2500 rpm	2400 rpm	0 ... 30 V, step size 1 V
Δn 150	2500 rpm	2350 rpm	0 ... 30 V, step size 1 V

Δn 200	2500 rpm	2300 rpm	0 ... 30 V, step size 1 V
Δn 250	2500 rpm	2250 rpm	0 ... 30 V, step size 1 V
Δn 300	2500 rpm	2200 rpm	0 ... 30 V, step size 1 V
Δn 350	2500 rpm	2150 rpm	0 ... 30 V, step size 1 V
Δn 400	2500 rpm	2100 rpm	0 ... 30 V, step size 1 V
Δn 450	2500 rpm	2050 rpm	0 ... 30 V, step size 1 V
Δn 500	2500 rpm	2000 rpm	0 ... 30 V, step size 1 V

Firstly, the experimental investigations were focussed on measuring the torque generated by each electric motor at each regime. The torque for variable speed motor was determined/estimated using the frequency converter. The torque for fixed speed motor is recorded using torque sensor. Before measurements, for the torque sensor calibration curve was obtained and integrated in the data acquisition system.

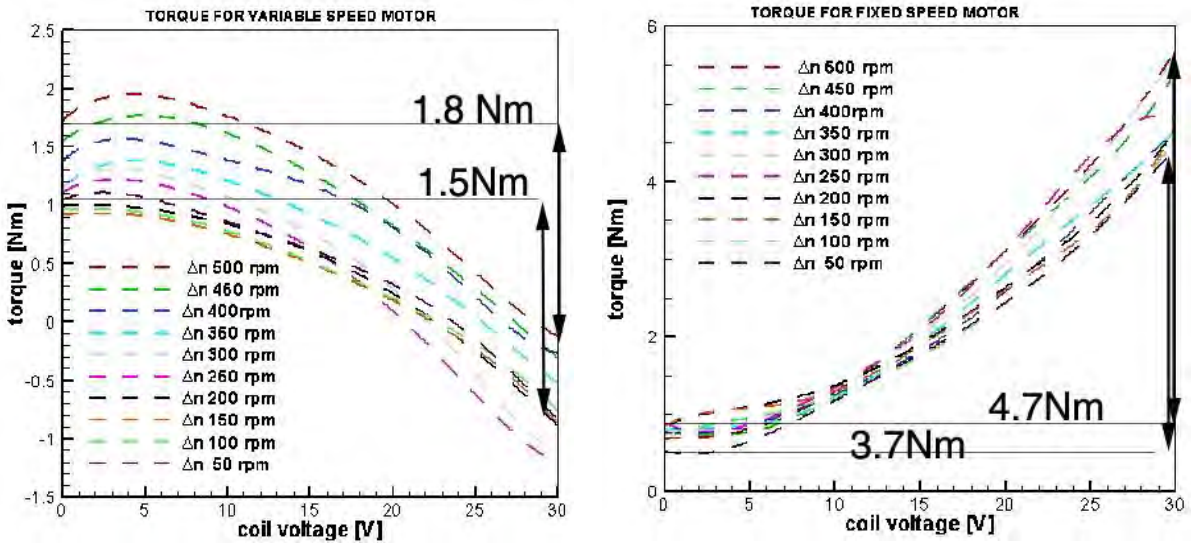

Figure 17. Measured torque for variable speed motor (left) and fixed speed motor (right) at 10 investigated regimes by modifying the applied voltage at the coil.

From the first evaluation, a small torque value of 1.5 Nm is observed for the variable speed motor at regimes with lower Δn=50 rpm and it rises to a value of 1.8 Nm for the highest Δn=500 rpm, Figure 5. Note that the torque value measured at 0 V is only due to viscosity of the MR fluid. The torque starts to increase once the voltage is applied on the coil, reaching a difference of 1.9 Nm for the lowest speed variation Δn of 50 rpm and 1.5 Nm for the highest speed variation Δn of 500 rpm, respectively.

The torque difference measured for the fixed speed motor is significant when the applied voltage at the coil varies from 0 V to 30 V. The reference torque value considered for the torque difference

corresponds to 0 V applied voltage at the coil. The torque difference is around 3.7 Nm at the lowest speed variation Δn of 50 rpm while the torque difference is approximately 4.7 Nm for the highest speed variation Δn of 500 rpm for the fixed speed motor, **Figure 18** right.

The torque difference measured for each electric motor (variable speed and fixed speed) is cumulated in a total torque. The total torque determined on each regime is plotted in Figure 18. The total torque is represented for three coil voltages of 10 V, 20 V and 30 V. One can be observed that the maximum torque value around 5.8 Nm is yielded at maximum applied voltage of 30 V. The clutch covers a maximum torque value measured with 33% larger that our requirements considered by the design specifications. The torque requirement has been determined from 3D numerical simulations performed on the pump system with axial rotor at variable speeds, [19].

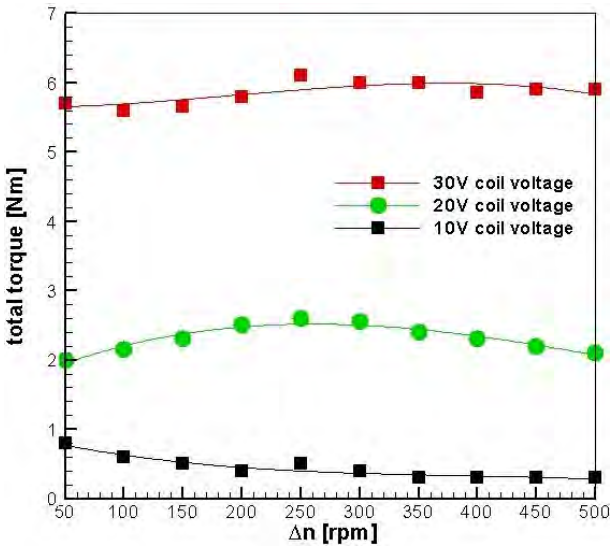

Figure 18. Total torque generated by the MR clutch at three voltage values applied to the coil.

A last analysis consists in measuring the external and internal temperature for the MR clutch, see Figure 19. The measurements have been performed in air with no cooling system. The acquired external temperature is recorded on the clutch exterior wall, while the internal temperature is registered at 1 mm close to MR fluid. The temperature is measured in order to observe the maximum temperature generated by the clutch which can modify the magnetic properties of the MR fluid. The recorded temperature corresponds to a complete measurement regime by varying the voltage between 0 - 30 V in a time interval of around 10 minutes.

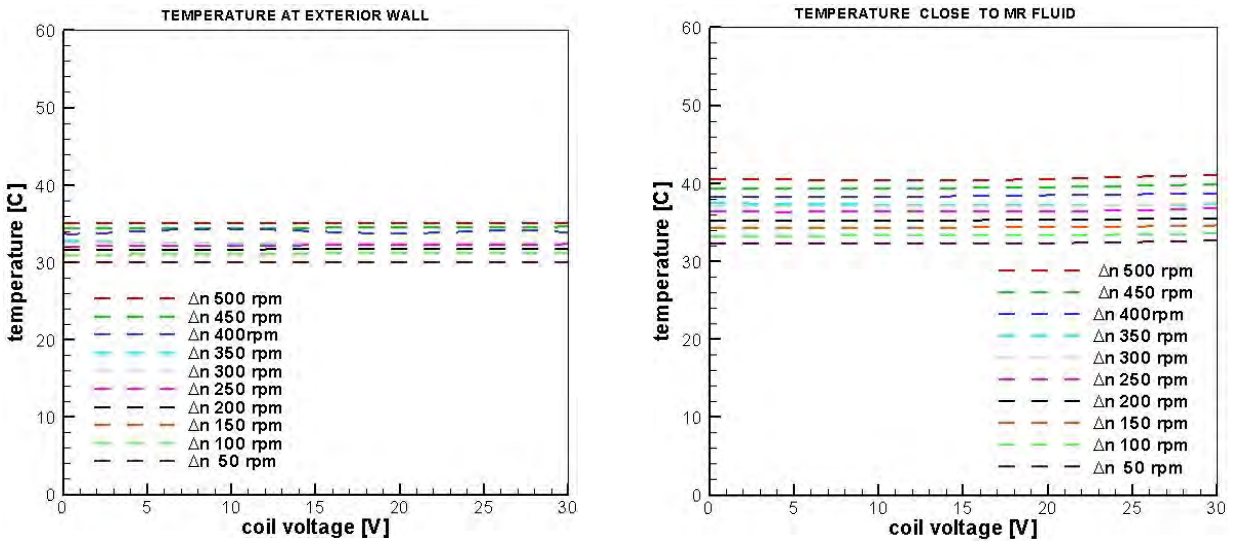

Figure 19. Temperature variation for each regime, measured at the exterior wall of the clutch and close to MR fluid.

According with the variation of the temperature, see Figure 19, the maximum temperature is acquired registered for the maximum speed difference as it is expected. The maximum temperature is approximately 42 °C close to the MR fluid. The temperature is small, due to high volume of the clutch and good dissipation of the heat inside the clutch. Even so, the maximum temperature does not reach the threshold temperature given by the producer for this type of MR fluid (150 °C).

As a result of this research, the MR clutch will be used for speed control of an axial rotor mounted in front of the pump impeller. The main purpose of the axial rotor installed in front of the pump impeller is to improve the cavitational behaviour of the pump increasing the minimum pressure on the impeller blades when the speed of the axial rotor is slow down with 15% with respect to the speed of the pump impeller, [19].

The design of the MR clutch was performed taking into consideration the geometrical constraints of the pump system. A challenge issue during the design stage was the design and analysis of the magnetic field of the MR clutch. The magnetic design of the MR clutch was performed in order to direct the magnetic flux density in the area where MR fluid is inserted in the device. According with numerical results, the maximum value of magnetic flux density is around 0.35 mT at the maximum current intensity of 1 A applied at the coil of the MR clutch in the gap where MR fluid is available in the clutch.

The MR clutch was tested on a test rig. The test rig serves for experimental investigation of different MR brakes and MR clutches required for our applications. Different MR fluids available on the market as well as several MR fluids developed and characterised by our laboratory are tested on this test rig. The experimental results have been performed on two directions: the torque measurements and temperature measurements. The total torque representing the torque cumulated from both sides of the MR clutch. The total torque measured on our test rig is around 5.8 Nm being with 33% larger than the value selected at the design. The external and internal temperature measured on the MR clutch help us

to observe the maximum temperature generated by the clutch, which can modify the magnetic properties of the MR fluid. During the measurements, the maximum temperature is registered at the maximum speed difference ($\Delta n = 500$ rpm) inside the MR clutch close to MR fluid and even so not exceeds the threshold temperature of the MR fluid. As a result, the MR clutch designed, built and tested for speed control of the axial rotor accomplishes the initial requirements for torque and temperature operation.

(C-ii) Control Methods for Diminishing the Hydraulic Instabilities in Hydraulic Turbines

Vortex rope dynamics and Timisoara swirl test case

To analyze the decelerated swirling flow from the conical diffuser of hydraulic turbines, can be used a turbine model, [20] and [21] or a surrogate model (swirl generator) [22]; [23]. In our case, a swirl generator, able to mimic the decelerated swirling flow in discharge cone was chosen [24]; [25].

The experimental test rig developed in our laboratory use a swirl generator, which serves to investigate the decelerated swirling flow and different control methods to mitigate the instabilities associated to vortex rope [26]; [27]; [28]. The main part of the entire test rig is the swirl apparatus included in the main hydraulic circuit with two components: swirl generator and the test section. The swirl generator disposed in the cylindrical part of the test section, with an interior diameter of Di =150 mm having three components: the ogive, the guide vane and the free runner. The ogive with four leaned struts helps to sustain the swirl generator and supply the jet. The stationary and rotating components of the swirl generator (guide vane and free runner) generates at the inlet in the conical diffuser a configuration of the flow similar with the corresponding flow downstream the Francis runner operated at partial discharge. The swirl generator ends with a nozzle with Dn = 30 mm located close to the throat section Dt = 100 mm of the conical diffuser. A secondary hydraulic circuit driven by an auxiliary pump supplies the jet through the nozzle. We obtained the cavitating vortex rope using the swirl apparatus presented in Fig. 1 (left). Note that for velocity measurements, the experimental data has done in over pressure conditions given by the measurement requirements. The main and secondary hydraulic circuits are full filled with water, which means no air volume is trapped inside. That is, why the density was taken constantly and equal with the water density value.

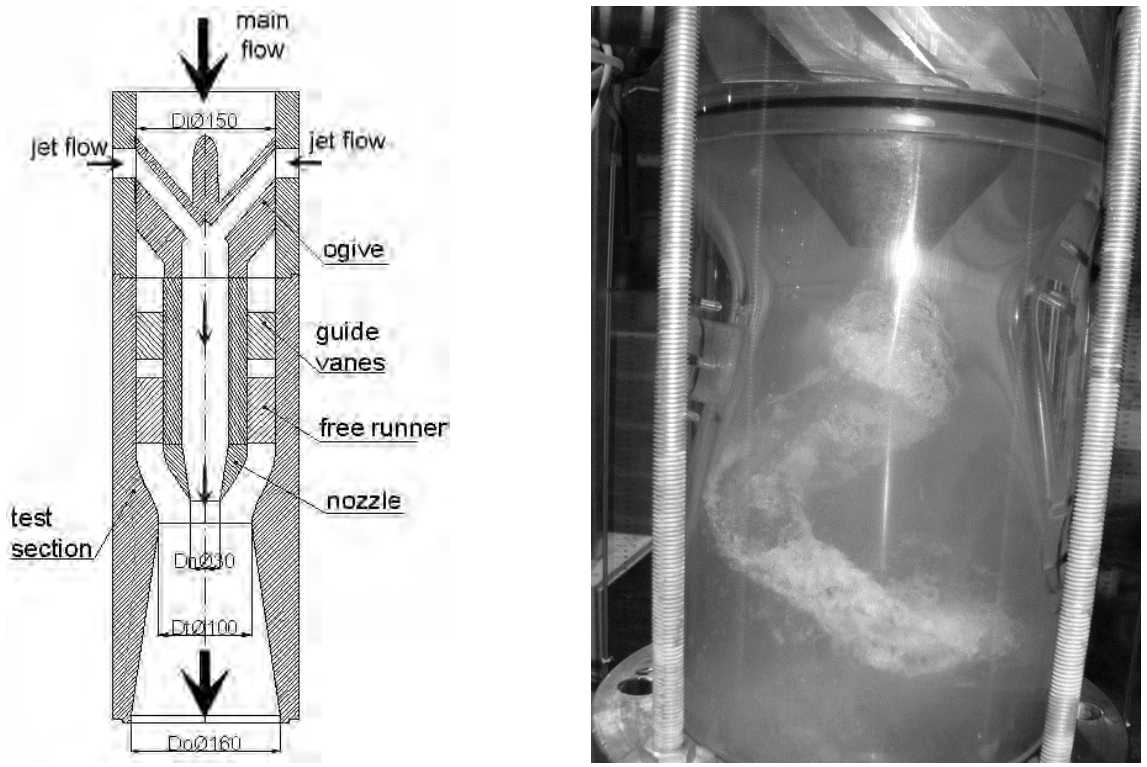

Figure 20. Schematic view of the swirl apparatus and test section from the experimental test rig (left) and visualisation of the cavitating vortex rope in the discharge cone of the test section (right), **[29].**

Reynolds' number of 3.8 x 10^5 corresponds to our investigation on the test rig, taking into account the main discharge of Q~30 l/s in the throat section with Dt = 100 mm. Experimental investigations have been performed with a water temperature distribution from 20°C to 25°C during each campaign. According to the above sentence, it is unnecessary to use a cooling system because the water volume from the rig is enough (~ 4 m^3). This is important to have negligible uncertainties due to temperature variations. To perform reliable measurements, on the test rig was implemented a speed acquisition system for the free runner. This system allows speed data reading of the runner during the measurements. Also, was designed a convergent – divergent test section, to perform velocity measurements [26]. Also, to have a precise measurement of the runner speed, it was implemented an acquisition system. The aluminum runner spins freely under the water flow action (there is no shaft attached to it). The speed acquisition system determines the speed, works in a non-invasive manner, and avoids any holes in the test section wall to keep away from leakage problems. Our solution to achieve these objectives is to sense the runner blades when they pass in front of a sensor. If using every blade (the runner has 10 blades), we can compute several values of speed for 360° rotation. In each aluminum blade was mounted a magnet which generates an impulse each time when is passing in front of the sensor. The magnetic sensor has a measurement accuracy of ±0.5% [30].

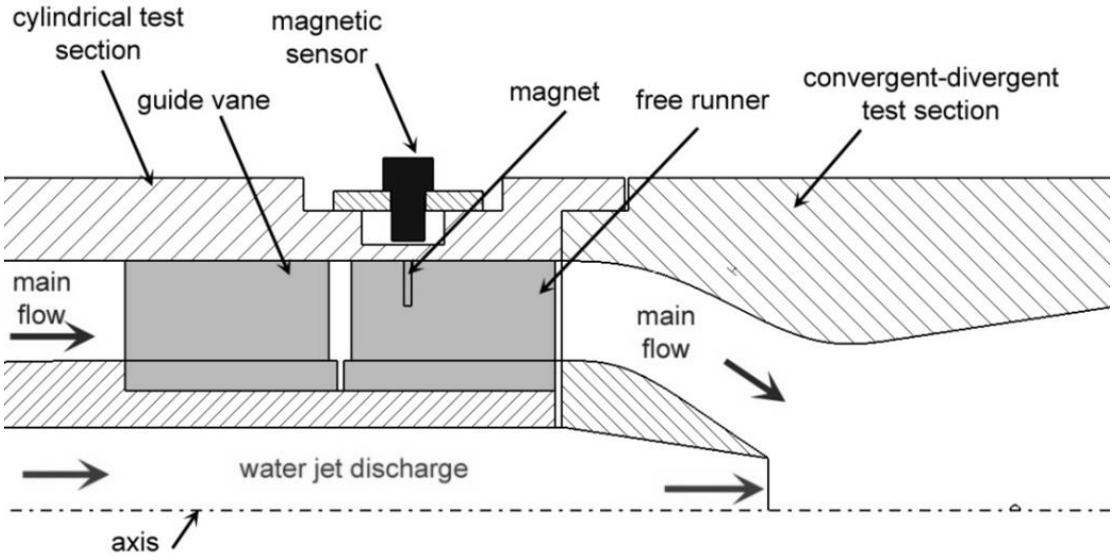

Figure 21. Sketch of the speed sensor mounted in the cylindrical part of the test section.

Having mounted the sensor and the magnets in the runner blades is obtained the dependency between speed of the runner and the main flow rate Q. We analyze the velocity profiles at a main flow rate of ~30 l/sec. The acquisition system for the runner speed allows measuring the time interval between two pulses given by the runner blades. We register at a speed of ~900 rpm at ~30 l/sec - Figure 22. In addition, from the linear fit of the measured points, we observed that the runner spins at a flow rate by 1 l/sec. This delay is due to the friction between the shaft and the Teflon bearing of the free runner.

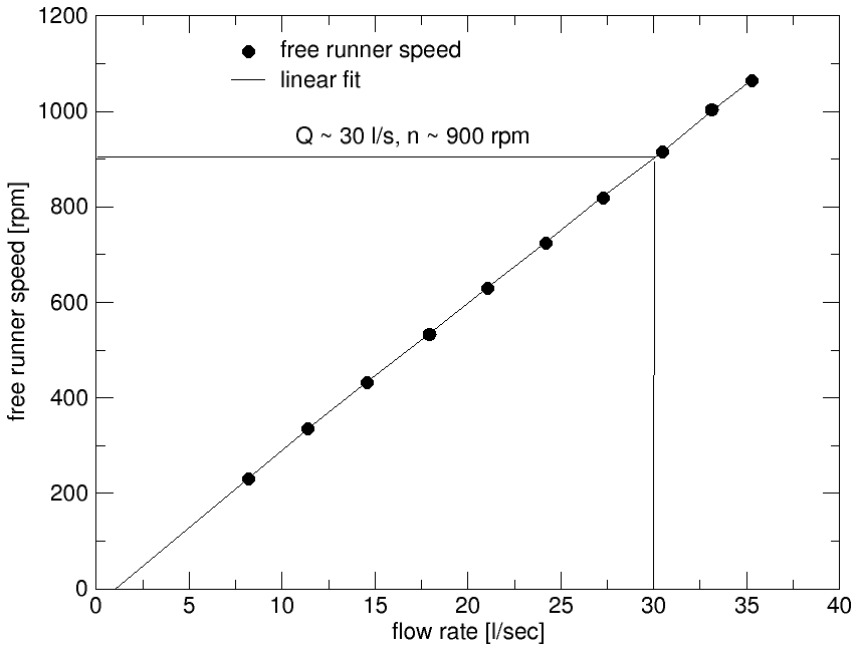

Figure 22. Speed of the free runner vs. main flow rate Q.

To perform velocity measurements, a convergent – divergent test section was designed. The first experimental test section was used only for measuring the pressure pulsations at the cone wall,

[31], [32]. The design of the new test section takes into account two conditions. The first condition is that the flow inside should not be influenced by the measuring windows, and a second condition is to mount three survey axes in the areas of interest (the convergent part, inlet and outlet in the divergent part). To check the velocity profile at the inlet of the test section, one surveys axis was installed in the convergent area, where we have only the flow given by the free runner and is not influenced by the swirling flow with vortex rope or water injection. We called the survey axis from the convergent part survey axis W0. The survey axis W0 was mounted in an inflection point where the curvature of the profile is zero. If the profile curvature is zero, it means that the section is a straight-line profile. In this way, placing the survey axis W0 in that area will not influence the flow. The survey axis W0 is perpendicular to the profile section and is mounted at a distance of 70 mm from the inlet test section. Similar to survey axis W0, we called next: survey axis W1 and survey axis W2. The divergent part of the test section is like a straight draft tube cone of a Francis turbine, having a similar angle (8.6°). Survey axis W1 is orthogonal to the interior profile of the test section at the inlet in divergent part and is mounted at 113 mm from the inlet test section. On this axis it is possible to check the flow, which is influenced by the vortex rope and water injection method, respectively. Similar conditions were imposed for survey axis W2, which is situated 168 mm from the inlet of the test section. For each survey axis was mounted an optical window. The optical windows accomplish the following properties: the interior and exterior surfaces are parallel, and the refraction index is equal to 1. A sketch of the test section with the optical windows can be observed on Figure 23.

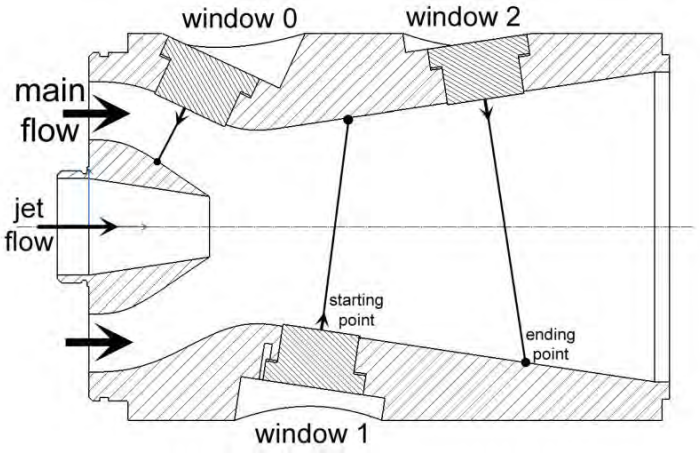

Figure 23. Sketch of the test section with optical windows and corresponding survey axis.

All measurements have the starting point on the wall of the windows and continue survey axis until we reach it on the wall of the test section, as shown in Figure 23.

A Dantec Dynamics LDA with a two-component system was used for experimental measurements. This is a non-contact system, which allows measuring two velocity components without disturbing the probe volume. The LDA system consists of an argon-ion source with 300 mW power and optical fiber that guides the beams to the flow. The main characteristics of the optical systems are the focal length of the probe 159.6 mm, beam diameter 2.2 mm and beam spacing 39.2

mm. Two pairs of beams with a wavelength of 488 nm and 514.5 nm are generated, and the probe includes a photomultiplier with an incorporated amplifier. All velocity measurements were acquired in the coincidence mode. A 3D traverse system was used to position the LDA probe on each measuring axis.

We made the measurements with a step size of 1 mm. To reflect the light produced by the laser in the test rig, silver particles were introduced. In addition, the features for experimental measurements were: i) the pressure measured at the manometer mounted on the lower reservoir was by 0.45 bar [27]; therefore, measurements were made over pressure. For, a flow rate of ~30 l/s the speed of the free runner was ~900 rpm, according to Figure 22. ii) the experimental test rig has been aired before and in the water were introduced silver particles required for laser measurements; iii) number of measured particles varies between 5000 and 50000 for each measuring point according to the adjustments and distance of the beams in water. We set the acquisition time at 30 seconds for each measuring point. To avoid vibrations caused by the movement of the traverse system, the measurements were made with a delay of 5 seconds for each point. Another constraint regarding the LDA measurements was to have a minimum number of acquired particles for each period.

According to our phenomenon from the test section, the main frequency varies between 15 Hz and 10 Hz (depending on the flow rate of injected water in the cone). In our measurements a frequency of acquisition was imposed at least 10 times larger than the frequency of the phenomenon. This criterion led us to have acquisition frequencies between 10 and 100 times larger than our frequency phenomenon. Thus, the LDA velocity signal has enough points to perform analyses as Fourier transform or signal reconstruction.

LDA system is an optical measuring system, which measures the scattered light of the seeding particle from the flow. The main condition to have a precise measurement is that the seeding particle follows the flow. When choosing particles for these measurements, we must consider the material from which the particles are made. In our case, we tested two types of particles: hollow glass spheres and silver-coated hollow glass spheres. The diameter of the hollow glass particles is 10 μm, with a density of 1,1 g/cm3. The diameter of the silver-coated hollow glass particles is also 10 μm, with a density by 1.4 g/cm3. In addition, the errors produced by these two types of seeding particles are identical.

For experimental measurements, we chose silver-coated hollow glass particles because the refraction of these particles is larger compared with hollow glass particles. In addition, we use special requirements for optical windows. They have flat parallel faces to enable a clear focal point for all laser beams.

The measurements have total uncertainty given by two components: random (precision) and systematic (bias) errors [33]. With velocity measurements, the random errors are larger than systematic errors, which are neglected. The velocity bias and system noise errors may be on the same

order of magnitude as precision errors. Repeatability of the measurements can estimate the random errors for the same survey axis maintaining the same operating conditions. The magnitude difference for repeated measurement points were calculated for each variable and the variance was determined from all replicated points. The overall calculated random error considers the average of all individual standard deviations. The estimated errors of the velocity profiles have a value between ±0.003 m/s and ±0.004 m/s. To calculate the bias velocity uncertainty is used the following formula, [34]:

$$v_b = \sqrt{\left(\overline{u} - \frac{1}{n}\sum_{i=1}^{n} u_i\right)^2} \quad (2)$$

where, $\overline{u}$ is the mean velocity for each volume probe; u_i is the measured velocity for each particle that passes the volume probe and n represent the sample number. The estimated bias for meridian velocity component has a value of 0.01 m/s, while for the circumferential one it was 0.005 m/s.

The first results, supposed to investigate the mean velocity field for swirling flow with vortex rope and swirling flow with the water jet method at different flow rates. All data measurements are in dimensionless form and for a main flow rate of ~30 l/s. The corresponding graphs for mean velocity profiles contain the length of the survey axis divided at the throat radius of the test and measured velocities divided at throat velocity. We chose the flow rates for the water jet to cover the partial water injection, the critical threshold jet and full water injection regimes, [1]. Four cases of water injection: 5%, 7%, 10% and 13% jet flow discharge from the main discharge were investigated. Figure 24 present the corresponding velocity profiles for the case of swirling flow with vortex rope and swirling flow with water injection for survey axis W1.

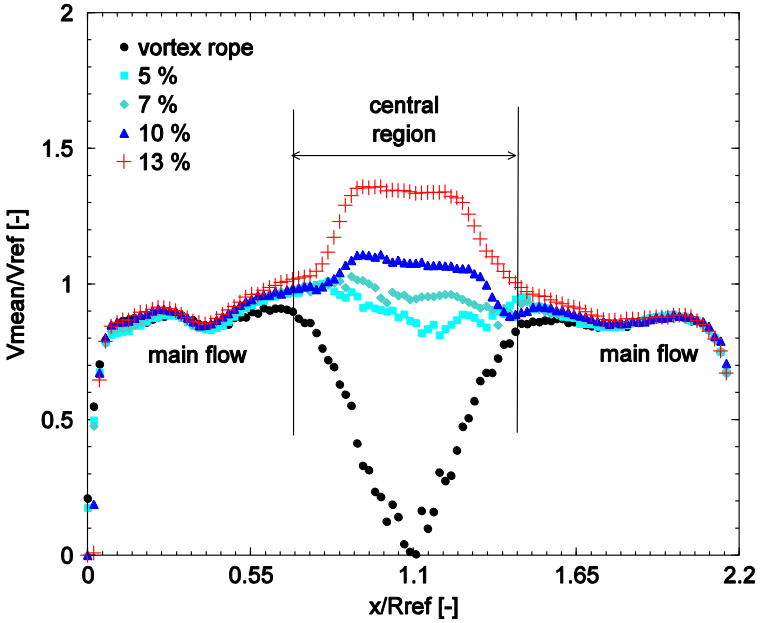

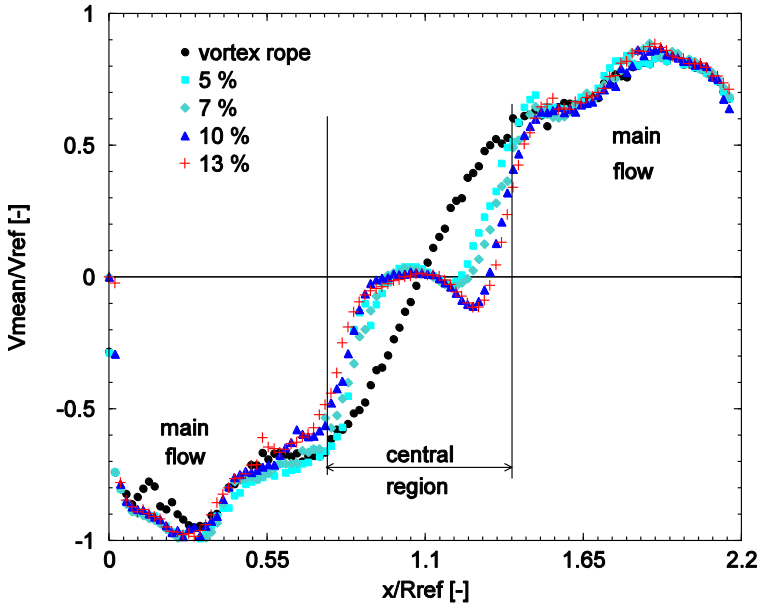

Figure 24. Meridian (up) and circumferential (down) velocity profiles for swirling flow with vortex rope at 4 flow rates of water injection, for survey axis W1.

In the case of window W2 (near to the outlet of the test section), the meridian velocity profile has a deficit of velocity close to the middle of survey axis, the main flow being pushed to the wall of the conical diffuser. When water is injected, the meridian velocity decreases close to the wall of the test section, with over 20%. This decrease corresponds to an increase in pressure recovery coefficient, having as a consequence a good conversion of energy in the cone. When the jet reaches at a discharge of 13% from the main discharge, the meridian velocity deficit from the middle of the cone is converted into a velocity excess near to the center axis. Between the center axis and the wall of the cone remains a velocity deficit area, which is uniform and does not produce pressure or velocity fluctuations.

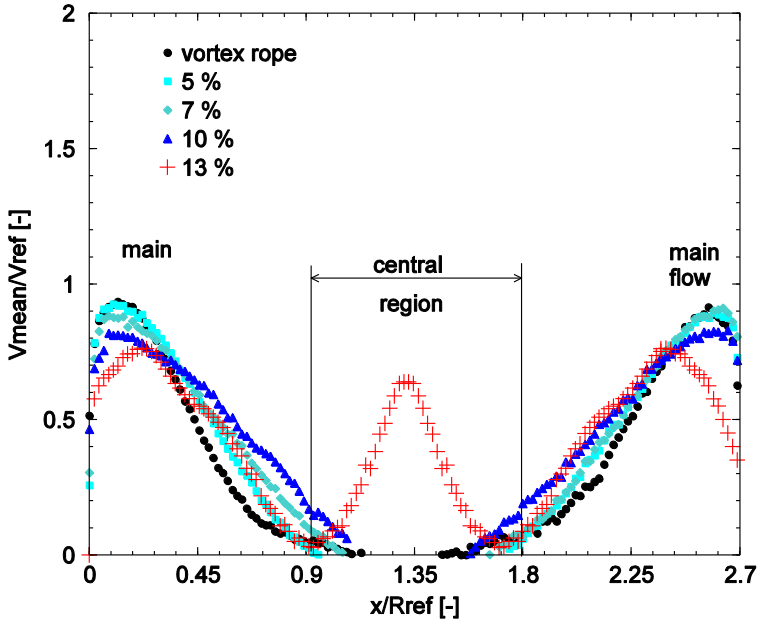

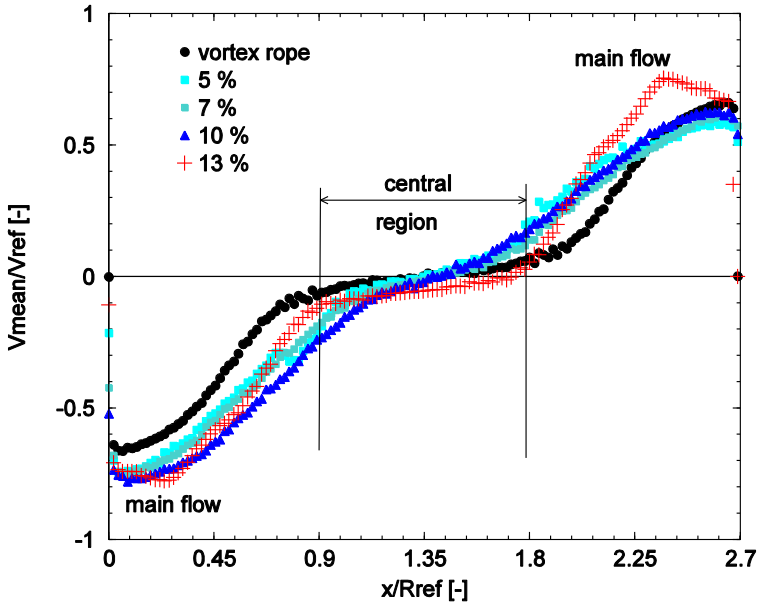

Figure 25. Meridian (up) and circumferential (down) velocity profiles for swirling flow with vortex rope at 4 flow rates with water injection for survey axis W2

Another analysis that involves the flow behaviour refers to RMS variations. This variation analysis is important to determine where, on the survey axis, the velocity fluctuations are higher or smaller.

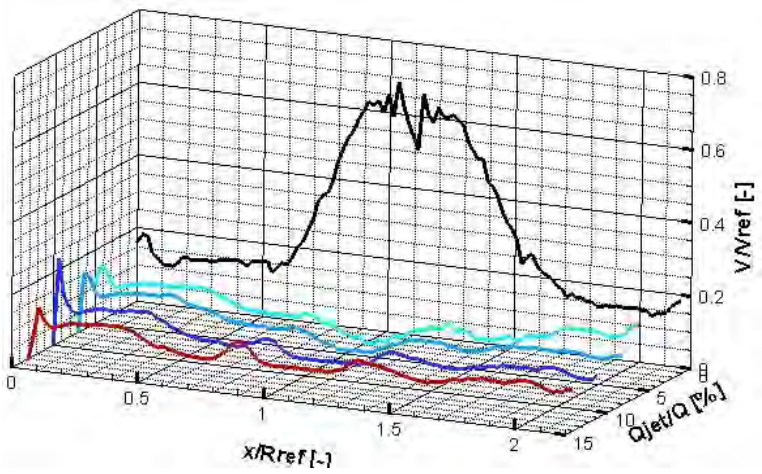

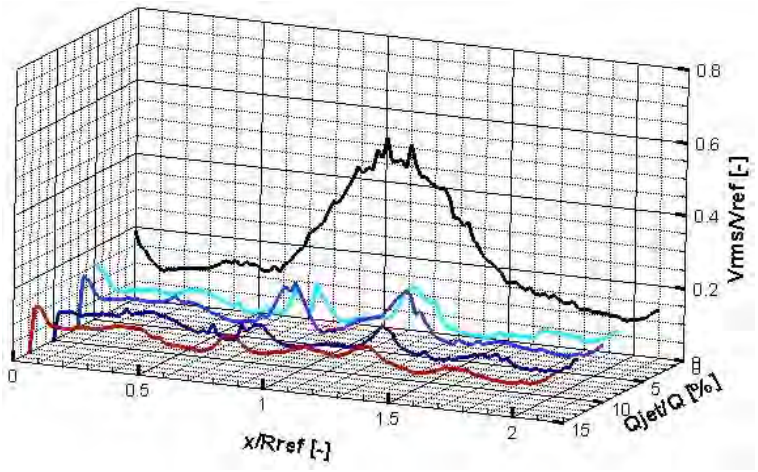

Figure 26. Variation of RMS for meridian (up) and circumferential (down) velocity profiles for swirling flow with vortex rope at 4 flow rates with water injection for survey axis W1.

In Figure 26 can be observed, for both velocity profiles, the variation of RMS is larger closer to the center axis. Close to the wall (extremities) the velocity fluctuations are small (in this area the main flow is concentrated), while in the center, the flow has large variations. When water is injected, the decrease of velocity fluctuations in all regions occurs. Because the survey axis is near to the inlet in the conical diffuser, the amount of discharge for water injection should not exceed 10% from the main discharge. However, the velocity fluctuations still exist in the cone, and it is necessary to look at the outlet of the test section (survey axis W2), to observe if the flow unsteadiness still exists.

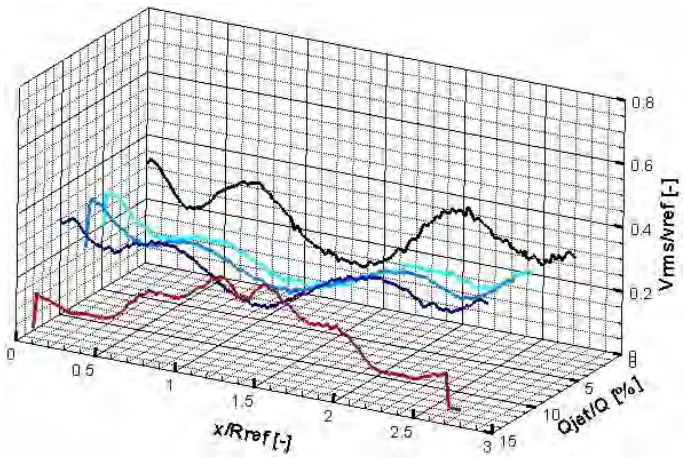

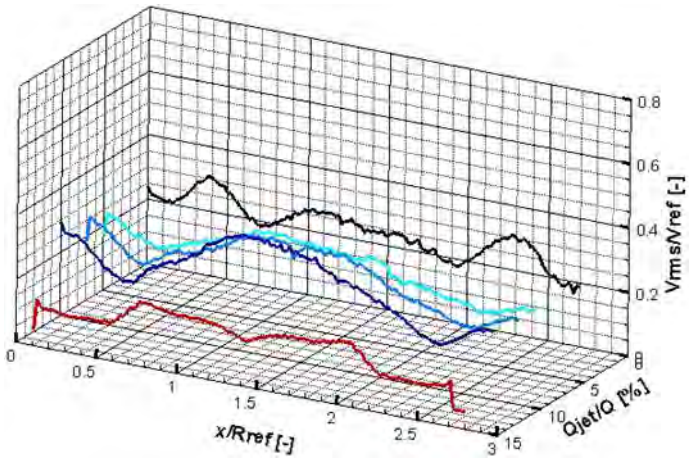

Figure 27. Variation of RMS for meridian (up) and circumferential (down) velocity profiles for swirling flow with vortex rope at 4 flow rates with water injection for survey axis W2.

For survey axis W2 at the outlet of the conical diffuser, a large variation for both velocity components occurs. In the case of meridian component, the variation of RMS decreases by over 60% close to the wall when the water injection occurs and has an increase in the center of the cone with 40%. The increase occurs because of the water jet supply in the center of the cone. In the case of circumferential velocity profile, the fluctuations reveal the fact that once the water is injected, at partial water discharge the vortex rope is pushed down in the cone leading to an increase of fluctuations by 5% - 20% in the center of the cone. Once the critical threshold jet passes, the velocity fluctuations are diminished with over 20% - 60% depending on the areas from the cone. At the full discharge water jet, the velocity fluctuations have almost a linear variation along the length of the cone.

The unsteady velocity field analysis using phase-average

This paragraph comprises an analysis of the unsteady velocity field from the convergent-divergent test section using phase-average. By using the phase-average analysis it is envisaged the reconstruction of the unsteady velocity field, the highlighting, evolution and behaviour of the vortex rope at different flow rates of the jet. The phase-average analysis starts from the measured components of the velocity:

$$u_i = \overline{u} + \hat{u} + u'_i \tag{3}$$

where, u_i is the instantaneous velocity measured with LDA which can be divided in three components $\overline{u}$ (mean velocity of the signal), $\hat{u}$ (time varying periodic part) and u_i' (turbulent fluctuation). From this (4), the phase-average velocity it is defines as:

$$\widehat{u} = \overline{u} + \hat{u} \tag{4}$$

We performed the measurements in phase with a reference signal. Having the velocity signal and a reference signal, were reconstructed the bins or phase intervals of the velocity signal. The

associated software for LDA post-processing data allows the number of bins and the width of each bin. In our case, we used 360 angle bins with a width of 2°.

To determine accurately the RMS for each bin, width of the bin must be as small as possible, with the condition that in each bin to have enough measured particles (in our case over 100 acquired particles). To have an analysis of phase average velocity depending by width of the bins, we initially tested a bin width of 1°, 2° and 3° with 360, 180 and 120 bins respectively for whole circumference. We reach a conclusion that increasing the bin width and decreasing the bins, the variation of phase average velocity is large, having also higher fluctuations of RMS. First, the reference signal for the phase average measurements chose the signal from the blades of the rotating runner. Having implemented the measuring system of the runner speed, the signal was used to generate the reference signal for the phase-average measurements.

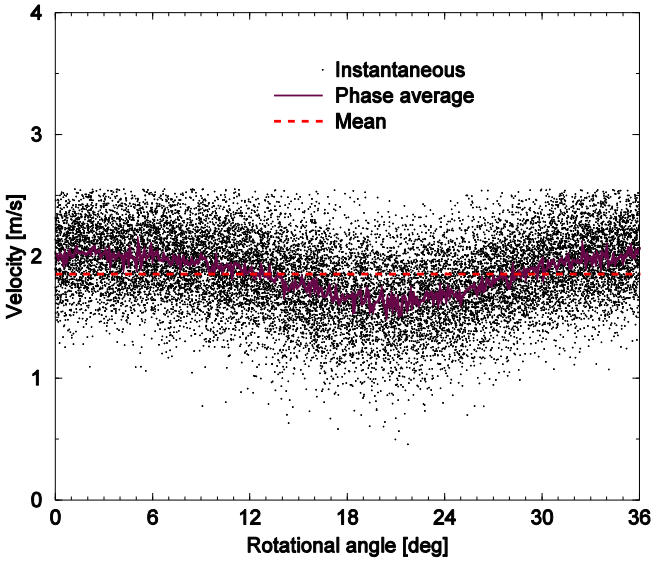

Figure 28. Decomposition of velocity for an inter-blade channel of the runner.

The runner blades signal was used to measure only the velocity profiles from the convergent part of the test section. Because the reference signal is given by each blade of the runner, we can reconstruct only an inter-blade channel, the rest of the channels being multiplied with the number of the blades. For each point from the survey axis was reconstructed with phase-average the velocity field from an inter-blade channel as shown in Figure 29.

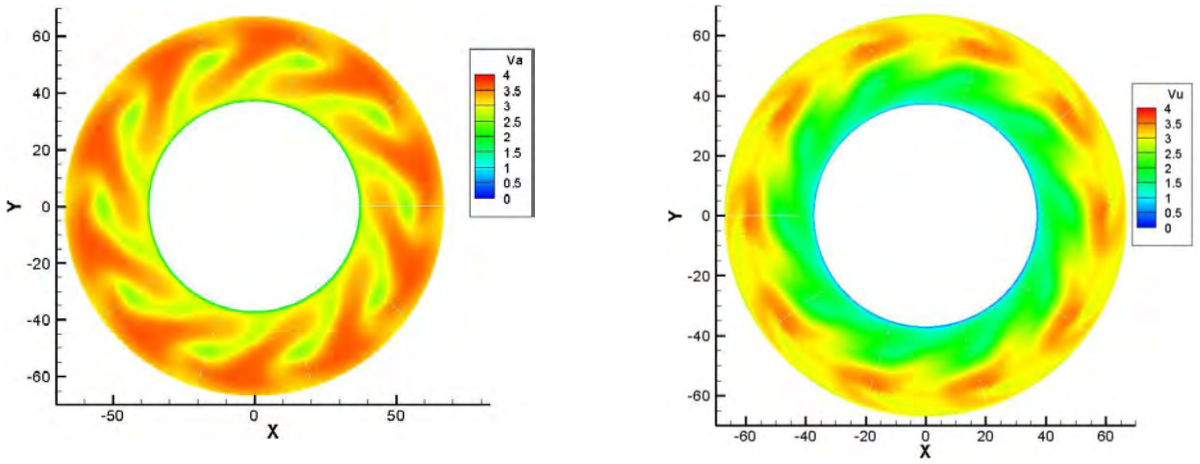

Figure 29. Phase-average meridian and circumferential velocity for window W0.

Figure 29 shows the influence of the free runner in both velocity fields (meridian and circumferential velocity fields). In the case of meridian velocity, the excess of the velocity close to the periphery and the weak from the blades occurs. For circumferential velocity, the influence of the blades is smaller comparing with the meridian one and an excess of velocity is observed near to periphery while near to the hub, the velocity has a uniform variation. In that way, the purpose of the runner is achieved, to spin freely with zero moment. It is mentioned that the water injection does not influence the velocity field in the case of this survey axis W0.

For the investigations of the flow in the divergent part of the test section, as a reference signal we chose it the pressure signal from the throat of the test section. To generate a digital signal, the pressure signal from the sensor (mounted at the inlet in the divergent part of the test section, PT1), passed a TTL generator. After it, passed a Band-Pass filter to cut the higher frequencies from the signal.

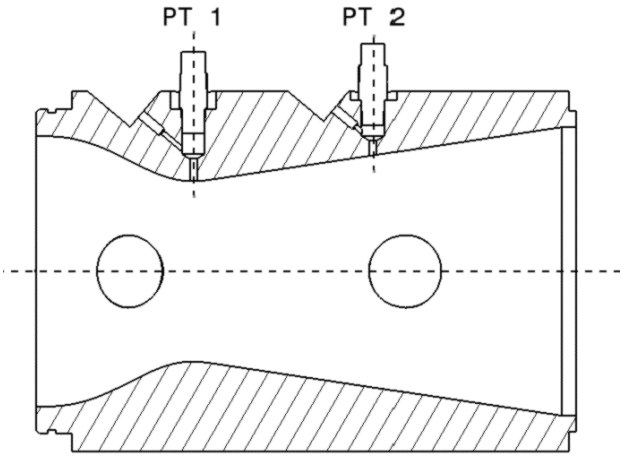

Figure 30. Pressure sensors implemented on the test section. PT1 is used as reference signal for phase-average.

In this way, the pressure signal it is transformed into a digital signal with identical frequency as the flow phenomenon from the test section. The original measured signal has almost a sinusoidal shape being influenced by the flow from the conical diffuser. The pressure sensor used to generate the reference signal has higher accuracy (0-2 bar range with a maximum measuring frequency by 10 kHz and an accuracy by 0.1%), being especially designed for these applications. To reconstruct the velocity field with phase-average, it is used only the first part from the survey axis up to the symmetry axis. The reconstruction starts from the wall of the measuring window and continues until the survey axis meets the symmetry axis of the test section.

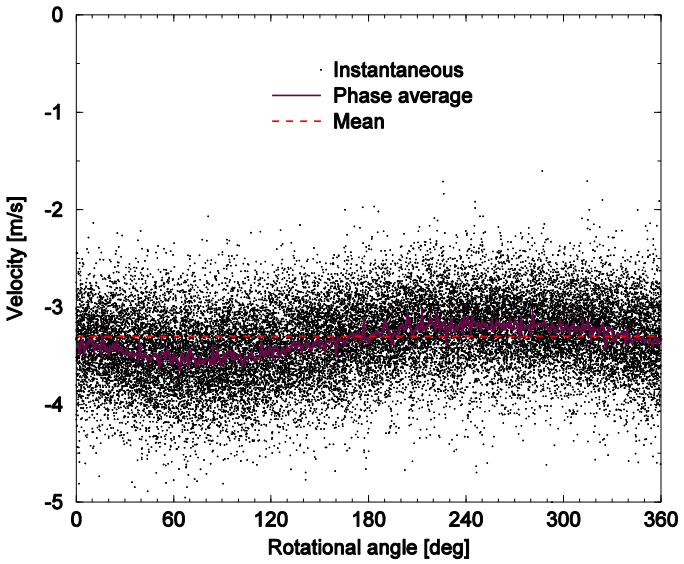

Figure 31. Velocity field decomposition in the divergent part of the test section.

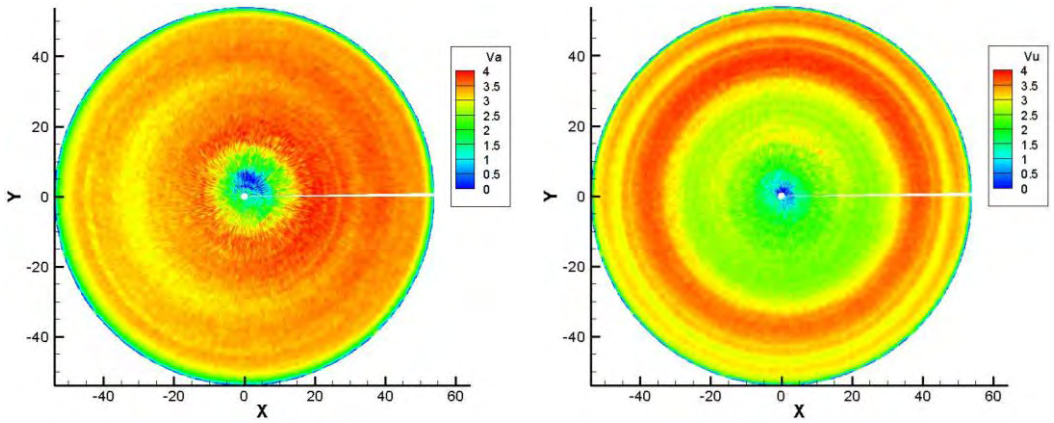

Figure 32. Phase-average meridian (left) and circumferential (right) velocity on window W1 for swirling flow with vortex rope.

For swirling flow with vortex, rope Figure 32, in instantaneous meridian velocity field, is observed the deficit of velocity near to the axis and an eccentric quasi-stagnant region. Also, in the middle of the survey axis, the velocity has an excess on one side and on the opposite side has a deficit. In the case of circumferential velocity profile, the velocity field is symmetrical. Compared with the

meridian component, when the velocity field has a smooth transition from the center to the periphery, in the case of circumferential one, the velocity has a sudden transition from the center area where there is a deficit to the periphery area, where there is an excess of velocity. After investigations of swirling flow with vortex rope, the next step was to analyze the velocity field when water injection method is used. The minimum flow jet discharge, which was investigated, is 5% of the main discharge.

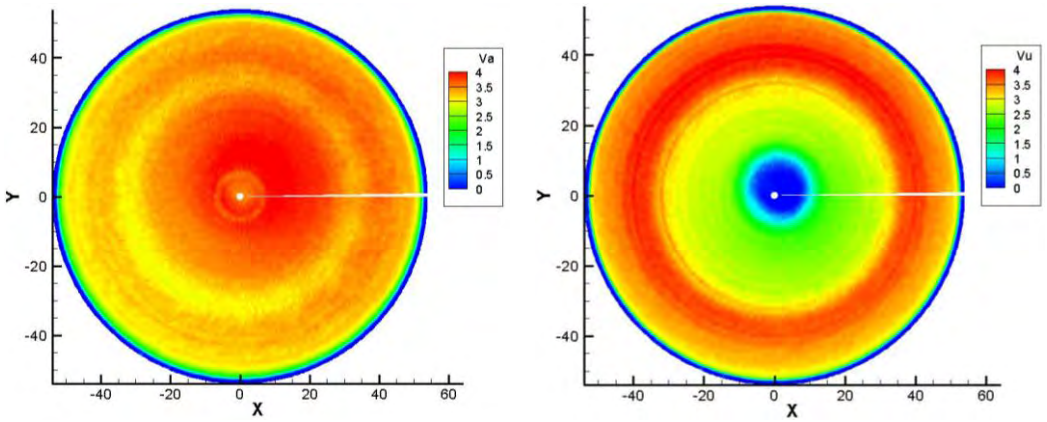

Figure 33. Phase-average meridian (left) and circumferential (right) velocity on window W1 for swirling flow with 5% water jet discharge.

From Figure 33 in the case of meridian velocity field, the water injection method at 5% jet discharge eliminates the velocity deficit from the center of the cone. Because the water jet, which is introduced, has only an axial component, the circumferential velocity field has zero value in the cone center and is eccentric because of the non-uniformity of the velocity field from the cone which is strong enough to shift the water jet.

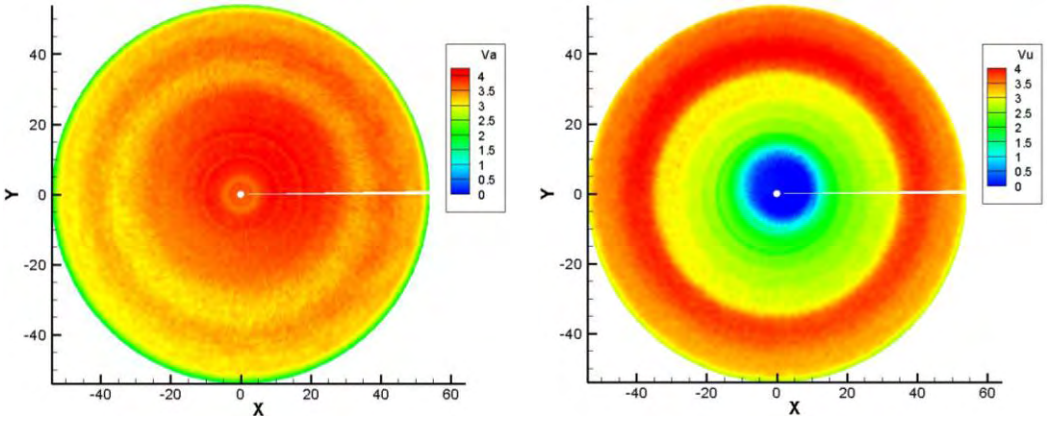

Figure 34. Phase-average meridian (left) and circumferential (right) velocity on window W1 for swirling flow with 7% water jet discharge.

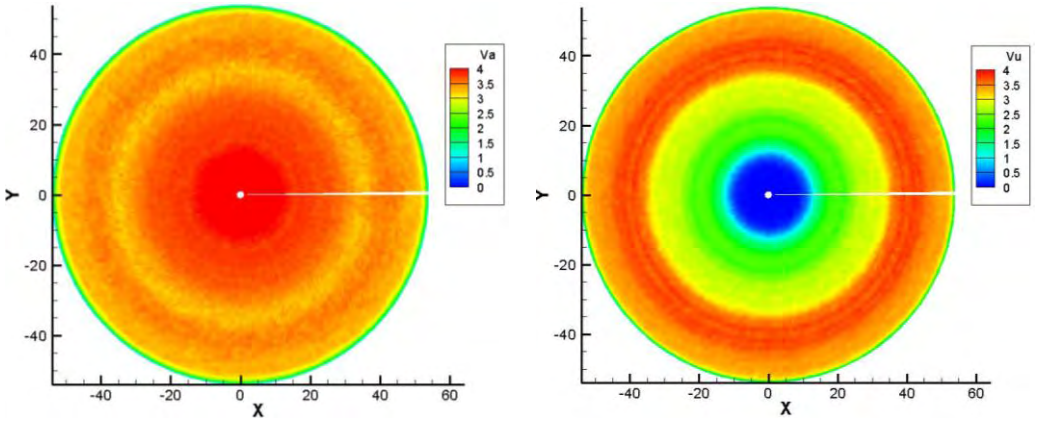

Figure 35. Phase-average meridian (left) and circumferential (right) velocity on window W1 for swirling flow with 10% water jet discharge

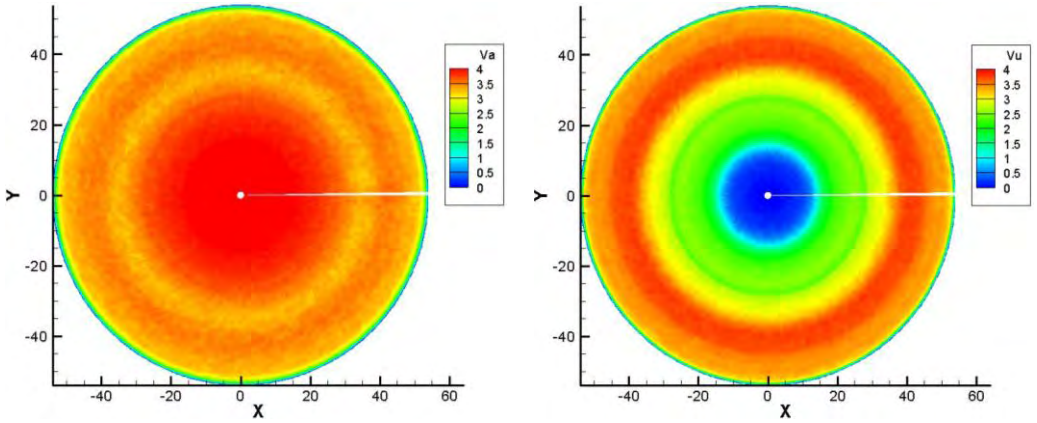

Figure 36. Phase-average meridian (left) and circumferential (right) velocity on window W1 for swirling flow with 13% water jet discharge.

When a 7% discharge of water is injected, the meridian velocity field starts to look symmetrically in the center of the cone because of the axial component of the water jet, while at the periphery the non-uniformity is almost eliminated. In circumferential velocity field, the water jet remains eccentrically, the swirling flow from the cone having enough strength to shift the water jet. When 10% discharge water is injected, in both velocity fields the influence of the vortex rope is insignificant. The flow is periodic and the influence of the water jet in both cases is important. For the full water injection (13% flow discharge), the velocity field is similar with 10% water injection. This analysis reveals that on this survey axis, near to the inlet of the divergent part of the cone, 10% water jet discharge is enough to eliminate the flow instabilities. Anyway, it is important to analyze survey axis W2, near to the outlet of the divergent part, to note if the vortex rope is mitigated for the same discharge flow rates as on survey axis W1.

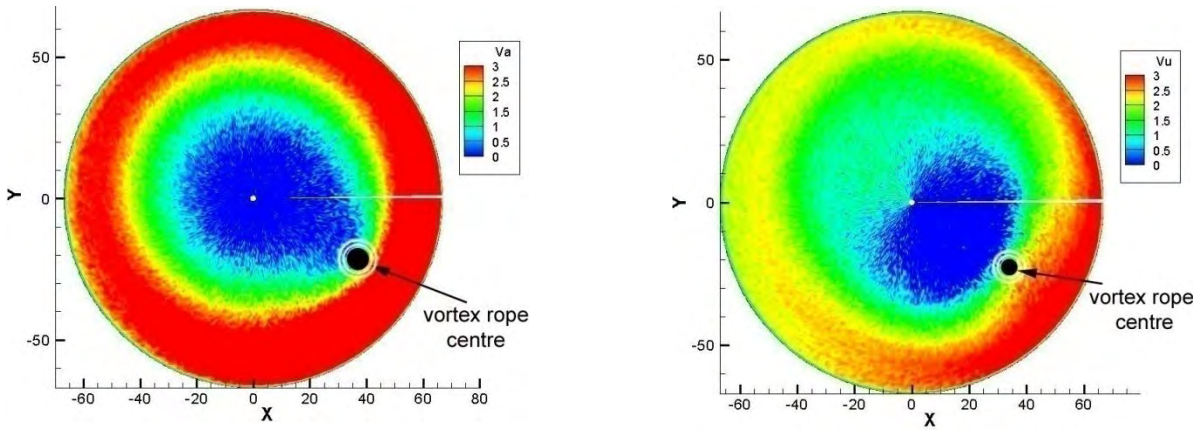

Figure 37. Phase-average meridian (left) and circumferential (right) velocity on window W2 for swirling flow with vortex rope.

For the corresponding survey axis W2, from the test section outlet, the influence of the vortex rope in the flow is important. In the case of meridian velocity is observed the quasi-stagnant region, which is developed in the middle of the cone. The influence of the vortex rope is observed also in the circumferential velocity profile, where the quasi-stagnant region is displaced from the center.

In addition, the velocity fluctuations (in Figure 27), confirm once again that the precessing vortex rope, which rotates around the quasi-stagnant region, gives the velocity unsteadiness. According to [33] the center of the vortex rope is found by analyzing the high and low velocity regions. Between these two regions, the vortex rope occurs.

When 5% water injection is used, in the meridian velocity field is observed that the quasi-stagnant region decreases, while the vortex rope is mitigated. In the case of circumferential velocity, the quasi-stagnant region diminishes and the flow near to the wall has a similar shape in all circumferences of the cone.

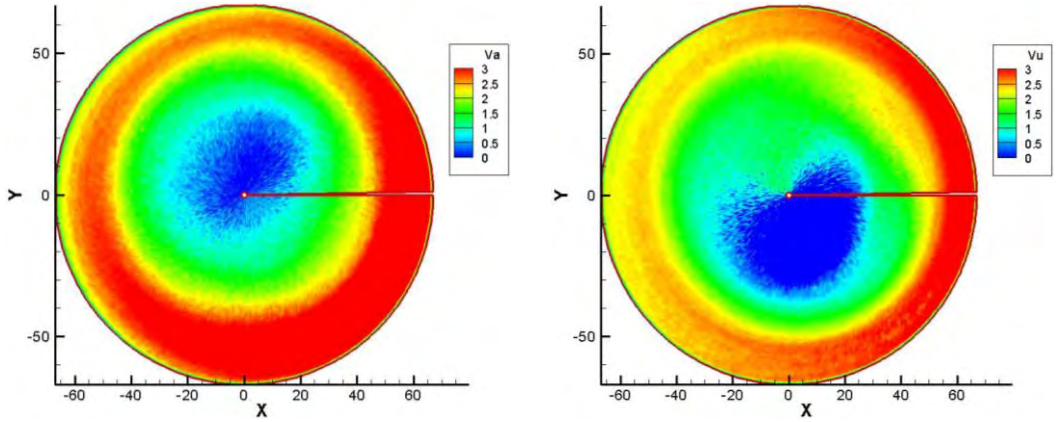

Figure 38. Phase-average meridian (left) and circumferential (right) velocity on window W2 for swirling flow with 7% water injection.

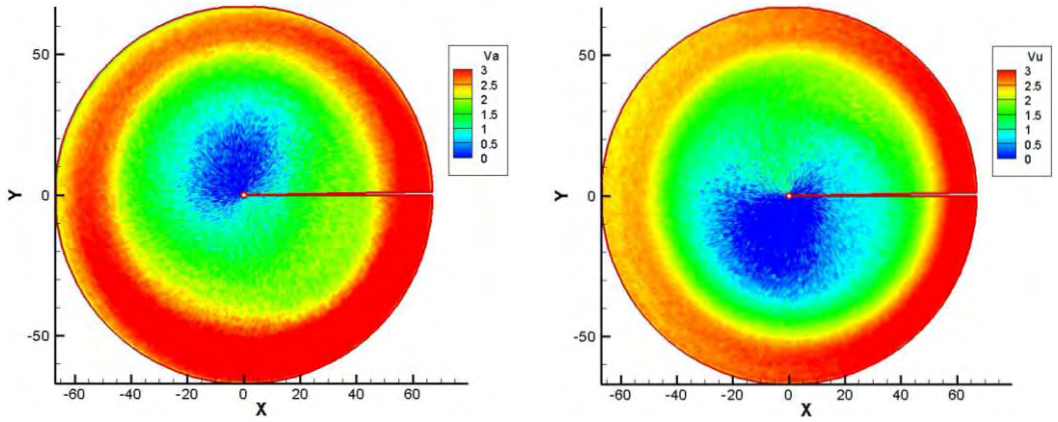

Figure 39. Phase-average meridian (left) and circumferential (right) velocity on window W2 for swirling flow with 10% water injection.

When 7% of water flow is injected for both velocity components, the quasi-stagnant region is mitigated, and the tendency is to be moved to the center of the cone. At 10% water injection in the case of meridian velocity, the quasi-stagnant region is mitigated with over 60% against the case of swirling flow with vortex rope and remain displaced from the center axis of the cone. The quasi-stagnant region in the case of circumferential velocity is mitigated with ~20% and is displaced to the center of the cone. Near to cone wall, the flow has a uniform distribution but still is influenced by the quasi-stagnant region. When the water jet discharge passes the critical threshold, the flow near the outlet of the test section is changed in comparison with the flow with the vortex rope. For the meridian velocity component, we observe four different zones in the flow field. Near to the wall is an excess of velocity, followed by a flow of medium velocity. Also, in the center of the cone is observed an excess of velocity followed by the quasi-stagnant region. All these areas have a uniform distribution in the cone. The water jet gives excess velocity from the center of the cone, while the main flow is concentrated near the cone wall. Anyway, the jet at this flow discharge can diminish completely the flow unsteadiness from the cone. In the case of the circumferential velocity profile, we distinguish three main zones. Near to the wall, an area with an excess of velocity corresponding to main flow, a velocity deficit area corresponding to the center of the cone and a transition area with a medium velocity. The velocity deficit area shows once again that the water jet has only an axial component, while the circumferential component is negligible.

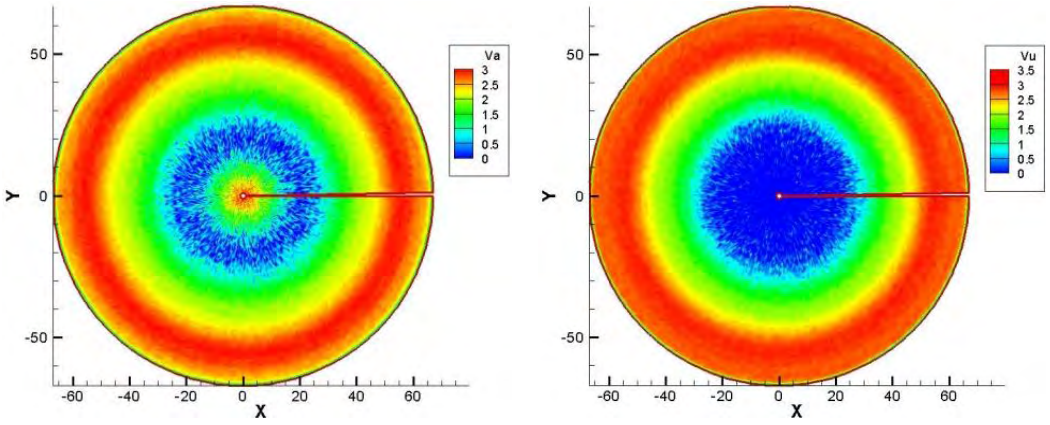

Figure 40. Phase-average meridian (left) and circumferential (right) velocity on window W2 for swirling flow with 13% water injection.

From the phase-average analysis of unsteady velocity field, it is clear that the flow behavior has changed from a swirling flow in an axial flow since the water injection occurs. In addition, all the negative effects produced by vortex rope as vibrations, noise, cracks of runner blades, are eliminated.

This study was continuing the work on the swirling flow control, using the water jet injection method in the conical diffuser of hydraulic turbines. In that way, LDA measurements and data signals processing have been done. We dedicate the first part of the paper to the test rig, whose main component is the test section and swirl generator, respectively. The test section with a convergent-divergent shape and 8.6° is similar to a real conical diffuser from Francis turbines. The cylindrical part of the test section which is mounted upstream the convergent-divergent part, has implemented a magnetic sensor for runner speed measurements. This was necessary to achieve runner speed. Also, three optical windows, each with measuring survey axis (W0 in the convergent part, W1, W2 at the inlet and outlet of the divergent part, respectively), are implemented on the test section. The purpose of the swirl apparatus is to generate a flow like the one from real Francis turbines, which operates at part load. The first results show that the vortex rope is obtained for a runner speed of ~900 rpm and a flow discharge of ~30 l/s. We dedicate the second part of the paper to the LDA measurements, of the swirling flow control method using water jet. LDA measurements of averaged velocity profiles and qualitative part of phase-average with and without water jet is analyzed in detail.

The main points are:

- The mean meridian velocity profiles for different water jet discharges show that the quasi-stagnant region associated with the vortex rope are mitigated since 7-10% water jet injection from the main discharge.

In addition, when the water jet occurs, the circumferential velocity in quasi-stagnant region is almost zero, given because the flow has only the axial component while we neglect the circumferential one. This analysis is reinforced by the RMS variation, which decreases when the water jet is introduced.

- For survey axis W0, the phase-average analysis shows an excess of meridian velocity near to periphery and a deficit to the hub. In that way, we achieve the purpose of the runner to spin freely with zero moment. We mention that the water injection does not influence the velocity field for this part of the test section.

- The phase-average analysis of swirling flow with vortex rope on the survey axis W1 and W2, reveals a good correlation with the quantitative results of mean velocity profiles. For W1, the vortex rope develops, with a velocity deficit near the center of the axis and an eccentricity corresponding to the quasi-stagnant region. We observe these features for the W2 survey axis. The quasi-stagnant region occupies an important area of the cone. We also observe the influence of the vortex rope in the circumferential velocity profile, where the quasi-stagnant region is displaced from the center. In addition, the center of the vortex rope is found by analyzing the high and low velocity regions.

- When the water jet is introduced, from 5% to 10%, the quasi-stagnant region is mitigated for both survey axis, even eliminated when the water jet achieves 13% from the main discharge.

To conclude, we can mitigate the swirling flow with vortex rope with the associated pressure and velocity fluctuations, using the axially water jet control method. The results presented above show the correct operation of this new method, which can change the flow behavior when the turbines operate at part load conditions.

Speed control with MR brake of the swirl generator free runner

A magneto-rheological brake (MRB) system was designed and installed to control the runner speed. As a result, the runner speed decreased up to 70% using the MRB system providing several swirling flow configurations at the discharge cone inlet covering a wide range (from part load to full load conditions).

The dimensionless flux of moment of momentum distribution versus dimensionless discharge was computed for several runner speed values based on experimental data, see Figure 41 (right). The same distribution is obtained for FLINDT Francis turbine proving the same behavior for the swirl generator [35]. The dimensionless discharge q is determined using the following formula:

$$q = \frac{Q}{\omega \cdot \pi \cdot R_{ref}^3}, Q = \int_A \vec{V} \cdot \vec{n} dA \quad (5)$$

where, is radial speed of the runner, R_{ref} is runner radius, represent the velocity vector and normal unit vector. The dimensionless flux of momentum was computed using the (6):

$$m_2 = \frac{M}{(\omega \cdot R_{ref})^3 \cdot \pi \cdot R_{ref}^2}, M = \int_A (U \cdot V_u) \vec{V} \cdot \vec{n} dA \quad (6)$$

where M is the dimensional flux of momentum, being determined just downstream of the runner based on LDV data, A is the cross section, V_u is the tangential velocity and U is the transport

velocity. As is observed in Figure 41 (right), at a runner speed value around 600 rpm the dimensionless flux of momentum has a vanishing value which from operating point of view, the runner works close to BEP. Four regimes corresponding to runner speed values of 925 rpm, 840 rpm, 800 rpm and 700 rpm are associated to the partial operating conditions with a positive m_2. When the runner slows down to more than 600 rpm, the m_2 starts to have an inverse value, which means that the runner starts to act as a hydraulic turbine operating at full load operation.

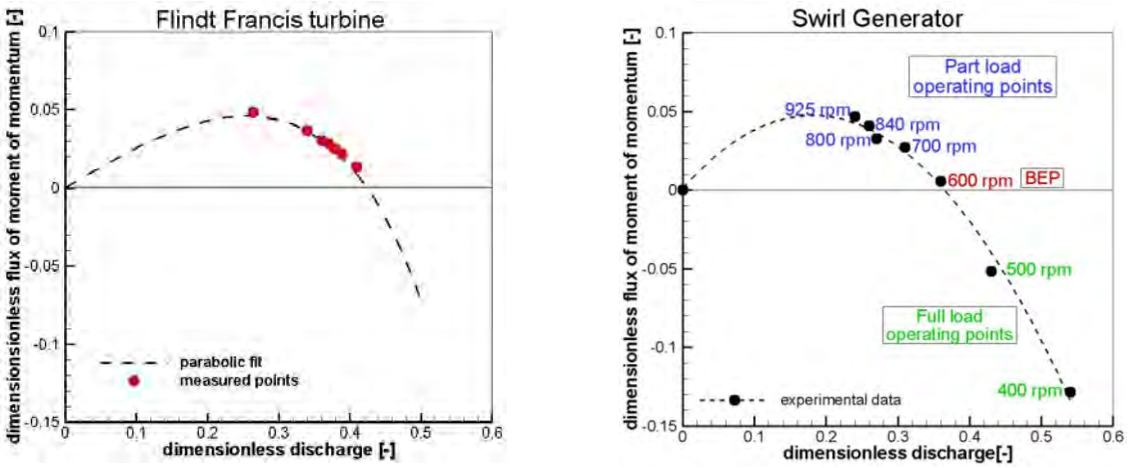

Figure 41. Dimensionless flux of moment of momentum calculated for FLINDT Francis turbine (left) and dimensionless flux of moment of momentum calculated for our swirl generator (right)

The intermediate values for runner speed and corresponding dimensionless discharge are presented in the next table.

Table 10. Runner speeds and corresponding operating regimes.

Runner speed *n* [rpm]	925	840	800	700	600	500	400
Operating regimes depending by m_2	positive $m_2>0$	positive $m_2>0$	positive $m_2>0$	positive $m_2>0$	vanishing $m_2\sim0$	negative $m_2<0$	negative $m_2<0$
Dimensionless discharge *q* [-]	0.23	0.248	0.27	0.309	0.36	0.342	0.54
Discharge coefficient with respect to BEP value [-]	0.7 (part load)	0.74 (part load)	0.75 (part load)	0.86 (part load)	1 (BEP)	1.19 (full load)	1.5 (full load)

As previously stated, the speed of the runner is reduced using an MRB system. This solution was chosen because it has some advantages as: small and robust, no mechanical parts, fast response time in order to control and low power consuming. In our case all the system was specially designed, because it was adapted to our geometric constraints and we benefit from the experience of Magneto-Rheological Laboratory in our department. As a working principle, magneto-rheological (MR) fluid is mounted between a rotating and a fixed piece. When a magnetic field (usually generated by a coil) passes, the MR fluid changes viscosity. Depending on the intensity of the magnetic field the viscosity is changing which makes the rotating part reduce the speed. A sketch with the MRB system and assembled components are presented in Figure 42.

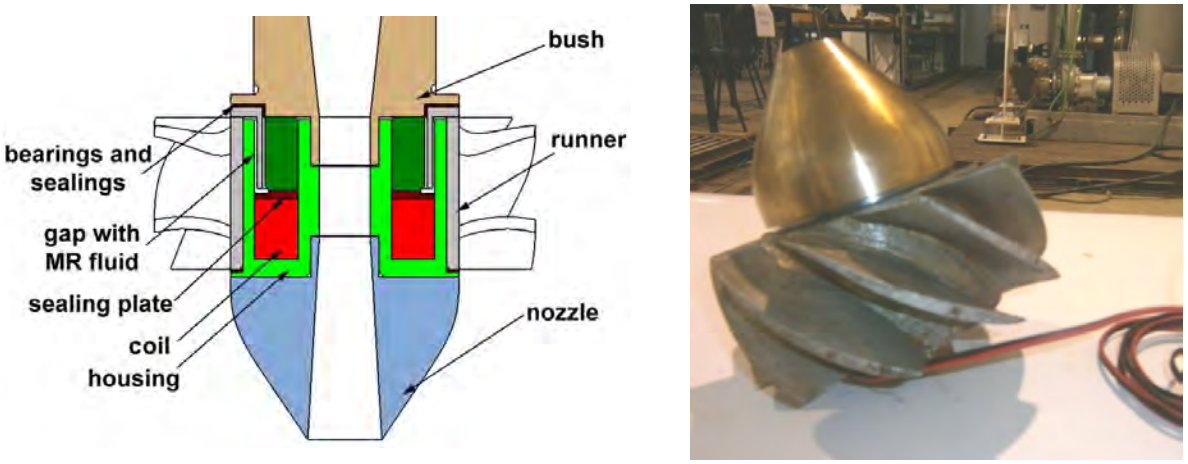

Figure 42. Sketch of the MRB system (left) and picture with mounted pieces (right), [36]

The runner was manufactured so that to be mounted the MRB system. The MRB system consists in iron housing, a coil, seals and bearings and the MR fluid. The housing is made of iron and was designed in order to close the magnetic field in the area where MR fluid is mounted. The coil is made by cupper wires, and a custom program was used to choose the number of wires and the wire thickness. A series of seals were used to keep the MR fluid separated by water (all system is surrounded by water), also these seals were used as bearings. The most important component by all systems is the MR fluid. We have chosen a MR fluid produced by LORD Corporation (MRF 336 AG). For the MR brake controlling the speed of the runner a quantity of 20 ml of MR fluid was necessary. The gap between rotating and fixed part is 1 mm and time response of the entire system is lower than 0.1 sec. Because the MRB system is working in water, no cooling system is necessary. A DC power supply with a maximum electrical voltage of 30V and a maximum electrical current of 5 A was used to control the magnetic field of the MR brake.

The purpose of this research was to assess the swirling flow from a draft tube cone at different operating regimes. The unsteady pressure measurements are used to analyze dynamic and energetic performances. With mean pressure is calculated the pressure recovery coefficient, the flow from the draft tube cone being analyzed from an energetical point of view. The unsteady pressure is used to

calculate the amplitude, frequency and type of conical diffuser unsteadiness, the flow from the draft tube cone being analysed from dynamically point of view. After the MRB system was installed and tested on the test rig, the pressure test section was mounted in order to perform experimental investigations. The top level located in the test section throat is considered the reference for pressure measurements and was noted L1, according to Figure 43. The rest of levels L2, L3 and L4 correspond to 50, 100 and 150 mm downstream in the draft tube cone, relative to L1. Eight capacitive pressure sensors were installed on the divergent part. Each level contains two opposite pressure sensors, in order to establish that pressure sensors indicate the same static pressure and determine type of unsteadiness from the draft tube cone. They have an accuracy of ±0.13% within a range of ±1 bar relative pressure. A main operating discharge of 30 l/s was used in experiments for all operating regimes. The speed of the runner was reduced from 925 up to 400 rpm, being respected by the regimes presented in Table 10. In order to check repeatability 10 experiments were performed for each regime. Each set corresponds to an acquisition time of 32s at a sampling rate of 256 samples/s.

From experimental investigation, the first analysis is to evaluate the energetic flow behaviour from the draft tube cone from part load regime (corresponding to design speed) up to full load regime (corresponding to lower runner speeds). The pressure recovery coefficient considers mean pressure and is calculated with the following equation:

$$c_p = \frac{\overline{p} - \overline{p}_{L1}}{\rho \cdot \frac{v_t^2}{2}} \tag{7}$$

where c_p is the pressure recovery coefficient, p_{L1} it means the pressure recorded at L1 level, $\overline{p}$ is the measured pressure downstream L1 level, ρ is the water density and v_t the bulk velocity in the throat section.

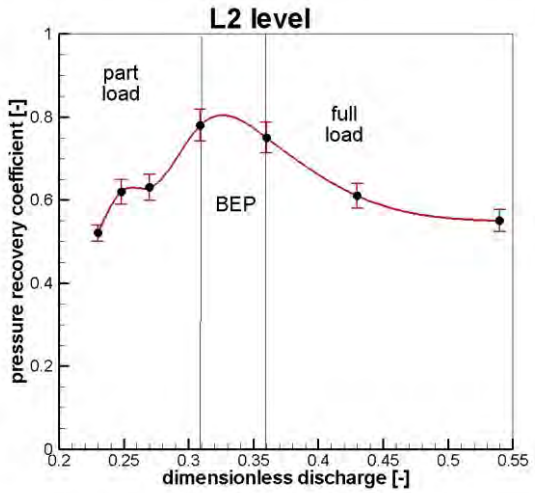

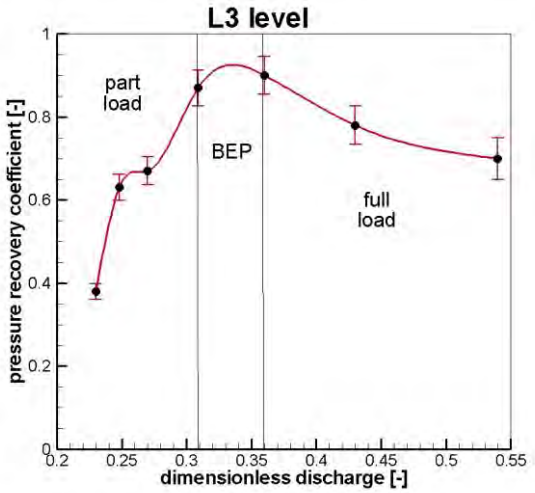

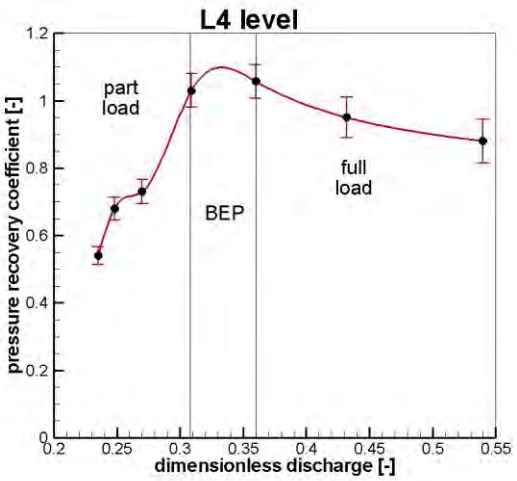

Figure 43. Pressure recovery coefficient on L2, L3 and L4 levels depending by dimensionless discharge

Figure 43 presents the variation of pressure recovery coefficient in three investigated levels: L2, L3 and L4. For all levels at partial discharge regimes the pressure recovery has a maximum of 0.7 in L4 level. When is reached at BEP the pressure recovery has maximum values in all levels, which confirms the role of the cone (to convert kinetic into pressure energy). When it reaches the full load regime the pressure recovery coefficient starts to decrease once departing from BEP, nevertheless due not reach at minimum values from partial discharge regimes. Figure 44 presents an evolution of pressure recovery coefficient in the length of the cone for three distinct cases. As is observed at partial discharge regime the role of the cone is functional only in the first third of the cone. At full load the cone recovers energy in all length of the cone with 0.75 less than at BEP. At partial discharge regime (q=0.23, for example) the pressure recovery coefficient is with 0.5 less approximately than BEP case.

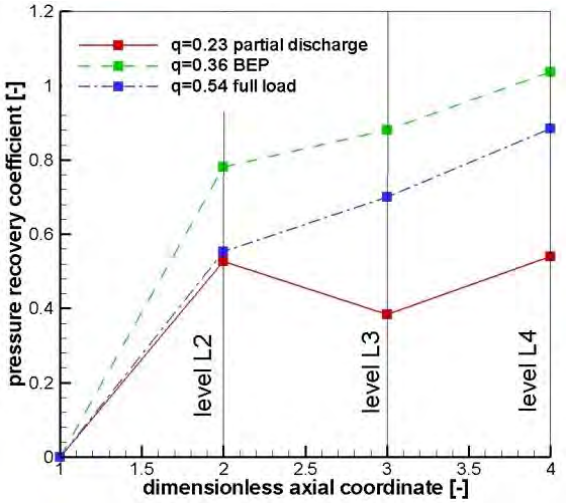

Figure 44. Evolution of pressure recovery coefficient at three distinct regimes in dimensionless length of the draft tube cone.

A second pressure analysis is to investigate the flow from a dynamical point of view. From the pressure signal was extracted the Fourier spectra. A new approach is employed to emphasize this signal. A second signal is reconstructed based on the acquired one, using the Parceval's theorem. The reconstructed signal has the same frequency as the first harmonic of the acquired signal and root mean square equivalent amplitude. A detailed analysis with this method is presented in [27].

For a discrete signal the amplitude and pressure fluctuations dimensionless form are defined as:

$$p_a = \frac{p_A}{\rho \cdot \frac{v_t^2}{2}} \tag{8}$$

where p_A represents the dimensional pressure amplitude or pressure fluctuation and the rest of terms are previously stated.

The second dimensionless parameter to be used is the Strouhal number, defined as:

$$Sh = f \cdot \frac{D_t}{v_t} \tag{9}$$

with f being the frequency of the flow from draft rube cone and Dt throat diameter of test section.

Dimensionless equivalent amplitude Figure 45 shows that at partial regimes different values are recorded depending by measured level. On L2 level and L3 level are situated the maximum amplitudes for partial regimes, which means that in the middle of the cone the vortex rope has the maximum eccentricity. At BEP the equivalent amplitude is approximately identical for the first three levels. As a result, the flow instabilities at this operating regime have no influence in the cone. When it is operated at full load regimes the equivalent amplitudes start to increase, having distinct values for each level. For L1 level the amplitude is approximately 4.5 times larger than at BEP, for L2 level 3 times larger, for L3 2 times larger, while at L4 level remain identical. Also, for q = 0.54 (full load regime) the amplitudes generate vibrations sensed in all experimental test rig. In the case of registered Strouhal number which is constant in all investigated levels of the cone, first at part load regime is decreasing reaching at a value of 0.7 smaller than at minimum q. As a comment is that at minimum q (925 rpm) the Strouhal number of the runner is similar with Strouhal number of the flow from the cone. When speed is reduced and q starts to increase the Strouhal number of the runner is different by Strouhal number of the flow from the cone. At full load regime the Strouhal number of the flow from the cone is increasing once that q increasing.

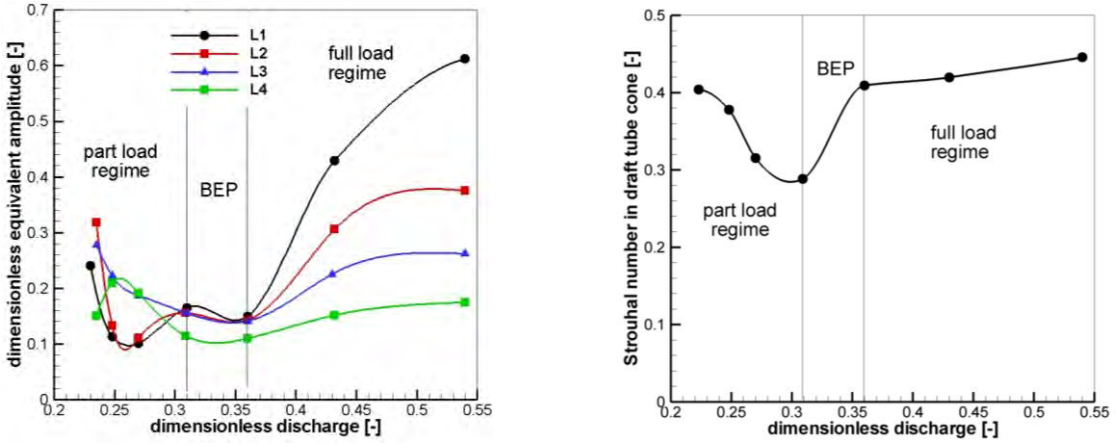

Figure 45. Dimensionless equivalent amplitude and Strouhal number for all levels depending by dimensionless discharge.

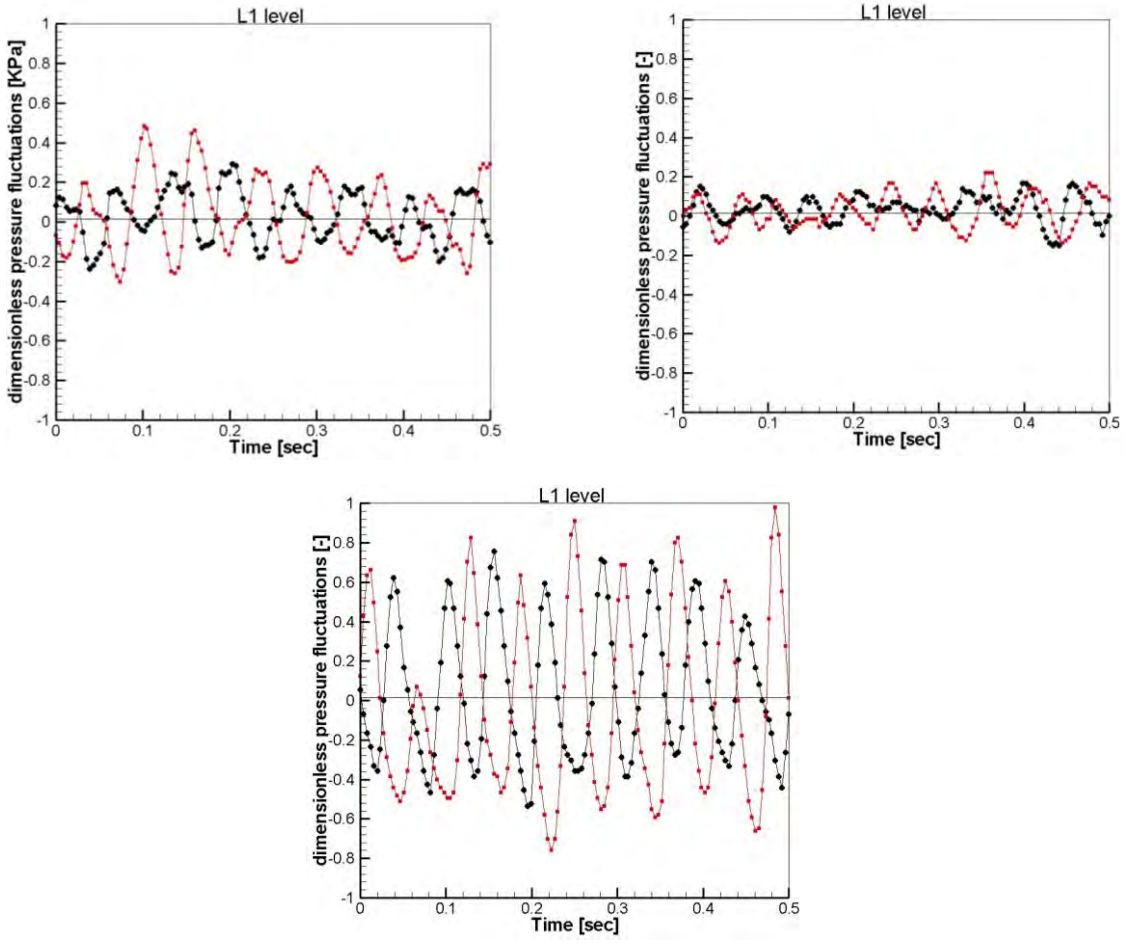

Figure 46. Registered dimensionless pressure fluctuations for L1 levels at three distinct flow regimes: part load regime q=0.23 (top left), BEP q=0.36 (top right) and full load q=0.54 (bottom).

A last analysis consists in evaluation of signal decomposition, keeping into account that on each level two pressure signals are registered on opposite sides. According to [37], there are two types of

draft tube cone pulsations. The plunging type acts as a water hammer in the length of the cone, while the rotating type acts in the cross sections of the cone. The rotating type is produced by flow instabilities as vortex rope due to its shape. First are represented both dimensionless pressure signals on same level. Figure 46 presents an example of how the registered signals for L1 level appear at three representative dimensionless discharges. The decomposition procedure to obtain rotating and plunging pulsation types is described in [27]. Also, pressure pulsations decomposition from the experimental data was using the procedure based on the Parceval's theorem.

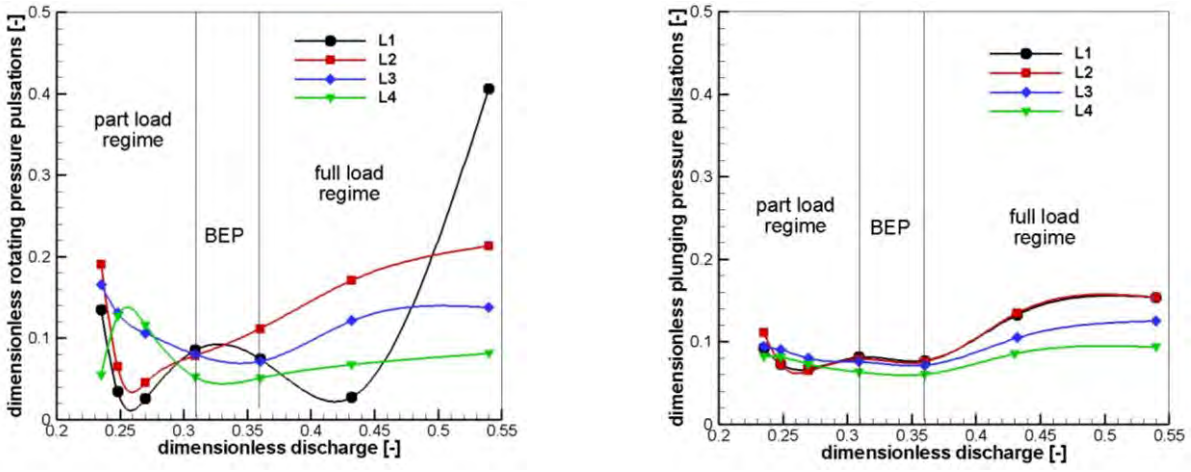

Figure 47. Dimensionless pressure signal decomposition into rotating (left) and plunging (right) type in all levels at different operating regimes.

The rotational component of pressure pulsation associated with the vortex rope is significant for part load regime and full load regime especially in the first three levels. If at part load regime the pressure fluctuation given by the vortex rope is higher in the middle of the cone (L2 and L3) levels, when it is reaching at full load regime the largest pulsation is registered at the cone throat. This significant decrease and level modification is given by the stagnant region which at full load is increasing in throat cone region, [38]. Once that stagnant region increases close to the throat also the plunging type pulsation is increasing.

This research presented the experimental measurements of decelerated swirling flow in a conical diffuser at different operating regimes. The speed of the runner of the swirl generator was controlled by an MR brake system. Accordingly with dimensionless discharge and dimensionless flux of moment of momentum, when the runner speed is reduced, it acts as a real runner operating from part load (design operation) up to overload regimes at constant guide vane opening. The pressure measurements were made in four levels in the cone, each level having two opposites' pressure transducers. The results are analyzed from two points of view: energetically and dynamically. From an energetic point of view, the mean pressure resulting pressure recovery coefficient. The amplitude, frequency and signal decomposition help to characterize the flow from a dynamic point of view. Pressure recovery coefficient shoved clearly that when the runner is operated at partial regime the

static pressure is recovered only in the first part of the cone, being observed only 50% pressure recovery than in BEP case. At full load regime the pressure recovery is at 75% in comparison with BEP. In the case of dynamical analysis, the equivalent amplitude has maximum values in the middle of the cone when it is working at partial discharge. This results from the shape of the vortex rope, with maximum eccentricity in the middle of the cone. At BEP the amplitudes registered the same values in all lengths of the cone, while at full load regime the maximum amplitude is registered at throat cone. This analysis cumulated with pressure signal discrimination showed that at full load regime the vortex rope has maximum amplitude at throat level, which leads to increase of stagnant region from this part of the cone.

Free runner control method for diminishing the vortex rope

Usually, to diminish the effects of pressure fluctuations induced by the hydraulic instabilities is limiting the operating range of the turbine. In this way, the task of energy compensator that hydroelectric power plants are having in the national electrical system is not always accomplished. Over the years different ways have been developed for extending the operating regimes with moderate development of hydraulic instabilities. Most existing solutions are related to the effects and not necessary to the cause of hydrodynamic instability. One of the most common solutions we can mention: filling the stalled region from the middle of the draft tube cone by air or by solid bodies [39], [40] or reducing the decelerated swirling flow close to the conical diffuser by mounting different fins or channels, , [41]. Anyway, all these methods deal with the effects of hydraulic instability, and not with the cause, which in our case is the decelerated swirling flow from the outlet of the runner turbine. Laboratory of Hydraulic Machinery and the Research Centre for Engineering of Systems with Complex Fluids (RCESCF) from the Politehnica University Timișoara, one of the main research directions is the investigation of the hydraulic machines.

The goal of this research was to design and investigate a new concept by using a free runner downstream on the main hydraulic runner turbine. The free runner concept supposes that rotates at the runaway speed with vanishing mechanical torque. The main purpose is to redistribute between the shaft and the periphery the total pressure and the moment of momentum such that the flux of total pressure and the moment of momentum are not altered. Moreover, the free runner does not modify the operating point of the main hydraulic turbine runner. The benefits of the free runner downstream the main runner turbine approach are: i) reducing the pressure pulsations (synchronous or asynchronous) from the draft tube cone, ii) optimal configuration for the swirling flow ingested by the draft tube cone, iii) minimum draft tube losses and maximum pressure recovery. Similar approaches have been presented by [42] by using a Francis turbine with tandem runners, or by using a stay apparatus downstream the Francis runner or RAPT concept for a radial axial pump turbine, [43]. The free runner concept (see the sketch in Figure 48) downstream the main turbine will add the required flexibility for the Francis turbine regulation and avoid the deterioration of hydraulic turbine components.

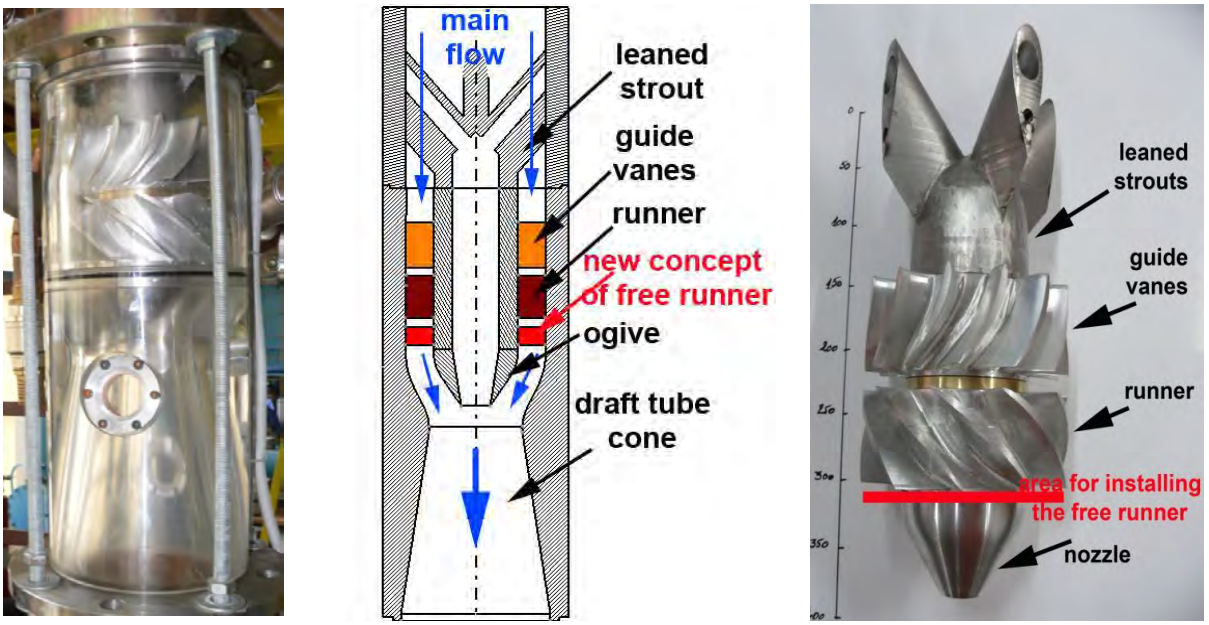

Figure 48. The existing experimental test rig with the swirl apparatus (left) and highlighting with red where the new free runner will be mounted (middle and right).

The principle of controlling the decelerated swirling flow by modifying the total pressure and the moment of momentum from the inlet of a conical diffuser has been studied theoretically [44], [45], [46]. According to this theory, the research aim is to offer an optimum configuration in the draft tube inlet. By the optimum configuration three conditions should be considered: minimum hydraulic losses, maximum pressure recovery and minimum pressure pulsations in the draft tube cone. By using the free runner, the total pressure from the outlet of the free runner and the inlet of the conical diffuser will be redistributed. The investigations undertaken from this research to minimize the effects of hydraulic instabilities and offer an optimal configuration in the draft tube cone will consist by experimental and numerical investigations. Experimental investigations consist by measurements of velocity profiles with Laser Doppler Velocimetry and pressure pulsations respectively. From the analysis of the experimental measurements the new concept of the free runner will be designed. Numerical investigations are carried out in the second part of the research and will assess quantitatively if by using the second runner, the hydraulic instability from the draft tube cone is reduced.

The main dimensions of the components from the swirl apparatus together with the dimensions of the free runner concept are presented in the table below.

Table 11. Hydraulic parameters for the test rig components.

Parameter	Value	Unit
Nominal discharge Qn	0,03	[m^3/s]
Main runner - rotational speed n	940	[rpm]

Main runner - tip diameter D_t	0,150	[m]
Main runner - hub diameter D_h	0,06	[m]
Main runner - blade number z	10	[-]
Free runner - rotational speed n_{fr}	850	[rpm]
Free runner - tip diameter D_{t-fr}	0,100	[m]
Free runner - hub diameter D_{h-fr}	0,03	[m]
Free runner - blade number z_{fr}	3	[-]

The numerical domain represented full 3D and consisted of 5.8 million mixed cells. First the numerical results were obtained without considering the presence of the free runner, and after the vortex rope was developed, the free runner with three blades was activated.

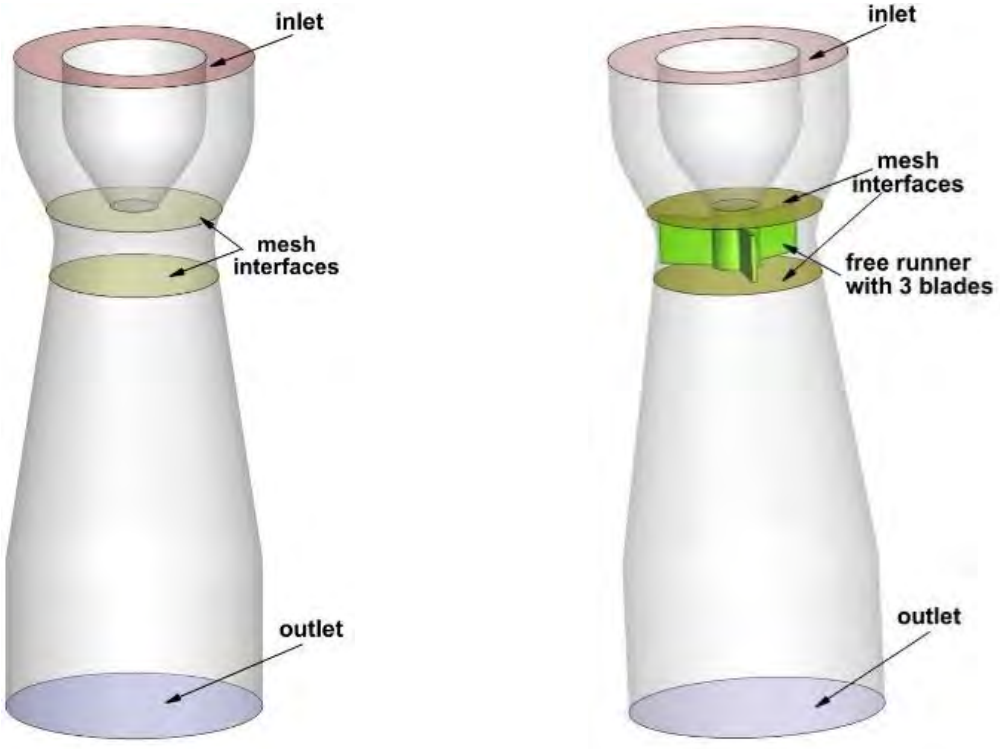

Figure 49. Full 3D domain: without free runner (left), with free runner (right), [47]

The numerical simulation was performed with the help of ANSYS Fluent 2021R1. The unsteady solver was employed, together with the Generalized k-ω (GEKO) model for modelling turbulence parameters. The velocity components together with the turbulence parameters, from the exit section of the swirl generator, obtained from experimental measurements, were imposed on the inlet boundary of the domain. On the outlet boundary the outflow condition was imposed. For all the wall boundary conditions the default set-up of the Fluent was retained, with No slip shear condition and

standard roughness model. In order to compute the interaction between the rotating domain, containing the free runner with 3 blades, and the static domain, the sliding mesh technique was employed, and two mesh interfaces were defined with the matching option activated, upstream and downstream of the free runner. The rotational speed imposed on the rotating domain was 850 rpm, corresponds to the free movement of the runner and was experimentally determined. To generate the vortex rope, first the presence of the free runner was "hidden" by defining the boundary condition on the blades as interior, and the volume was set as water. After the vortex rope was generated, the free runner was activated by imposing the wall boundary condition on the blades, and the volume was set as solid. As solution methods, the scheme of SIMPLEC was employed for computing the pressure-velocity coupling. The spatial discretization was set to Second Order Upwind for pressure, momentum and turbulence parameters and to Least Squares Cell Based for the gradient. The transient formulation was set to Bounded Second Order Implicit. The time step was set as 0.001 seconds, corresponding to a movement of the free runner of approximately 5°, and 15 iterations were considered for each time step. The numerical simulation was carried out for a flow time of 4.458 seconds for the case without the free runner and for a flow time of 2.505 seconds for the case with the free runner.

A first step in the analysis of the new concept is the validation of the velocity profiles obtained from the 3D numerical simulation against the experimental results. The measurements have been validated in the convergent part of the test section on the W0 survey axis. The comparison between the experimental analysis and the 3D numerical simulation shows that the numerical results agree very well with the experimental values. The comparison was centered on two velocity components: the meridional velocity and the circumferential velocity. Note that the experimental velocity components were used to validate the results from numerical simulations, not as boundary conditions.

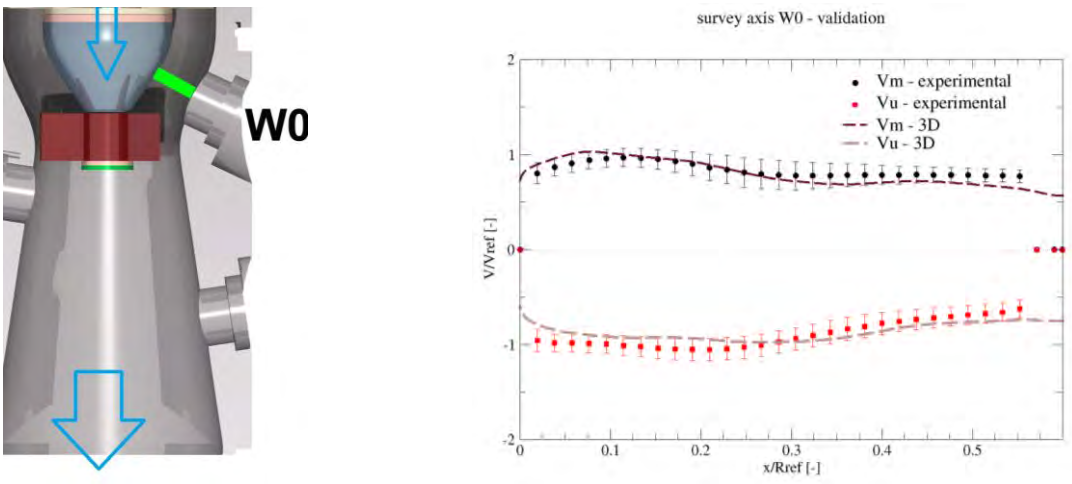

Figure 50. Validation of the velocities measured experimentally with the LDV on the survey axis W0 with the velocity profiles obtained from the 3D numerical simulation).

Considering the good validation of the numerical investigation, the next step is the analysis of the flow and of the pressure from the numerical simulation for the investigated cases: without and with free runner. Figure 51 presents the flow evaluation in the conical diffuser for both cases, by analyzing the formation of the vortex rope. To visualize the vortex rope, a constant pressure iso-surface was plotted, with green color, and the vortex cores of the flow filed were calculated and plotted, the red-colored spheres. The pictures show that the vortex rope is present in the conical diffuser in the case without a free runner (left part of the images). It is forming close to the ogive and continues 2/3 from the length of the conical diffuser. When the free runner is inserted into the extension of the ogive, the vortex rope starts to decrease in length and thickness. It forms at the end of the shaft of the free runner and continues approximately 1/3 from the length of the conical diffuser.

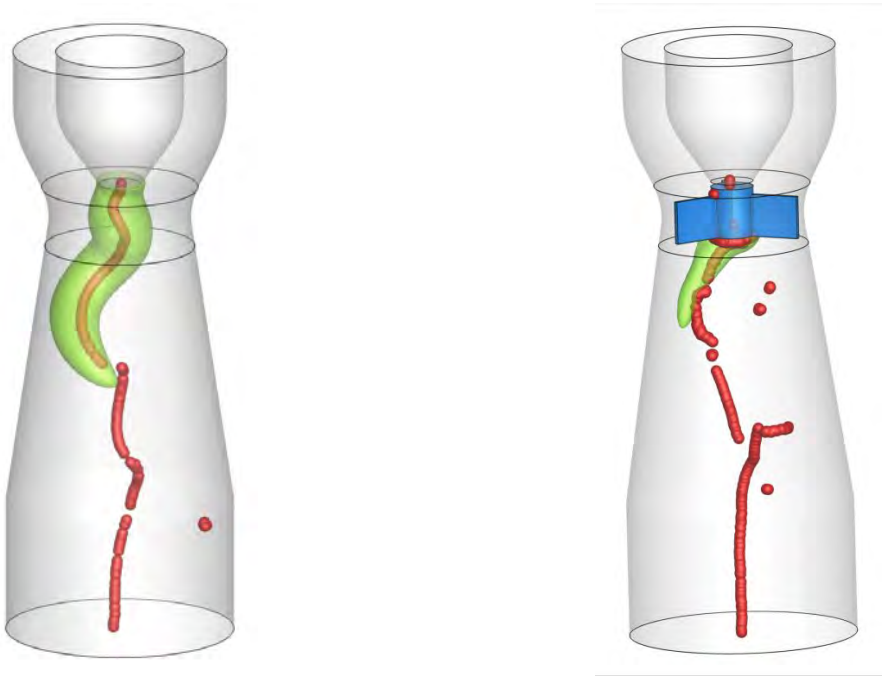

Figure 51. Visualization of the vortex rope for the case: without and with free runner.

Another analysis consists of evaluating the unsteady pressure registered 100 mm downstream of the inlet in the conical diffuser, as shown in Figure 52. The unsteady pressure is registered from the numerical simulation and after the FFT was performed. The analysis of the FFT shows the main frequency of the vortex rope (15.6 Hz). In the case without free runner, the maximum amplitude reaches a value of 2000 Pa. When the free runner is introduced, the maximum amplitude reaches a value of 1500 Pa, which means a reduction of 25 %. Nevertheless, it is pointed out that in this case is tested a simple free runner with only three straight blades.

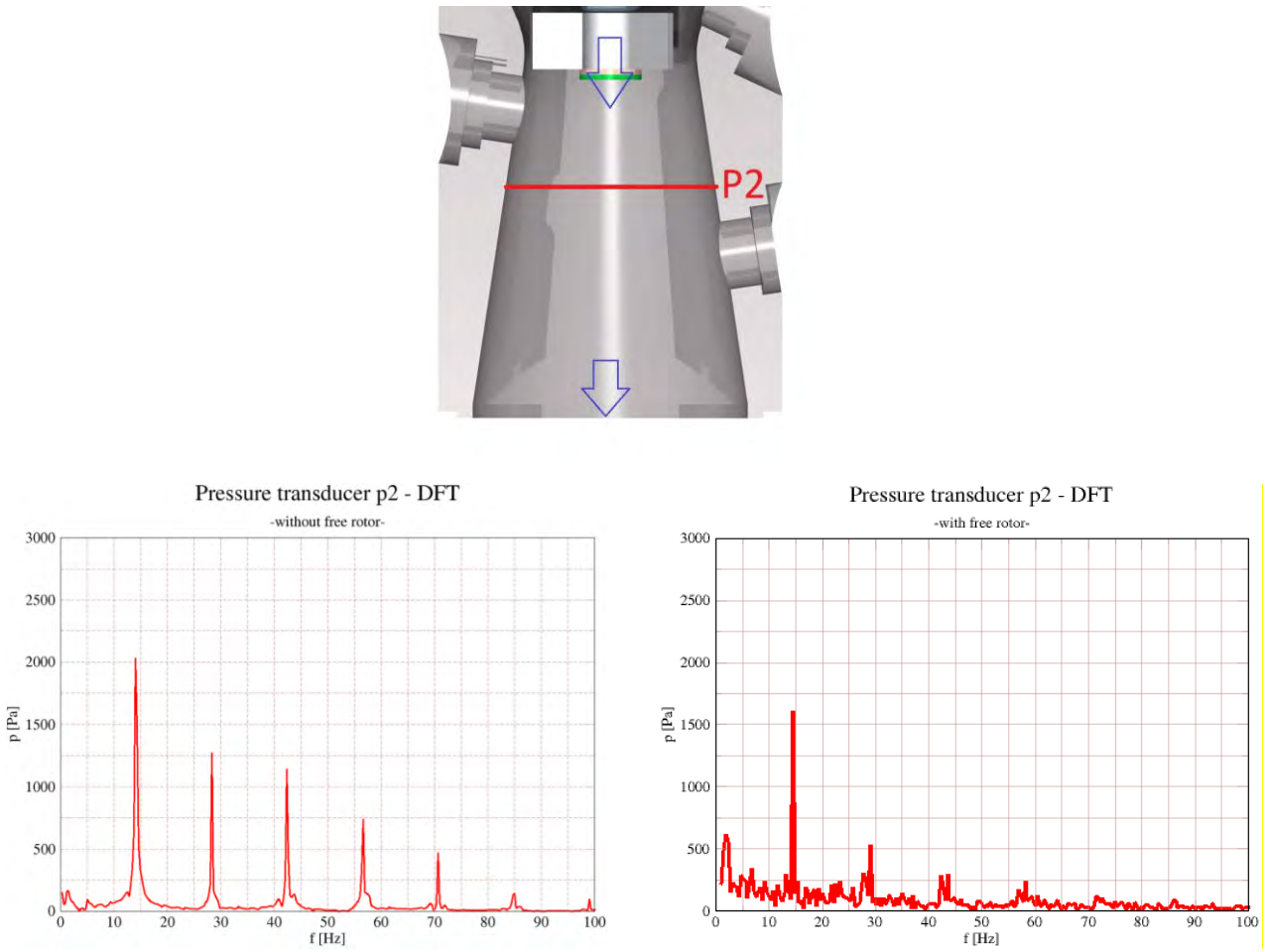

Figure 52. Evolution of the unsteady pressure (Fast Fourier transform) in the conical diffuser without free runner and with free runner.

In order to proof the concept, it was used the test rig from Politehnica University Timisoara laboratory. The test rig is a surrogate which mimics the swirling flow from the outlet of a Francis turbine operated at part load conditions (at 70% from the nominal flow). The main components of the test rig are the swirl generator and the convergent-divergent test section – as conical diffuser [48].

The main components of the swirl generator are the struts, the stator, the main runner, and the ogive. All those components are assembled in the Plexiglas test-section with an inner diameter of 0.150 m and an outer diameter of 0.2 m. The divergent part of the test section has the same angle as the conical diffuser of a real hydraulic turbine. The vortex rope generated by the swirl generator is presented in Figure 53.

Figure 53. The swirl generator with the main components and the convergent-divergent test section (left). The visualization of the vortex rope obtained in the divergent part of the test section (middle). The visualization of the flow in the divergent part (draft tube cone) when the free runner is installed in the extension of the swirl generator.

The acquisition system contains a Laser Doppler Velocimetry (LDV) to acquire the meridian and circumferential velocity components together with pressure pulsations. During the measurements, the nominal discharge was maintained at a constant value of 0.03 m3/s, and all the measurements were performed in overpressure conditions of 0.3 bar. Details regarding the LDV system and pressure transducers are very well described in [49].

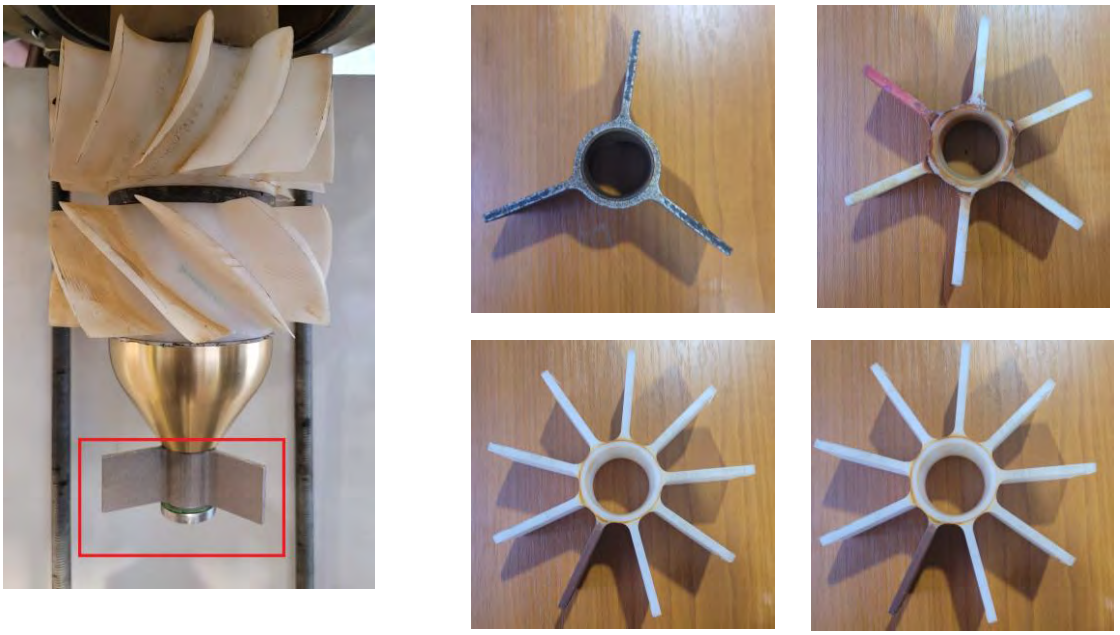

measured speeds of the free runners on the experimental test rig	3 blades	6 blades	9 blades	12 blades
	846 rpm	885 rpm	820 rpm	760 rpm

Figure 54. Experimental setup with the free runner mounted on the extension of the swirl generator. The free runner rotates freely (zero moment) on the shaft which is mounted on the ogive.

The proposed straight free runner for investigation, was mounted at the minimum radius of the test section, having the radius at the periphery of 0.1 m, and at the hub of 0.03 m. The measured rotational speed of the flat free runner is presented in Figure 54 with respect to the runaway speed. To proof this concept four straight free runners have been tested in the laboratory.

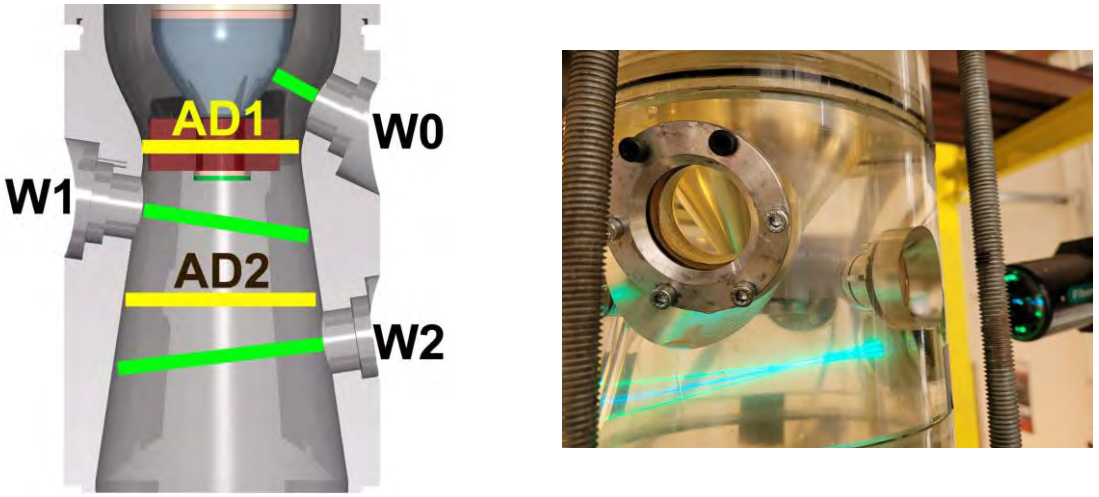

Figure 55. Position of window W0, W1 and W2 (left), the survey axes for velocity profiles. The position of AD1 and AD2 wall pressure measurements. Velocity measurements on the test section (right).

According with Figure 55, the free runners have been mounted in the extension of the swirl generator, more precisely is connected to the ogive. The ogive was modified to sustain a shaft and, on the shaft, have been mounted the free runners. The experimental results concentrated on mean velocity profiles. The mean velocity profiles are presented in dimensionless form with respect the equations below. The length of survey axis W0 was divided with the reference radius, in our case the radius at the throat between convergent and divergent area of the test section. The circumferential and meridional velocity was divided with the velocity from the throat.

$$x/Rref = \frac{L_{surveyaxis}}{D_t/2} = \frac{L[m]}{0.05[m]}[-] \quad , \quad V/Vref = \frac{V_{(m^*,u)measured}[\frac{m}{sec}}{V_{throat}[\frac{m}{sec}[-]} \qquad (10)$$

The measured velocity considers only the flow rate from the main circuit (in our case ~0.03 m3/sec). In addition, for each point the value of RMS was analyzed (Random Mean Square). On the

second hand, the experimental results are presented and analyzed for the unsteady pressure measured at the wall of the test section, which was measured in parallel with the velocity. Considering the free runner is a supplementary component added exactly at the inlet in the conical diffuser, a first evaluation was the analysis of the surface occupied by the free runners. At the inlet in the conical diffuser, according with Figure 56, the surface occupied when the free runner is inserted in increased by three times when the free runner with twelve blades is inserted. This means that when a secondary runner is mounted at the inlet in the conical diffuser, the number of blades should be limited to respect the hydraulic losses as much as possible. Moreover, if we analyze the measured speed on the test rig, see Figure 54, is increasing up to 6 blades and after is decreasing due to higher number of blades and higher hydraulic loses generated by the runner itself.

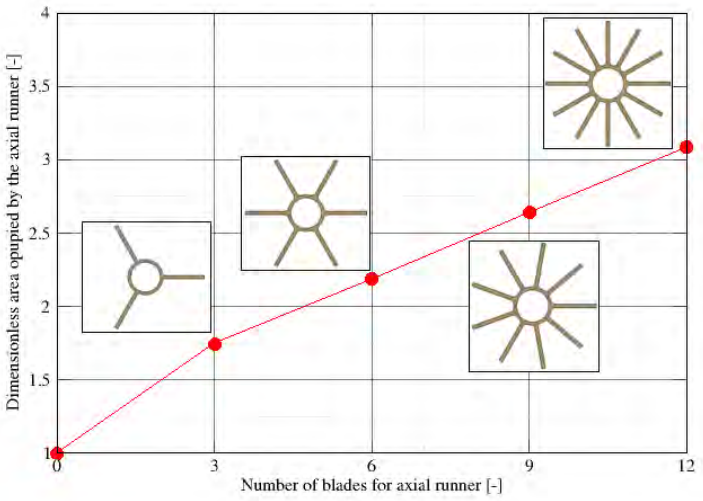

Figure 56. Analysis of the dimensionless area at the inlet of the conical diffuser for the swirling flow with vortex rope (0 number of blades) and with free runners.

As a first conclusion, when analyzing the increase of the surface and the measured speed of the free runners, the free runner with 6 blades ensures a maximum speed with relative minimum hydraulic losses induced by the supplementary component (the free runner) on the hydraulic circuit. On the second part of the experimental results, the velocity profiles have been measured on three survey axis W0, W1 and W2 (according with Figure 55) for 5 individual cases (one with the development of the vortex rope and four with different number of blades for the free runner: 3, 6, 9, 12 blades). For each survey axis have been measured two velocity components: the meridian component and circumferential component.

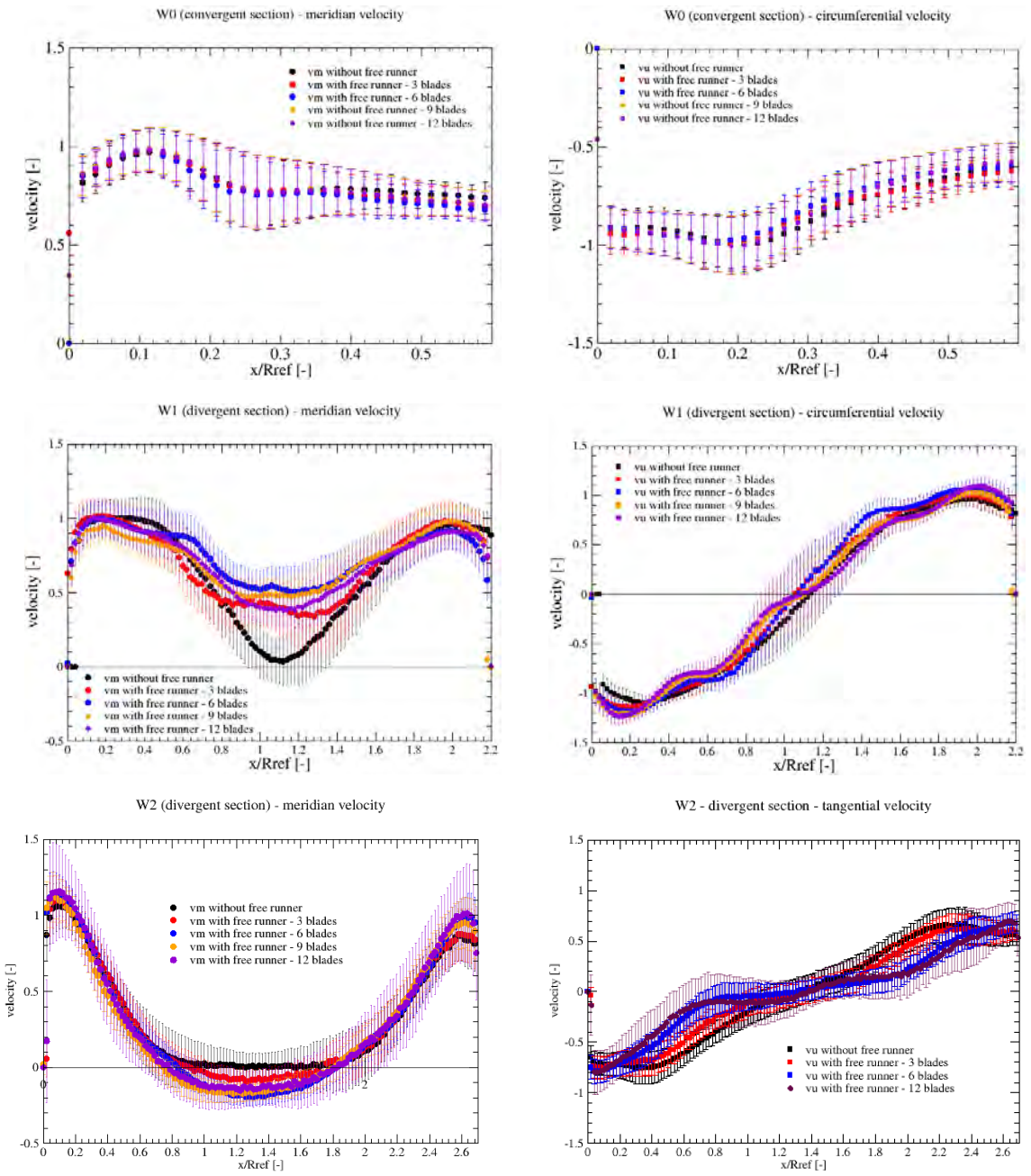

Figure 57. Mean meridian (vm) and circumferential (vu) velocity profiles on three survey axis from the test section, for the case without free runners (with vortex rope) and free runners with 3, 6, 9, 12 blades.

In W0 survey axis, see Figure 57 up, the influence of the free runners is negligible, due the fact that the measurement axis is between the main runner and the free runner. As a result, the meridian velocity has an excess of velocity close to periphery (between 0 – 0.1 on x/R_{ref}) and a velocity deficit close to the hub, in the middle of the test section (between 0.5 – 0.6 on x/Rref). If we are looking in the literature, this type of the flow is addressed to the decelerated swirling flow, especially when the hydraulic turbines operate at part load operation. In W1 survey axis, see Figure 57 middle, when no free runner is installed, a stagnant region is formed in the middle of the conical diffuser and the vortex rope appears. When the free runners are installed, the stagnant region is transforming into a velocity

deficit region. Moreover, from on each investigated free runner, the velocity deficit region modifies, the optimum flow being obtained by the free runner with 6 blades. This it is observed also for the circumferential velocity component, where the swirl is acting as a rigid solid body rotation. In the case of W2 survey axis, which is located at the outlet of the conical diffuser, the free runners influence over the flow are minimum, all the free runners providing a velocity deficit in the middle of the conical diffuser. The last analysis consisted of Fourier transform of the pressure signal acquired at the wall of the conical diffuser on two levels: AD 1 and AD 2.

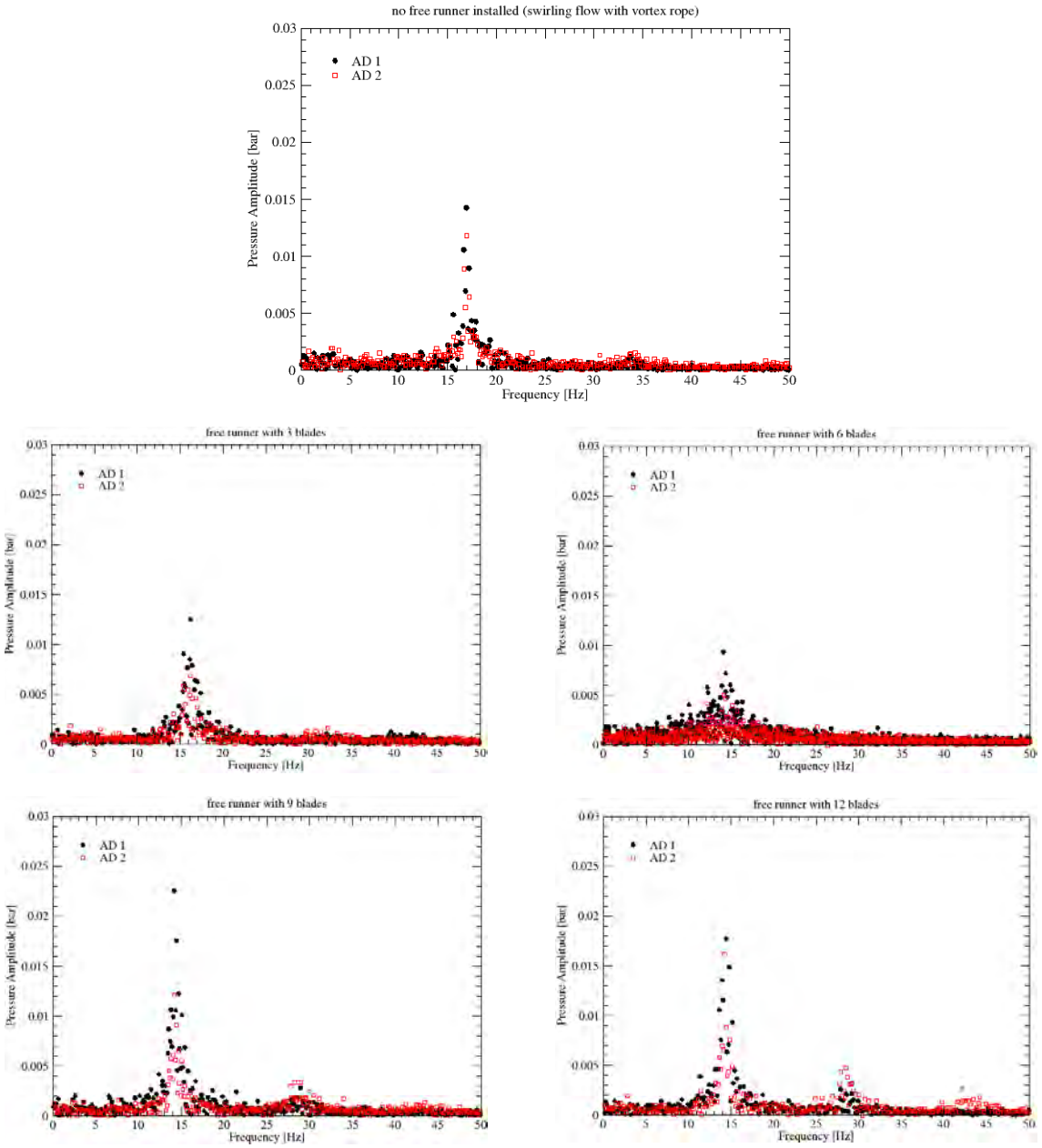

Figure 58. FFT analysis for two points (AD1 and AD2) on the conical diffuser for the case with vortex rope (up) and the free runners with 3, 6, 9, 12 blades (left - right).

The Fourier transform reveals the main harmonic of the amplitude (associated to the development of the vortex rope in the conical diffuser) and the modification once the free runners are inserted. According with Figure 58 and Figure 59, the associated frequency of the swirling flow is decreasing from a maximum value of 16,96 Hz (which corresponds of the flow with vortex rope) at a lower frequency of 14.10 Hz (which corresponds of the flow with 6, 9 and 12 blades). If we analyze the amplitude on AD 1 and AD 2, is decreases with approximately 30% for the free runner with 6 blades and after is increases if the number of the blades of the free runner increases.

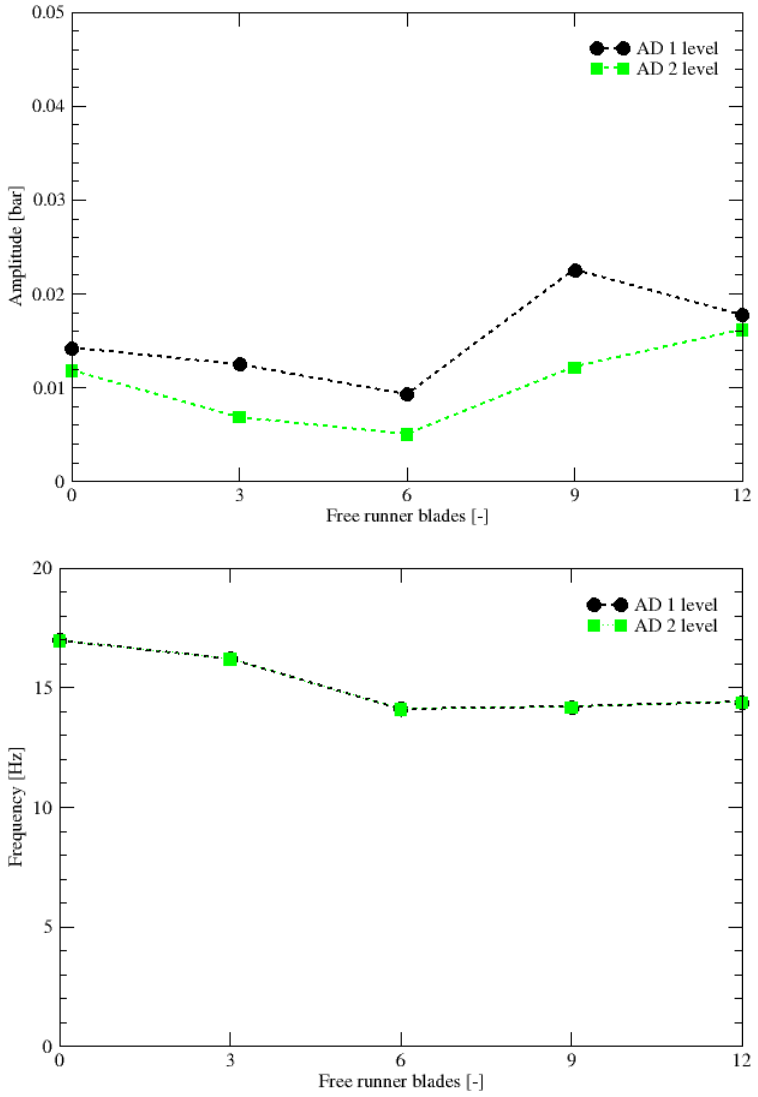

Figure 59. Evolution of the frequency and maximum amplitude on AD 1 and AD 2 levels on the draft tube cone wall for the case with vortex rope (0 free runner blades) and with free runners (3, 6, 9, 12 blades).

The experimental investigations performed in analysis propose a new concept of free runner mounted downstream the main hydraulic runner. The approach assumes that the free runner rotates at the runaway speed and is mounted in the extension of the hydraulic turbine (in our case of the swirl generator). The free runner was attached with the help of a shaft to the ogive and four free

runners have been tested. The free runners had 3, 6 9 and 12 straight blades. The numerical and experimental results concluded that the free runner with 6 blades reduces the frequency of the generated vortex rope and the amplitude with 30% approximately. Nevertheless, the free runner mounted at the inlet in the conical diffuser generates hydraulic losses and supplementary investigations should be considered for a complete characterization of the concept.

Radial-axial water jet for increasing the flexibility in operation of hydraulic turbines

In the last decade, a new active control method has been proposed and patented by Resiga et al. [50], [51], axial water injected through the runner's crown along the draft tube cone. The method was intensively experimented by Bosioc et al. [1], [27] in the laboratory, where the control method proved the efficiency and diminish the flow instabilities from the draft tube cone. The method addresses directly the cause of flow instabilities, and it acts on dynamic behavior (by reducing the pressure fluctuations and vibrations) and flow behavior (modifies the structure of the flow, by eliminating the formation of the vortex rope). As a result, the water jet injection through the runner crown has been tested in other laboratories on model turbines and has been implemented in real hydropower plants, [52], [53]. Anyway, the major obstacle on implementing this control method in the power plants on large scale, is related by the higher volume of water (more than 15% from the main flow rate) necessary to be axially injected through the ogive in the draft tube cone.

Recently a series of numerical investigations, reheated the idea of water injection in the draft tube cone, [54] with similar results in diminishing the flow instabilities from the draft tube cone at part load operation. The investigations performed by two different research collectives [54], [55] concentrated on ogive or nozzle modification with the purpose to reduce the amount of water necessary for injection. The results show that a radial-axial water jet can reduce the effects of the vortex rope while using a water jet flow rate of approximately 10% from the main operating flow rate or even less.

The main goal of this study was to investigate a new concept by using an actuator mounted at the end of the ogive. The actuator will provide a radial-axial water jet in the draft tube cone. According with Figure 60, the swirl generator which consist by the fixed stay vanes and the runner and continues with the ogive, has an actuator (shown in red) with the possibility to move and positioning at the inlet in the draft tube cone. In comparison with the axial water jet control technique already validated in the laboratory, the concept for radial-axial water jet it comes with the following advantages: 1) efficient jet - reduces the amount of flow rate for water injection from 14% up to 10%; 2) efficient jet - the displacement system has the possibility to provide axial or radial-axial or radial jets, depending by the hydrodynamic instability developed in the drat tube cone. The main purpose of the new concept of efficient jet is to add flexibility in operation for the hydraulic turbines to avoid the draft tube performance deterioration at off-design operating conditions. Moreover, the main runner operation is not influenced, and the radial-axial water jet will function only when the machine is operated at part load or full load with the development of the vortex rope.

The principle of modulating the decelerated swirling flow within the conical diffuser has been investigated through numerical analysis [55]. In alignment with this theoretical framework, the research objective is to provide an optimal configuration at the draft tube cone inlet. To achieve this optimum configuration, three conditions must be addressed: minimizing hydraulic losses,

maximizing pressure recovery, and minimizing pressure pulsations within the draft tube cone. The implementation of a radial-axial water jet facilitates the fulfilment of these conditions with the least energy required for radial-axial water injection.

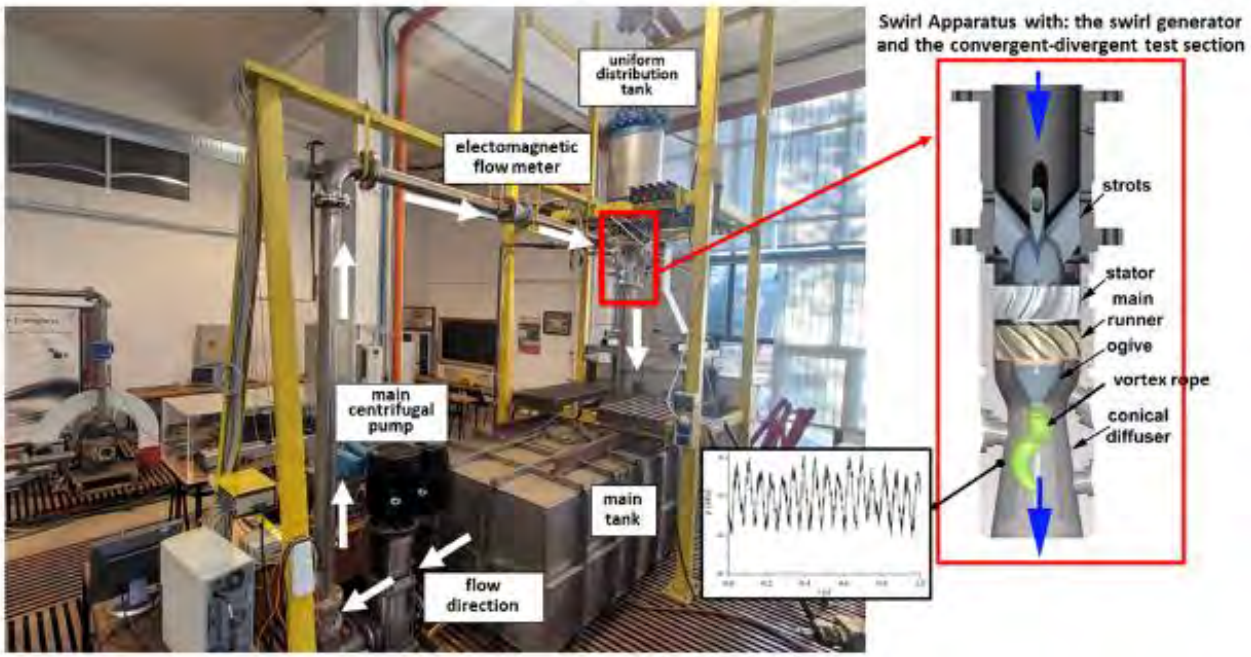

Figure 60. The test rig from the laboratory similar with the numerical model employed in this study.

The computational model utilized for evaluating the radial axial jet within the discharge cone of hydraulic turbines is linked to the swirl apparatus present within the laboratory environment. This swirl apparatus facilitates the investigation of various control methodologies aimed at alleviating flow instabilities associated with the vortex rope phenomenon. The apparatus, integrated into the primary hydraulic circuit of the test rig, comprises two principal components: the swirl generator and the test section. The swirl generator itself is composed of three parts: the ogive, the stator, and the main runner, which are installed within a cylindrical Plexiglas section with an internal diameter of 0.150 m, as illustrated in Figure 60. At the inlet of the conical diffuser, the stator and main runner generate a rotating flow analogous to that observed downstream of a Francis runner operating at 70% of the nominal flow rate, [36].

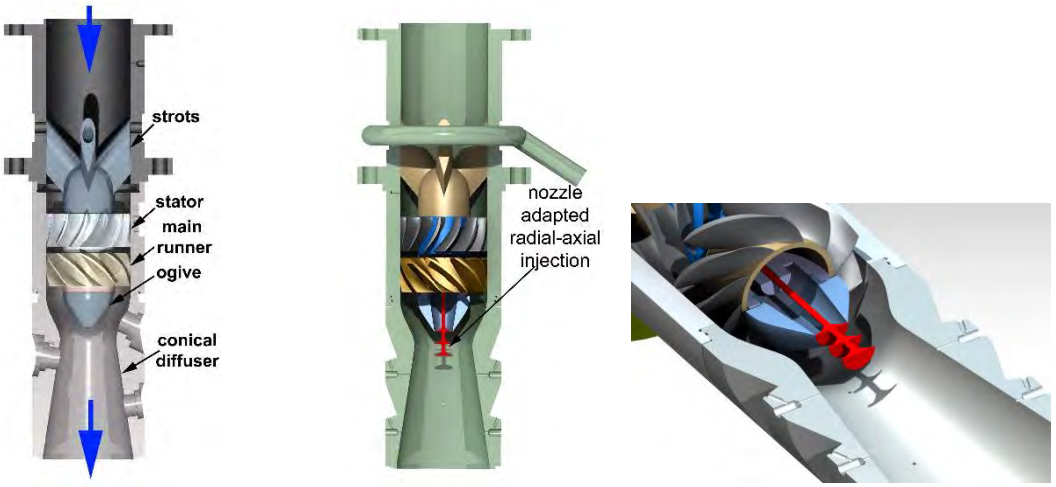

Figure 61. The swirl apparatus and test section from the experimental test rig are illustrated. The left image depicts the original configuration, whereas the right image displays the setup with the device designed to facilitate a radial axial jet rig.

The main dimensions of the components from the swirl apparatus together with the dimensions of the radial axial concept are presented in Table 12.

The computational domain pertains to the convergent-divergent segment of the swirling flow apparatus developed at Politehnica University Timisoara, [56]. The convergent segment is delineated by the annular inlet section and the throat, as depicted in Figure 62. Figure 62 illustrates the computational domain inclusive of the jet injection device. A mixed mesh, comprising approximately 2.8 million cells, has been generated. For each scenario, boundary conditions are prescribed utilizing a velocity profile at the domain's inlet and an outflow condition at the outlet section. The inflow boundary conditions are derived by computing the flow upstream of the numerical domain from our preceding research work. Consequently, the inlet velocity profile (covering axial, radial, and circumferential velocity components) in addition to the turbulent quantities (kinetic energy and turbulence dissipation rate) corresponding to a runner speed of 920 rpm are applied to the annular inlet section. Figure 63, shows the velocity profiles from the inlet test section. Two flow rates values were tested for the jet injection device: 1.5 l/s and 3 l/s. For the two values of the flow rate of the jet, corresponding constant velocity values were imposed on the outer section of the jet injection device.

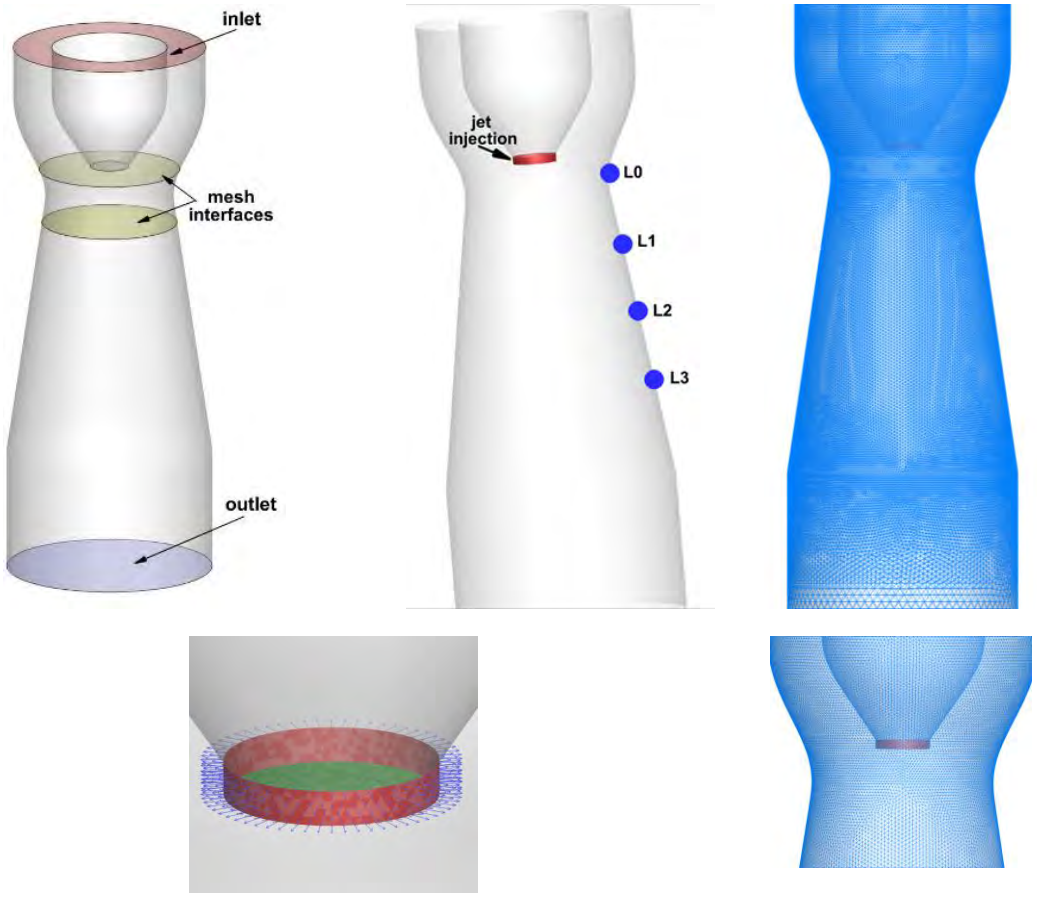

Figure 62. Full 3D domain: with the development of the vortex rope (left), with nozzle for radial axial jet injection (right)

Three-dimensional unsteady numerical simulations, both with and without jet injection, were undertaken utilizing Ansys FLUENT 2023 R2 software to evaluate the efficacy of the novel approach in mitigating the vortex rope. In modelling the turbulent flow within the domain, the k-ω GEKO turbulence model was employed. This turbulence model has been recently introduced into Ansys FLUENT and is more adept at accurately capturing the flow characteristics specific to hydraulic machines. The advantage of this turbulence model lies in its flexibility to encompass a wide array of applications. The model offers free parameters that may be adjusted for specific application types, without adversely affecting its fundamental calibration. This attribute constitutes a potent tool for model optimization; however, it necessitates a thorough understanding of the coefficients' impact to prevent mistuning. It is vital to underscore that the model possesses strong default settings, enabling its application without modification, although any adjustments should be substantiated by high-quality experimental data. The time step applied for the unsteady simulation for all the investigated cases was t = 0.002 s. All numerical solutions were converged down to residuals as low as 10^{-4}. Pressure monitors, L0…L3, have been placed on 4 levels on the cone wall, at 50 mm on each other, in order to acquire the pressure evolution of the flow phenomena.

Table 12. Hydraulic parameters for the numerical setup.

Parameters	Value	Unit
Nominal discharge Qn	0,03	[m^3/s]
Main runner - rotational speed n	920	[rpm]
Main runner - tip diameter D_t	0,150	[m]
Main runner - hub diameter D_h	0,06	[m]
Main runner - blade number z	10	[-]
Nozzle opening	5	[mm]
Control 1 - Flow rate injection	1.5	[l/s]
Control 1 – Precent from main flow	5	[%]
Control 2 - Flow rate injection	3	[l/s]
Control 2 – Percent from main flow	10	[%]

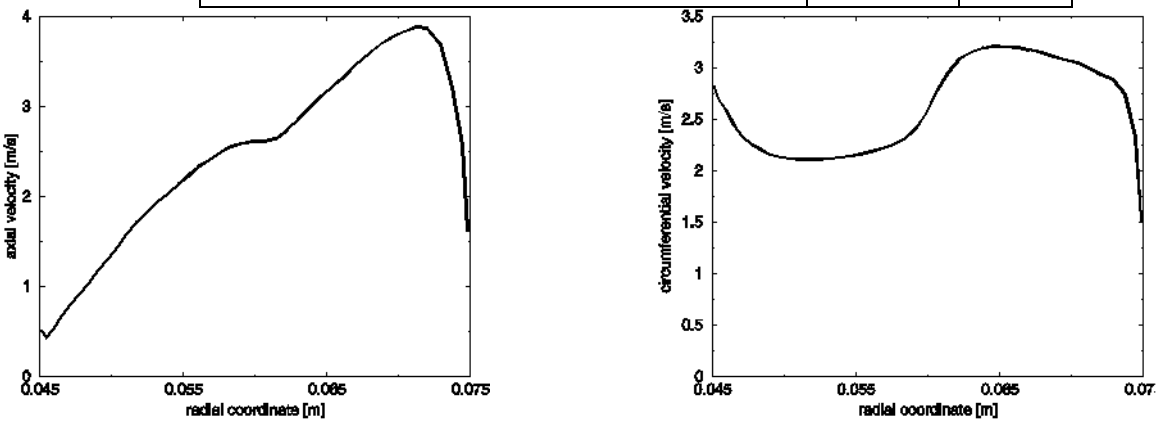

Figure 63. Velocity profiles from the inlet test section

The validation of the numerical case with the vortex rope and having implemented the velocity profiles from Figure 63, was performed and discussed in [47]. The subsequent step involves the analysis of the flow and pressure obtained from the numerical simulation for the scenarios investigated: the vortex rope and two cases for the control: 5% and 10% axial radial injection. Figure 64 illustrates the evaluation of the flow within the conical diffuser for all scenarios, focusing on the formation of the vortex rope. To visualize the vortex rope, a constant pressure iso-surface was plotted, represented in green, and the vortex cores of the flow field were calculated and depicted as grey. The images depict that the vortex rope is present in the conical diffuser in the context of all cases. It forms near the ogive and extends over two-thirds of the conical diffuser's length. When the radial axial jet

is introduced into the extension of the ogive, the vortex rope begins to increase in both length and thickness for 5% flow rate and start to decrease for 10%.

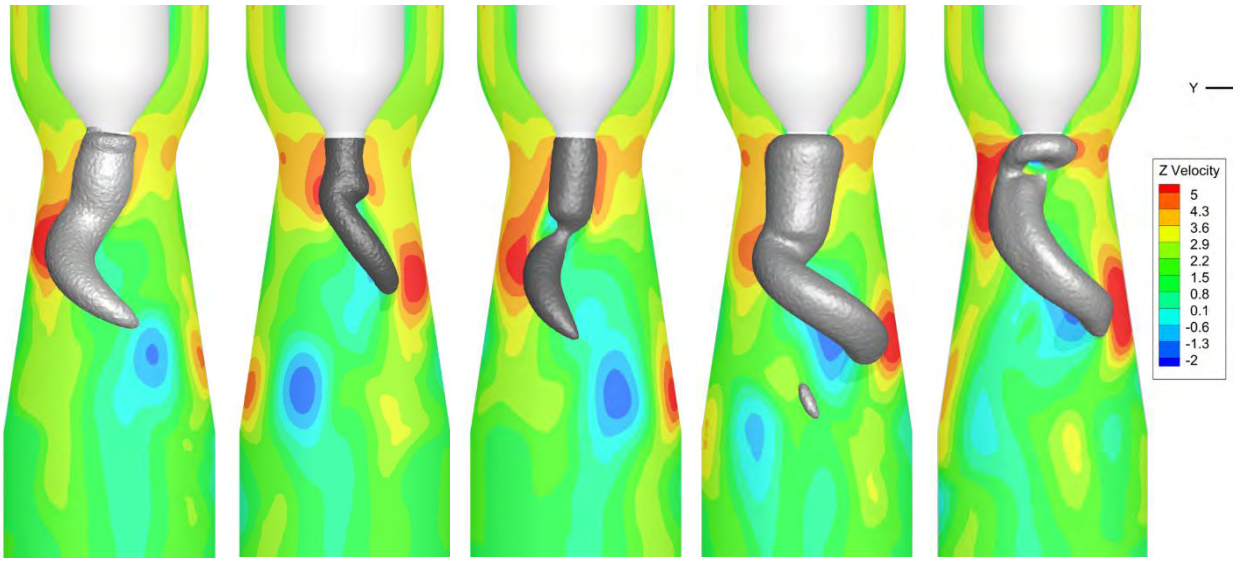

Figure 64. Numerical visualisation of the vortex rope contour on axial velocity for all investigated cases.

An additional analysis involves the assessment of unsteady pressure recorded on levels L0, L1, L2 and L3 downstream from the inlet within the conical diffuser, as depicted in Figure 65. The unsteady pressure data is obtained from numerical simulation, followed by the execution of FFT. The FFT analysis identifies the primary frequency of the vortex rope as 13 Hz. In the absence of control with axial radial jet, the maximum amplitude attains a value of 4000 Pa. Upon the introduction of the radial axial jet, the maximum amplitude is, and the frequency does not change for 5% flow rate injection. At the maximum flow jet injection of 10% the amplitudes and the frequency in the draft tube cone are di minished completely.

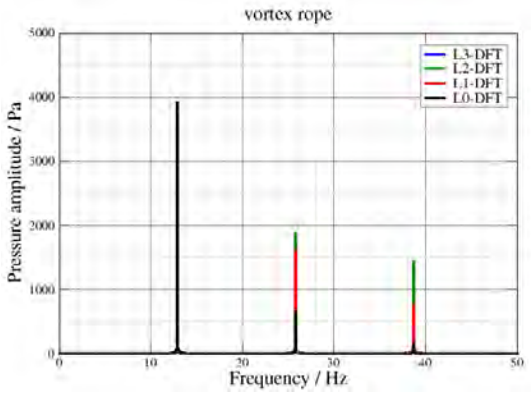

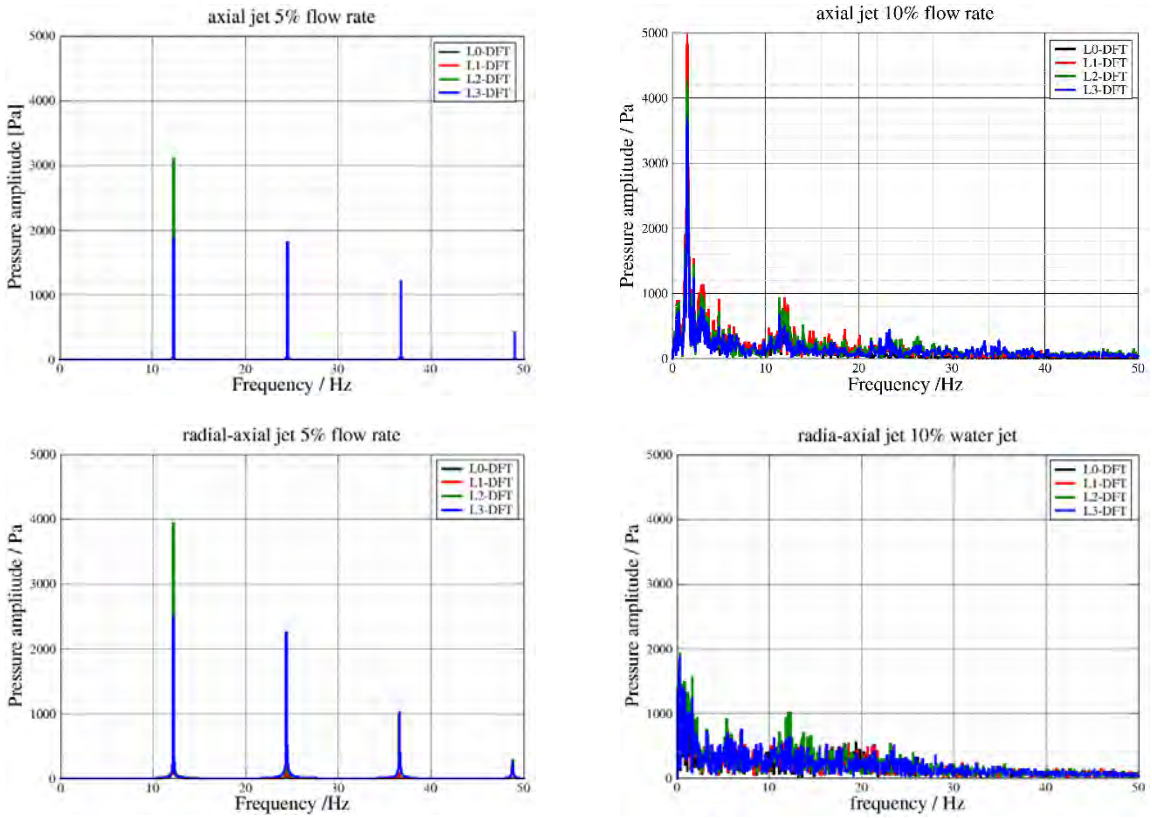

Figure 65. FFT numerical unsteady pressure results for all 5 investigated cases.

This study proposed a method to reduce hydraulic instabilities in draft tube cones by utilizing a radial-axial water jet. Recent numerical investigations have shown that water injection, especially with modifications to the nozzle, can diminish flow instabilities at part load operations, reducing the flow rate required from 14% to about 10%. The study introduces a new concept using an actuator mounted on the ogive to provide a flexible radial-axial water jet that adjusts to different hydrodynamic conditions. This approach aims to prevent performance deterioration in hydraulic turbines at off-design conditions without affecting the main runner's operation. Numerical simulations with the swirl apparatus and the radial-axial jet injection device were conducted. The Ansys FLUENT 2023 R2 software, employing the k-ω GEKO turbulence model, was used for simulations, offering flexibility and accuracy for hydraulic machine flows. The study tested two flow rates (1.5 l/s and 3 l/s) for the jet injection, which account for 5% and 10% of the main flow, respectively. Results indicated that radial-axial jet introduction changes the vortex rope characteristics within the draft tube, with increased length and thickness at 5% flow rate and reduced presence at 10%. Unsteady pressure analysis showed that the maximum amplitude of vortex-induced pressure pulsations was significantly reduced with higher flow rate injections, indicating improved hydraulic stability.

(C-iii) Control Methods for Diminishing the Hydraulic Instabilities In Centrifugal Pumps

Pump test rig. Design of test section for velocity and unsteady pressure investigation.

In hydropower systems among hydropower plants there are integrated pumping stations (PS). The main purpose is to consume the excess energy produced by the fluctuating wind or solar power to store energy. Also, the PS can be found in water supplies for cities, pipelines for gas and petrol, cooling units for the energy, chemical and metallurgical industry. The PS is expensive and cannot be replaced completely, preferably being refurbished.

Usually, these pumps can reach high values of flow rate at high efficiency with an acceptable development of cavitation phenomena. The pumps have constructive differences besides regular pumps in order to ensure a higher flow rate. Consequently, the complex shape of the suction-elbow with symmetric inlet generates an non-uniform flow field, which is ingested by impeller, [57], [43]. Consequently, the incidence angle on the impeller blades is significantly modified during one complete rotation. These mismatches induce additional losses that are referred to incidence losses which affect hydraulic performances, pump efficiency, total head, power input and required net positive suction head (NPSH) if cavitation is considered. These phenomena's also generate stronger unsteady flow conditions, such as stall, wakes, turbulence and pressure fluctuations, which affect the overall mechanical behavior of the pump with vibration, noise and radial and axial forces on the rotor, Error! Reference source not found..

Several investigations of the flow upstream the impeller have underlined the unsteady flow generated by the suction elbow and shaft. Ludtke [58], performed a detailed experimental investigation of the flow in radial and tangential suction chambers of a compressor in order to identify the flow structure. Three flow separation regions are identified based on these investigations: the first region is located where the pipe diverges, the second one is displaced on the convex side of the inlet bend where the flow turns from radial to axial and the third zone is behind the shaft. As a result, the hydrodynamic performances of the pump are deteriorated as well as unsteady phenomena are generated. Different engineering solutions can be evaluated in order to diminish the non-uniformity generated by the suction elbow. The straight engineering solution is to change the suction elbow, but it is unfeasible from economical point of view. Alternatively, an inducer can be installed in front of the impeller, Anton [59]. According to Anton, the inducer is an economically feasible solution, which could be mounted upstream the pump impeller in order to increase the pressure at the pump inlet. In this case, the non-uniformity flow will be decreased, and the static pressure will be increased at the impeller inlet. Consequently, efficiency remains practically unchanged while the cavitational behavior is improved. The inducer is an important part of many industrial pumps and rocket turbo pumps for which very low inlet pressure is available Error! Reference source not found.

Although the use of inducers is frequent today, several aspects of their operation remain difficult to model, especially in unsteady-state two-phase flow cavitating regimes. From the assembly between inducer and centrifugal impeller, the inducer usually works in cavitation and is often replaced. Schilling et al. [43], introduce a new concept of an axial rotor combined pump impeller. The axial rotor is an axial bladed rotor; the main task is to generate a sufficiently high-pressure level in front of the pump impeller in order to avoid any kind of cavitation of the pump inlet. The numerical analysis investigates the comparison between pump impeller without and with axial rotor hydrodynamics considering the flow given by the symmetrical suction elbow. After, is presented the experimental test rig, and the three-dimensional computational domains, boundary conditions and numerical setup. The experimental pump characteristics are validated against numerical simulations and the pump hydrodynamics are analysed for the case of the pump impeller with and without axial rotor.

An experimental test rig was developed at Politehnica University of Timisoara for assessing global performances (efficiency and cavitational) of centrifugal pumps. The test rig is completely manufactured from stainless steel. It is equipped with two tanks (each with the capacity of 1 m^3), pipes, DN80 electromagnetic flow meter, valves which allow isolation of test section for quick mounting of different pump impellers which will be tested. The inlet and outlet pipes diameters are 0.1 m and 0.08 m, respectively. The test rig has mounted a symmetrical suction elbow scaled model (which is manufactured by Plexiglas), used in general for the pumping stations units [60].

At the inlet of the pump impeller (pipe diameter 0.1 m), the test rig is equipped with a gauge transducer able to measure the pressure range between -1 ÷ +2.5 bar, while a manometer registers the pressure range between 0 ÷ 6 bar at the outlet of the pump. All the electrical signals from different sensors are connected to a dedicated acquisition data system, [61]. The main hydraulic pump parameters are presented in below table:

Table 13. Hydraulic parameters from the test rig.

Parameter	Value	Unit
Nominal pumping head H_n	44	[m]
Nominal discharge Q_n	0.0335	[m^3/s]
Nominal speed n	2900	[rpm]
Power at nominal discharge P_n	20	[kW]
Nominal efficiency	72	[%]
Characteristic speed n_q	30	[-]

The experimental investigations have been performed to assess the global performances (efficiency and cavitation) for both impellers with and without axial rotor, [62].

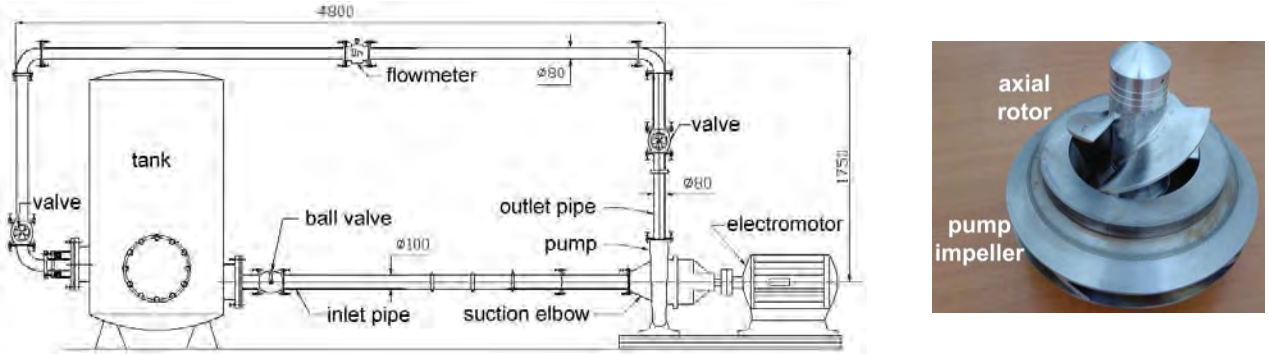

Figure 66. The experimental test rig from UPT. The dimensions are given in mm (left). The pump impeller investigated together with the axial rotor (right).

In order to investigate the pump hydrodynamics with and without the axial rotor in front of the pump impeller, 3D numerical investigation is performed. The analysis will focus on the flow field generated by the symmetrical suction elbow and ingested by the pump impeller. The numerical domain corresponds to the pump assembly for two investigated cases. For the first case (case A), the numerical domain corresponds to the cylindrical inlet pipe, symmetrical suction elbow, a cylindrical part (between the suction elbow and the pump impeller), the pump impeller, the volute and the cylindrical outlet pipe, see Figure 67 left. The impeller model with 5 blades corresponds to a prototype pump installed in a pumped storage power plant from Romania [63], [64]. The 3D numerical domain includes a cylindrical inlet pipe, a symmetrical suction elbow, an axial rotor with three blades, a pump impeller, and a volute together with cylindrical outlet pipe for the second investigated case (labelled case B). The axial rotor was designed to increase the static pressure at the pump impeller inlet improving the cavitational behavior. Additionally, a more uniform flow field at the inlet of the pump impeller is expected to be obtained downstream to axial rotor. Therefore, a surface (identical with the pump impeller inlet) in order to analyze the flow non uniformities for both cases was defined.

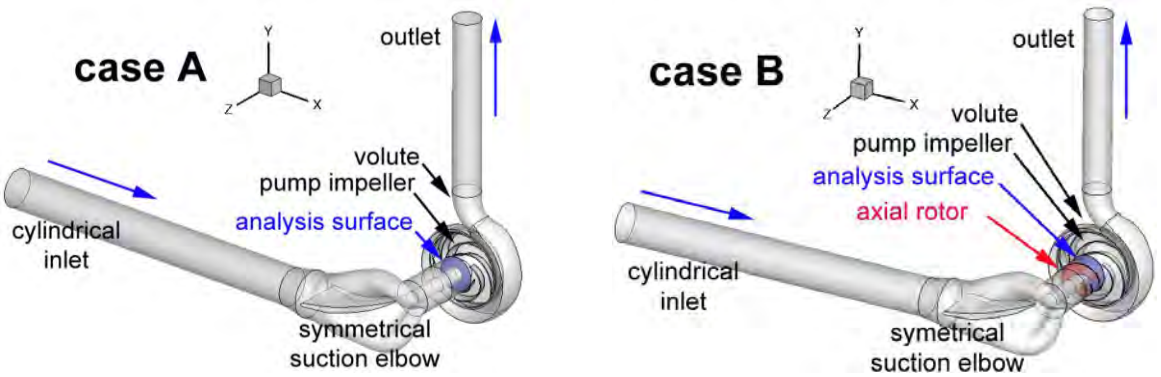

Figure 67. Tridimensional computational domains include elbow, without (left)/ with (right) axial rotor, pump impeller and volute prepared for numerical simulation.

A structured mesh of 3.3 M cells is used for case A while 4.1 M cells for the case B, respectively. The computational domains for both cases are presented in Figure 67, while Table 14 includes the detailed numerical simulation conditions.

Table 14. Mesh data and numerical conditions for the investigated cases.

Case	A	B
Type of the mesh	hexahedral	hexahedral
Total number of mesh cells	3.382.675	4.110.925
	Numerical setup	
Case	A	B
pump impeller speed	3000 rpm	3000 rpm
axial rotor speed	[-]	3000 rpm
Discharge	0.0335 m^3/s	0.0335 m^3/s
Turbulence model	k-ω SST	k-ω SST
Inlet conditions	normal velocity 3.525 m/s	normal velocity 3.525 m/s
Outlet conditions	static pressure 4 bar	static pressure 4 bar

FLUENT [65] software was used for the flow computation considering the k-ω SST turbulence model. The second order schemes and SIMPLE algorithm for coupling velocity-pressure fields are selected. The threshold value for numerical solution convergence is imposed below to 1e-6. The simulation time step, dt= 1 ms is considered in this computation with 20 inner iterations on each time step. Moreover, the mean static pressure measured experimentally at the outlet of the pump, is imposed at the outlet section of the numerical domain in both cases.

From experimental investigation and numerical simulation, the first analysis consisted of evaluating and validating the pumping head without and with axial rotor. Both cases have been compared taking into consideration the similar discharge and same pump impeller speed. For case A, the numerical simulation estimates the pumping head with 6.6% more, see Table 15. The numerical simulation estimates the pumping head with 6% more than measured value in the case of pump impeller coupled with axial rotor (case B).

Table 15. Comparison the pumping head between experimental and numerical cases.

	Cases	Discharge [m³/s]	Head [m]	Error [%]
without axial rotor (case A)	Experimental investigation	0.0335	45.2	6.6%
	3D numerical simulation		48.2	
with axial rotor (case B)	Experimental investigation		45.2	6%
	3D numerical simulation		47.9	

One can observe in Table 15 that the pumping head remains practically unchanged when the axial rotor is installed in front of the pump impeller, [62]. However, the axial rotor is expected to increase the static pressure and flow incidence on the impeller blades. Accordingly, our analysis focus on following two aspects: (i) the distribution of the minimum static pressure and (ii) the distribution of the flow at the inlet of the pump impeller.

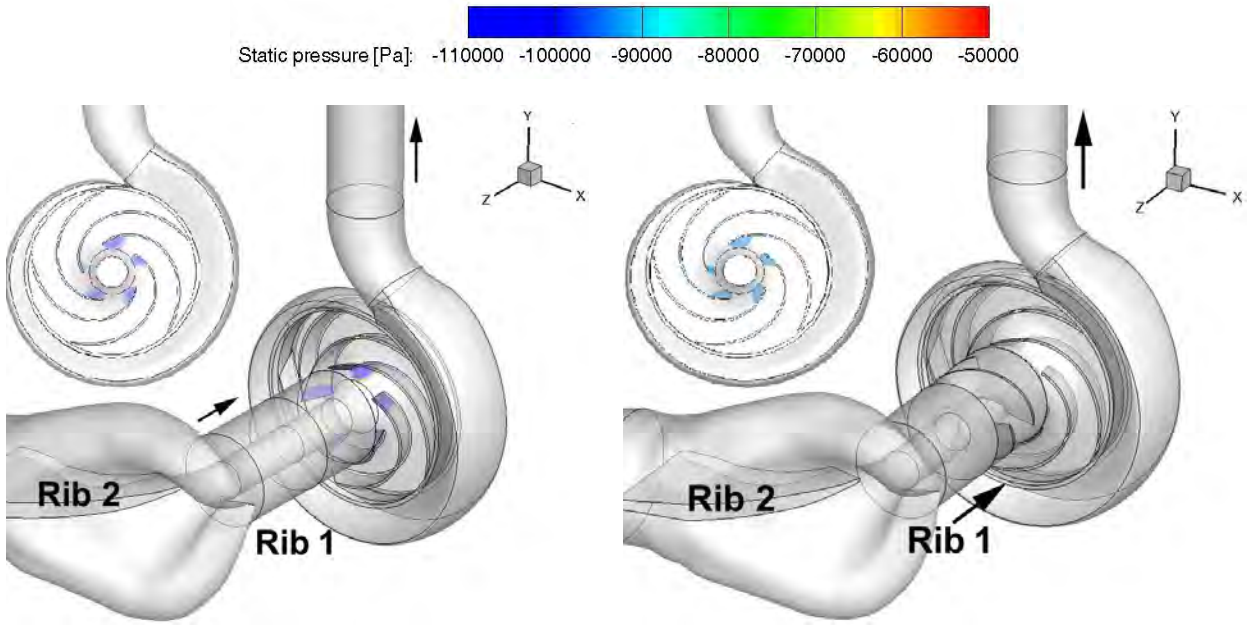

Figure 68. Minimum pressure regions: case A (left), case B (right)

The location of the minimum pressure in both cases is evidenced in Figure 68. As it is expected, the minimum pressure region (light blue spot) is identified for case A (pump impeller only) on the suction side of each pump impeller blade near to the leading edge. Moreover, the minimum static pressure region is significantly different from one blade to another due to the non-uniform flow field generated by the suction elbow. The minimum pressure region is passed from the pump impeller blades to the inducer blades when the axial rotor is mounted in front of the pump impeller (case B). Moreover, the extension of the regions with minimum static pressure is diminished. As a result, the

cavitational behaviour of the pump is improved. This statement is supported by the experimental investigations performed on the test rig [61].

The tangential velocity component has a non-uniform distribution provided by vortices generated by three-dimensional complex geometry of the symmetrical suction elbow mounted upstream to the pump impeller. This provides a circumferential distribution of the relative flow angle β at the leading edge of the blades of the pump impeller, which causes unsteady loadings on its. A cross section located at the inlet of the pump impeller is defined (see Figure 67 - *analysis surface*) in order to be investigated the distribution of the relative flow angle β for both cases. The relative flow angle β distribution on this cross section is only generated by the symmetrical suction elbow for the case A while its distribution for case B is mainly influenced by the axial rotor and less by the symmetrical suction elbow.

The relative flow angle β is defined according to the following formula:

$$\beta = arctan\left(\frac{v_m}{u - v_u}\right) \tag{11}$$

where:

$$v_m = \sqrt{v_a^2 + v_r^2} \tag{12}$$

$$u = r \cdot \omega \tag{13}$$

$$\omega = \frac{\pi \cdot n}{30} \tag{14}$$

The relative flow angle β takes into consideration the meridian velocity v_m (composed by in axial velocity v_a and radial velocity v_r), the transport velocity u and the tangential velocity v_u.

According with Figure 69 for the case with pump impeller only (case A), the relative flow angle β has a consistent variation near the sleeve and casing. The maximum non-uniformity of the relative flow angle is concentrated in two opposite regions. For this case the variation is between ±10°, while in the middle of the surface the relative flow angle varies between ±5°.

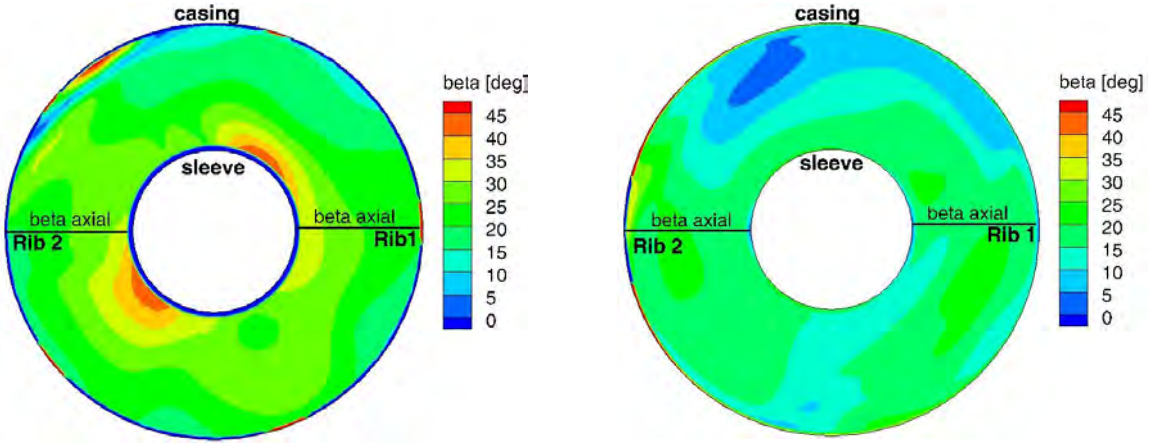

Figure 69. Distribution of the relative flow angle β on the cross section located at the

inlet of the pump impeller for both cases: case A (left) and case B (right)

When the axial rotor is installed in front of the pump impeller (case B), a maximum variation is observed near the casing of ±10°, while in the middle of the surface and close to the sleeve the maximum variation is between ±3°. From the quantitative evaluation of the relative flow angle, one can observe a large non uniformity for case A. Once the axial rotor is mounted in front of the pump impeller, the relative flow angle β became more uniform on cross section located upstream to the pump impeller. However, it can be seen a minimum area near the casing due to the non-uniformity created by the symmetrical suction elbow and ingested by the axial rotor.

Particularly, the relative flow angle β is determined on the horizontal lines located downstream to both ribs (Rib 1 and Rib 2) in order to be quantified the flow field deviation from axial flow, Figure 70.

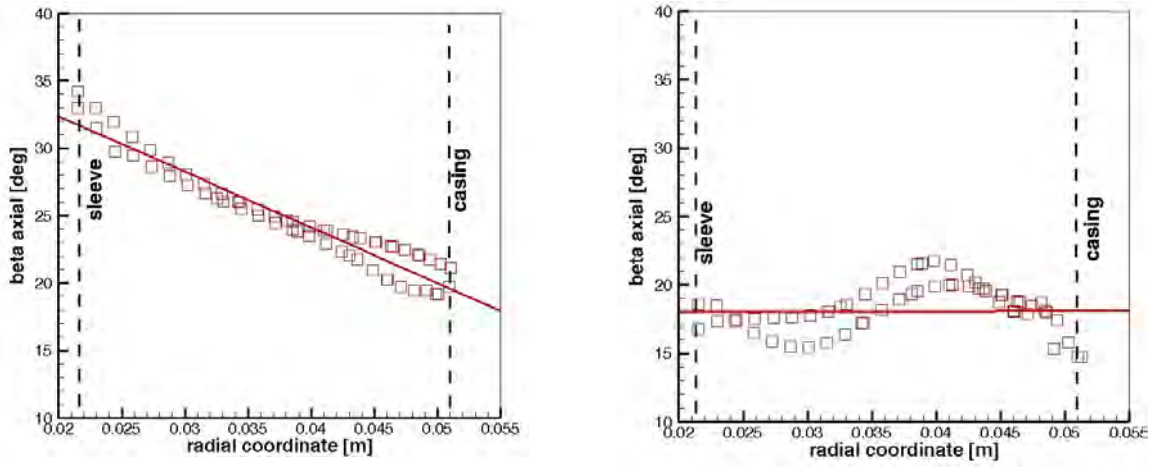

Figure 70. The radial distribution of the relative flow angle β on the horizontal lines located downstream to both ribs: case A (left) and case B (right)

As a result, this distribution reveals an excess near the sleeve and a deficit near the casing for case A (pump impeller only - left). When the axial rotor is mounted in front of the pump impeller (case B) the distribution can be considered practically constant from sleeve to casing. From a hydrodynamic point of view, a constant radial distribution of the relative flow angle from sleeve to casing is preferred, [66].

The deviation angle (i) from axial flow is computed extracting the radial distribution of the relative flow angle associated to the axial flow inlet (Figure 70) and from the relative flow angle at the inlet of the pump impeller plotted in Figure 69. For case A the deviation angle is directly affected by the flow from the symmetrical suction elbow, while for case B the deviation angle takes into consideration the flow from the symmetrical suction elbow and the influence of the axial rotor mounted in front of the pump impeller. Accordingly, the incidence angle was calculated with the following formula:

$$i = \beta - \beta_{axial} \tag{15}$$

Consequently, a non-uniform deviation angle can be observed for case A, Figure 71. This non-uniform flow from the impeller inlet induces an unsteady loading on the pump impeller blades. For case B the deviation angle tends to have a constant distribution, leading to a more uniform blade loading.

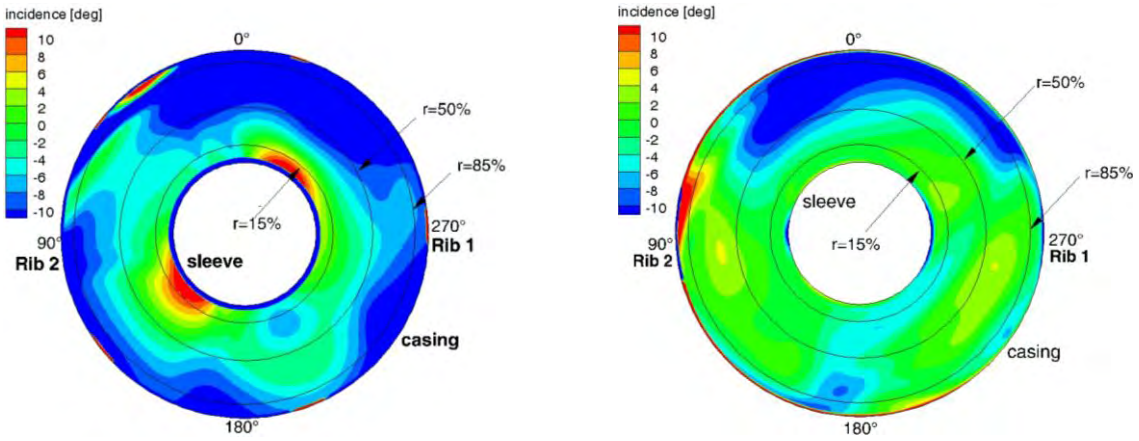

Figure 71. The deviation angle map on the cross section located at the inlet of the pump impeller: case A (left) and case B (right)

On the other hand, in order to quantitatively evaluate the deviation angle three circles (near to hub labelled, r=15% near the sleeve, in the middle r=50%, and near to casing r=85%) are figured out in Figure 71. The distribution of the deviation angle for both cases is shown in Figure 72.

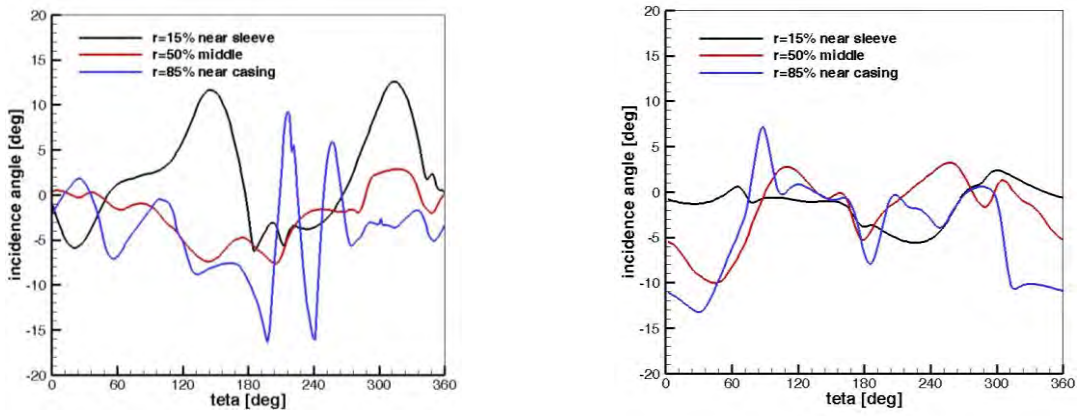

Figure 72. The deviation angle plotted on three circles located on the cross section located at the pump impeller inlet: case A (left) and case B (right)

For pump impeller only (case A), the deviation angle has a variation of ±10° near the sleeve and casing. When the axial rotor is used (case B), the deviation angle varies near the casing, while in the middle and near the sleeve is approximately obtained a constant distribution on all section. In our case, a more uniform deviation angle is obtained for case B using the axial rotor in front of the pump impeller. In this case the appropriate deviation angle covers 85% on the inlet cross section,

while for case A the appropriate deviation angle covers only 40% on the inlet cross section of the pump impeller, respectively. Clearly, a more uniform flow field is ingested by the pump impeller when an axial rotor is installed upstream to it in order to "mix" the non-uniformity generated by the suction elbow.

The study presented experimental and full 3D numerical investigations performed into a centrifugal pump in order to evaluate the hydrodynamic behavior at the pump impeller inlet. Two cases are investigated: the first case with pump impeller only and the second case with the axial rotor mounted in front of the same pump impeller. The axial rotor was designed in order to increase the static pressure at the pump inlet in order to improve the cavitation behavior. Firstly, the pumping head is experimentally obtained. The numerical results for both cases are validated against experimental data to assess the accuracy of the numerical procedure. Secondly, the minimum static pressure was identified based on numerical investigation. The analysis showed that once the axial rotor is mounted, the minimum pressure increases and moreover is moved from the leading edge of the impeller blades to the inducer domain. As a result, when the axial rotor is mounted in front of the pump, the impeller improves the cavitational behavior. Next, the non-uniformity flow generated by suction elbow is deeply analyzed because it is ingested by the impeller. The relative flow angle β and the deviation angle I have been calculated at the pump impeller inlet. When the axial rotor is used, the deviation angle is improved with 40%. As a result, a more uniform flow field is ingested by the pump impeller when an axial rotor is installed upstream to it to "mix" the non-uniformity generated by the suction elbow.

MR clutch for variable speed of the axial inducer.

Several investigations of the flow upstream the impeller have underlined the unsteady phenomena generated by the suction elbow and shaft, [58], [63]. They performed a detailed experimental investigation of the flow in radial and tangential suction chambers of a compressor or centrifugal pumps in order to identify the flow structure. Three flow separation regions are identified based on these investigations: the first region is located where the pipe diverges, the second one is displaced on the convex side of the inlet bend were the flow turns from radial to axial and the third zone is behind the shaft. As a result, the hydrodynamic performances of the pump are deteriorated as well as unsteady phenomena are generated.

Different engineering solutions can be evaluated to diminish the non-uniformity generated by the suction elbow. The straight engineering solution is to change the suction elbow, but it is unfeasible from economical point of view. Alternatively, an inducer can be installed in front of the impeller, [59], [43]. An inducer is a device attached to the impeller eye that is usually shaped like a screw that helps to increase the static pressure of the impeller. The inducer transfers the "low pressure" point from the eye of the pump impeller to the entrance of the inducer itself. The inducer is manufactured with constant blade thickness and rounded leading and trailing edges. The inducer is installed on the pump shaft together with the impeller spinning with the same speed. In this case, the flow non-uniformity will be decreased, and the static pressure will be increased at the impeller inlet. Consequently, the efficiency behaviour remains unchanged while the cavitational behaviour is improved. The inducer is an important part of many industrial pumps and the rocket turbo pumps for which very low inlet pressure is available. From the assembly between inducer and centrifugal impeller, the inducer usually works in cavitation and is often replaced, [15]. Moisa et al. designed an axial rotor with 3 blades. The axial rotor design procedure is based on inverse design method where the inflow and outflow conditions are known. Axial flow is considered as an upstream condition while the downstream swirling flow is suited for the pump impeller inlet, respectively. The key ingredient in this procedure is the loading shape which provides the blade geometry of the axial rotor from leading edge to trailing edge. The axial rotor terminology has been coined by Schilling et al. According with Schilling, the axial rotor is an axial bladed rotor with profiled blades while the inducer has a simple construction with bended blades; the main task of it is to generate a sufficiently high-pressure level at the impeller inlet. Our experimental investigations had clearly assessed the cavitational behavior of the pump with an axial rotor at a constant speed of 3000 rpm, [67].

On this study a new concept is numerically explored in order to assess the cavitational behavior improvement on a wide operating range for a pump. This new method proposes variable speed for the axial rotor while the speed of the pump impeller is constant**,** [14]. The speed of the axial rotor can be slow down or speed up in order to adapt the inflow at the inlet of the pump impeller. The purpose of the study is to investigate numerically and experimentally the new concept. First,

three-dimensional numerical simulation is performed for all domains of the pump considering the cylindrical inlet, the elbow, the axial rotor and the collector. The axial rotor was simulated at different speeds from 2000 rpm to 3000 rpm (with a step of 100 rpm) while the pump impeller speed is kept constant at 2500 rpm. Second, the pumping head is numerically computed and validated against experimental data on the case with both axial rotor and pump impeller at constant speed of 2500 rpm. Next, the minimum pressure value is identified for all cases to assess the cavitational behavior against variable speed of the axial rotor. Also, the pressure coefficient is plotted on the middle of the blade (0.5 span wise) for the axial rotor and pump impeller blades from the numerical simulation. As a result, the minimum value of the static pressure on both axial rotor and impeller blades is identified revealing its tendency against variable speed of the axial rotor. Having confirmation of the concept from the numerical simulation, then the experimental investigations are performed to assess its performance and limitations. Next, a clutch was designed, manufactured and tested in the laboratory. Up to now, experimental tests have identified the operating domain for the clutch and efficiency tests have been determined.

The test rig on which the tests are performed is equipped with two tanks (each with the capacity of 1 m^3), pipes, DN80 electromagnetic flow meter, valves which allow isolation of test section for quick mounting of different pump impellers. The inlet and outlet pipes diameters are 0.1 m and 0.08 m, respectively. A suction elbow manufactured by Plexiglas is installed in front of the pump to allow visualization of the cavitating vortices at different operating conditions.

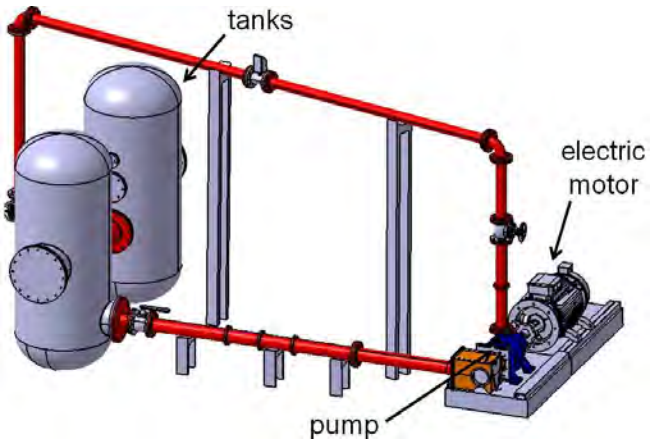

Figure 73. Sketch of the experimental test rig

The main design characteristics for the pump are nominal discharge 0.0335 m^3/s, nominal pumping head 44 m, nominal speed 3000 rpm and power at nominal discharge 20 kW. For the axial rotor the main design specifications are as follows: nominal discharge 0.03 m^3/s and nominal speed 3000 rpm. A gauge transducer is installed on the inlet pipe with the pressure range of -1 ÷ +2.5 bars, while a manometer available on the outlet pipe of the pump registers the relative pressure range between 0 ÷ 6 bars. All the electrical signals from different sensors are connected to a dedicated acquisition data system. In a first step, experimental investigations have been performed to validate

the global performances with the numerical results at 2500 rpm for the centrifugal pump and the axial rotor. On the second step, the test rig serves investigating the new control method with variable speed for the axial rotor. The experimental investigations concentrated on determining the operating regime of the axial rotor and global performances of the pump.

The 3D computational domains correspond to the pump assembly with axial rotor available on the experimental test rig. The 3D computational domains include a cylindrical inlet pipe, a suction elbow, the axial rotor with three blades, the pump impeller with five blades and the volute together with cylindrical outlet pipe, see Figure 2. The axial rotor was designed to improve the pump cavitational behavior [15]. It was numerically proved that the flow field non-uniformity delivered by the axial rotor to the pump inlet is diminished with respect to the flow non-uniformity provided by the suction elbow, [68].

3D numerical investigations are performed with a variable speed for the axial rotor, while the pump impeller has constant speed. The numerical analysis focuses on the analysis of the minimum static pressure from all 3D numerical domains and analysis of the static pressure coefficient on the axial rotor and pump impeller blades for the new investigated method.

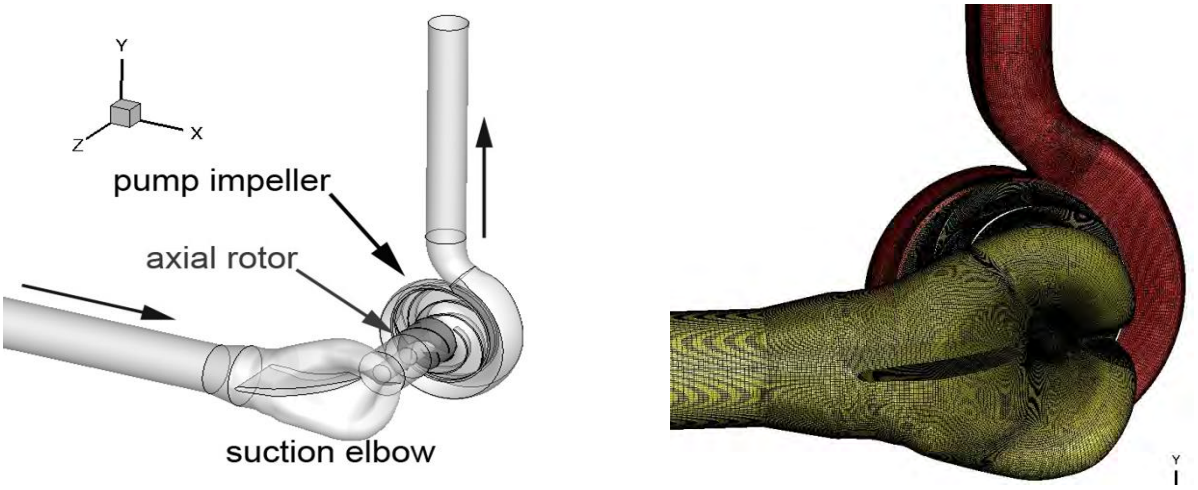

Figure 74. 3D computational domains and mesh for analysis of the centrifugal pump

The numerical simulation uses a structured mesh of 4.1 million cells. For all the cases investigated FLUENT software was used with the k-ω SST turbulence model. For coupling the velocity-pressure fields is used the SIMPLE algorithm and the second order schemes. The convergence for the numerical solution was set to 1e-6. 20 inner iterations have been considered for each step and each step is imposed to 1 msec. The main information regarding the computational domains and the setup is presented in Table 16:

Table 16: Setup and information's regarding the numerical simulation.

Mesh Type	Hexahedral/structured
Pump impeller speed	2500 rpm
Axial rotor speed	2000 ÷ 3000 rpm - 11 investigated cases
Discharge	0.02768 m^3/sec
Turbulence model	k-ω SST
Inlet conditions	normal velocity 3.525 m/s
Outlet conditions	static pressure 2 bar

According to Table 16, the pump impeller is simulated in all cases at a speed of 2500 rpm and a discharge Q = 0.02768 m^3/sec. For the design of the pump impeller was used a speed of 3000 rpm and a discharge of Q_n = 0.0335 m^3/sec. For this investigation a smaller speed for the pump impeller was considered 2500 rpm. Similarly, the axial rotor was designed at 1.2Q = 0.0402 with a speed of 3000 rpm.

A structured mesh with 4.7 M cells is considered for all computational domains. 1.6 M cells are considered for the inlet pipe and suction elbow domain. The axial rotor has approximately 0.9 M cells, around 1.2 M cells have the pump impeller computational domain and 1 M cells on the volute together with outlet pipe. Three interfaces located between the suction elbow - axial rotor, axial rotor - impeller and the impeller - volute are employed in the computation. The grid independency was clarified in [69], accordingly the numerical investigation related in the paper has the optimum mesh.

From the experimental investigation and numerical simulation, the first analysis consisted in evaluation of the pumping head with the axial rotor for one case only: pump impeller and axial rotor at same speed 2500 rpm and nominal discharge value Q = 0.02768 m^3/s. The experimental pumping head was 34.7 m, while the numerical value is 33.9 m. One can observe that the pumping head deviation between numerical value and experimental data is approximately 2%.

Once the numerical model was validated, our numerical analysis focuses on three aspects: (i) the minimum static pressure obtained for each speed value of the axial rotor (ii) the distribution of static pressure coefficient on the axial rotor and pump impeller blades and (iii) the total torque generated by the axial rotor and speed decrease and speed increase.

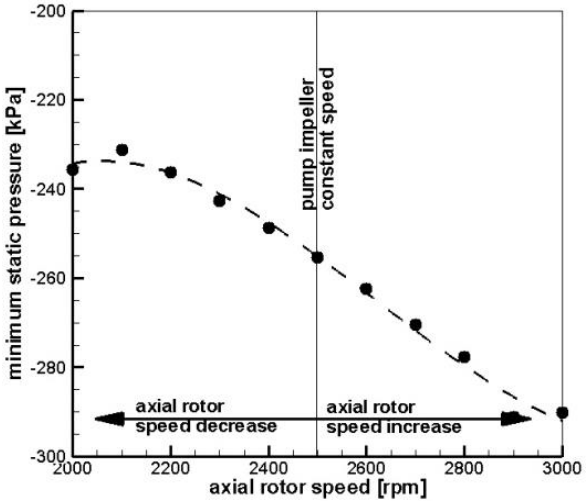

Figure 75. Minimum static pressure for 3D numerical simulation domain of the pump

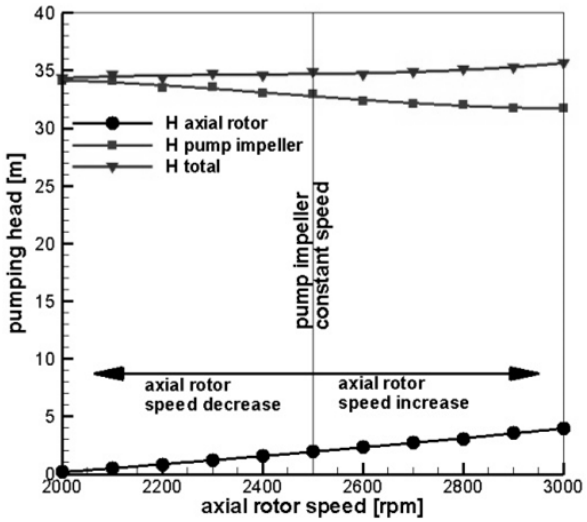

Figure 76. Evolution of total pumping head for each component (axial rotor and pump impeller) at a variable speed of the axial rotor.

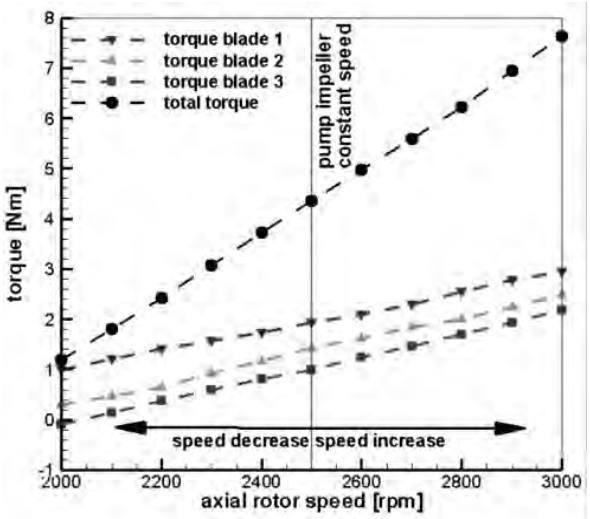

Figure 77. Evolution of total moment for the axial rotor at variable speed.

The first graph from the evaluation of the numerical simulation was to represent the minimum static pressure calculated in all 3D numerical domains for each speed of the axial rotor, Figure 75. The purpose of this is to assess the cavitational behavior of the pump. In Figure 75, it is observed that for decreasing the axial rotor speed, the static pressure increases by approximately 8% (improves the cavitational behavior in the pump). The minimum static pressure decreases when the axial rotor increases speed, as a result the pump is sensitive at the cavitation. Note that the minimum static pressure is always on the axial rotor blades. It is clearly shown that at nominal discharge, the minimum static pressure is increased and the cavitational behavior is improved when the speed of the axial rotor is slow down. Moreover, if it is determined the total pumping head, remains constant for all regimes. The head is balanced between the axial rotor and pump impeller. An important component on this analysis was to calculate the torque on each axial rotor blade, followed by the total torque generated by the axial rotor, see Figure 77. One can observe that at same speed as the pump impeller (2500 rpm), the total torque generated by the axial rotor is 4.5 Nm, the total torque increases at 7.5 Nm (with 66 % more) when the axial rotor speeds up and at minimum speed for the axial rotor the total torque is around 1Nm. Accordingly, the calculated total torque and the speed will be the main parameters in order to design the clutch for the pump. A first conclusion regarding the axial rotor with variable speed is that global performances of the pump are not modified; an increase of the static pressure with approximately 8% is registered when the axial rotor slows down.

The second numerical investigation consists in the analysis of the static pressure coefficient. The static pressure coefficient is defined as follows:

$$c_p = \frac{\mathrm{p} - \mathrm{p_{inlet}}}{\rho g H} \tag{16}$$

where p represents the static pressure and p_{inlet} represent the average static pressure at the inlet of the axial rotor.

The evaluation of the pressure coefficient for the axial rotor and pump impeller was made for the middle of the blade at 0.5 span wise. On this span wise, the analysis was performed for one blade of the axial rotor and one blade of the pump impeller, Figure 78. The speed of the axial rotor was modified from 2000 rpm to 3000 rpm with a step of 100 rpm, while the pump impeller speed was kept constant at 2500 rpm. The pressure coefficient at 2500 rpm for axial rotor and pump impeller is considered as reference (gray with points) in all plots. Also, the graphs contain variation of cavitation coefficient σ, calculated according to the following equation:

$$\sigma = \frac{\mathrm{p_{inlet}} - \mathrm{p_v}}{\rho g H} \tag{17}$$

where p_{inlet} is the static pressure at pump impeller inlet, p_v is the vaporization pressure at 10°C.

In case of slowing down the speed of axial rotor (2400 rpm), the pressure coefficient on the axial rotor remains approximately unchanged with respect to the speed reference (2500 rpm), see Figure **79**. Conversely, on the pump impeller pressure side the coefficient is decreasing close to the leading edge. Moreover, on the suction side it is observed that pressure increases close to the leading edge with 60%. This increase will lead to less cavitation on the pump impeller blades. If the speed of the axial rotor slows down to more than 2300 rpm up to 2000 rpm, the minimum pressure is increased both on axial rotor and pump impeller blades. When the axial rotor increases the speed (3000 rpm) it is observed that on the pressure side we have the same pressure coefficient as for reference 2500 rpm, see Figure **79**, down.

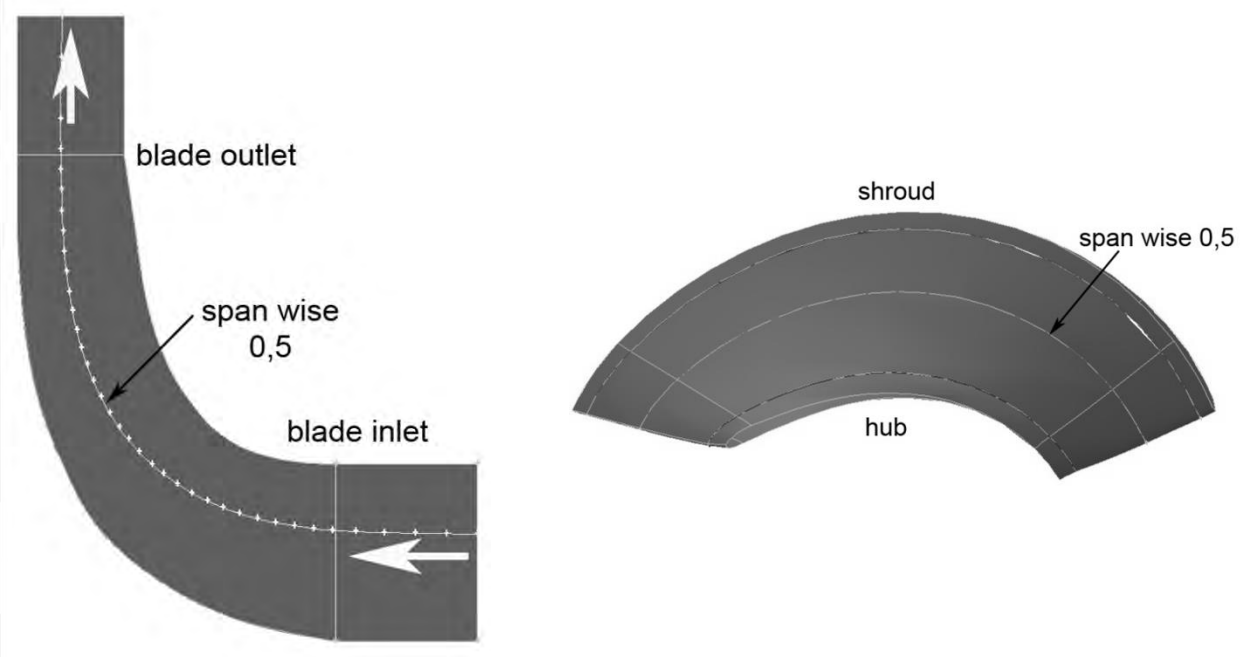

Figure 78. Location of the investigated span wises for pump impeller (left) and axial rotor (right).

Moreover, on the suction side of the pump impeller the pressure is improved close to the leading edge. As a conclusion, if the speed of the axial rotor slows down, the impact point at the inlet of the pump impeller moves on the suction side of the blade, and when the speed increase the impact point tends to pass on the pressure side of pump impeller blade. Nevertheless, the variable speed of the axial rotor increases the pressure at the pump impeller blade inlet, improving the cavitational behavior.

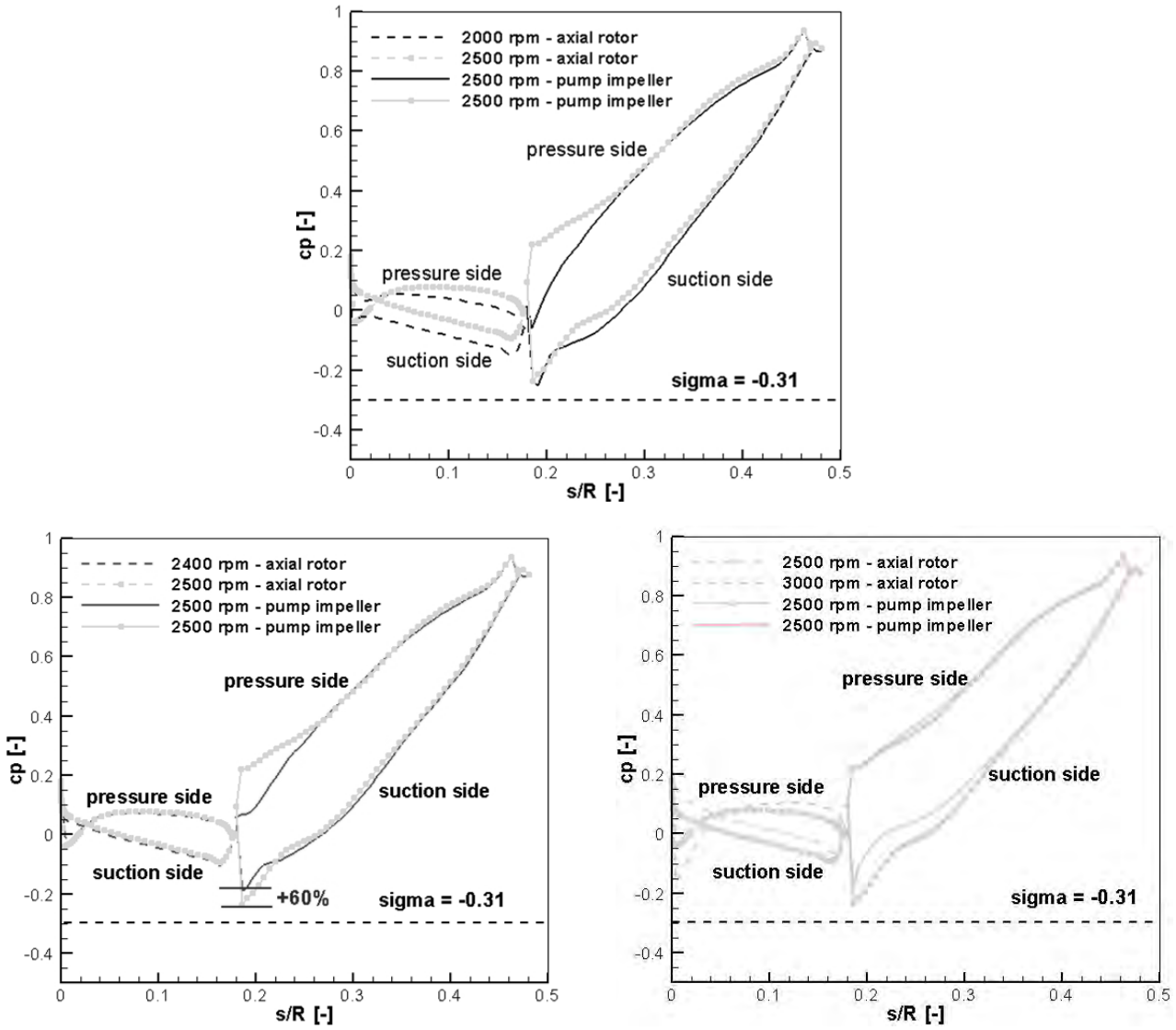

Figure 79. Blade loadings for the axial rotor and the pump impeller at 2000, 2400 and 3000 rpm speeds for axial rotor and speed reference at 2500 rpm.

To have a clear image regarding the evolution of the pressure coefficient, Figure **80** presents the evolution of the minimum value of the pressure coefficient on the blade of the pump impeller. The best operating conditions for the blades of the pump impeller are given when the axial rotor has lower speeds. The operating domain of the axial rotor is between 2400 - 2200 rpm, while the pump impeller has the same speed of 2500 rpm.

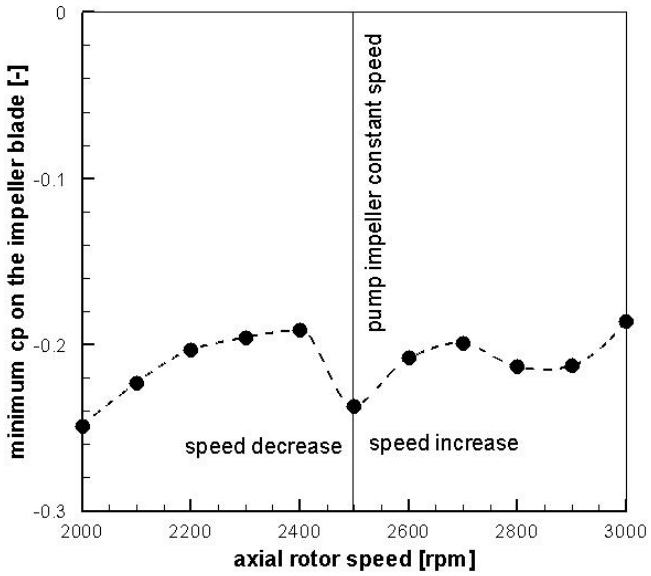

Figure 80. Minimum static pressure coefficient for the pump impeller blade.

According to numerical investigations performed on the pump (cylindrical inlet, suction elbow, axial rotor with variable speed, pump impeller and collector), when the axial rotor is slowing down with maximum 15% from the speed of the pump impeller (2200 rpm minimum speed), the minimum value of the static pressure on impeller blades is increasing. As a result, for the experimental investigations, the decision was made to design and test a device which will reduce the speed of the axial rotor only. The device used is a clutch with the function to keep the same speed for the pump impeller as the speed of the electrical motor and reduce the speed for the axial rotor in a controlled way. The clutch is a magneto-rheological device used to impose speed controlled by the viscosity of the magneto-rheological fluids.

Magneto-rheological fluids have been applied at the beginning of 1948, when Rabinow [5] developed a clutch device. According with Rabinow, the advantages of using this kind of clutches with magneto-rheological fluids are the amount of electrical power necessary to control is negligible while the time response is also small. Since then, magneto-rheological fluids have been implemented in many applications. Several important applications can be found in: sensors [70], actuators [71], dampers [72] [6], brakes [3], [4], seals (especially in the case of gas transporting installations [73].

Magneto-rheological clutches are an important research direction concerning these smart materials. Some of the advantages are convenient low-power control (through electrically generated magnetic field) and very good torque to weight ratio. The latter recommends them for applications where small devices able to generate high value of torque are needed, [9], [10]. The electrical control possibility (the magnetic field can easily be electrically generated and controlled) is a very important advantage. The next figure presents a sketch of our pump equipped with the magneto-rheological clutch for slowing down the axial rotor.

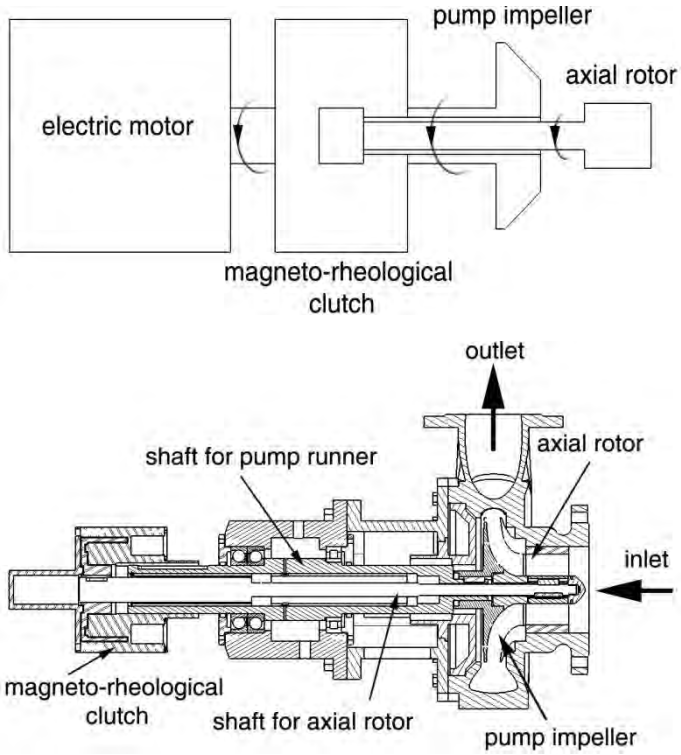

Figure 81. Pump solution for variable speed of the axial rotor with MR clutch, sketch (up) and detail on the chosen pump clutch solution (down).

According to the sketch presented in the above figure (Figure **81** up); the chosen solution has an electrical motor in order to drive the clutch and the pump impeller. The pump is designed that the speed of the electric motor and the pump impeller should be the same, while the clutch serves as a coupling for the pump impeller and a gear for the axial rotor. Note that the axial rotor on this configuration can have same speed as the pump impeller or less. In the clutch an important component is the coil, which helps to modify the magnetic field inside the clutch and the viscosity of the magneto-rheological fluid responsible for the speed control, respectively. The coil power and the magnetic field inside the gap where the magneto-rheological fluid is inserted have been measured at the beginning of the tests, to check the system functionality.

The first experimental evaluation was performed to measure the speed of the axial rotor for three separate cases, as in Figure 82. To measure the speed, a waterproof proximity sensor was mounted close to the axial rotor blades and was connected in the acquisition data system. In the first case (axial rotor runaway speed), the axial rotor was connected at the shaft without the clutch. For the second case (axial rotor with MR clutch 0 V) the axial rotor was connected with the magneto-rheological clutch, but no electrical current was applied. For this case, only the viscous effects of the magneto-rheological fluid have been considered.

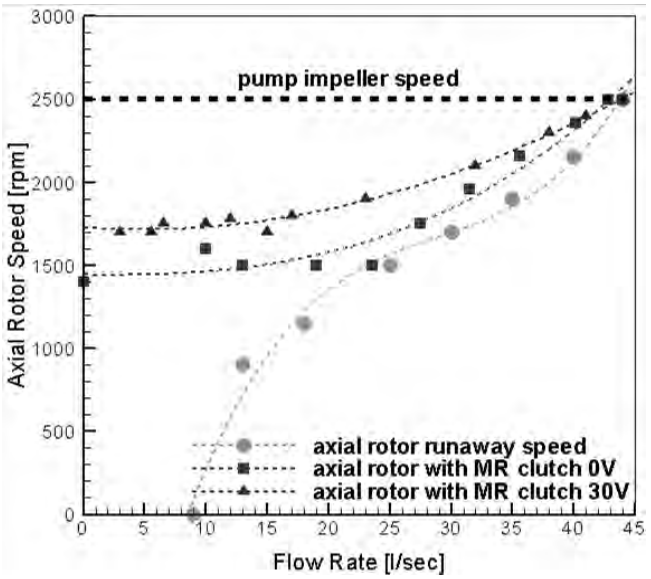

Figure 82. MR clutch operating domain for three investigated cases: axial rotor at runaway speed, axial rotor with clutch at 0 v and axial rotor with clutch at 30 v.

For the third case, the magneto-rheological clutch was connected at the DC source and 30 V were applied on the coil. Accordingly, the viscosity of the magneto-rheological fluid was increased. The speed measurement of the axial rotor gives us the operating range for each case. As a result, at the maxim flow rate of 44 l/sec, the axial rotor has the same speed for all three cases (2500 rpm). When it is operated at runaway speed, the axial rotor is blocked (0 rpm) at 9 l/sec (30% from the nominal flow rate). When the axial rotor is attached at the magneto-rheological clutch and 0 V applied, the minimum speed is around 1400 rpm (44 % less than pump impeller speed). When the magneto-rheological clutch is activated (30 V applied on the coil), the minimum speed for the axial rotor is around 1750 rpm (30 % less than pump impeller speed). Note that the operating domain for the MR clutch can be modified by using another magneto-rheological fluid (with other viscosity) or by increasing the coil voltage.

Next, a second experimental analysis consisted of evaluating the global performances of the pump when the axial rotor has variable speed for the classical configuration in pumps (rigid pump impeller and axial rotor) and the cases when the clutch is connected with the axial rotor at 0 V and 30 V applied voltage at the coil clutch. The global performances are presented in dimensionless forms as follows: discharge coefficient, head coefficient, power coefficient and efficiency.

The discharge coefficient is defined as follows:

$$\varphi = \frac{\mathrm{Q}}{\pi \omega R_{ref}^3} \tag{18}$$

, where ω represent the angular speed of the pump impeller, R_{ref} represent the reference radius, in our case the inlet of the pump.

The head coefficient is calculated with the formula:

$$\psi = \frac{2gH}{\omega^2 R_{ref}^2} \tag{19}$$

The power coefficient was calculated with the formula:

$$\lambda = \frac{P_m}{\rho\omega^3 R_{ref}^5} \tag{20}$$

Efficiency:

$$\eta = \frac{\rho gQH}{P_m} \tag{21}$$

According to Figure 83 a), the head coefficient remains approximately constant, with a variation of ± 2 %, for all investigated cases. Even if the axial rotor has variable speed for two cases (MR clutch at 0 and 30 V) the head coefficient remains the same for all cases, while the pumping head for the axial rotor and pump impeller is balanced between. In the case of the measured power coefficient, a difference of 10% larger for cases with magneto-rheological clutch for small flow rates is observed. This is related to the fact that a series of new bearings and seals have been mounted on the pump for the shaft of the pump impeller and the shaft of the axial rotor. Also, this difference is observed in the efficiency of the pump, which is smaller in the case of using the magneto-rheological clutch. As a conclusion, for the experimental tests performed up to now, the head coefficient remains approximately unchanged, while the power coefficient and the efficiency is smaller in case of using the magneto-rheological clutch for the pump due to new bearings and seals. Further cavitational investigations will tell us if the behavior can be improved how it was demonstrated in numerical simulations performed up to now.

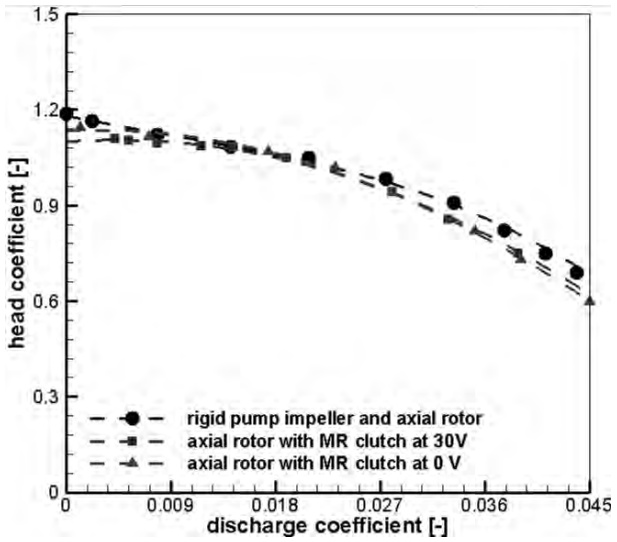

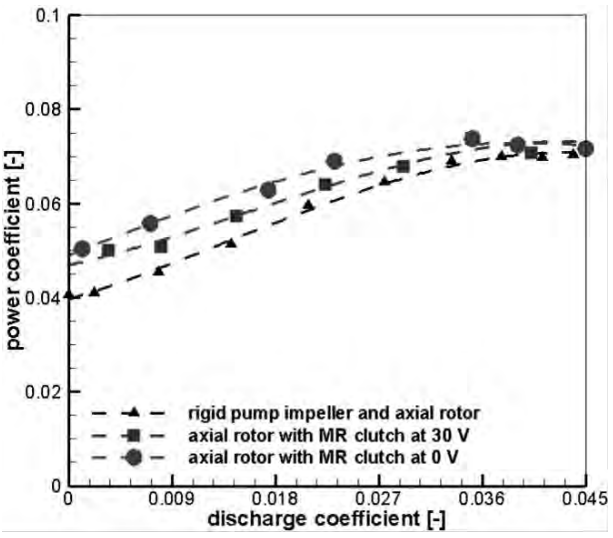

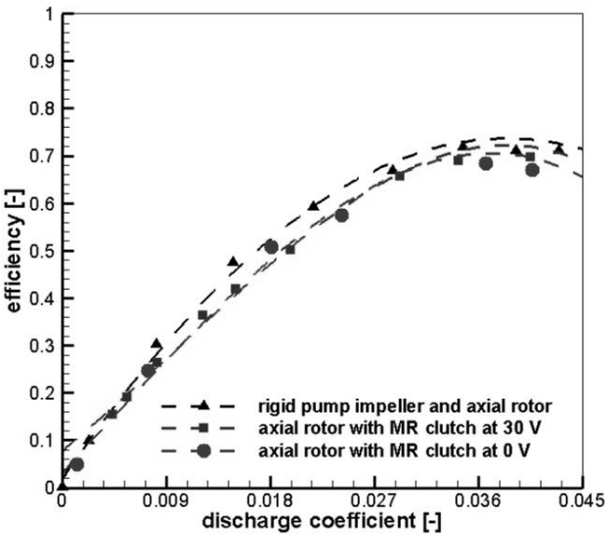

Figure 83. Experimental investigations of the global performances (head coefficient, power coefficient and efficiency) for the pump with axial rotor at variable speed.

The method proposes variable speed for the axial rotor while the speed of the pump impeller is kept constant. Extensive numerical investigations reveal the efficiency of this method. The numerical results establish an increase of the minimum static pressure from the numerical domain (8%) when the speed of the axial rotor is reduced by 15% from the speed of the pump impeller. Also, when the speed of the axial rotor slows down, the pressure coefficient (especially on the pump impeller blades) is improved.

Having validation of the numerical investigation, the method was put into practice on the laboratory. A magneto-rheological clutch was chosen to control the speed of the axial rotor. The reason for choosing this speed controller is related to small dimensions, easy to control and robustness.

In the last part, the operating regime for the magneto-rheological clutch and the global performances for the pump with this method have been measured. The global performance proves that the head coefficient remains approximately constant, even if the axial rotor has variable speed. The power coefficient and the efficiency are diminished due to the seals attached to the centrifugal pump. Further, experimental cavitational investigations will indicate the efficiency of the new method.

(C-iv) Performance assessment in hydraulic turbomachines

Dynamic measurements in hydraulic machines.

A significant part of my research development in the field of hydraulic turbomachinery was achieved through an international research project funded by an International Short Visit Grant from the Swiss National Science Foundation (SNSF). The research was conducted at the Hydraulic Machinery Laboratory of HES-SO Valais-Wallis, Switzerland, as part of the project titled "Development and Implementation of a Dynamic Method to Measure the Performances of Hydraulic Machines" (Project No. IZK0Z2_163500, 2015), under the coordination of Prof. Dr. Eng. Cécile Münch-Alligné. This project focused on the development and validation of a dynamic measurement methodology designed to capture the transient behavior and real-time performance of hydraulic machines. During the four-month research period (June–September 2015), I was directly involved in the experimental campaign, including the installation and calibration of instrumentation, acquisition of high-resolution dynamic data, and post-processing using both time-domain and frequency-domain analysis techniques. The work was carried out in close collaboration with Dr. Eng. Vlad Hasmatuchi, whose expertise in experimental hydraulics supported the successful implementation of the dynamic measurement system.

The implementation of the so-called “sliding-gate” dynamic method to measure in a faster way (up to ten times) the efficiency characteristics on hydraulic turbomachinery is presented. The new model testing measurement method is successfully applied on two different cases dedicated to recover the energy lost in release valves of water supply networks: a 2.65 kW double-regulated laboratory prototype of an in-line axial microturbine with two independent variable speed counter-rotating runners; a 11 kW multi-stage centrifugal pump as turbine (PAT) with variable speed.

The universal test rig of the HES-SO Valais/Wallis, Switzerland, dedicated to assessing hydraulic performances of small-power turbomachines, has been employed. The applied procedure consists, in a first step, on measuring the 3D hill-chart of a given testing model (turbine or pump) by the classical static point-by-point method. Then, a second digitizer is added to acquire synchronized dynamic signals of the sensors in parallel with the existing acquisition/control system of the test rig. The dynamic measurements of efficiency are performed at different constant speeds of the test rig recirculating pumps while increasing and/or decreasing the speed of the testing model runner(s) from zero to maximum, and vice versa, slowly enough in order to keep a steady-state operation. In the end, the resulting 3D efficiency hill-charts of the two tested machines obtained by the dynamic and by the classical static point-by-point measurement methods are compared, with the measurement precision and repeatability particularly emphasized.

Historically, the main objective of model testing was to cast predictions on the performances of an industrial machine. Nowadays, it plays the additional role of addressing a large number of

contracts guarantees, [74]. Furthermore, while the progress of technologies employed on the test rigs has conducted to an increasing level of measurement accuracy, the role of the experimenter remains crucial to ensure reliable and accurate measurements.

In hydraulic turbine development, for both new- or refurbishment projects, either of large or of small scale, model tests remain often mandatory. Further, numerical simulation has been established as a complementary relatively cost-efficient tool to predict hydraulic efficiency and flow hydrodynamics mainly in the normal operating range. However, regarding the characteristics at off-design conditions, experimental investigation remains often irreplaceable. In addition, the dynamic behavior in transient operation can sometimes be drawn only experimentally.

According to the IEC [75] standard recommendations, hydraulic performance is retrieved by steady-state point-by-point measurements over the whole operating range of a turbomachine. This classical method, beyond the fact that is largely proved, it allows reliable and accurate measurements. However, requiring a large time necessary to reach a steady operating condition and usually several additional dozens of seconds of acquisition time to calculate valid average values of different parameters, the method is relatively time expensive.

Focusing on small hydro (as well as on mini-, micro-, and pico-hydro), [76], as the budget allocated to the development is much more limited (compared to the large-hydro), the total men-hours investment dedicated to the performance measurements must be reduced as much as possible. From this aspect, with the main purpose of reducing the time necessary to perform the full hydraulic performance tests of a turbomachine, a new dynamic method has been implemented and validated in [77]. This technique is an adaptation of the so-called "sliding-gate" method, successfully used for index testing of Francis and Kaplan units [78]. It consists of applying the general procedure for standard testing, but instead of using discrete gate positions, data is collected while the guide vanes are moved slowly and continuously through the desired operating range. During the tests, the motion of the gates must be slow enough so that quasi- steady-state operating condition is ensured. The "sliding-gate" method uses the same instrumentation as the classical point-by-point one, with the advantage of obtaining continuous efficiency curves over the whole operating range and with a significant reduction of the total required time to perform the tests [79]. The current work comes with two examples of implementation and validation of dynamic efficiency measurements on hydraulic turbomachinery model testing: a double-regulated axial counter-rotating variable speed microturbine and a centrifugal multi-stage variable speed pump-as-turbine. First, the experimental setup, including the employed hydraulic test rig and the two case studies are introduced. Then, the instrumentation and the experimental methodology are presented. The results focus first on the selection and validation of the optimal acceleration/deceleration ramps of the runners to ensure a steady-state condition for the dynamic measurements. Finally, the resulting hydraulic hill-charts obtained by the two methods are compared.

The universal hydraulic test rig of the HES-SO Valais//Wallis - Switzerland (see Figure 84) dedicated to small-power turbomachines has been employed to perform the hydraulic performance measurements. Its configuration, instrumentation and operation follow the IEC 60193 [75] standard recommendations on hydraulic model testing. The closed-loop circuit of the test rig is supplied by three recirculating multistage centrifugal pumps connected in parallel. The variable speed pumps (2x18.5 kW and respectively 1x5.5 kW) can deliver a maximum discharge of about 100 m^3/h and a maximum pressure of 160 mWC. The testing variable-speed model is placed in the upper part of the circuit, upstream a free-surface pressurized reservoir. The latest allows simulating a given setting level of the model, either positive or negative, and thus investigating also the cavitation performances. The operation of the test rig is ensured by an automatic system. Its customized LabVIEW interface allows for real-time measurements and displays the instantaneous values of pumps speed, discharge, testing head, water temperature, Thoma number etc. The autonomous regulation system can keep constant the pumps speeds, of the testing head or the discharge values. Finally, the wireless communication architecture between the hydraulic test rig and the measurement/monitoring systems (e.g. testing model control system) ensures safe centralization of data, storage and sharing.

Main characteristics:

Maximum head: **160 mWC**

Maximum discharge: **±100 m^3/h**

Generating power: **20 kW**

Pumping power: **2x 18.5 kW & 1x 5.5 kW**

Maximum pumps speed: **3'500/3000 rpm**

Total circuit volume: **4.5 m^3**

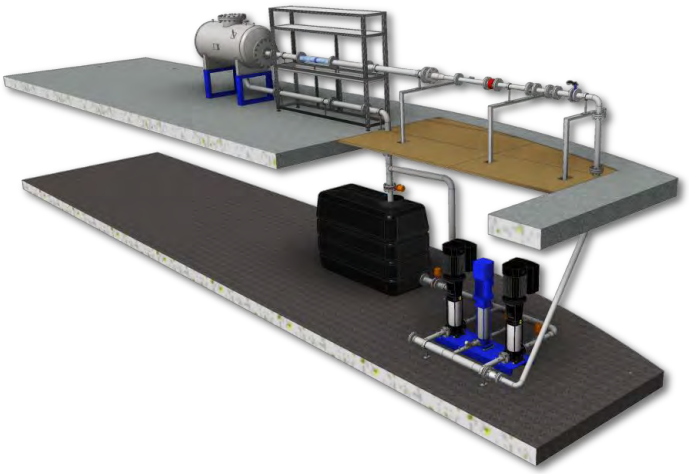

Figure 84. Hydraulic test rig (2015 version) of the HES-SO Valais//Wallis – Switzerland.

Case studies: Counter-rotating microturbine – bulb version

The first case study consists of a fully instrumented laboratory prototype of an axial microturbine with counter-rotating runners (see Figure 85) dedicated to recover the energy lost in release valves of water supply networks. Its multi-stage concept, like the one of centrifugal pumps, makes it appropriate for high head operating conditions, specific to the Pelton turbines. Indeed, each stage, composed by two counter-rotating axial runners, generally used at low head and large discharge conditions, recovers a fraction of the total head. The one-stage turbine of 2.65 kW is composed by two counter-rotating runners with respectively 5 and 7 blades. The outer diameter of the runners, as well as the pipe diameter, is 100 mm; the turbine inner diameter is 80 mm. The tested

version includes a band installed at the periphery of each runner, provided with a labyrinth, in order to limit the leakage between the tip of the blades and the outer fixed wall. At the nominal operating point (a discharge of 37.5 m^3/h and a head of 20 m), for a ratio $\alpha = N_A/N_B = 1$ between the runners absolute rotational speed, its hydraulic efficiency, obtained by numerical simulation, reaches 85% [80]. The optimal operation of the turbine is ensured by the relative rotational speed between the two runners along with their absolute rotational speed.

Further, the runners are driven by two independent electrical generators specially designed for this turbine, placed into the upstream and downstream bulbs respectively. Two frequency converters are used to drive the variable speed electrical generators at the desired constant rotational speed value, whatever the sign of the mechanical torque. Finally, for each runner, an incremental encoder, used mainly for the rotational speed driving, along with a torque meter ensure the mechanical power measurements. In addition, the wet and the dry regions of the machine are separated using a sealed magnetic coupling.

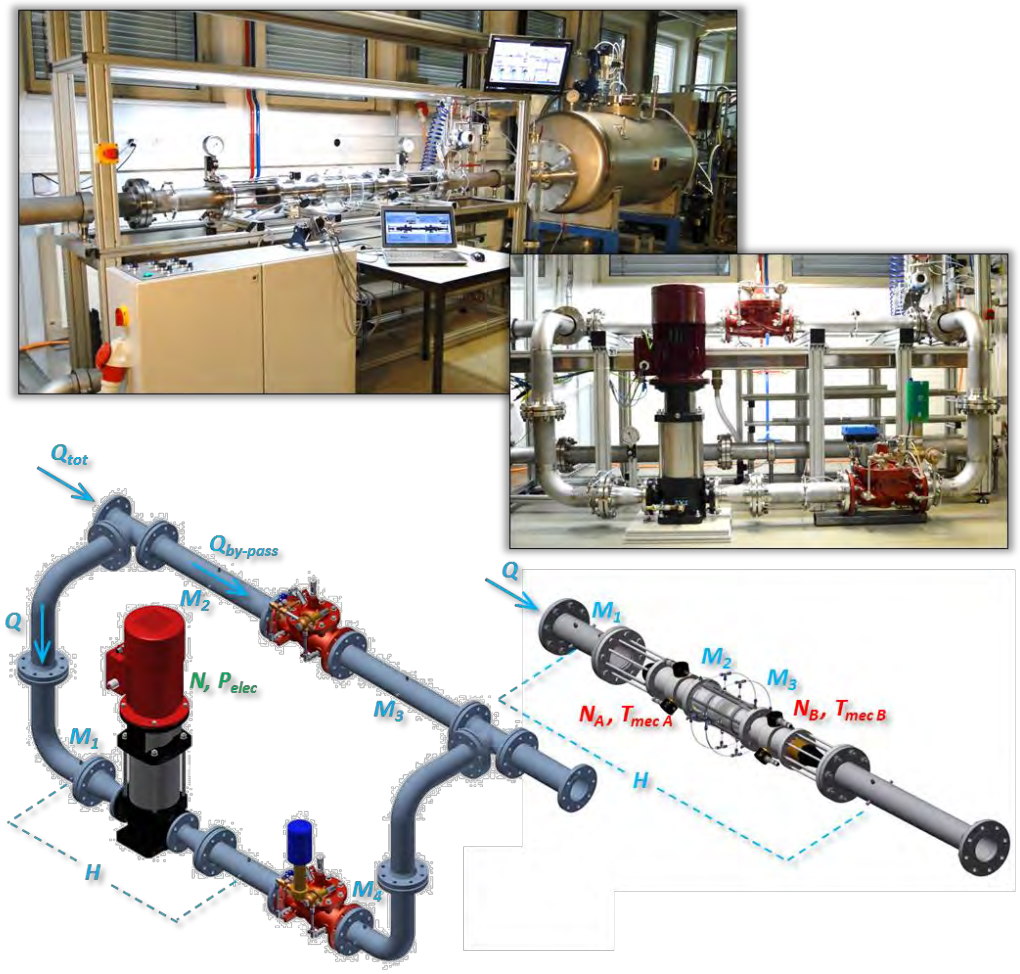

Figure 85. Experimental setup of the counter-rotating microturbine and of the PAT installed on the hydraulic test rig.

Case studies: Multi-stage centrifugal pump as turbine (PAT)

Running a standard pump as turbine is often a cost-efficient solution to recover the extra available energy of the water supply systems, and not only [81]. However, prior to the installation, its operation and control in turbine mode must be investigated, [82]. Indeed, if the hydraulic characteristics may be derived using, for example, the experimental data provided by Chapallaz et al. [83], the hydrodynamic stability mainly outside the normal operating range remains difficult or even impossible to predict without experimental tests.

In this context, a second case study dedicated to the energy recovery in water supply networks, consisting of an 11kW multi-stage centrifugal pump used as turbine (Ebara EVMG32 5-0F5/11) has been considered - see Figure 85. Its five radial-axial runners (with 5 blades each) have an inlet diameter of 136 mm and an outlet diameter of 67.5 mm. The turbine is regulated only with the help of the variable rotational speed of the runners. The permanent magnet synchronous generator, Leroy-Sommer LSRPM 132 M, with a nominal power of 15.8 kW, has been driven, in this case as well, by a frequency converter able to keep constant the desired rotational speed value, whatever the sign of the mechanical torque and the rotational speed. Concerning the instrumentation, the machine is equipped with an incremental encoder necessary for the rotational speed driving only. Therefore, for this case only the electrical power of the generator has been measured.

One may state here that the turbine has been tested in a hydraulic configuration similar to the one of the pilot site, where it has been already installed. The release valve installed on the by-pass branch, which plays the role of an existing release valve on a drinking water supply network, ensures the extra flow passage when the requested discharge is larger than the maximum flow rate of the turbine. The second release valve, placed downstream the turbine, limits the pressure at the outlet of the main branch, and therefore secures the network, whatever the operating conditions of the turbine. Moreover, in the case of discharges lower than the minimum value allowed for the turbine, or in the case of a failure, this release valve is able to cut completely the main branch, the whole discharge passing automatically through the by-pass one. Anyway, during the performance tests on the turbine, the by-pass release valve remained closed all the time, while the one of the turbine branch has been kept completely opened.

The characteristics of the main employed instruments necessary to recover the hydraulic performances of the testing model along with the testing conditions are provided in Table 17. On the one hand, the test rig is equipped with an electromagnetic flowmeter for the discharge Q, two differential pressure transducers for the head H and the setting level H_S respectively and three additional capacitive absolute pressure transducers for the static pressure at the wall $M_{1,2,3}$. The latest are connected through wall static pressure collectors, as may be seen in Figure 85. A PT100 transducer for the water temperature T and three optical tachometers for the rotational speed of the recirculation pumps $N_{p1, 2, 3}$ come to complete the main instruments.

On the other hand, the axial microturbine is equipped with two incremental encoders and two torque meters, one for each counter-rotating runner, necessary for the driving of the electrical generators and for the computation of mechanical power. Finally, an incremental encoder and a high-precision electrical multimeter are used to drive the PAT's electrical generator and to compute the electrical power.

Regarding the measurement of quantities related to the test rig (including the hydraulic power), a National Instruments (NI) cRIO 9074 autonomous digitizers, equipped with various acquisition/control modules, is used. A NI cDAQ 9174 digitizer is then employed to drive the testing model and to record the values of the rotational speed of the runners, of the mechanical torque of the runners (microturbine) and of the electrical power of the generator (PAT).

Table 17. Characteristics of the main instruments.

Acronym	Measured quantity	Sensor type	Range	Precision
Q	Discharge	Electromagnetic flowmeter	0..±100 [m^3/h]	± 0.5 [%]
H	Head	Differential pressure sensor	0..16 [bar]	± 0.1 [%]
H_s	Setting level	Differential pressure sensor	0..5 [bar]	± 0.2 [%]
$M_{1, 2, 3, 4}$	Absolute static pressure	Capacitive pressure transducer	0..10/20 [bar]	± 0.05 [%]
T	Temperature	PT100 transducer	0..100 [°C]	± 0.1 [%]
$N_{p1, 2, 3}$	Pumps rotational speed	Tachometer	0..1000 [Hz]	-
$T_{mec\ A, B}$	Mechanical torque	Torque meter	0..±7.5 [Nm]	± 1 [%]
$N_{A, B}$	Turbine rotational speed	Incremental encoder	0..7500 [rpm]	2048 [ppr]
P_{elec}	Electrical power	Precision electrical multimeter	0..1000 [Vtrms] 0..32 [Atrms]	± 0.03 [%]
N	Turbine rotational speed	Incremental encoder	0..6000 [rpm]	4096 [ppr]

In the case of classical static point-by-point method, both digitizers perform measurements and compute the average and the standard deviation values for all parameters over 8 seconds at 50 Hz (user-configurable, depending on the stability of the operating condition). In the case of dynamic measurements, a second cDAQ 9174 digitizer has been installed to acquire synchronized dynamic signals of the sensors in parallel with the existing acquisition/control systems of the test rig and of

the testing model. Its acquisition frequency has been set to 100 Hz, considered fast enough to cope with the frequency response of the employed sensors.

The experimental protocol employed to measure the hydraulic performances of both the microturbine and PAT is provided in Figure 86. First, all the instruments have been calibrated and/or rechecked before the beginning of measurements. Considering the classical point-by-point method, the measurements have been performed for 11 different testing head values to build the full efficiency 3D hill-chart of the microturbine. Moreover, 9 values of constant ratio α between the runner's absolute rotational speed were systematically considered for each constant testing head. That makes a total of more than 1'000 acquired operating points. In the case of the PAT, the measurements have been performed at 10 different constant rotational speed values of the recirculating pumps. For each recirculating pumps constant rotational speed value, more than 12 different runner rotational speed values of the PAT have been acquired, which makes a total of more than 120 operating points necessary to draw the full-3D efficiency characteristic of the machine.

Then, focusing on the dynamic method, first the optimal acceleration/deceleration ramps of the electrical drives have been identified in order to ensure a quasi- steady-state operation of the testing model. The main objective was to reduce at maximum time of measurement time, while avoiding measurement errors and hysteresis on the acquired characteristics. Then, the hydraulic efficiency measurements have been performed at 9 different test rig recirculating pumps constant rotational speed values while increasing and decreasing the speed of the microturbine/PATs runner(s) from minimum to maximum and vice versa. In the case of the microturbine, for each recirculating pump's constant rotational speed value 11 different constant runners absolute rotational speed ratios have been tested. Finally, the results obtained by the dynamic method have been validated with the ones obtained by the classical static point-by-point measurements method.

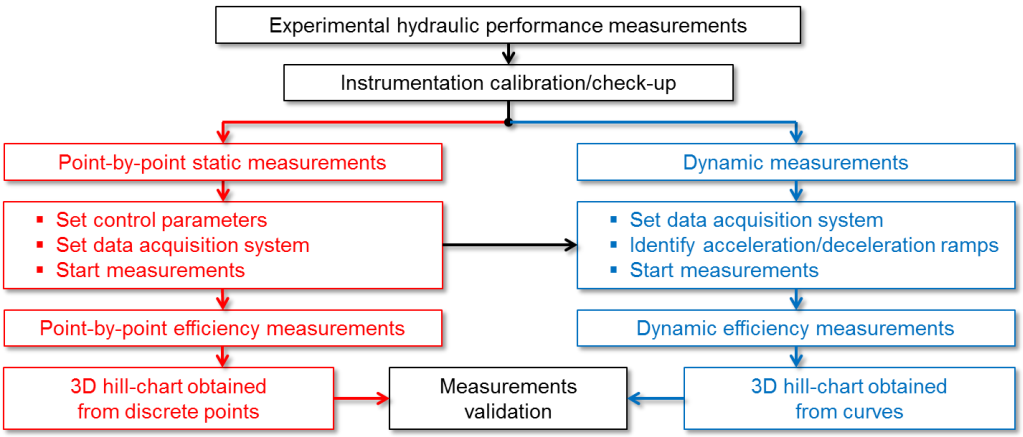

Figure 86. Flowchart of the employed experimental protocol.

The hydraulic-to-electrical efficiency $\eta_{h\text{-}elec}$ can be expressed as the product between the hydraulic-to-mechanical efficiency $\eta_{h\text{-}mec}$ and the electrical efficiency of the generator η_{elec}:

$$\eta_{h-elec} = \eta_{h-mec} \cdot \eta_{elec} = \eta_h \cdot \eta_m \cdot \eta_{elec} = \left(\eta_e \cdot \eta_q \cdot \eta_{rm}\right) \cdot \eta_m \cdot \eta_{elec} \ [\%] \quad (22)$$

Further, $\eta_{h\text{-}mec}$ results from the product between the hydraulic η_h and the bearing efficiency η_m, with the hydraulic efficiency η_h including the efficiency of the disc friction η_{rm}, the energetic efficiency η_e as well as the volumetric efficiency η_q. In the case of the microturbine, considering its reduced size and geometrical complexity, only the hydraulic-to-mechanical efficiency $\eta_{h\text{-}m}$, given by the ratio between the mechanical power P_{mec} recovered by both runners and the hydraulic power P_h of the whole one-stage turbine, could be measured:

$$\eta_{h-mec} = \frac{P_{mec}}{P_h} = \frac{\sum(\omega_i \cdot T_{mec\,i})}{\rho \cdot Q \cdot E} \ [\%] \quad (23)$$

In the case of the PAT, since the machine is not equipped with a torquemeter, only the hydraulic-to-electrical efficiency, given by the ration between the electrical power of the generator P_{elec} and the hydraulic power has been measured:

$$\eta_{h-elec} = \frac{P_{elec}}{P_h} = \frac{P_{elec}}{\rho \cdot Q \cdot E} \ [\%] \quad (24)$$

$$E = g \cdot H \ [J \cdot kg^{-1}] \quad (25)$$

Regarding the hydraulic power, whilst the discharge Q is directly measured, the total specific energy E (23)is calculated with the value of the head H. As illustrated in Figure 85, for both tested cases, the inline inlet and outlet cross sections of the machine are equal. Considering the Bernoulli's equation, for this particular case the calculation of the total head can performed only from the difference of the static pressure between the inlet and the outlet, directly measured with the help of the differential pressure sensor.

$$\eta^* = \frac{\eta_{h-mec\,/\,h-elec}}{max\left(\eta_{h-mec\,/\,h-elec}\right)} \ [-] \quad (26)$$

$$\eta^{*\prime} = \eta^* - \eta^*_{interp} \ [-] \quad (27)$$

The first step before performing dynamic measurements is to find the optimal acceleration/deceleration ramp of the runner(s) speed in order to stay in quasi- steady-state operating condition during the measurement process. To this end, the speed of the three recirculating pumps of the test rig has been set and maintained constantly at a value of 1500 rpm in the case of the microturbine, or 2000 rpm in the case of the PAT. Then, for the microturbine, considering a constant runner's absolute rotational speed ratio α = 1, the runners speed was uniformly increased from 1000 rpm to 2000 rpm and then decreased back to 1000 rpm. The same

procedure was applied in the case of the PAT for the range from 750 to 2250 rpm. In total, 6 (for the microturbine) and respectively 4 (for the PAT) different acceleration/deceleration ramps of respectively 10, 25, 30, 40, 60, 90 and 120 sec/1000 rpm have been addressed.

Counter-rotating microturbine **PAT**

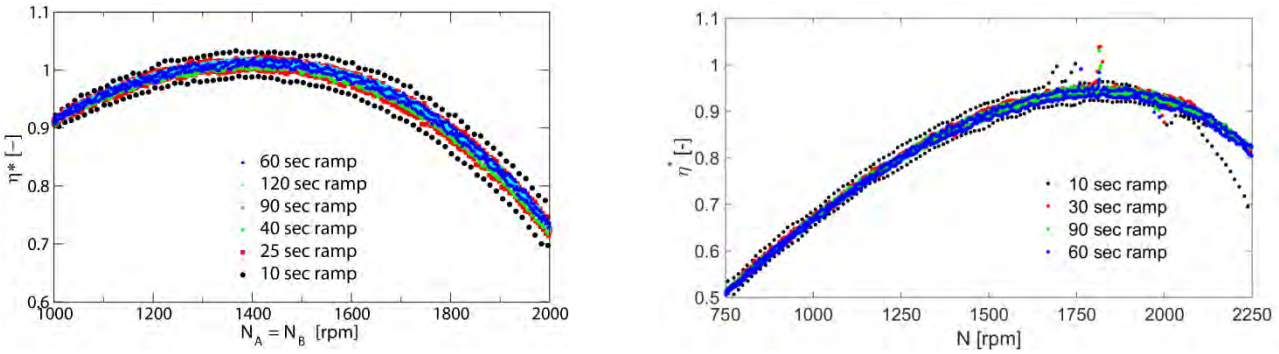

Figure 87. Influence of the acceleration/deceleration ramp of the runner(s) speed on the efficiency for fixed inflow conditions (pumps speed N_p = 1500/2000 rpm).

Counter-rotating microturbine **PAT**

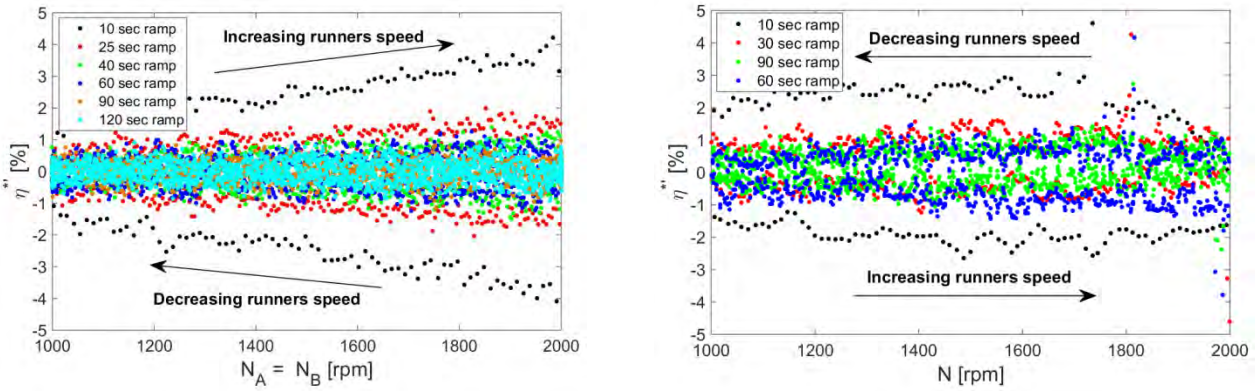

Figure 88. Efficiency fluctuation during an increasing/decreasing cycle at fixed inflow conditions (pumps speed N_p = 1500/2000 rpm) for different speed acceleration/deceleration ramps.

In Figure 88, the resulting influence of the acceleration/deceleration ramp of the runner(s) speed on the efficiency for fixed inflow conditions is provided. Efficiency is scaled with the maximum measured value determined from the static measurements. One may notice here hysteresis and large measurement errors on the resulting efficiency for speed ramps below 40 sec/1000 rpm.

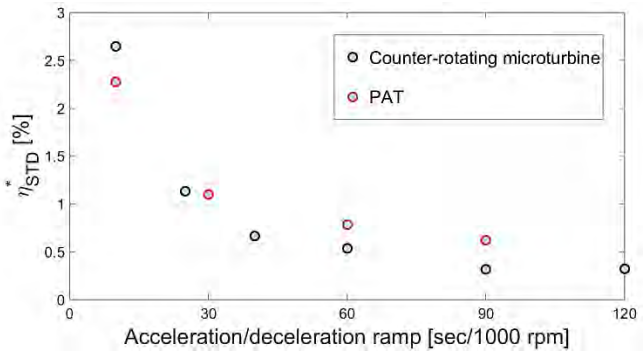

Acc./dec. ramp [sec/1000 rpm]	η^*_{STD} [%]	
	Microturbine	**PAT**
10	2.6467	2.2774
25	1.1363	-
30	-	1.0995
40	0.6693	-
60	0.5369	0.7863
90	0.3167	0.6246
120	0.3213	-

Figure 89. Resulting efficiency STD depending on the speed acceleration/deceleration ramp.

Then, the Figure 89 presents the influence of the speed acceleration/deceleration ramp on the magnitude of the efficiency fluctuations (due to measurement errors) $\eta^{*'}$ compared to the average efficiency obtained by curve fitting. Accordingly, for both tested cases, the hysteresis effect tends to become insignificant for speed ramps larger than 40 sec/1000 rpm. The evolution of the resulting standard deviation (STD) of the efficiency fluctuation η^*_{STD} with the speed ramp, provided in Figure 89, confirms this assertion. Consequently, as an acceptable compromise between the measurement time and the measurement precision (efficiency errors below 1% for both cases) a speed acceleration/deceleration ramp of 60 sec/1000 rpm has been selected for the further dynamic efficiency measurements.

The comparison between the efficiency obtained by dynamic and by static point-by-point measurement methods, for fixed inflow conditions (recirculating pumps speed of N_p = 1500/2000 rpm), is given in Figure 90. In the case of the discrete point-by-point method the speed of the turbine runner(s) has been modified in steps of 250 rpm from 0 to 3000 rpm, whilst is the case of the dynamic method it has been continuously increased, and then decreased, from 0 to 3000 rpm and vice versa. A good agreement between the results obtained by the two methods, with a maximum error of 1% between the mean values, may be observed for both tested cases, on the whole operating range, including off-design conditions. In the case of the microturbine, the negative efficiency values are given by a negative mechanical torque of the runners, corresponding to the turbine brake operating mode.

Counter-rotating microturbine **PAT**

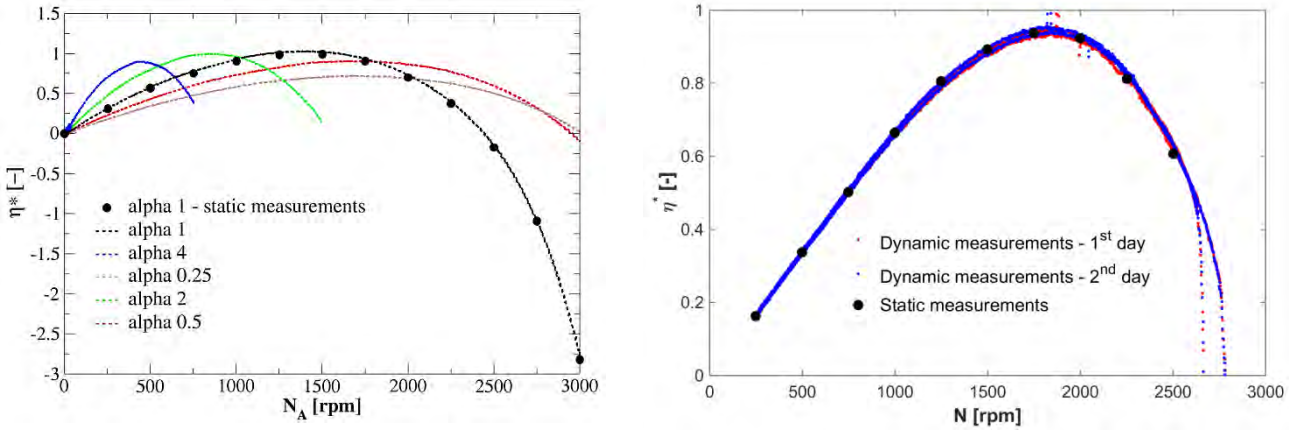

Figure 90. Comparison between dynamic and static efficiency measurements for fixed inflow conditions (recirculating pumps speed N_p = 1500/2000 rpm).

In the case of the PAT, accentuated hysteresis, specific to S-shaped characteristic curves, is noticed for high rotational speed values. To this end, considering the speed, the discharge and the power factors, the resulting S-shaped 4-quadrants characteristic curves of the PAT measured through the dynamic method are provided in Figure 91. Focusing on the discharge-speed characteristic, all the measurements are clustered on only one S-shaped curve. Indeed, this is explained by the fact that the machine has not been designed with any distributor, its characteristic being similar to the one of a pump-turbine at fixed guide vanes opening angle. However, on a power-speed representation, depending on the recirculating pump's speed, several S-shaped characteristics and hysteresis are noticed. Concerning the hydraulic configuration of the test rig for these 4-quadrants measurements, no special adjustment has been applied, the machine running smoothly between the turbine and reverse-pump modes, and vice versa.

$$N_{ED} = \frac{\mathrm{N} \cdot D_{ref}}{60 \cdot \sqrt{E}} \; [-] \tag{28}$$

$$Q_{ED} = \frac{\mathrm{Q}}{D_{ref}^2 \sqrt{E}} \; [-] \tag{29}$$

$$P_{ED}^{*} = \frac{P_{elec}}{\rho \cdot D_{ref}^2 E^{1.5}} \; [-] \tag{30}$$

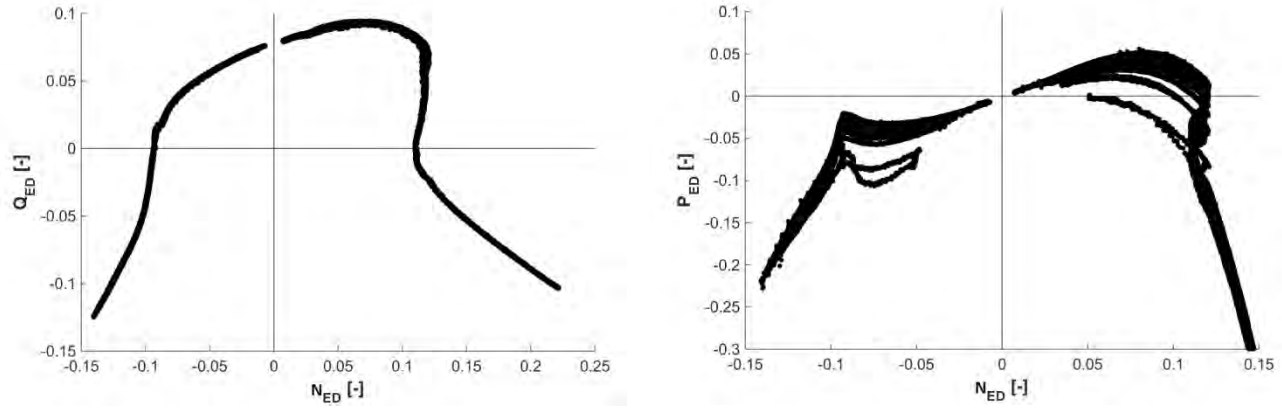

Figure 91. Resulting 4-quadrant characteristic curves of the PAT obtained with the dynamic measurements method.

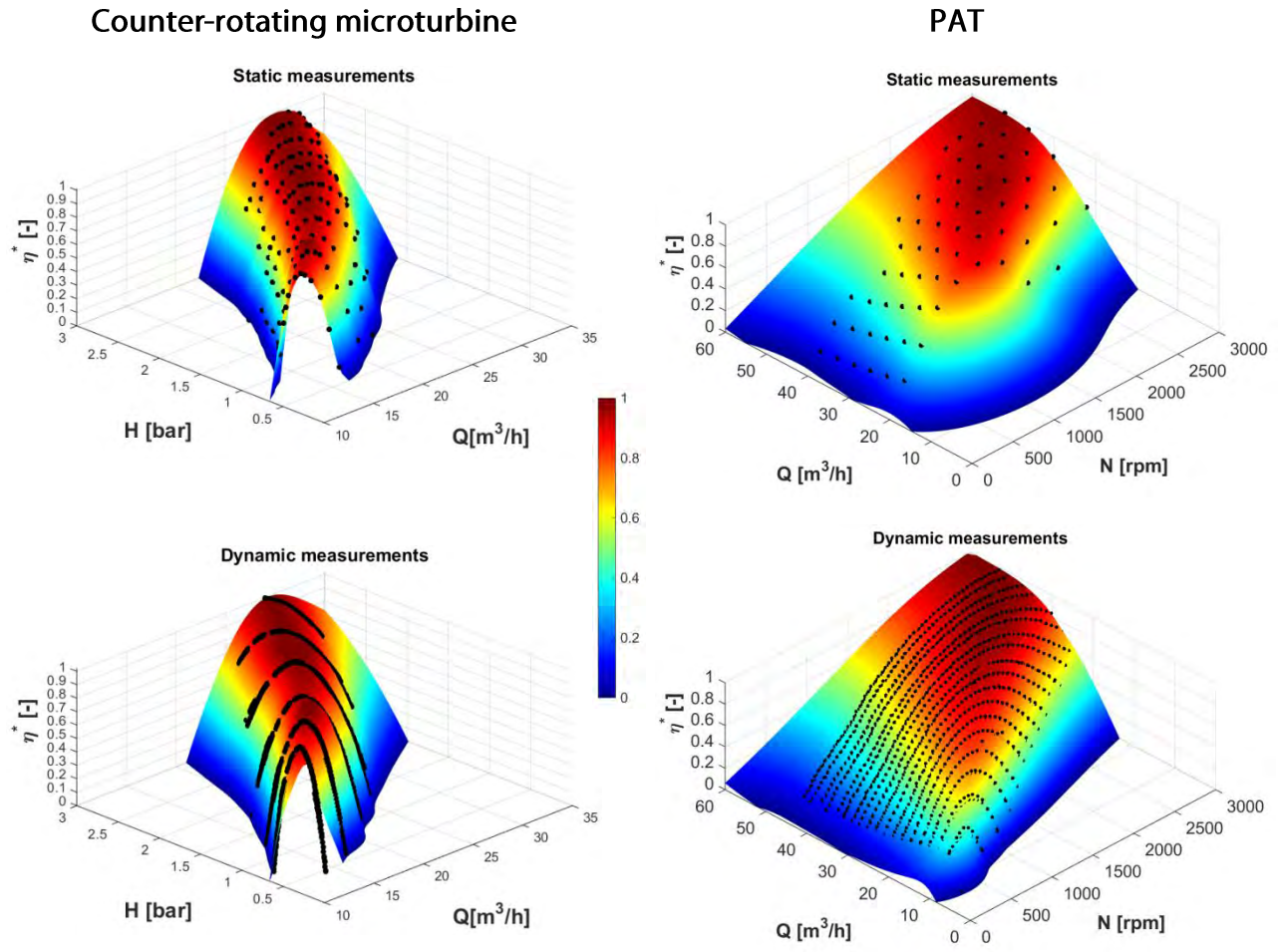

Figure 92. Resulting efficiency 3D hill-charts obtained by the classical static point-by-point and by the dynamic measurement methods.

The resulting efficiency 3D hill-charts obtained by the classical static point-by-point and by the dynamic measurement methods are provided in Figure 92. From a qualitative point of view the results obtained by the dynamic method are in a good agreement with the ones obtained by the static method for both tested cases.

Indeed, a satisfactory match between the two resulting 3D hill-surfaces (see the superposition of the fitted surfaces in Figure 93) validates the new proposed dynamic measurements method. The differences between the two hill-chart surfaces are mainly due to the quality of the interpolation and due to the number and the position of the available operating points. A more refined grid of operating points along with a more adapted surface interpolation method should reduce these artificial differences. Finally, in the case of the microturbine, if for the static measurements method, the measured operating points cross horizontally the final Q-H characteristic, in the case of the dynamic method the intersection with a typical characteristic of a pump is noticed from the distribution of operating points.

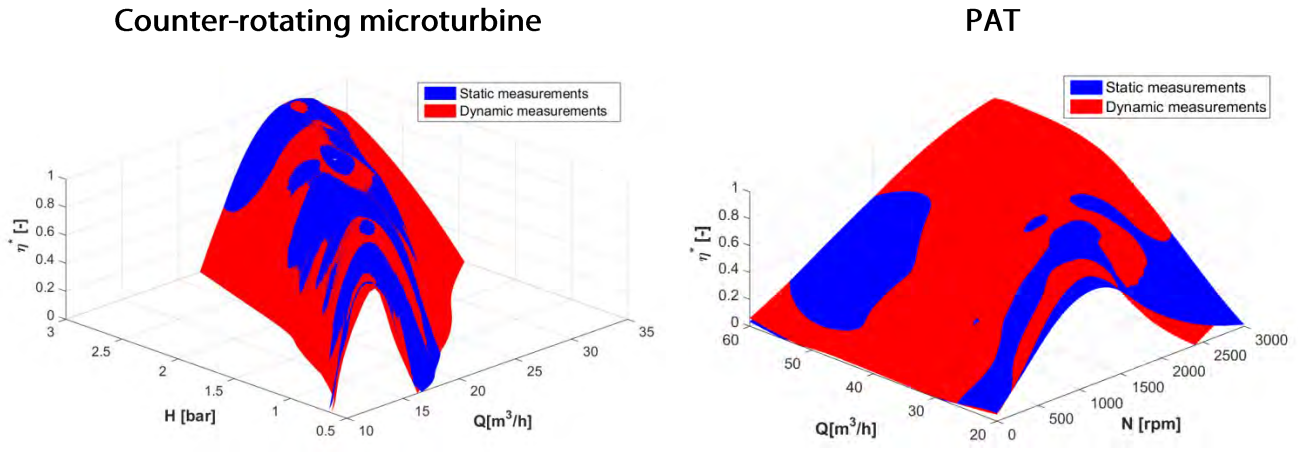

Figure 93. Validation of resulting 3D hill-charts obtained by the dynamic measurements method with the results of the classical static point-by-point method.

The implementation of the so-called "sliding gate" dynamic method to measure in a faster way (up to ten times) the efficiency characteristics on hydraulic turbomachinery has been presented. The new model testing measurement method has been successfully applied on two different cases dedicated to recover the energy lost in release valves of water supply networks: a 2.65 kW double-regulated laboratory prototype of an in-line axial microturbine with two independent variable speed counter-rotating runners and a 11 kW multi-stage centrifugal pump as turbine with variable speed.

The measurements have been carried out on the universal test rig of the HES-SO Valais/Wallis, Switzerland, dedicated to assessing hydraulic performances of small-power turbomachines following the IEC standard recommendations. The applied procedure consisted, in a first step, on measuring the 3D hill-chart of a given testing model (turbine or pump) by the classical static point-by-point method. Then, a second digitizer has been installed to acquire synchronized dynamic signals of the sensors in parallel with the existing acquisition/control systems of the test rig and of the testing model. The dynamic measurements of efficiency have been performed at different constant speeds of the test rig recirculating pumps while increasing and/or decreasing the speed of the testing model runner(s) from zero to maximum, and vice versa, slowly enough in order to keep a steady-state operation. Finally, the resulting 3D efficiency hill-charts of the two tested machines obtained by the

dynamic have been validated with the results obtained by the classical static point-by-point measurement method. Moreover, the S-shaped 4-quadrants characteristics of the PAT have been also successfully measured using the new dynamic method.

In conclusion, this approach is particularly gainful for small-hydro due to the reduced time required to perform the hydraulic efficiency tests. The same method could be interesting to rapidly identify the regions dominated by hydrodynamic instabilities within the operating range of a turbomachine.

Measurements and investigations in hydraulic turbines (cam surface determination for double regulated bulb turbines).

The cam surface determination was performed for the CHE Slatina, a double regulated bulb turbine, during the project: BC76/2022: Modernizare HA1 Slatina – Determinarea unei came combinatorice optimizată din punct de vedere al vibrațiilor și randamentului, Director: Prof. Dr. Eng. Romeo Susan-Resiga. For double regulated hydraulic turbines, such as vertical axis Kaplan or horizontal axis Kaplan (bulb) turbines, the high efficiency on a wide operating range is insured by the proper correlation of the guide vanes opening and runner blades opening with the operating point. The operating point can be specified either by head and discharge or by head and power.

Figure 94, shows the hill chart for the bulb turbine investigated in this study, installed in a hydropower plant on the Olt river in Romania. In the abscissa there is the shaft power of the turbine and the ordinate corresponds to the net head. The red lines correspond to various values of the runner blade opening angle φ and the green lines to the guide vanes opening angle α. The iso-lines for turbine efficiency η_t are the solid blue lines. The allowed operating range is bounded by the black dashed line, with limitations for maximum and minimum power and net head. Such diagrams are usually determined for a model turbine in the laboratory on specialized test rigs. When implemented in-situ, the opening angles are replaced by the displacement of the hydraulic pistons that open/close either the guide vanes or the rotor blade, usually as a percent from the maximum displacement. When implemented on the prototype turbine, the hill chart is usually checked with in-situ index tests, for which the main uncertainty is introduced by the discharge measurements.

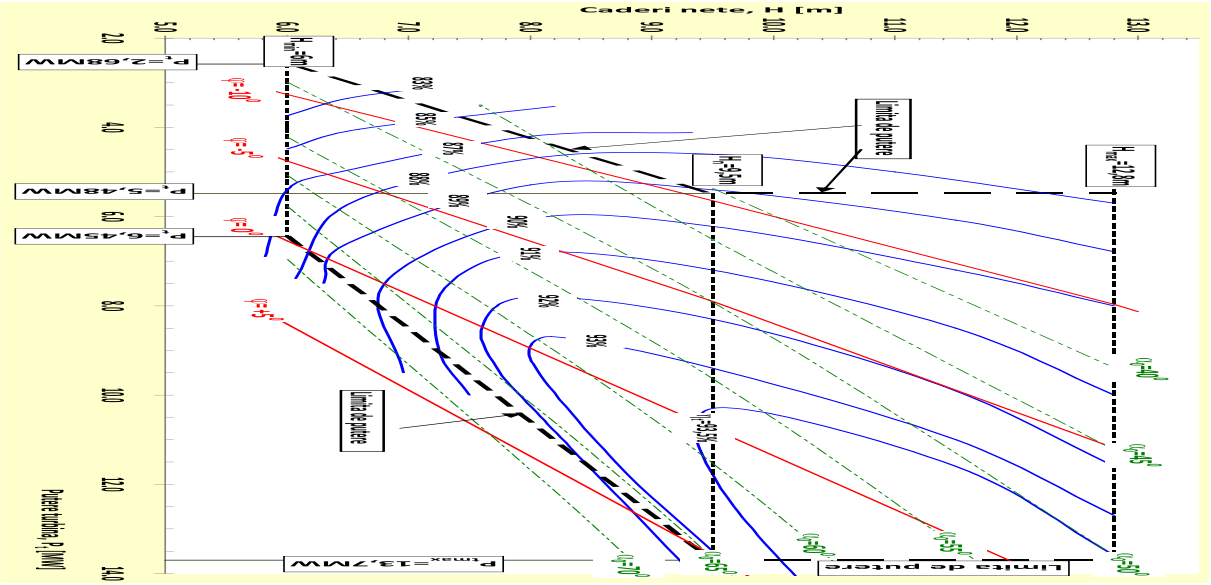

Figure 94. The hill chart of the bulb turbine investigated in this paper, [84].

The surfaces for runner blades opening and guide vanes opening as function of the hydro-unit power and net head can be inferred from Figure 94 and represented using Multivariate Adaptive Regression Splines (MARS) method conveniently implemented in MATLAB with the package ARES as

shown in Figure 95. This method has been employed in [85] to update and optimize the CAM of Kaplan turbines to account for wear and tear generated by frequency control operation.

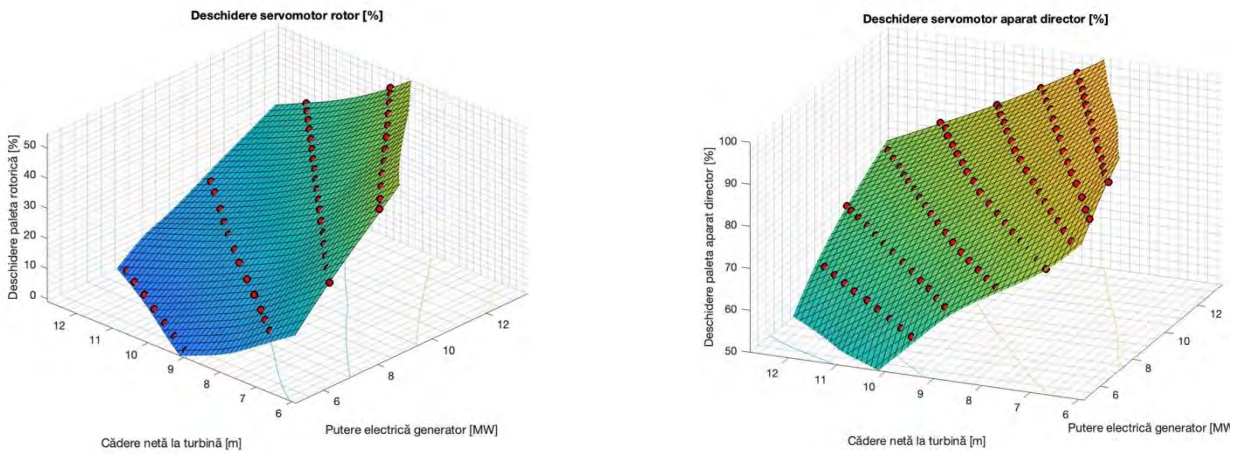

Figure 95. Surfaces for rotor blades opening $PR[\%](P,H)$, left picture, and guide vanes opening $AD[\%](P,H)$, where the turbine shaft power from Figure 94 is converted into electrical power, measured in-situ, using the data available for generator efficiency.

Moreover, the hydro-unit efficiency (the so-called hill chart) can also be recovered from Figure 94 with the same MARS method, as shown in Figure 96.

In practice, the surfaces from Figure 96 are converted in isolines and implemented in the turbine regulating unit, such that for the available net head H/m , measured in the power plant, and the prescribed unit power P/MW the corresponding guide vanes opening AD/% and runner blades opening PR/% are automatically set such that the efficiency is maximized at each operating point, as shown in Figure 96.

However, it happens that sometimes the diagram in Figure 94 is not either accurate or does not correspond to the actual turbine. In this case, the turbine operation is obviously severely hindered, with high levels of vibration above the standard limits, and an erratic vibrations amplitude evolution.

In this paper we address such a practical problem, and present the methodology employed for in-situ measurements that updated the cam surfaces, and finally allowing the normal operation of the turbine.

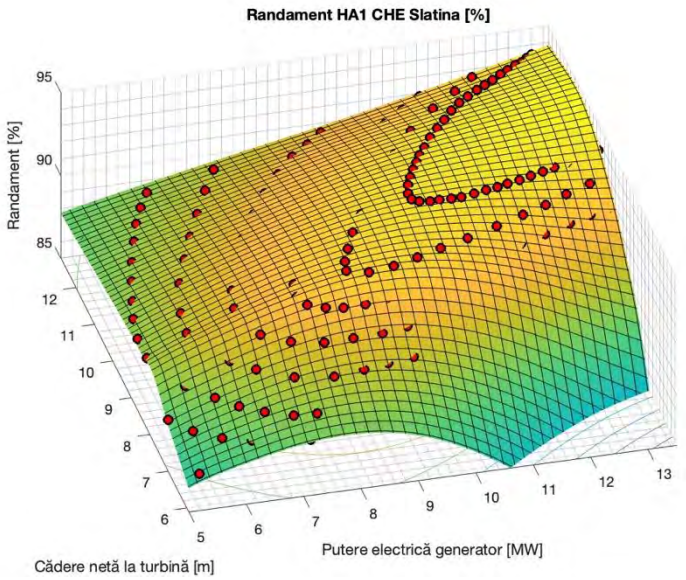

Figure 96. The hill chart for the bulb turbine reconstructed using MARS with data from Figure 94.

The main challenge when performing efficiency measurements for in-situ index tests is that there are large uncertainties in discharge measurements compared to the controlled environment in laboratory test rigs. In our case, in spite of the efforts to have reliable and reproducible discharge measurements it became clear that we have to find an alternative way to determine the correct cam.

A practical way to overcome the above difficulty is to perform tests at constant power [86]. The main idea is that for a prescribed power value, and at the available net head, we increase the guide vane opening AD/% and correspondingly decrease the runner blade opening PR/% such that the power remains constant. Obviously, when performing such test, the turbine regulating unit is in manual mode. Conversely, when closing the guide vanes AD/% one should open the runner blades to keep the power constant. When plotting PR/% versus AD/% one obtains a typical hyperbolic curve such as in Figure 97, where data are taken from [87].

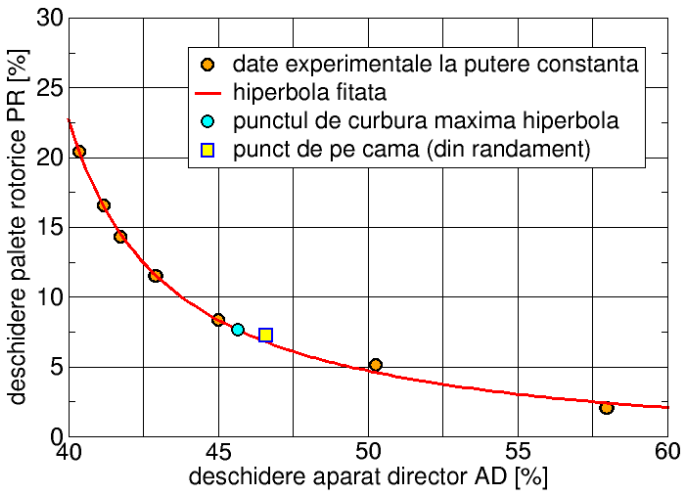

Figure 97. Index test at constant power (data from [78].

One can fit the measured data (orange points in Figure 97) with a hyperbola, as in equation (31), using the least squares method to find the coefficients A_0, A_1 and A_2.

$$PR = A_2 + \frac{A_0}{AD - A_1} \tag{31}$$

The point of maximum curvature of this hyperbola is given by,

$$\begin{aligned} AD &= A_1 + \sqrt{A_0} \\ PR &= A_2 + \sqrt{A_0} \end{aligned} \tag{32}$$

This point of maximum curvature is displayed with the blue circle in Figure 97. The main observation is that this maximum curvature point is, within measurement error, quite close to the maximum efficiency point shown with yellow square in Figure 97. As a result, one can approximate quite well the points of maximum efficiency (on-cam points) by the points of maximum curvature from the constant power index tests.

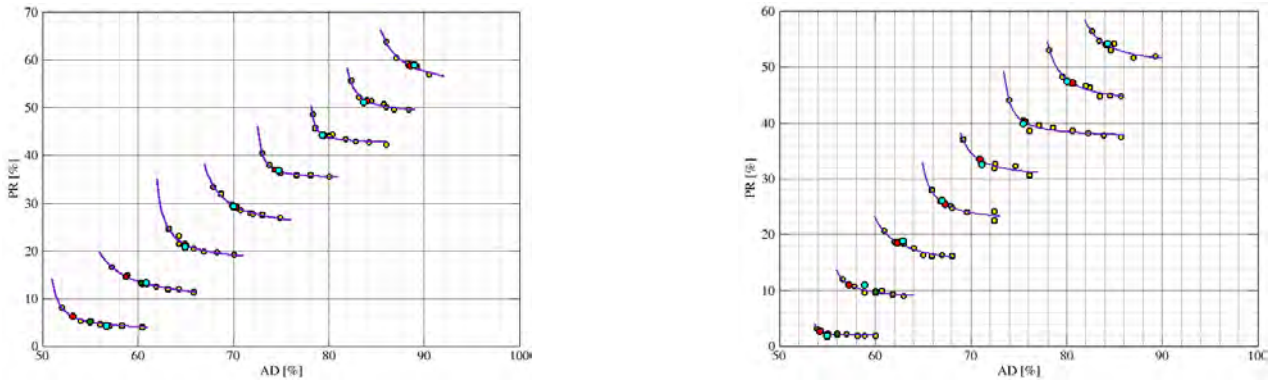

Figure 98. Index tests at constant power performed in-situ on a bulb turbine.

Table 18. On-cam points determined by index tests at constant power.

Electrical Power [MW]	Net head [m]	Guide vane opening	Runner blade opening
13.03	10.02	84.15	54.00
12.07	10.12	80.62	47.05
11.00	10.24	75.63	40.06
9.95	10.33	71.03	33.31
9.00	10.45	67.35	25.41
7.98	10.49	62.35	18.58

7.08	10.57	60.02	9.66
6.01	10.65	56.02	2.10
13.02	9.47	88.56	58.70
11.97	9.61	84.02	51.32
11.05	9.72	79.50	44.13
10.05	9.84	74.32	37.04
9.00	9.95	70.31	29.16
7.91	10.06	64.99	21.29
7.05	10.17	60.41	13.34
6.02	10.26	55.0	5.05

An example of actual measurements on a bulb turbine is shown in Figure 98. Index tests at constant power performed in-situ on a bulb turbine., with the points of maximum curvature, associated with maximum efficiency, presented in Table 18. Note that for such index tests the turbine head does not need to be kept constant for long periods of time. It is enough to have a constant head during the measurements for a given power value. This is a major advantage for in-situ measurements, where the turbine net head cannot be controlled as in the laboratory test rigs.

Using the new on-cam points determined experimentally with index test at constant power as in Section 2, we have updated the surfaces from Figure 94. The hill chart of the bulb turbine investigated in this paper, . The new surfaces include the experimental points with a large weight, using the same least squares.

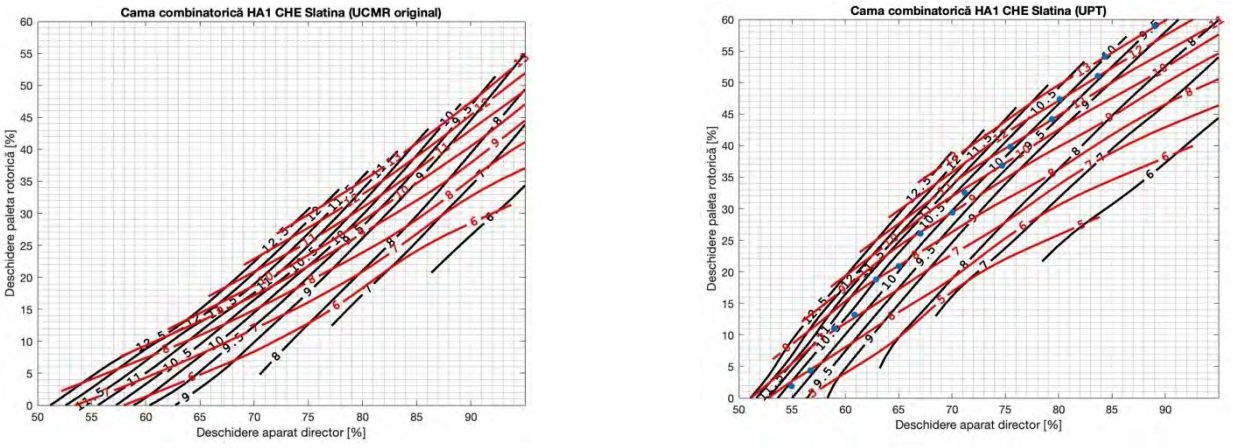

Figure 99. The CAM surface represented as isolines of constant head [m] (black solid lines) and of constant power [MW] (red solid lines). Left picture is the original CAM surface and the right picture is the updated one.

One can clearly notice from figure 6 the significant change in the CAM surfaces updated with the points determined experimentally in-situ with index test at constant power. Although in-situ there are limited possibilities to perform measurements with a large range of net head values, it is possible to adjust the CAM surface even with a small set of net heads [87]. Nevertheless, as seen from Table 18, using the MARS method there is no need to keep the same net head for the experimental points.

In the end, the CAM surface implemented in the regulating unit of the bulb turbine examined in this paper is presented in Figure 100.

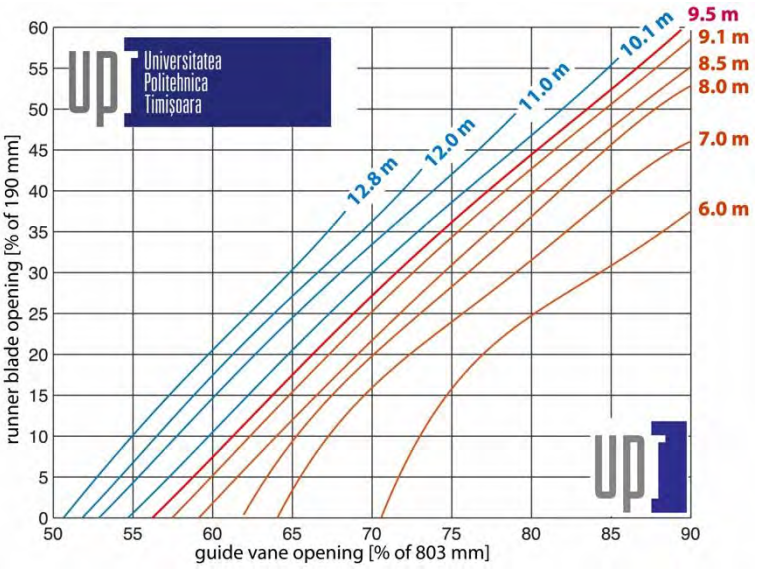

Figure 100. The CAM implemented in the regulating unit of the bulb turbine. Only half of the constant head curves are shown, for readability. The nominal head is 9.5 m. For a prescribed power value, the regulating unit sets the guide vanes and runner blade opening on the corresponding net head curve.

The study presented a methodology for correcting or updating the CAM surface for double regulated hydraulic turbines using in-situ index tests at constant power. It is shown that the points (guide vane opening, rotor blade opening) determined at constant head and constant power are arranged on a hyperbola. The maximum curvature point of such a hyperbola is a very good approximation for the on-cam point of maximum efficiency. However, the constant power index tests do not rely on discharge measurements, which are affected by large uncertainties for in-situ measurements.

Data processing using the Multivariate Adaptive Regression Splines (MARS) is a robust approach and allows considering new experimental data to correct existing cam surfaces in the least squares sense.

The new corrected and updated CAM allows the stable operation of the bulb turbine, with a reduced level of vibration. In practice, constant power index tests can be periodically and

automatically performed on operating double regulating turbines, to collect data that allows updating the cam surface.

(D) ACADEMIC CAREER DEVELOPMENT PLAN

(D-i) Scientific development plans

My research activity has been consistently centred on the field of hydraulic machinery, with a particular emphasis on hydraulic turbines and centrifugal pumps. As evidenced by my scientific contributions and experimental work, I have concentrated on the investigation, development, and laboratory testing of innovative solutions aimed at mitigating hydrodynamic instabilities that arise during the operation of these machines. These instabilities, such as vortex rope produce large pressure pulsations and swirling flow instabilities and can affect the structural integrity of hydraulic turbines operating under variable load conditions.

A key objective of my research has been to explore control mechanisms, both passive and active, capable of suppressing or stabilizing unsteady flow behaviour within hydraulic turbines and centrifugal pumps. My work includes the application of magneto-rheological (MR) components, variable-speed axial inducers, free-runner control and water jet control systems. These efforts are directed toward increasing the operational flexibility of hydraulic machines, enhancing their reliability, and aligning their performance with modern energy system demands.

When placed in the broader European context, the relevance of this research becomes even more pronounced. The European electrical system is one of the most complex, interconnected, and technologically advanced systems globally. It is characterized by a diverse energy mix, extensive cross-border transmission infrastructure, and a strong and growing commitment to sustainable energy development. As of 2022, the total electricity generation within the EU-27 reached approximately 2,700 terawatt-hours (TWh).

The EU's energy policy has placed considerable emphasis on decarbonization, with a clear trajectory toward the phasing out of coal-fired power plants. This shift has been particularly evident since the early 2000s, as numerous member states have either decommissioned or scheduled the retirement of coal-based generation units, replacing them with renewable energy technologies and flexible natural gas generation to maintain grid stability.

By 2022, renewable energy sources, including hydropower, accounted for over 39% of the EU's total electricity production. This transformation is underpinned by ambitious policy instruments such as the European Green Deal with the aim to achieve a 55% reduction in greenhouse gas emissions by 2030. These policies promote systemic electrification, increased energy efficiency, and substantial investment in clean technologies.

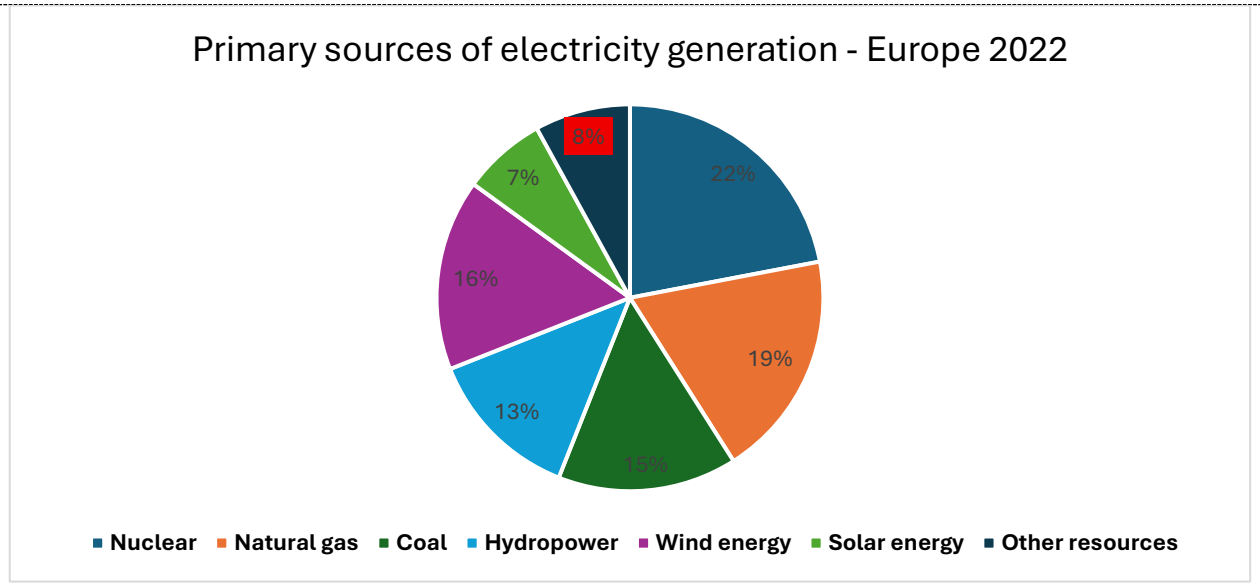

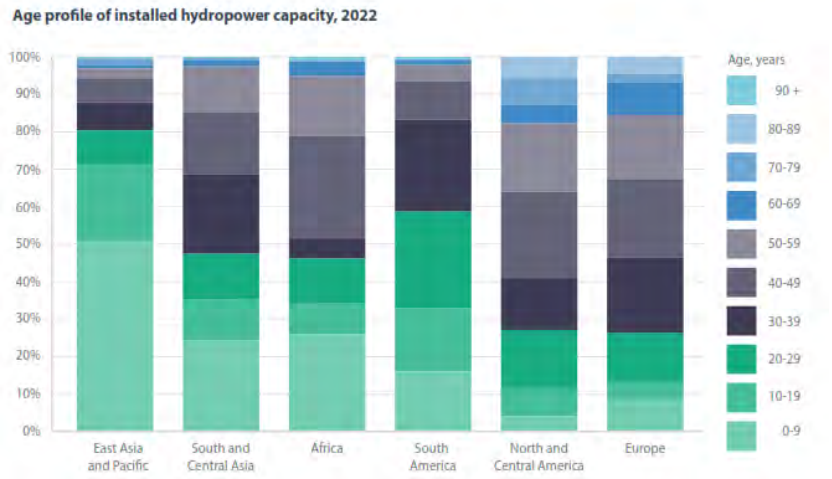

Figure 101. Percentage of Europe electricity generation and the age profile of installed hydropower over the globe. It can be seen clearly that Europe has the oldest installed hydraulic turbines which are necessary to be refurbished in the next 5 years and further, [88], [89].

Within this framework, hydropower remains a foundational component of Europe's low-carbon electricity supply. As of 2022, the installed hydropower capacity across Europe was approximately 250 gigawatts (GW). The leading contributors to this capacity are Norway, France, Italy, Austria, and Switzerland. Hydropower generates approximately 12–15% of the continent's electricity, though this figure varies significantly by country. For instance, Norway derives over 90% of its electricity from hydroelectric sources, positioning it as a benchmark for hydropower utilization and efficiency.

Despite its maturity, the European hydropower sector, originally commissioned over 40 years ago, now requires substantial upgrades to sustain output, improve flexibility, and meet modern environmental standards. According to Quaranta (2023) and Quaranta et al. (2024), approximately 67% of existing European hydropower stations will necessitate major modernization by 2030.

Hydropower in Europe is entering a critical era of rehabilitation and renewal—not solely through the construction of new facilities, but more importantly, by enhancing existing infrastructure through modern control methods, upgraded turbines, and the integration of digital intelligence. These investments are essential not only for enabling deeper integration of intermittent renewable energy sources, but also for ensuring the long-term reliability and sustainability of the continent's energy system.

In direct connection with current practice in European hydropower, the team from the Research Centre for Engineering with Complex Fluids, led by Prof. Dr. Eng. Romeo Susan-Resiga, has been actively engaged over the past decade in a series of complex projects in collaboration with the hydropower industry, especially with SPEEH Hidroelectrica S.A. These projects have covered a wide range of topics, including consultancy, technical expertise, and applied research in hydraulic machinery. I have been involved across the full spectrum of engineering activities, including turbine commissioning, on-site power plant measurements, turbine model testing, and technical document analysis.

In parallel, I have consistently developed and coordinated the activities of the Hydraulic Machinery Laboratory within the Faculty of Mechanics at Politehnica University Timișoara. This effort has resulted in a continuously upgraded research infrastructure, made possible through the successful implementation of four national research projects and two industrial contracts, which have led to the acquisition of new test rigs and the refurbishment of older experimental test rigs. Importantly, these laboratory developments have also created a dynamic and supportive environment for training and supervising young researchers. The knowledge and experience gained from industrial collaborations and from the laboratory now serve as a strong foundation for mentoring and guiding the next generation of researchers and professors.

(D-ii) Professional and academic plans

Since the beginning of my academic career at the Faculty of Mechanics, Politehnica University Timișoara, I have pursued several strategic directions that support both professional growth and institutional development, with the overarching goal of enhancing academic excellence and research capacity. These directions include:

- the continuous development and modernization of course content, ensuring alignment with the latest scientific advancements and technological trends.
- the supervision and mentoring of students in the preparation of bachelor's and master's theses, as well as the guidance of doctoral students within ongoing research programs.
- the recruitment and integration of young academics from among recent PhD graduates, with the aim of strengthening and diversifying the existing research team within our group.
- the continuation of research activities in the field of hydraulic machinery, with dissemination of results in internationally indexed journals and at prestigious scientific conferences.
- application for research grants and the establishment of long-term collaborations with industrial partners, to enable joint projects in hydraulic machinery.

In response to current environmental and economic challenges, I have introduced new topics into teaching activities. These include Pumps as Turbines (PaTs), a cost-effective and scalable solution for energy recovery in rural or isolated regions, and fish-friendly turbines, which are becoming increasingly relevant under emerging environmental regulations and climate adaptation strategies.

To support the applied component of my academic activities, I have contributed to the development of a modern teaching infrastructure, which includes laboratories equipped with dedicated test rigs for each experiment corresponding to the subjects I coordinate. These facilities ensure that students can bridge theoretical knowledge with practical skills in a realistic and engaging environment.

In parallel, I provide continuous support to PhD students conducting research within the Hydraulic Machinery Laboratory, offering them access to experimental infrastructure and scientific mentoring. Given that my research focuses on flow control in hydraulic turbomachines, and of having coordinated four nationally funded research projects (financed by UEFISCDI), I intend to remain active involved in future competitive grant calls. Additionally, I aim to expand collaborations with companies in the hydraulic machinery sector by initiating applied research contracts that address practical engineering challenges and innovation needs in industry.

In conclusion, I consider that the role of the modern academic extends well beyond the traditional scope of teaching. It includes mentoring and creating meaningful learning experiences that inspire students to engage in scientific inquiry and technical innovation. Whether through

collaborative research projects, study visits, or extracurricular involvement, my goal is to create a dynamic academic environment, one that integrates teaching with sustained research among students and PhD students.

(E) ANNEX WITH SCIENTIFIC AND PROFESSIONAL ACHIEVEMENTS.

The list of the ten selected published manuscripts based on which the present habilitation thesis is written

The list of selected manuscripts forming the basis of this habilitation thesis is presented below. The publications are grouped according to the four research domains, which are further detailed the content.

MAGNETO-RHEOLOGICAL FLUIDS (MRF) AND ITS APPLICATIONS IN HYDRAULIC MACHINERY

[1] Bosioc, A., Beja, T., Muntean, S., Borbath, I., & Vekas, L. (2017). Experimental investigations of MR Fluids in air and water used for brakes and clutches. 1st International Conference on Materials Design and Applications, MDA 2016. 65, pg. 197-207. Porto: Springer Verlag - Advanced Structured Materials. doi:10.1007/978-3-319-50784-2_16.

[2] Bosioc, A., Ardelean, T., Szakal, R., Muntean, S., Borbath, I., & Vekas, L. (2019). Experimental investigations of a MR clutch for a centrifugal pump. In Advanced Structured Materials (Vol. 98, pg. 253-263). Springer Verlag. doi:10.1007/978-3-030-02257-0_19.

CONTROL METHODS FOR DIMINISHING THE HYDRAULIC INSTABILITIES IN HYDRAULIC TURBINES

[3] Bosioc, A., Muntean, S., Tanasa, C., Susan-Resiga, R., & Vekas, L. (2014). Unsteady pressure measurements of decelerated swirling flow in a discharge cone at lower runner speeds. 27TH IAHR SYMPOSIUM ON HYDRAULIC MACHINERY AND SYSTEMS (IAHR 2014). 22, p. 032008. Montreal: IOP Conference Series-Earth and Environmental Science. doi:10.1088/1755-1315/22/3/032008

[4] Javadi, A., Bosioc, A., Nilsson, H., Muntean, S., & Susan-Resiga, R. (2016). Experimental and Numerical Investigation of the Precessing Helical Vortex in a Conical Diffuser, With Rotor-Stator Interaction. JOURNAL OF FLUIDS ENGINEERING-TRANSACTIONS OF THE ASME, 138(8), 081106. doi:10.1115/1.4033416

[5] Bosioc, A., & Tanasa, C. (2020). Experimental study of swirling flow from conical diffusers using the water jet control method. Renewable Energy, 152, 385-398. doi: 10.1016/j.renene.2020.01.080

[6] Bosioc, A., Szakal, R., Stuparu, A., & Susan-Resiga, R. (2023). Numerical Analysis of the Flow by Using a Free Runner Downstream the Francis Turbine. International Journal of Turbomachinery Propulsion and Power, 8(2), 14. doi:10.3390/ijtpp8020014

CONTROL METHODS FOR DIMINISHING THE HYDRAULIC INSTABILITIES IN CENTRIFUGAL PUMPS

[7] Muntean, S., Susan-Resiga, R., Bosioc, A., Constantin, S., Maxim, D., Tanasa, C., Vekas, L., Borbath, I., Anton, L. (2019) Equipment for Reducing Cavitational Effects and Leveling Flow at Turbo

Pumps Inlet. Romania Brevet nr. RO131578-B1.

[8] Bosioc, A., Mos, D., Muntean, S., & Anton, L. (2019). Analysis Of a Centrifugal Pump Equipped With an Axial Rotor with Variable Speed. Proceedings Of the Asme/Jsme/Ksme Joint Fluids Engineering Conference. 3B, p. V03BT03A046. San Francisco: ASME JSME KSME Joint Fluids Engineering Conference Proceedings.

ADVANCED DIAGNOSTIC AND TESTING METHODS FOR PUMPS AND TURBINES IN ENERGY APPLICATIONS

[9] Hasmatuchi, V., Bosioc, A., Luisier, S., & Munch-Alligne, C. (2018). A Dynamic Approach for Faster Performance Measurements on Hydraulic Turbomachinery Model Testing. Applied Sciences-Basel, 8(9), 1426. doi:10.3390/app8091426

[10] Susan-Resiga, R., Bosioc, A., & Muntean, S. (2025). In-situ updating of the cam surface for double regulated bulb turbine. 9th Meeting of the IAHR WorkGroup on Cavitation and Dynamic Problems in Hydraulic Machinery and System, IAHRWG 2023. 1483. Timisoara: IOP Conference Series: Earth and Environmental Science. doi:10.1088/1755-1315/1483/1/012043

Experimental Investigations of MR Fluids in Air and Water Used for Brakes and Clutches

Alin Ilie Bosioc, Trandafir Emanuel Beja, Sebastian Muntean, Istvan Borbáth and Ladislau Vékás

1 Introduction

Magnetic fluids have been developed at the beginning of the 1948, when Rabinow [1] developed a clutch device. According with Rabinow, the advantages of using this kind of clutch with magnetic fluids are: the amount of electrical power necessary to control is small and time response is also small. Since then the magnetic fluids have been implemented in many applications. Several important applications can be found in: sealing's (especially in the case of gas transporting installations) [2, 3], sensors [4], dumpers [5, 6].

Magneto-rheological brakes (MRB) are one important research direction concerning these smart materials. Some of the advantages are convenient low-power control (through electrically generated magnetic field) and very good torque to weight ratio. The latter recommends them for applications where small devices able to generate high value of torque are needed, [7, 8]. The electrical control possibility

A.I. Bosioc (✉) · T.E. Beja
Hydraulic Machinery Department, University Politehnica Timişoara, Mihai Viteazu, no. 1, Timisoara, BV, Romania
e-mail: alin.bosioc@upt.ro

T.E. Beja
e-mail: emanuel_beja@yahoo.com

S. Muntean · L. Vékás
Center for Advanced Research in Engineering Sciences, Romanian Academy, Mihai Viteazu, no. 24, Timişoara, BV, Romania
e-mail: seby@acad-tim.tm.edu.ro

L. Vékás
e-mail: vekas.ladislau@gmail.com

I. Borbáth
SC. Roseal S.A., Str. Nicolae Balcescu, no. 5A, Odorheiu Secuiesc, Romania
e-mail: borbathistvan@roseal.eu

L.F.M. da Silva (ed.), *Materials Design and Applications*,
Advanced Structured Materials 65, DOI 10.1007/978-3-319-50784-2_16

(1)

Experimental Investigations of a MR Clutch for a Centrifugal Pump

A. I. Bosioc, T. Ardelean, R. Szakal, S. Muntean, I. Borbath and L. Vékás

Abstract A magneto-rheological clutch was designed and built in order to modify the speed of an axial rotor mounted in front of a centrifugal pump. The main goal by modifying the speed of the axial rotor is to increase the operating regimes with less cavitation and to uniform the flow at the inlet of the pump impeller. The magneto-rheological clutch is tested separately on a preliminary test rig, in order to analyse in detail, the working parameters (generated torque, the interior and exterior temperature). Also, the test rig serves testing different MR fluids available on the market as well as several MR fluids developed and characterized in our laboratory. The preliminary test rig consists in one fixed (2500 rpm) and one variable speed electric motors (2000–2500 rpm), a torque transducer (0–20 Nm), the magneto-rheological clutch, temperature sensors as well as a control and acquisition system. The aim of this study is to provide a first experimental evaluation of the magneto-rheological clutch designed and built for a special application. First, the paper presents the problem and our solution using the MRC. Second, we focus on the magneto-rheological clutch and the test rig; the magnetic and mechanical design of the clutch is presented, while for the test rig the operating conditions will be described. The third part analyses the

A. I. Bosioc (✉) · T. Ardelean · R. Szakal · S. Muntean
University Politehnica Timişoara, Bv. Mihai Viteazu, No. 1, 300222 Timişoara, Romania
e-mail: alin.bosioc@upt.ro

T. Ardelean
e-mail: timotei.ardelean@yahoo.com

R. Szakal
e-mail: raul.szakal@student.upt.ro

S. Muntean
e-mail: seby@acad.tim.tm.edu.ro

S. Muntean · L. Vékás
Romanian Academy - Timişoara Branch, Bv. Mihai Viteazu, No. 24, 300224 Timişoara, Romania
e-mail: vekas.ladislau@gmail.com

I. Borbath
SC. Roseal S.A., Odorheiu Secuiesc, Str. Nicolae Balcescu, No. 5A, 535600 Odorheiu Secuiesc, Romania
e-mail: borbathistvan@roseal.eu

L. F. M. da Silva (ed.), *Materials Design and Applications II*, Advanced
Structured Materials 98, https://doi.org/10.1007/978-3-030-02257-0_19

(2)

27th IAHR Symposium on Hydraulic Machinery and Systems (IAHR 2014) IOP Publishing
IOP Conf. Series: Earth and Environmental Science 22 (2014) 032008 doi:10.1088/1755-1315/22/3/032008

Unsteady pressure measurements of decelerated swirling flow in a discharge cone at lower runner speeds

A I Bosioc[1], S Muntean[2], C Tanasa[1], R Susan-Resiga[1,2] and L Vékás[2]
[1] Department of Hydraulic Machinery, University Politehnica Timisoara, Bv. Mihai Viteazu, No. 1, Ro-300222, Timisoara, Romania
[2] Center for Advanced Research in Engineering Sciences, Romanian Academy – Timisoara Branch, Bv. Mihai Viteazu, No. 24, Ro-300223, Timisoara, Romania

E-mail: alin.bosioc@upt.ro

Abstract. The decelerated swirling flow in the draft tube cone of hydraulic turbines (especially turbines with fixed blades) is responsible for self-induced instabilities which generates pressure pulsations that hinder the turbine operation. An experimental test rig was developed in order to investigate the flow instabilities. A new method was implemented to slow down the runner using a magneto rheological brake in order to be extended the flow regimes investigated. As a result, the experimental investigations are performed for 7 operating regimes in order to quantify the flow behaviour from part load operation to overload operation. The unsteady pressure measurements are carried out on 4 levels in the cone. The unsteady pressure measurements on the cone wall consist in quantifying of three aspects: i) the pressure recovery coefficient obtained based on mean pressure provides the energetic assessment on the draft tube cone; ii) the unsteady quantities (dominant amplitude and frequency) are determined revealing the dynamic behaviour; iii) the plunging and rotating components of the pressure pulsation. As a result, this new method helps us to investigate in detail the flow instability for different operating regimes and allows investigating various flow control solutions.

1. Introduction

Currently there is a growing demand for renewable energy in the industrialized countries. However, these energy sources (e.g. solar, wind) introduce a fluctuating behaviour in the grid. Therefore, the hydraulic turbines have to operate far away from the best efficiency point (BEP) covering a wide area. An important component of the hydraulic turbines with low and medium head is the draft tube cone due to the most important energy is recovered along to this part [1]. The hydraulic losses increase sharply with a significant decrease in efficiency when the turbines operate far away from the best efficiency point. Also, the self induced instabilities are generated in the draft tube cone (e.g. vortex rope) leading to strong pressure pulsations.

Different control methods have been introduced and tested in order to mitigate the vortex rope effects. Kurokawa et al. [2] proposed J-Groove method which consists in mounting radial groves on the draft tube cone. Thike [3] and Falvey [4] have tested different extensions of runner cone to suppress the stagnant region and associated vortex rope. Recently, a new control method was proposed [5] and successfully tested experimentally which involves using an axial water jet to the runner cone [6]. The results clearly showed that using the optimum amount of jet water, the stagnant region and the vortex rope are completely eliminated from the draft tube cone. Foroutan and Yavuzkurt [7] have reached at a similar conclusion, when tested numerically water injection method on a Francis turbine.

The vortex rope effects are present both at partial discharge and at full load discharge. The experimental test rig developed in laboratory was design to investigate one operating regime. A new solution was tested by lowering the runner speed in order to extend the investigation at several swirling flow configurations. This solution covers a wide range of discharge values from 0.7 up to 1.54 from best efficiency point discharge at constant guide vane opening.

(3)

Experimental and Numerical Investigation of the Precessing Helical Vortex in a Conical Diffuser, With Rotor–Stator Interaction

A. Javadi[1]
Division of Fluid Dynamics, Department of Applied Mechanics, Chalmers University of Technology, Göteborg SE-412 96, Sweden
e-mail: ardalan.javadi@chalmers.se

A. Bosioc
Assistant Professor
Department of Hydraulic Machinery, University Politehnica Timişoara, Bv. Mihai Viteazu, No. 1, Timişoara Ro-300222, Romania
e-mail: alin.bosioc@upt.ro

H. Nilsson
Professor
Division of Fluid Dynamics, Department of Applied Mechanics, Chalmers University of Technology, Göteborg SE-412 96, Sweden
e-mail: hani@chalmers.se

S. Muntean
Center for Advanced Research in Engineering Sciences, Romanian Academy—Timişoara Branch, Bv. Mihai Viteazu, No. 24, Timişoara Ro-300223, Romania
e-mail: seby@acad-tim.tm.edu.ro

R. Susan-Resiga
Professor
Department of Hydraulic Machinery, University Politehnica Timişoara, Bv. Mihai Viteazu, No. 1, Timişoara Ro-300222, Romania
e-mail: romeo.resiga@upt.ro

The flow unsteadiness generated in a swirl apparatus is investigated experimentally and numerically. The swirl apparatus has two parts: a swirl generator and a test section. The swirl generator which includes two blade rows, one stationary and one rotating, is designed such that the emanating flow at free runner rotational speed resembles that of a Francis hydroturbine operated at partial discharge. The test section consists of a conical diffuser similar to the draft tube cone of a Francis turbine. Several swirling flow regimes are produced, and the laser Doppler anemometry (LDA) measurements are performed along three survey axes in the test section for different runner rotational speeds (400–920 rpm), with a constant flow rate, 30 l/s. The measured mean velocity components and its fluctuating parts are used to validate the results of unsteady numerical simulations, conducted using the Reynolds-averaged Navier–Stokes (RANS) computational fluid dynamics (CFD) code ANSYS CFX. Furthermore, phase-averaged pressure measured at two positions in the draft tube is compared with those of numerical simulations. A dynamic mesh is used together with the sliding general grid interfaces (GGIs) to mimic the effect of the rotating runner. The delayed detached-eddy simulation method, conjugated with the Spalart–Allmaras turbulence model (DDES-SA), is applied to achieve a deep insight about the ability of this advanced modeling technique and the physics of the flow. The RNG k–ε model is also used to represent state-of-the-art of industrial turbulence modeling. Both models predict the mean velocity reasonably well while DDES-SA presents more realistic flow features at the highest and lowest rotational speeds. The highest level of turbulence occurs at the highest and lowest rotational speeds which DDES-SA is able to predict well in the conical diffuser. The special shape of the blade plays more prominent role at lower rotational speeds and creates coherent structures with opposite sign of vorticity. The vortex rope is captured by both turbulence models while DDES-SA presents more realistic one at higher rotational speeds.
[DOI: 10.1115/1.4033416]

1 Introduction

Hydraulic turbomachines have played an important role in the procurement of renewable energy for more than a century. Accompanied with the context of extensive technological development, their design for efficiency and reliability has reached an excellent point of quality. The fixed-speed turbines in the power plants work most efficiently at the design point that delineates the best combination of the speed, head, and discharge. At the design point, water turbines generally operate with little swirl entering the draft tube and without flow separations from the draft tube walls, whereas at off-design, at both full and part load, the flow leaving the turbine has a large tangential component. The hydraulic efficiency drops sharply due to this tangential component. It is known that a mitigated level of residual swirl downstream the runner delays boundary layer separation at the draft tube wall in the conical section, and thus aids the pressure recovery [1]. The large swirl intensities, however, can decrease the performance by forming an on-axis recirculation region [2]. Chauvin et al. [1] showed that there is a narrow range of swirl intensities that prevents both recirculation and separation. When swirl increases, a vortex breakdown occurs. The vortex breakdown is an abrupt change in the core of a slender vortex and typically develops downstream into a recirculatory "bubble" or a helical pattern [3–6]. The breakdown in a pipe with constant cross section is an inviscid process, where a slight viscosity of the fluid, divergence or convergence of the pipe, or increment of tangential vorticity at the inlet are perturbations from the inviscid case. The characteristics of various breakdown states, or modes, in swirling flows depend on the swirl number, the Reynolds number (Re), and geometry-induced axial pressure gradients in the flow. The swirl number is defined as

$$Sr = \frac{\int_{r_1}^{r_2} \rho UW r^2 dr}{R_2 \int_{r_1}^{r_2} \rho W^2 dr} \quad (1)$$

where R_2 is the outer radius of the cross section where Sr is calculated, R_1 is the inner radius of the cross section, and W and U are the mean axial and tangential velocity. The velocity components are averaged circumferentially and temporarily. The inclusion of a slight swirl (Sr = 0.1) at the inlet can reduce the helical precession speed and may cause the rotation of the precessing helical vortex to be against the mean swirl [7]. Several states of precession are presented as the swirl intensity increases, in which the helical precession, as well as the spiral structure, reverses the direction of rotation [8]. When the swirl increases to Sr = 0.5, a central recirculation zone occurs, which is a typical manifestation of vortex

[1]Corresponding author.
Contributed by the Fluids Engineering Division of ASME for publication in the JOURNAL OF FLUIDS ENGINEERING. Manuscript received May 12, 2015; final manuscript received April 5, 2016; published online June 6, 2016. Assoc. Editor: Bart van Esch.

(4)

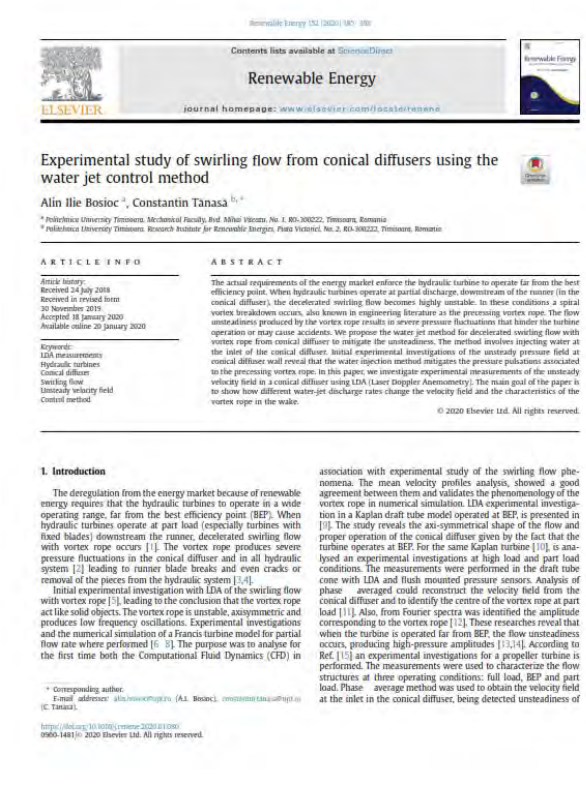

Contents lists available at ScienceDirect

Renewable Energy

journal homepage: www.elsevier.com/locate/renene

Experimental study of swirling flow from conical diffusers using the water jet control method

Alin Ilie Bosioc [a], Constantin Tănasă [b,*]

[a] Politehnica University Timisoara, Mechanical Faculty, Bvd. Mihai Viteazu, No. 1, RO-300222, Timisoara, Romania
[b] Politehnica University Timisoara, Research Institute for Renewable Energies, Piata Victoriei, No. 2, RO-300222, Timisoara, Romania

ARTICLE INFO

Article history:
Received 24 July 2018
Received in revised form
30 November 2019
Accepted 18 January 2020
Available online 20 January 2020

Keywords:
LDA measurements
Hydraulic turbines
Conical diffuser
Swirling flow
Unsteady velocity field
Control method

ABSTRACT

The actual requirements of the energy market enforce the hydraulic turbine to operate far from the best efficiency point. When hydraulic turbines operate at partial discharge, downstream of the runner (in the conical diffuser), the decelerated swirling flow becomes highly unstable. In these conditions a spiral vortex breakdown occurs, also known in engineering literature as the precessing vortex rope. The flow unsteadiness produced by the vortex rope results in severe pressure fluctuations that hinder the turbine operation or may cause accidents. We propose the water jet method for decelerated swirling flow with vortex rope from conical diffuser to mitigate the unsteadiness. The method involves injecting water at the inlet of the conical diffuser. Initial experimental investigations of the unsteady pressure field at conical diffuser wall reveal that the water injection method mitigates the pressure pulsations associated to the precessing vortex rope. In this paper, we investigate experimental measurements of the unsteady velocity field in a conical diffuser using LDA (Laser Doppler Anemometry). The main goal of the paper is to show how different water-jet discharge rates change the velocity field and the characteristics of the vortex rope in the wake.

© 2020 Elsevier Ltd. All rights reserved.

1. Introduction

The deregulation from the energy market because of renewable energy requires that the hydraulic turbines to operate in a wide operating range, far from the best efficiency point (BEP). When hydraulic turbines operate at part load (especially turbines with fixed blades) downstream the runner, decelerated swirling flow with vortex rope occurs [1]. The vortex rope produces severe pressure fluctuations in the conical diffuser and in all hydraulic system [2] leading to runner blade breaks and even cracks or removal of the pieces from the hydraulic system [3,4].

Initial experimental investigation with LDA of the swirling flow with vortex rope [5], leading to the conclusion that the vortex rope act like solid objects. The vortex rope is unstable, axisymmetric and produces low frequency oscillations. Experimental investigations and the numerical simulation of a Francis turbine model for partial flow rate where performed [6–8]. The purpose was to analyse for the first time both the Computational Fluid Dynamics (CFD) in association with experimental study of the swirling flow phenomena. The mean velocity profiles analysis, showed a good agreement between them and validates the phenomenology of the vortex rope in numerical simulation. LDA experimental investigation in a Kaplan draft tube model operated at BEP, is presented in [9]. The study reveals the axi-symmetrical shape of the flow and proper operation of the conical diffuser given by the fact that the turbine operates at BEP. For the same Kaplan turbine [10], is analysed an experimental investigations at high load and part load conditions. The measurements were performed in the draft tube cone with LDA and flush mounted pressure sensors. Analysis of phase averaged could reconstruct the velocity field from the conical diffuser and to identify the centre of the vortex rope at part load [11]. Also, from Fourier spectra was identified the amplitude corresponding to the vortex rope [12]. These researches reveal that when the turbine is operated far from BEP, the flow unsteadiness occurs, producing high-pressure amplitudes [13,14]. According to Ref. [15] an experimental investigations for a propeller turbine is performed. The measurements were used to characterize the flow structures at three operating conditions: full load, BEP and part load. Phase average method was used to obtain the velocity field at the inlet in the conical diffuser, being detected unsteadiness of

* Corresponding author.
E-mail addresses: alin.bosioc@upt.ro, (A.I. Bosioc), constantin.tanasa@upt.ro (C. Tănasă).

https://doi.org/10.1016/j.renene.2020.01.090
0960-1481/© 2020 Elsevier Ltd. All rights reserved.

(5)

International Journal of Turbomachinery Propulsion and Power

MDPI

Article

Numerical Analysis of the Flow by Using a Free Runner Downstream the Francis Turbine

Alin Ilie Bosioc [1,*], Raul Szakal [2], Adrian Stuparu [1] and Romeo Susan-Resiga [1]

[1] Department of Mechanical Machines, Equipment and Transportation, Politehnica University Timişoara, Bv. Mihai Viteazu, No.1, RO-300222, Timişoara, Romania
[2] Romanian Academy – Timişoara Branch, Bv. Mihai Viteazu, No. 24, RO-300223, Timişoara, Romania
* Correspondence: alin.bosioc@upt.ro

Abstract: The current requirements of industrialized countries require the use of as much renewable energy as possible. One significant problem with renewable energy is that the produced power fluctuates. Currently, the only method available for energy compensation in the shortest time is given by hydroelectric power plants. Instead, hydroelectric power plants (especially the plants equipped with hydraulic turbines with fixed blades) are designed to operate in the vicinity of the optimal operating point with a maximum ±10% deviation. The energy market requires that hydraulic turbines operate in an increasingly wide area between -35 - 20% from the optimum operating point. Operation of hydraulic turbines far from the optimum operating point involves the appearance downstream of the turbine of a decelerated swirling flow with hydraulic instabilities (known in the literature as the vortex rope). The main purpose of the paper is to investigate numerically a new concept by using a free runner downstream on the main hydraulic runner turbine more precisely in the draft tube cone. The free-runner concept supposes that rotates at the runaway speed with vanishing mechanical torque. The main purpose is to redistribute the total pressure and the moment between the shaft and the periphery. In addition, the free runner does not modify the operating point of the main hydraulic turbine runner.

Keywords: free runner concept, hydraulic turbines, numerical simulation, Laser Doppler Velocity measurements, draft tube cone, validation, vortex rope, visualization, unsteady pressure.

1. Introduction

In the last decades, market policy has focused on the development of renewable energy. Renewable energy (solar and wind) introduces a large fluctuating component in the electrical grid. As a consequence, many hydroelectric power plants are operated to flatten the fluctuation of wind and solar power [1]. Although operated in an off-design condition for grid services (part load and high load), hydraulic turbines experience an abrupt decrease in terms of efficiency [4]. An excess of residual swirl is ingested by the draft tube, downstream the turbine runner. The residual swirl that occurs at off-design conditions is a consequence of the mismatch between the flow generated by the wicked gates and the angular momentum extracted by the turbine runner [5]. The most harmful phenomena developed in the draft tube of hydraulic turbine are those at part-load operating conditions. At these regimes, the residual swirl ingested by the conical diffuser of the draft-tube leads to development of so-called vortex rope [6-10]. The vortex rope is a self-induced hydrodynamic instability which can be characterized by a well-defined predominant fundamental frequency. In general, the fundamental frequency of the vortex ropes varies 0.2 – 0.4 times the rotational frequency of the turbine runner, Ciocan et al. [11]. The vortex rope leads to severe pressure fluctuations that interrupt the safe operation of the hydraulic turbine [12-14]. Many approaches have been considered to mitigate the undesirable effect of the vortex rope or to fully understand the flow behavior. Both passive (not require

Citation: To be added by editorial staff during production.

Academic Editor: Firstname Lastname

Received: date
Revised: date
Accepted: date
Published: date

Copyright: © 2023 by the authors. Submitted for possible open access publication under the terms and conditions of the Creative Commons Attribution (CC BY-NC-ND) license (https://creativecommons.org/licenses/by-nc-nd/4.0/).

Int. J. Turbomach. Propuls. Power **2023**, *8*, x. https://doi.org/10.3390/xxxxx www.mdpi.com/journal/ijtpp

(6)

(19) OFICIUL DE STAT PENTRU INVENȚII ȘI MĂRCI București

ROMÂNIA

(11) RO 131578 B1

(51) Int.Cl.
F04D 29/66
F04D 27/02
F16D 37/02

BREVET DE INVENȚIE

(21) a 2016 00484

(45) Data publicării mențiunii acordării invenției: 28/03/2018 BOPI nr. 3/2018

(73) Titular:
- UNIVERSITATEA "POLITEHNICA" DIN TIMIȘOARA, PIAȚA VICTORIEI NR.2, TIMIȘOARA, TM, RO

(72) Inventatori:
- MUNTEAN SEBASTIAN, BD. CETĂȚII NR. 48, SC. E, ET. 2, AP. 11, TIMIȘOARA, TM, RO
- SUSAN-RESIGA ROMEO-FLORIN, STR. TIMIȘ NR. 18, BL. 32, SC. A, ET. 1, AP. 4, TIMIȘOARA, TM, RO
- BOSIOC ILIE ALIN, STR. MARMURA NR. 3, TIMIȘOARA, TM, RO
- CORSTANTIN SORIN-RĂZVAN, CALEA ȘAGULUI NR. 78, BL. 22, SC. D, AP. 4, TIMIȘOARA, TM, RO
- MARIN DANIEL-IOSIF, STR. OȘLANDEI NR. 4, ET. X, AP. 12, TIMIȘOARA, TM, RO
- TĂNĂSA CONSTANTIN, STR. SIRIUS NR. 19, BL. 62, SC. D, AP. 8, ET. 8, TIMIȘOARA, TM, RO
- VEKAS LADISLAU-NICOLAE, STR. SIMION BĂRNUȚIU, BL. 11A, SC. A, ET. 7, AP. 27, TIMIȘOARA, TM, RO
- BORBÁTH ISTVÁN, STR. STRĂNDULUI NR. 8, ODORHEIU SECUIESC, HR, RO
- ANTON LIVIU-EUGEN, BD. CONSTANTIN BRĂNCOVICI LOBBA NR. 30, AP. 8, TIMIȘOARA, TM, RO

(74) Mandatar:
CABINET DE PROPRIETATE INDUSTRIALĂ TUDOR ICLĂNZAN, PIAȚA VICTORIEI NR.5, SC.D, AP.2, TIMIȘOARA

(56) Documente din stadiul tehnicii:
US 2015004435 A1; GB 1497711

(54) ECHIPAMENT PENTRU REDUCEREA EFECTELOR CAVITAȚIONALE ȘI UNIFORMIZAREA CURGERII LA INTRAREA ÎN TURBOPOMPE

RO 131578 B1

Examinator: ing. PATRICHE CORNEL

(7)

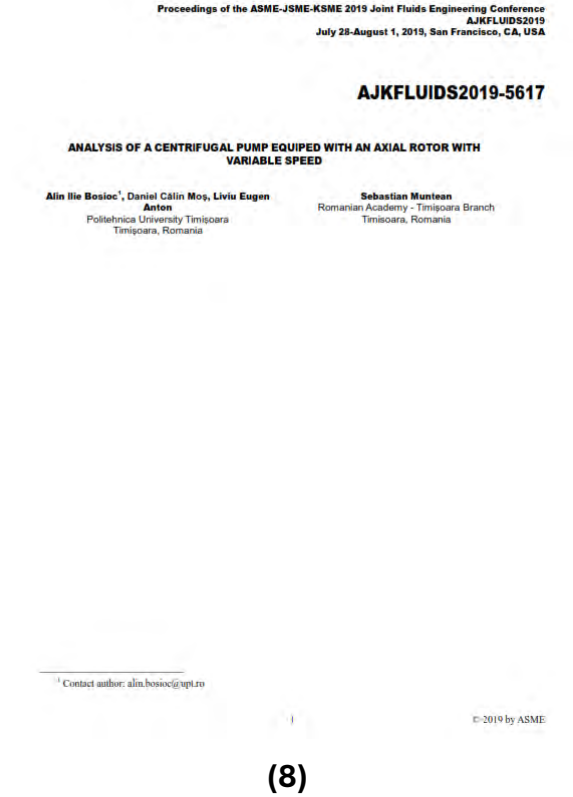

Proceedings of the ASME-JSME-KSME 2019 Joint Fluids Engineering Conference
AJKFLUIDS2019
July 28-August 1, 2019, San Francisco, CA, USA

AJKFLUIDS2019-5617

ANALYSIS OF A CENTRIFUGAL PUMP EQUIPED WITH AN AXIAL ROTOR WITH VARIABLE SPEED

Alin Ilie Bosioc[1], Daniel Călin Moș, Liviu Eugen Anton
Politehnica University Timișoara
Timișoara, Romania

Sebastian Muntean
Romanian Academy - Timișoara Branch
Timișoara, Romania

[1] Contact author: alin.bosioc@upt.ro

© 2019 by ASME

(8)

applied sciences

MDPI

Article

A Dynamic Approach for Faster Performance Measurements on Hydraulic Turbomachinery Model Testing

Vlad Hasmatuchi [1,*], Alin Ilie Bosioc [2], Sébastien Luisier [1] and Cécile Münch-Alligné [1]

[1] School of Engineering, Systems Engineering Institute, University of Applied Sciences and Arts Western Switzerland Valais, Route du Rawyl 47, CH-1950 Sion, Switzerland; sebastien_luisier@hotmail.com (S.L.); cecile.muench@hevs.ch (C.M.-A.)

[2] Department of Hydraulic Machinery, University Politehnica Timisoara, Bv. Mihai Viteazu 1, RO-300222 Timisoara, Romania; alin.bosioc@upt.ro

* Correspondence: vlad.hasmatuchi@hevs.ch; Tel.: +41-27-606-8825

Received: 20 July 2018; Accepted: 14 August 2018; Published: 21 August 2018

check for updates

Featured Application: Reducing the time required to assess or improve the performances of hydraulic machines is a crucial aspect for small-hydro applications. Indeed, the investments for applied research and development for this type of technologies are limited. In this paper, an alternative approach to measure the performance is evaluated and came out to be up to ten times faster than standard methods.

Abstract: During the design and optimization of hydraulic turbomachines, the experimental evaluation of hydraulic performances beyond the best efficiency point and for off-design conditions remains essential to validate the simulation process and to finalize the development. In this context, an alternative faster method to measure the efficiency of hydraulic turbomachines using a dynamic approach has been investigated. The so-called "sliding-gate" dynamic measurement method has been adapted and implemented on the hydraulic test rig of the HES-SO Valais//Wallis, Sion, Switzerland. This alternative approach, particularly gainful for small-hydro for which the investment devoted to development is limited, has been successfully assessed on two cases for drinking water networks energy recovery. A 2.65 kW double-regulated laboratory prototype of a tubular axial micro-turbine with two independent variable speed counter-rotating runners and a 11 kW multi-stage centrifugal pump-as-turbine (PAT) with variable speed have been selected. The hydraulic efficiency results obtained by dynamic measurements are compared to the ones obtained by the classical steady point-by-point method. This dynamic method, suitable not only for hydraulic machinery, allows: (i) reducing significantly (up to 10×) the time necessary to draw the complete efficiency characteristics of a hydraulic machine; (ii) rapidly detecting the hydrodynamic instabilities within the operating range of the machine.

Keywords: dynamic measurements; experimental testing; efficiency; hydraulic turbomachines; small-hydro

1. Background

Hydropower, small and large, remains the most important source of renewable energy for electrical power production providing 16.4% of the world electricity mix in 2016 [1]. In Switzerland, hydropower provides 56.7% of the electricity of the country, 5.7% coming from small-hydro (see [2]), considering plants with an "annual average used" capacity up to 10 MW [3]. Indeed, there are more than 1300 small-scale hydropower plants in operation, with an installed capacity of approximately

(9)

IAHRWG-2023 IOP Publishing
IOP Conf. Series: Earth and Environmental Science **1483** (2025) 012043 doi:10.1088/1755-1315/1483/1/012043

In-situ updating of the cam surface for double regulated bulb turbine

R Susan-Resiga[1,2*], A Bosioc[1], S Muntean[2] and M Boarnă[3]

[1] Politehnica University Timişoara, Romania

[2] Romanian Academy – Timişoara Branch, Romania

[3] Hidroelectrica SA – Slatina Branch, Romania

[*] romeo.resiga@upt.ro

Abstract. For double regulated turbines, the correlation between guide vanes opening (GVO) and runner blades opening (RBO) with the operating point (turbine head and power) is provided by the so-called combination (CAM) curve/surface. Operating the machine "on-cam" should provide an efficiency maximization and a low level of vibration. For a refurbished bulb turbine it was found that the implemented CAM was rather far from being optimal, with unexpectedly erratic evolution of vibration level above the expected level. The index tests previously performed in-situ were unreliable due to rather large uncertainties in discharge measurements. The challenge was to verify and update the cam surface with in-situ measurements, without primarily relying on discharge measurements. The paper presents such an approach, together with the cam surface updating methodology.

1. Introduction

For double regulated hydraulic turbines, such as vertical axis Kaplan or horizontal axis Kaplan (bulb) turbines, the high efficiency on a wide operating range is insured by the proper correlation of the guide vanes opening and runner blades opening with the operating point. The operating point can be specified either by head and discharge or by head and power.

Figure 1 shows the hill chart for the bulb turbine investigated in this paper, installed in a hydropower plant on the Olt river in Romania. In the abscissa there is the shaft power of the turbine and the ordinate corresponds to the net head. The red lines correspond to various values of the runner blade opening angle φ and the green lines to the guide vanes opening angle α. The iso-lines for turbine efficiency η_t are the solid blue lines. The allowed operating range is bounded by the black dashed line, with limitations for maximum and minimum power and net head. Such diagrams are usually determined for a model turbine in the laboratory [1,2,3], on specialized test rigs. When implemented in-situ, the opening angles are replaced by the displacement of the hydraulic pistons that open/close either the guide vanes or the rotor blade, usually as a percent from the maximum displacement, i.e. $\alpha[°] \rightarrow GVO[\%]$ and $\varphi[°] \rightarrow RBO[\%]$. When implemented on the prototype turbine, the hill chart is usually checked with in-situ index tests, for which the main uncertainty is introduced by the discharge measurements [4].

The correlations between turbine operating point given by shaft power P_t and net head H, on one hand, and the efficiency $\eta_t(P_t, H)$, guide vane opening angle $\alpha(P_t, H)$ and runner blade opening angle $\varphi(P_t, H)$, on the other hand, are surfaces that can be mathematically represented using the Multivariate

(10)

First page from the list of ten representative published manuscripts based the habilitation thesis is written.

Published Books

[1] Bosioc, A. (2017). Mecanica Fluidelor și Mașini Hidraulice - Suport de Curs și Aplicații de Calcul. Timisoara: Editura Politehnica, [90].

[2] Tanasa, C., & Bosioc, A. (2017). Tehnici de control a curgerii cu rotație în difuzoarele conice. Timisoara: Editura Politehnica, [49].

[3] Stuparu, A., & Bosioc, A. (2021). Pompe Centrifuge. Timisoara: Editura Politehnica, [91].

[4] Stuparu, A., Bosioc, A., & Ciocan, T. (2024). Proiectarea Mașinilor Hidraulice Axiale. Timisoara: Editura Politehnica, [92].

Book Chapters

[1] Muntean, S., Susan-Resiga R., Bosioc, A., Cimpian, V., Nedelcu, D. and Safta, C., "Vortex Flows in Turbomachines," in *Vortex Dominated Flows*, Timisoara, Romania, Ed. Eurostampa, 2009, [93].

[2] Muntean, S., Bosioc, A., Szakal, R., Vekas, L., & Susan-Resiga, R. (2017). Hydrodynamic investigations in a swirl generator using a magneto-rheological brake. 1st International Conference on Materials Design and Applications, MDA 2016. 65, pp. 209-218. Porto: Springer Verlag - Advanced Structured Materials. doi:10.1007/978-3-319-50784-2_17, [94]

[3] Bosioc, A., Beja, T., Muntean, S., Borbath, I., & Vekas, L. (2017). Experimental investigations of MR Fluids in air and water used for brakes and clutches. 1st International Conference on Materials Design and Applications, MDA 2016. 65, pp. 197-207. Porto: Springer Verlag - Advanced Structured Materials. doi:10.1007/978-3-319-50784-2_16, [16]

[4] Bosioc, A., Ardelean, T., Szakal, R., Muntean, S., Borbath, I., & Vekas, L. (2019). Experimental investigations of a MR clutch for a centrifugal pump. In Advanced Structured Materials (Vol. 98, pp. 253-263). Springer Verlag. doi:10.1007/978-3-030-02257-0_19, [18]

[5] Szakal, R., Bosioc, A., Muntean, S., Susan-Resiga, D., & Vekas, L. (2019). Experimental investigations of a magneto-rheological brake embedded in a swirl generator apparatus. In Advanced Structured Materials (Vol. 98, pp. 265-279). Springer Verlag. doi:10.1007/978-3-030-02257-0_20, [95]

Patents

[1] Susan-Resiga, R., Tanasa, C., Bosioc, A., Ciocan, T., Stuparu, A., & Muntean, S. (2017). Method and equipment for controlling the swirling flow through the conical diffuser of hydraulic turbines. Romania Patent No. RO130075-B1, [96].

[2] Muntean, S., Susan-Resiga, R., Bosioc, A., Constantin, S., Maxim, D., Tanasa, C., . . . Anton, L. (2019). Equipment For Reducing Cavitational Effects and Leveling Flow at Turbo Pumps Inlet. Romania

Patent No. RO131578-B1, [14].

[3] Susan-Resiga, R., Muntean, S., Tanasa, C., Bosioc, A., Ciocan, T., & Popescu, C. (2019). Equipment for controlling instabilities of swirl flow from the conical diffuser of hydraulic turbines. Romania Patent No. RO131408-B1, [97].

[4] Susan-Resiga, R., Bosioc, A., Tanasa, C., Stuparu, A., & Szakal, R. (2022). Equipment for eliminating instabilities generated by swirling flow from draft tube cone of hydraulic turbine e.g. Francis turbine. Romania Patent No. RO135938-B1, [98].

[5] Susan-Resiga, R., Tanasa, C., & Bosioc, A. (2023). Device for reducing instabilities of swirl flow in conical diffuser of hydraulic turbines. Romania Patent No. RO137523-B1, [99].

ROMÂNIA

DUPLICAT

ELIBERAT INVENTATORULUI
în baza Art.34 alin.(2),
din Legea nr.64/1991 republicată

OFICIUL DE STAT PENTRU INVENȚII ȘI MĂRCI

Brevet de invenție

Nr. 130075

Acordat în temeiul Legii nr.64/1991 privind brevetele de invenție, republicată în Monitorul Oficial al României, Partea I, nr.613, din 19 august 2014.

Titular: UNIVERSITATEA POLITEHNICA DIN TIMIȘOARA, TIMIȘOARA, TM, RO

Titlul invenției: METODĂ ȘI ECHIPAMENT PENTRU CONTROLUL CURGERII CU ROTAȚIE DIN DIFUZORUL CONIC AL TURBINELOR HIDRAULICE

Inventatori: SUSAN-RESIGA ROMEO-FLORIN, TIMIȘOARA, TM, RO; TĂNASĂ CONSTANTIN, TIMIȘOARA, TM, RO; BOSIOC ALIN ILIE, TIMIȘOARA, TM, RO; CIOCAN TIBERIU, COMUNA SANDRA, TM, RO; STUPARU ADRIAN-CIPRIAN, TIMIȘOARA, TM, RO; MUNTEAN SEBASTIAN, TIMIȘOARA, TM, RO

Descrierea invenției, revendicările și desenele la care se face referință în acestea, fac parte integrantă din prezentul brevet de invenție.
Durata brevetului de invenție este de 20 ani, cu începere de la data de 13/08/2014, cu condiția plății taxelor anuale de menținere în vigoare a brevetului.

Director General

București, Data eliberării 28/04/2017

ROMÂNIA

DUPLICAT

ELIBERAT INVENTATORULUI
în baza Art.34 alin.(2),
din Legea nr.64/1991 republicată

OFICIUL DE STAT PENTRU INVENȚII ȘI MĂRCI

BREVET DE INVENȚIE

Nr. 131408

Acordat în temeiul Legii nr.64/1991 privind brevetele de invenție, republicată în Monitorul Oficial al României, Partea I, nr.613, din 19 august 2014.

Titular: UNIVERSITATEA POLITEHNICA DIN TIMIȘOARA, TIMIȘOARA, TM, RO

Titlul invenției: ECHIPAMENT PENTRU CONTROLUL INSTABILITĂȚILOR CURGERILOR CU VÂRTEJ DIN DIFUZORUL CONIC AL TURBINELOR HIDRAULICE

Inventatori: SUSAN-RESIGA ROMEO-FLORIN, TIMIȘOARA, TM, RO; MUNTEAN SEBASTIAN, TIMIȘOARA, TM, RO; TĂNASĂ CONSTANTIN, TIMIȘOARA, TM, RO; BOSIOC ILIE ALIN, TIMIȘOARA, TM, RO; CIOCAN TIBERIU, COMUNA SANDRA, TM, RO; POPESCU CONSTANTIN, TIMIȘOARA, TM, RO

Descrierea invenției, revendicările și desenele la care se face referință în acestea, fac parte integrantă din prezentul brevet de invenție.
Durata brevetului de invenție este de 20 ani, cu începere de la data de 12/05/2016, cu condiția plății taxelor anuale de menținere în vigoare a brevetului.

Director General

București, Data eliberării 30/09/2019

ROMÂNIA

DUPLICAT

ELIBERAT INVENTATORULUI
în baza Art.34 alin.(2),
din Legea nr.64/1991 republicată

OFICIUL DE STAT PENTRU INVENȚII ȘI MĂRCI

BREVET DE INVENȚIE

Nr. 131578

Acordat în temeiul Legii nr.64/1991 privind brevetele de invenție, republicată în Monitorul Oficial al României, Partea I, nr.613, din 19 august 2014.

Titular: UNIVERSITATEA" POLITEHNICA" DIN TIMIȘOARA, TIMIȘOARA, TM, RO

Titlul invenției: ECHIPAMENT PENTRU REDUCEREA EFECTELOR CAVITAȚIONALE ȘI UNIFORMIZAREA CURGERII LA INTRAREA ÎN TURBOPOMPE

Inventatori: MUNTEAN SEBASTIAN, TIMIȘOARA, TM, RO; SUSAN-RESIGA ROMEO-FLORIN, TIMIȘOARA, TM, RO; BOSIOC ILIE ALIN, TIMIȘOARA, TM, RO; CONSTANTIN SORIN-RĂZVAN, TIMIȘOARA, TM, RO; MAXIM DANIEL-IOSIF, TIMIȘOARA, TM, RO; TANASA CONSTANTIN, TIMIȘOARA, TM, RO; VEKAS LADISLAU-NICOLAE, TIMIȘOARA, TM, RO; BORBATH ISTVAN, ODORHEIUL SECUIESC, HR, RO; ANTON LIVIU-EUGEN, TIMIȘOARA, TM, RO

Descrierea invenției, revendicările și desenele la care se face referință în acestea, fac parte integrantă din prezentul brevet de invenție.
Durata brevetului de invenție este de 20 ani, cu începere de la data de 05/07/2016, cu condiția plății taxelor anuale de menținere în vigoare a brevetului.

Confirm cele de mai sus prin semnarea și aplicarea sigiliului
Director General

București, Data eliberării 29/03/2019

ROMÂNIA

OSIM

OFICIUL DE STAT PENTRU INVENȚII ȘI MĂRCI

Brevet de invenție

Nr. 135938

Acordat în temeiul Legii nr 64/1991 privind brevetele de invenție, republicată în Monitorul Oficial al României, Partea I, nr 613, din 19 august 2014.

Titular: UNIVERSITATEA "POLITEHNICA" DIN TIMIȘOARA, TIMIȘOARA, TM, RO

Titlul invenției: ECHIPAMENT PENTRU ELIMINAREA INSTABILITĂȚILOR GENERATE DE CURGEREA CU VÂRTEJ DIN DIFUZORUL CONIC AL TURBINELOR HIDRAULICE

Inventatori: SUSAN-RESIGA ROMEO-FLORIN, TIMIȘOARA, TM, RO; BOSIOC ILIE ALIN, TIMIȘOARA, TM, RO; TĂNASĂ CONSTANTIN, TIMIȘOARA, TM, RO; ȘTUPARU ADRIAN-CIPRIAN, TIMIȘOARA, TM, RO; SZAKAL RAUL-ALEXANDRU, COMUNA BARU, HD, RO

Descrierea invenției, revendicările și desenele la care se face referință în acestea, fac parte integrantă din prezentul brevet de invenție.
Durata brevetului de invenție este de 20 ani, cu începere de la data de 08/04/2022, cu condiția plății taxelor anuale de menținere în vigoare a brevetului.

Confirm cele de mai sus prin semnarea și aplicarea sigiliului
Director General

București, Data eliberării 30/07/2024

ROMÂNIA

OSIM

OFICIUL DE STAT PENTRU INVENȚII ȘI MĂRCI

Brevet de invenție

Nr. 137523

Acordat în temeiul Legii nr 64/1991 privind brevetele de invenție, republicată în Monitorul Oficial al României, Partea I, nr 613, din 19 august 2014.

Titular: UNIVERSITATEA "POLITEHNICA" DIN TIMIȘOARA, TIMIȘOARA, TM, RO

Titlul invenției: DISPOZITIV PENTRU REDUCEREA INSTABILITĂȚILOR CURGERII CU ROTAȚIE DIN DIFUZORUL CONIC AL TURBINELOR HIDRAULICE

Inventator: SUSAN-RESIGA ROMEO-FLORIN, TIMIȘOARA, TM, RO; TĂNASĂ CONSTANTIN, TIMIȘOARA, TM, RO; BOSIOC ILIE ALIN, TIMIȘOARA, TM, RO

Descrierea invenției, revendicările și desenele la care se face referință în acestea, fac parte integrantă din prezentul brevet de invenție.
Durata brevetului de invenție este de 20 ani, cu începere de la data de 07/10/2022, cu condiția plății taxelor anuale de menținere în vigoare a brevetului.

Confirm cele de mai sus prin semnarea și aplicarea sigiliului
Director General

București, Data eliberării 30/09/2024

Obtained patens in quality of corresponding author or coauthor.

ISI Papers and Conference Proceedings

[1] Tanasa, C., Bosioc, A., Muntean, S., & Susan-Resiga, R. (2011). FLOW-FEEDBACK CONTROL TECHNIQUE FOR VORTEX ROPE MITIGATION FROM CONICAL DIFFUSER OF HYDRAULIC TURBINES DRAFT TUBE. PROCEEDINGS OF THE ROMANIAN ACADEMY SERIES A-MATHEMATICS PHYSICS TECHNICAL SCIENCES INFORMATION SCIENCE, 12(2), 125-132.

[2] Bosioc, A., Susan-Resiga, R., Muntean, S., & Tanasa, C. (2012). Unsteady Pressure Analysis of a Swirling Flow With Vortex Rope and Axial Water Injection in a Discharge Cone. JOURNAL OF FLUIDS ENGINEERING-TRANSACTIONS OF THE ASME, 134(8), 081104. doi:10.1115/1.4007074

[3] Bosioc, A., Muntean, S., Susan-Resiga, R., Vekas, L., & Bernad, S. (2013). Numerical Simulation of the Swirl Generator Discharge Cone at Lower Runner Speeds. 11TH INTERNATIONAL CONFERENCE OF NUMERICAL ANALYSIS AND APPLIED MATHEMATICS 2013, PTS 1 AND 2 (ICNAAM 2013. 1558, pp. 204-207. Athens: AIP Conference Proceedings. doi:10.1063/1.4825456

[4] Tanasa, C., Bosioc, A., Susan-Resiga, R., & Muntean, S. (2013). Experimental investigations of the swirling flow in the conical diffuser using flow-feedback control technique with additional energy source. 26TH IAHR SYMPOSIUM ON HYDRAULIC MACHINERY AND SYSTEMS. 15, p. 062043. Beijing: IOP Conference Series-Earth and Environmental Science. doi:10.1088/1755-1315/15/6/062043

[5] Bernad, S., Bosioc, A., Totorean, A. S., & Bernad, E. (2013). Vortices in by-pass graft flow. 11th International Conference of Numerical Analysis and Applied Mathematics 2013, ICNAAM 2013. 1558, pp. 160-163. AIP Conference Proceedings. doi:10.1063/1.4825445

[6] Bernad, S., Totorean, A., Bosioc, A., Stanciu, R., & Bernad, E. (2013). Numerical investigation of Dean vortices in a curved pipe. 11th International Conference of Numerical Analysis and Applied Mathematics 2013, ICNAAM 2013. 1558, pp. 172-175. AIP Conference Proceedings. doi:10.1063/1.4825448

[7] Tanasa, C., Susan-Resiga, R., Muntean, S., & Bosioc, A. (2013). Flow-Feedback Method for Mitigating the Vortex Rope in Decelerated Swirling Flows. JOURNAL OF FLUIDS ENGINEERING-TRANSACTIONS OF THE ASME, 135(6), 061304. doi:10.1115/1.4023946

[8] Bosioc, A., Muntean, S., Tanasa, C., Susan-Resiga, R., & Vekas, L. (2014). Unsteady pressure measurements of decelerated swirling flow in a discharge cone at lower runner speeds. 27TH IAHR SYMPOSIUM ON HYDRAULIC MACHINERY AND SYSTEMS (IAHR 2014). 22, p. 032008. Montreal: IOP Conference Series-Earth and Environmental Science. doi:10.1088/1755-1315/22/3/032008

[9] Bosioc, A., & Tanasa, C. (2014). LDA measurements of unsteady velocity field for decelerated swirling flows with vortex rope in a discharge cone. UPB Scientific Bulletin, Series D: Mechanical Engineering, 76(2), 243-250.

[10] Draghici, I., Muntean, S., Bosioc, A., & Anton, L. (2014). LDV measurements of the velocity field on the inlet section of a pumped storage equipped with a symmetrical suction elbow for variable discharge values. 27TH IAHR SYMPOSIUM ON HYDRAULIC MACHINERY AND SYSTEMS (IAHR 2014). 22, p. 032017. Montreal: IOP Conference Series-Earth and Environmental Science. doi:10.1088/1755-

1315/22/3/032017

[11] Bernad, S., Bosioc, A., Bernad, E., & Craina, M. (2014). Comparison between experimentally measured flow patterns for straigth and helical type graft. Bio-Medical Materials and Engineering, 24 (1), pp. 853-860. doi:10.3233/BME-130877

[12] Javadi, A., Bosioc, A., Nilsson, H., Muntean, S., & Susan-Resiga, R. (2014). Velocity and pressure fluctuations induced by the precessing helical vortex in a conical diffuser. 27TH IAHR SYMPOSIUM ON HYDRAULIC MACHINERY AND SYSTEMS (IAHR 2014). 22, p. 032009. Montreal: IOP Conference Series-Earth and Environmental Science. doi:10.1088/1755-1315/22/3/032009

[13] Totorean, A., Bosioc, A., Bernad, S., & Susan-Resiga, R. (2014). Identification and visualization of vortices in by-pass graft flow. Proceedings of the Romanian Academy Series A - Mathematics Physics Technical Sciences Information Science, 15(1), 52-59.

[14] Bosioc, A., Muntean, S., Susan-Resiga, R., Borbath, I., & Vekas, L. (2015). Numerical Analysis of the Temperature Field in A Magneto-Rheological Brake. INTERNATIONAL CONFERENCE OF COMPUTATIONAL METHODS IN SCIENCES AND ENGINEERING 2015 (ICCMSE 2015). 1702, p. 080002. Athens: AIP Conference Proceedings. doi:10.1063/1.4938797

[15] Bernad, E., Bernad, S., Totorean, A., Hudrea, C., Bosioc, A., & Crainic, N. (2015). Fluid dynamics in 45 degrees arterial by-pass model. In Z. Kalogiratou, T. E. Simos, & T. Monovasilis (Ed.), International Conference of Computational Methods in Sciences and Engineering 2015, ICCMSE 2015. 1702, p. 080010. Athens: American Institute of Physics Inc. doi:10.1063/1.4938805

[16] Bernad, E., Hudrea, C., Bernad, S., Totorean, A., & Bosioc, A. (2015). Luminal flow alteration in presence of the stent. In Z. Kalogiratou, S. T., & T. Monovasilis (Ed.), International Conference of Computational Methods in Sciences and Engineering 2015, ICCMSE 2015. 1702, p. 080011. Athens: American Institute of Physics Inc. doi:10.1063/1.4938806

[17] Bernad, S., Totorean, A., Bosioc, A., Crainic, N., Hudrea, C., & Bernad, E. (2015). Fluid mechanics in stented arterial model. International Conference of Computational Methods in Sciences and Engineering 2015, ICCMSE 2015. 1702. Athens: American Institute of Physics Inc. doi:10.1063/1.4938803

[18] Bernad, S., Bosioc, A., Bernad, E., & Craina, M. (2015). Helical type coronary bypass graft performance: Experimental investigations. Bio-Medical Materials and Engineering, 26, S477 - S486. doi:10.3233/BME-151337

[19] Tanasa, C., Susan-Resiga, R., Muntean, S., Stuparu, A., Bosioc, A., & Ciocan, T. (2015). Numerical Assessment of a Novel Concept for Mitigating the Unsteady Pressure Pulsations Associated to Decelerating Swirling Flow with Precessing Helical Vortex. INTERNATIONAL CONFERENCE OF COMPUTATIONAL METHODS IN SCIENCES AND ENGINEERING 2015 (ICCMSE 2015) (p. 080003). Athens: AIP Conference Proceedings. doi:10.1063/1.4938798

[20] Totorean, A., Bernad, S., Bosioc, A., Hudrea, C., Bernad, E., & Susan-Resiga, R. (2015). The influence of number of turns to helicity variations at the outlet sections in helical geometries with

applications for by-pass graft. International Conference of Computational Methods in Sciences and Engineering 2015, ICCMSE 2015. 1702, p. 080007. Athens: American Institute of Physics Inc. doi:10.1063/1.4938802

[21] Totorean, A., Bosioc, A., Bernad, S., & Susan-Resiga, R. (2015). Critical flow regions in the coronary by-pass graft anastomosis. Proceedings of the Romanian Academy Series A - Mathematics Physics Technical Sciences Information Science, 16(2), 168-175.

[22] Bosioc, A., Muntean, S., Draghici, I., & Anton, L. (2016). Hydrodynamic Analysis of the Flow in an Axial Rotor and Impeller for Large Storage Pump. 28TH IAHR SYMPOSIUM ON HYDRAULIC MACHINERY AND SYSTEMS (IAHR2016). 49, p. 032016. Grenoble: IOP Conference Series-Earth and Environmental Science. doi:10.1088/1755-1315/49/3/032016

[23] Draghici, I., Muntean, S., Bosioc, A., Ginga, G., & Anton, L. (2016). UNSTEADY PRESSURE FIELD ANALYSIS AT PUMP INLET EQUIPPED WITH A SYMMETRICAL SUCTION ELBOW. PROCEEDINGS OF THE ROMANIAN ACADEMY SERIES A-MATHEMATICS PHYSICS TECHNICAL SCIENCES INFORMATION SCIENCE, 17(3), 237-244.

[24] Hasmatuchi, V., Bosioc, A., & Munch-Alligne, C. (2016). On the Dynamic Measurements of Hydraulic Characteristics. 28TH IAHR SYMPOSIUM ON HYDRAULIC MACHINERY AND SYSTEMS (IAHR2016). 49, p. 062001. Grenoble: IOP Conference Series-Earth and Environmental Science. doi:10.1088/1755-1315/49/6/062001

[25] Bernad, S., Bosioc, A., Bernad, E., Petre, I., & Totorean, A. (2016). Flow characteristics in narrowed coronary bypass graft. International Conference of Numerical Analysis and Applied Mathematics 2015, ICNAAM 2015. 1738, p. 030025. Rhodes: AIP Conference Proceedings. doi:10.1063/1.4951781

[26] Bernad, S., Totorean, A., Bosioc, A., Petre, I., & Bernad, E. (2016). Stent implantation influence wall shear stress evolution. International Conference of Numerical Analysis and Applied Mathematics 2015, ICNAAM 2015. 1738, p. 030027. Rhodes: American Institute of Physics Inc. doi:10.1063/1.4951783

[27] Javadi, A., Bosioc, A., Nilsson, H., Muntean, S., & Susan-Resiga, R. (2016). Experimental and Numerical Investigation of the Precessing Helical Vortex in a Conical Diffuser, With Rotor-Stator Interaction. JOURNAL OF FLUIDS ENGINEERING-TRANSACTIONS OF THE ASME, 138(8), 081106. doi:10.1115/1.4033416

[28] Muntean, S., Bosioc, A., Draghici, I., & Anton, L. (2016). Hydrodynamic Analysis of the Flow Field Induced by a Symmetrical Suction Elbow at the Pump Inlet. 28th IAHR Symposium on Hydraulic Machinery and Systems (IAHR). 49, p. 032014. Grenoble: IOP Conference Series-Earth and Environmental Science. doi:10.1088/1755-1315/49/3/032014

[29] Muntean, S., Tanasa, C., Bosioc, A., & Mos, D. (2016). Investigation of the Plunging Pressure Pulsation in a Swirling Flow with Precessing Vortex Rope in a Straight Diffuser. 28TH IAHR SYMPOSIUM ON HYDRAULIC MACHINERY AND SYSTEMS (IAHR2016). 49, p. 082010. Grenoble: IOP Conference Series-Earth and Environmental Science. doi:10.1088/1755-1315/49/8/082010

[30] Tanasa, C., & Bosioc, A. (2016). Experimental and Numerical Investigation of a Draft Tube Cone at Lower Runner Speeds. PROCEEDINGS OF THE INTERNATIONAL CONFERENCE ON NUMERICAL ANALYSIS AND APPLIED MATHEMATICS 2015 (ICNAAM-2015). 1738, p. 030019. Rhodes: AIP Conference Proceedings. doi:10.1063/1.4951775

[31] Susan-Resiga, R., Muntean, S., Stuparu, A., Bosioc, A., Tanasa, C., & Ighisan, C. (2016). A variational model for swirling flow states with stagnant region. EUROPEAN JOURNAL OF MECHANICS B-FLUIDS, 55(1), 104-115. doi:10.1016/j.euromechflu.2015.09.002

[32] Bernad, S., Bosioc, A., Totorean, A., Petre, I., & Bernad, E. (2017). Wall Shear Stress Evolution in Carotid Artery Bifurcation. PROCEEDINGS OF THE INTERNATIONAL CONFERENCE ON NUMERICAL ANALYSIS AND APPLIED MATHEMATICS 2016 (ICNAAM-2016). 1863, p. 30020. Rhodes: American Institute of Physics Inc. doi:10.1063/1.4992173

[33] Bosioc, A., Stuparu, A., & Susan-Resiga, R. (2017). Numerical Analysis of Temperature and Torque in A Magneto-Rheological Clutch. International Conference on Numerical Analysis and Applied Mathematics (ICNAAM). 1863, p. 030015. Rhodes: AIP, Mathematics, AppliedPhysics, Applied. doi:10.1063/1.4992168

[34] Draghici, I., Atanasoaiei, C., Bosioc, A., Muntean, S., & Anton, L. (2017). Experimental analysis of the global performances for a pump with symmetrical suction elbow at two speeds. Sustainable Solutions for Energy and Environment Conference, EENVIRO 2016. 112, pp. 225-231. Bucharest: Energy Procedia - ELSEVIER SCIENCE BV, Energy & FuelsEnvironmental Sciences. doi:10.1016/j.egypro.2017.03.1090

[35] Mos, D., Muntean, S., Bosioc, A., Tanasa, C., & Susan-Resiga, R. (2017). Experimental Investigation of the Unsteady Pressure Field in Decelerated Swirling Flow with 74° Sharp Heel Elbow. HYPERBOLE SYMPOSIUM 2017 (HYDROPOWER PLANTS PERFORMANCE AND FLEXIBLE OPERATION TOWARDS LEAN INTEGRATION OF NEW RENEWABLE ENERGIES). 813, p. 012046. Porto: Journal of Physics Conference Series. doi:10.1088/1742-6596/813/1/012046

[36] Totorean, A., Hudrea, C., Bosioc, A., & Bernad, S. (2017). FLOW FIELD EVOLUTION IN STENTED VERSUS STENOSED CORONARY ARTERY. PROCEEDINGS OF THE ROMANIAN ACADEMY SERIES A-MATHEMATICS PHYSICS TECHNICAL SCIENCES INFORMATION SCIENCE, 18(3), 248-255.

[37] Hasmatuchi, V., Bosioc, A., Luisier, S., & Munch-Alligne, C. (2018). A Dynamic Approach for Faster Performance Measurements on Hydraulic Turbomachinery Model Testing. Applied Sciences-Basel, 8(9), 1426. doi:10.3390/app8091426

[38] Bosioc, A., Sebastian, M., & Anton, L. (2018). Numerical Simulation of an Axial Rotor with Variable Speed in a Pump Impeller. INTERNATIONAL CONFERENCE OF NUMERICAL ANALYSIS AND APPLIED MATHEMATICS (ICNAAM 2017). 10.1063/1.5043667, p. 030017. Thessalonik: AIP Conference Proceedings. doi:10.1063/1.5043667

[39] Stuparu, A., Baya, A., Bosioc, A., Anton, L., & Mos, D. (2018). Modelling the Operation Curves of two Similar High Power Centrifugal Pumps. INTERNATIONAL CONFERENCE OF NUMERICAL ANALYSIS

AND APPLIED MATHEMATICS (ICNAAM 2017). 1978, p. 030005. Thessalonik: AIP Conference Proceedings. doi:10.1063/1.5043655

[40] Bosioc, A., Mos, D., Draghici, I., Muntean, S., & Anton, L. (2019). Experimental analysis of a pump equipped with an axial rotor with variable speed. 29TH IAHR SYMPOSIUM ON HYDRAULIC MACHINERY AND SYSTEMS. 240, p. 032021. IOP Conference Series-Earth and Environmental Science. doi:10.1088/1755-1315/240/3/032021

[41] Bosioc, A., Mos, D., Muntean, S., & Anton, L. (2019). ANALYSIS OF A CENTRIFUGAL PUMP EQUIPPED WITH AN AXIAL ROTOR WITH VARIABLE SPEED. PROCEEDINGS OF THE ASME/JSME/KSME JOINT FLUIDS ENGINEERING CONFERENCE. 3B, p. V03BT03A046. San Francisco: ASME JSME KSME Joint Fluids Engineering Conference Proceedings.

[42] Muntean, S., Bosioc, A., Draghici, I., & Anton, L. (2019). INVESTIGATION AND ANALYSIS OF THE FLOW FIELD INDUCED BY A SYMMETRICAL SUCTION ELBOW AT THE PUMP INLET. PROCEEDINGS OF THE ASME/JSME/KSME JOINT FLUIDS ENGINEERING CONFERENCE. 3B, p. V03BT03A024. San Francisco: ASME JSME KSME Joint Fluids Engineering Conference Proceedings.

[43] Tanasa, C., Bosioc, A., Muntean, S., & Susan-Resiga, R. (2019). A Novel Passive Method to Control the Swirling Flow with Vortex Rope from the Conical Diffuser of Hydraulic Turbines with Fixed Blades. Applied Sciences-Basel, 9(22), 4910. doi:10.3390/app9224910

[44] Muntean, S., Bosioc, A., Marsavina, L., Galatanu, S., Draghici, I., & Anton, L. (2019). Failure analysis of the rainwater axial pumps installed in a wastewater pumping station. 29TH IAHR SYMPOSIUM ON HYDRAULIC MACHINERY AND SYSTEMS. 240, p. 032022. IOP Conference Series-Earth and Environmental Science. doi:10.1088/1755-1315/240/3/032022

[45] Stuparu, A., Baya, A., Bosioc, A., Anton, L., & Mos, D. (2019). Experimental investigation of a pumping station from CET power plant Timisoara. 29TH IAHR SYMPOSIUM ON HYDRAULIC MACHINERY AND SYSTEMS. 240, p. 032018. IOP Conference Series-Earth and Environmental Science. doi:10.1088/1755-1315/240/3/032018

[46] Tanasa, C., Stuparu, A., Bosioc, A., & Susan-Resiga, R. (2019). Numerical Analysis of Pulsating Water Jet Method for Mitigating the Vortex Rope. 2019 INTERNATIONAL CONFERENCE ON ENERGY AND ENVIRONMENT (CIEM) (pp. 423-428). Bucuresti: IEEE, Environmental Sciences & Ecology.

[47] Bosioc, A., & Tanasa, C. (2020). Experimental study of swirling flow from conical diffusers using the water jet control method. Renewable Energy, 152, 385-398. doi:10.1016/j.renene.2020.01.080

[48] Muntean, S., Mos, D., Szakal, R., Bosioc, A., & Susan-Resiga, R. (2021). Influence of the elbow shape on the unsteady pressure field in decelerated swirling flows. 30TH IAHR SYMPOSIUM ON HYDRAULIC MACHINERY AND SYSTEMS (IAHR 2020). 774, p. 012116. IOP Conference Series-Earth and Environmental Science. doi:10.1088/1755-1315/774/1/012116

[49] Szakal, R., Mecea, D., Bosioc, A., Borbath, I., & Muntean, S. (2021). DESIGN AND TESTING A MAGNETO-RHEOLOGICAL BRAKE WITH CYLINDRICAL CONFIGURATION. PROCEEDINGS OF THE ROMANIAN ACADEMY SERIES A-MATHEMATICS PHYSICS TECHNICAL SCIENCES INFORMATION

SCIENCE, 22(2), 189-197.

[50] Szakal, R., Muntean, S., Bosioc, A., Susan-Resiga, R., & Vekas, L. (2021). 3D numerical investigations of the swirling flow in a straight diffuser for the variable speed values of the rotor obtained with a magneto-rheological brake. 30TH IAHR SYMPOSIUM ON HYDRAULIC MACHINERY AND SYSTEMS (IAHR 2020). 774, p. 012019. IOP Conference Series-Earth and Environmental Science. doi:10.1088/1755-1315/774/1/012019

[51] Susan-Resiga, R., Muntean, S., Bosioc, A., & Stuparu, A. (2021). Stabilisation of the swirl exiting a Francis runner far from the best efficiency point. 30TH IAHR SYMPOSIUM ON HYDRAULIC MACHINERY AND SYSTEMS (IAHR 2020). 774, p. 012113. IOP Conference Series-Earth and Environmental Science. doi:10.1088/1755-1315/774/1/012113

[52] Stuparu, A., Susan-Resiga, R., & Bosioc, A. (2021). CFD Simulation of Solid Suspension for a Liquid-Solid Industrial Stirred Reactor. Applied Sciences-Basel, 11(12), 5705. doi:10.3390/app11125705

[53] Stuparu, A., Susan-Resiga, R., & Bosioc, A. (2021). Improving the Homogenization of the Liquid-Solid Mixture Using a Tandem of Impellers in a Baffled Industrial Reactor. Applied Sciences-Basel, 11(12), 5492. doi:10.3390/app11125492

[54] Bosioc, A., Szakal, R., Stuparu, A., & Susan-Resiga, R. (2023). Numerical Analysis of the Flow by Using a Free Runner Downstream the Francis Turbine. International Journal of Turbomachinery Propulsion and Power, 8(2), 14. doi:10.3390/ijtpp8020014

[55] Bosioc, A., Szakal, R., Tanasa, C., Gherghe, G., & Susan-Resiga, R. (2024). The influence of the free runners on the decelerated swirling flow from the draft tube cone of hydraulic turbines. 32ND IAHR SYMPOSIUM ON HYDRAULIC MACHINERY AND SYSTEMS. 1411, p. 012065. Roorkee: IOP Conference Series-Earth and Environmental Science. doi:10.1088/1755-1315/1411/1/012065

[56] Tanasa, C., Bosioc, A., Stuparu, A., Muntean, S., & Susan-Resiga, R. (2024). A Perspective Review of Passive Techniques Applied to Control the Swirling Flow Instabilities from the Conical Diffuser of Hydraulic Turbines. Applied Mechanics Reviews, 76(1), 010801. doi:10.1115/1.4056895

[57] Tanasa, C., Stuparu, A., Bosioc, A., Terteci, C., Belgiu, G., & Nanu, S. (2025). Innovative Device to Control Self-Induced Instabilities Associated with the Swirling Flow from the Discharge Cone of Hydraulic Turbines. Actuators, 14(3), 13. doi:10.3390/act14030126

BDI papers and Conference Proceedings

[1] Susan-Resiga, R., Bosioc, A., & Muntean, S. (2025). In-situ updating of the cam surface for double regulated bulb turbine. 9th Meeting of the IAHR WorkGroup on Cavitation and Dynamic Problems in Hydraulic Machinery and System, IAHRWG 2023. 1483. Timisoara: IOP Conference Series: Earth and Environmental Science. doi:10.1088/1755-1315/1483/1/012043

[2] Bosioc, A., Stuparu, A., Tanasa, C., & Susan-Resiga, R. (2025). Flat free runner with outer ring for reducing the hydraulic instabilities developed in the discharge cone of a Francis turbine. 9th Meeting

of the IAHR WorkGroup on Cavitation and Dynamic Problems in Hydraulic Machinery and System, IAHRWG 2023. Timisoara: IOP Conference Series: Earth and Environmental Science. doi:10.1088/1755-1315/1483/1/012034

[3] Szakal, R., Bosioc, A., & Sebastian, M. (2025). Unsteady pressure field analysis in different configurations of decelerated swirling flow with 90° sharp heel elbow. 9th Meeting of the IAHR WorkGroup on Cavitation and Dynamic Problems in Hydraulic Machinery and System, IAHRWG 2023. 1483. Timisoara: IOP Conference Series: Earth and Environmental Science. doi:10.1088/1755-1315/1483/1/012011

[4] Bosioc, A., Szakal, R., Tanasa, C., & Susan-Resiga, R. (2022). Experimental Investigation of a Free Runner Concept Downstream of Francis Turbines. 31st IAHR Symposium on Hydraulic Machinery and Systems, IAHR 2022. 1079, p. 012018. Trondheim: IOP Conference Series: Earth and Environmental Science. doi:10.1088/1755-1315/1079/1/012018

[5] Bosioc, A., Tanasa, C., Stuparu, A., & Susan-Resiga, R. (2022). Free runner concept downstream of Francis turbines. International Conference of Computational Methods in Sciences and Engineering 2021, ICCMSE 2021. 2611, p. 030002. Heraklion: American Institute of Physics Inc. doi:10.1063/5.0119430

[6] Susan-Resiga, R., Bosioc, A., & Stuparu, A. (2023). Enhanced affinity law for centrifugal pumps at variable speed. 14th International Conference on Hydroinformatics, HIC 202. 1136. Bucharest: IOP Conference Series: Earth and Environmental Science. doi:10.1088/1755-1315/1136/1/012056

[7] Draghici, I., Bosioc, A., Muntean, S., & Anton, L. (2014). Experimental investigation of the non-uniform inflow generated by the symmetrical suction elbow of a large pump. UPB Scientific Bulletin, Series D: Mechanical Engineering, 76(3), 207-2014.

[8] Tanasa, C., Muntean, S., Bosioc, A., Susan-Resiga, R., & Ciocan, T. (2016). Influence of the air admission on the unsteady pressure field in a decelerated swirling flow. UPB Scientific Bulletin, Series D: Mechanical Engineering, 78(3), 161-170.

[9] Bernad, E., Bernad, S., Totorean, A., Bosioc, A., & Sargan, I. (2017). Flow patterns in helical-type graft: Biomedical applications. International Journal of Design and Nature and Ecodynamics, 12(1), 30-43. doi:10.2495/DNE-V12-N1-30-43.

Contracts - Director

[1] Numerical simulation of heat convection for a washing machine heating system function of the thickness of limestone layer, beneficiary: ZOPPAS Industries, ctr. nr. BC 96/2014, period: 2014.

[2] Servicii de măsurători magneto-reologice, beneficiary: INCDTIM Cluj-Napoca, ctr. nr. BC 65/2022, period: 2020.

National research projects – Director

[1] Dispozitiv magneto-reologic pentru controlul curgerii cu rotație, beneficiary: UEFISCDI, PN-II-RU-PD-2011-3-0165, PD 32/2011, period: 2011-2013

[2] Solutie inovatoare de dispozitiv magneto-reologic pentru imbunatatirea performantelor pompelor centrifuge, beneficiary: UEFISCDI, PN-TE-2014-4-1089, TE 62/2015, period: 2015-2017.

[3] Rotor liber pentru controlul curgerii cu rotatie la iesirea din turbinele hidraulice, beneficiary: UEFISCDI, PN-III-P1-1.1-TE-2019-1594, TE 179/2020, period: 2020-2022.

[4] Control cu jet de apă energetic-eficient pentru creșterea flexibilității în operare a turbinelor hidraulice, beneficiary: UEFISCDI, PN-IV-P7-7_1-PED-2024-1113, PED 20/2025, period: 2025-2026.

Contracts – Member

[1] Servicii expert- asistenta tehnica, emitere rapoarte , participare sedinte de lucru si audieri in cadrul actiunii de arbitraj international ICC22482/MHM, BC26/2020, period 2020-2021;

[2] Servicii de expertiză și asistență tehnică în cadrul acțiunii de arbitraj Dosar nr. 8/2021 aflat pe rolul Curții de Arbitraj Comercial Internațional de pe lângă Camera de Comerț și Industrie a României; BC105/2021, period 2022;

[3] Modernizare HA1 Slatina - Determinarea unei came combinatorice optimizată din punct de vedere al vibrațiilor și randamentului, BC76/2022, period 2022;

[4] Servicii de asistenta tehnica de specialitate pentru testarea pe model a turbinelor aferente obiectivului de investitii "Retehnologizare CHE Vidraru", BC43/2025, period 2025.

National research projects – Member

[1] Instabilități auto-induse ale curgerii cu rotație în turbine hidraulice la regimuri departe de regimul optim, beneficiary: UEFISCDI, PCE-2012-4-0634, period: 2013-2016.

[2] Cresterea competitivitatii COLTERM prin optimizarea tehnologiei de antrenare cu turatie variabila a pompelor centrifuge de termoficare de mare putere, beneficiary: UEFISCDI, PN-III-P2-2.1-BG-2016-0190, period: 2016-2018.

[3] Reducerea Curgerii Decelerate cu Vârtej din Difuzoarele Conice Utilizand Jet de Apă Pulsator, beneficiary: UEFISCDI, PN-II-RU-TE-2014-4, CTR. 61, period: 2015-2017.

[4] Transfer de cunoastere pentru cresterea timpului de functionare a pompelor pluviale pentru sistemele de apa uzata, beneficiary: UEFISCDI, PN-III-P2-2.1-BG-2016-082, period: 2016-2018.

[5] Un nou tip de vana pentru controlul si reducerea instabilitatii curgerii cu rotatie din difuzorul conic al turbinelor hidraulice, beneficiary: UEFISCDI, 732PED /2022, period: 2022-2024.

[6] IRiS ajustabil pentru controlul instabilitatilor auto-induse generate de curgerea cu rotatie din difuzorul conic al turbinelor hidraulice, beneficiary: UEFISCDI, PN-IV-P7-7_1-PED-2024-1209, PED 22/2025, period: 2025-2026.

Member in organizing committees of Workshops and Conferences

[1] 9th IAHR Meeting of the Workgroup on Cavitation and Dynamic Problems in Hydraulic Machinery and Systems, October 10-12, 2023, Conference Center of the University Politehnica Timisoara, Romania
[2] 9th German-Romanian Workshop on Turbomachinery Hydrodynamics, 16-18 July 2013, Timişoara;
[3] 7th German-Romanian Workshop on Turbomachinery Hydrodynamics, 26-28 May 2011, Timişoara.
[4] 25th IAHR Symposium on Hydraulic Machinery and Systems, 20-24 September 2010, Timişoara.
[5] 5th German-Romanian Workshop on Turbomachinery Hydrodynamics, 2-4 July 2009, Timişoara.
[6] 2nd IAHR International Meeting of the Workgroup on Cavitation and Dynamic Problems in Hydraulic Machinery and Systems, 24-26 October 2007, Timişoara.
[7] 3rd German-Romanian Workshop on Turbomachinery Hydrodynamics, 10-12 May 2007, Timişoara

Mobility and international collaborations

[1] Mobility projects for researchers (MC 186/18.11.2024) at Department of Fluid Mechanics and Hydraulic Machinery, University of Rijeka, Croatia, Research stage for 3D reconstruction of hydraulic machinery, financed by UEFISCDI Romania PN-IV-P2-2.2-MC-2024-0309, 2024.
[2] Mobility projects for researchers (MC2017) at HES-SO Valais-Wallis, Switzerland, Image-based velocity measurement method using a high-speed camera without laser, financed by UEFISCDI Romania project PN-III-P1-1.1-MC-2017-1620, 2017.
[3] International Short Visit Grant, FNS Switzerland, HES-SO Valais-Wallis, Switzerland, Development and implementation of a dynamic method to measure the performances of hydraulic machines, financed by the FNS Switzerland project IZK0Z2_163500, 2015.
[4] International collaboration with: Chalmers University of Technology, Department of Applied Mechanics, Division of Fluid Dynamics, Gothenburg, Sweden, (Prof. Nilsson Hakan, Javadi Ardalan, Petit Olivier), 2010-2016.

Awards

[1] Ioan de Sabata Award for excellence in teaching in the university year 2022-2023, from Politehnica University Timisoara, 2023.
[2] Eminent Researcher for results in didactic and research activity, from Asociatia Orizonturi Universitare, 2016.

[3] Certificate of Merit in research activity from Timisoara City Hall, 2016.

[4] Diploma for significant research results, from Academia Oamenilor de Stiinta, 2016.

Awards obtained for research and academic results.

References

[1] A. Bosioc, Controlul curgerii cu rotație în conul tubului de aspirație al turbinelor hidraulice, PhD Thesis, vol. 90, Timisoara: Editura Politehnica, Seria 9: Inginerie Mecanică, 2011.

[2] K. Karakoc, E. Park and A. Suleman, "Design considerations for an automotive magnetorheological brake," *Mechatronics,* vol. 18, no. 8, pp. 434-447, 2008.

[3] W. H. Li and H. Du, "Design and experimental evaluation of a magnetorheological brake," *International Journal of Advanced Manufacturing Technology,* vol. 21, no. 7, pp. 508-515, 2003.

[4] Q. H. Nguyen and S. B. Choi, "Selection of magnetorheological brake types via optimal design considering maximum torque and constrained volume," *Smart Materials and Structures,* vol. 21, no. 1, p. 015012, 2012.

[5] J. Rabinow, "The Magnetic Fluid Clutch," *Transactions of the American Institute of Electrical Engineers,* vol. 67, pp. 1308-1315, 1948.

[6] N. Filip-Vacarescu, C. Vulcu and D. Dubina, "Numerical study of a hybrid damping system composed of a buckling restrained brace with a magneto rheological damper," *Proceedings of the Romanian Academy Series A - Mathematics Physics Technical Sciences Information Science,* vol. 18, no. 3, pp. 273-280, 2017.

[7] A. Baya, "Experimental investigation of the vortex rope into a simplified draft tube and its flow control," *Acta Tehnica Napocensis, Series: Applied Mathematics and Mechanics,* vol. II, pp. 243-249, 2009.

[8] D. Susan-Resiga and L. Vekas, "Yield stress and flow behaviour on concentrated ferrofluid-based magneto-rheological fluids," *Rheologica Acta,* pp. 645-653, 2014.

[9] H. Bose, T. Gerlach and J. Ehrlich, "Magnetorheological torque transmission devices with permanent magnets," in *13th International Conference on Electrorheological Fluids and Magnetorheological Suspensions, ERMR 2012*, 2013.

[10] F. Bucchi, P. Forte, F. Fredo, A. Musolino and R. Rizzo, "A fail-safe magnetorheological clutch excited by permanent magnets for the disengagement of automotive auxiliaries," *Journal of Intelligent Material Systems and Structures,* vol. 25, no. 16, pp. 2102-2114, 2014.

[11] R. Rizzo, A. Musolino and H. Lai, "An Electrodynamic/Magnetorheological Clutch Powered by Permanent Magnets," *IEEE Transactions on Magnetics,* vol. 53, no. 2, p. 7744661, 2017.

[12] L. Vekas, "Ferrofluids and magnetorheological fluids," in *CIMTEC 2008 - Proceedings of the 3rd International Conference on Smart Materials, Structures and Systems - Smart Materials and Micro/Nanosystems*, 2008.

[13] R. Ahamed, S. Choi and M. Ferdaus, "A state of art on magneto-rheological materials and their potential applications," *Journal of Intelligent Material Systems and Structures,* vol. 29, no. 10, pp. 2051-2095, 2018.

[14] S. Muntean, R. Susan-Resiga, A. Bosioc, S. Constantin, D. Maxim, C. Tanasa, L. Vekas, I. Borbath and L. Anton, "EQUIPMENT FOR REDUCING CAVITATIONAL EFFECTS AND LEVELING FLOW AT TURBO PUMPS INLET". Romania Patent RO131578-B1, 2019.

[15] I. Moisa, R. Susan-Resiga and S. Muntean, "Pump inducer optimization based on cavitation criterion," *Proceedings of the Romanian Academy Series A - Mathematics Physics Technical Sciences Information Science,* vol. 14, no. 4, pp. 317-325, 2013.

[16] A. Bosioc, T. Beja, S. Muntean, I. Borbath and L. Vekas, "Experimental investigations of MR Fluids in air and water used for brakes and clutches," in *1st International Conference on Materials Design and Applications, MDA 2016*, Porto, 2017.

[17] R. Szakal, A. Bosioc, I. Borbath and S. Muntean, "COMPARATIVE ANALYSIS OF TWO MAGNETORHEOLOGICAL CLUTCHES WITH DIFFERENT GEOMETRIC CONFIGURATIONS," *PROCEEDINGS OF THE ROMANIAN ACADEMY, Series A,* vol. 26, no. 2, pp. 165-172, 2025.

[18] A. Bosioc, T. Ardelean, R. Szakal, S. Muntean, I. Borbath and L. Vekas, "Experimental investigations of a MR clutch for a centrifugal pump," in *Advanced Structured Materials*, vol. 98, Springer Verlag, 2019, pp. 253-263.

[19] A. Bosioc, D. Mos, S. Muntean and L. Anton, "ANALYSIS OF A CENTRIFUGAL PUMP EQUIPPED WITH AN AXIAL ROTOR WITH VARIABLE SPEED," in *PROCEEDINGS OF THE ASME/JSME/KSME JOINT FLUIDS ENGINEERING CONFERENCE*, San Francisco, 2019.

[20] J. Arpe, "Analyse du champ parietale d'un diffuser coude de turbine Francis," Ecole Politechnique de Lausanne, Switzerland, 2003.

[21] O. Kirschner, J. Grupp and H. Schmidt, "Experimental investigation of vortex control in a straight draft tube model," in *4th German-Romanian Workshop on Turbomachinery Hydrodynamics*, Stuttgart, Germany, 2008.

[22] J. Kurokawa, A. Kajigaya, J. Matusi and H. Imamura, "Supression of the swirl in a conical diffuser by use of J-Groove," in *Proceedings of the 20th IAHR Symposium on Hydraulic Machinery and Cavitation*, Charlotte, North Carolina, USA, 2000.

[23] A. Ojima and K. Kamemoto, "Vortex method simulation of 3D and unsteady vortices in a swirling flow apparatus experimented in "Politehnica" University of Timisoara," in *25th IAHR Symposium on Hydraulic Machinery and Systems, Online at: IOP Conf. Series: Earth and Environmental Science*, Timisoara, Romania, 2010.

[24] R. Susan-Resiga, S. Muntean, C. Tanasa and A. Bosioc, "Hydrodynamic design and analysis of a swirling flow generator," in *The 4th German Romanian Workshop on TurboMachinery Hydrodynamics*, Stuttgart, Germany, 2008.

[25] O. Petit, A. Bosioc, H. Nilsson, S. Muntean and R. Susan-Resiga, "A swirl generator case study for OpenFOAM," in *25TH IAHR SYMPOSIUM ON HYDRAULIC MACHINERY AND SYSTEMS*, Timisoara, 2010.

[26] A. Bosioc, C. Tanasa, S. Muntean and R. Susan-Resiga, "2D LDV measurements of swirling flow in a simplified draft tube," in *The 14th International Conference on Fluid Flow Technologies*, Budapest, Hungary, 2009.

[27] A. Bosioc, R. Susan-Resiga, S. Muntean and C. Tanasa, "Unsteady Pressure Analysis of a Swirling Flow With Vortex Rope and Axial Water Injection in a Discharge Cone," *JOURNAL OF FLUIDS ENGINEERING-TRANSACTIONS OF THE ASME,* vol. 134, no. 8, p. 081104, 2012.

[28] C. Tanasa, A. Bosioc, R. Susan-Resiga and S. Muntean, "Experimental investigations of the swirling flow in the conical diffuser using flow-feedback control technique with additional energy source," in *26TH IAHR SYMPOSIUM ON HYDRAULIC MACHINERY AND SYSTEMS*, Beijing, 2013.

[29] A. Bosioc and C. Tanasa, "Experimental study of swirling flow from conical diffusers using the water jet control method," *Renewable Energy,* vol. 152, pp. 385-398, 2020.

[30] S. Muntean, A. Bosioc, R. Stanciu, C. Tanasa and R. Susan-Resiga, "3D Numerical Analysis of a Swirling Flow Generator," in *4th International Meeting on Cavitation and Dynamic Problems in Hydraulic Machinery and Systems*, Belgrade, 2011.

[31] A. Bosioc, C. Tanasa, S. Muntean and R. Susan-Resiga, "PRESSURE RECOVERY IMPROVEMENT IN A CONICAL DIFFUSER WITH SWIRLING FLOW USING WATER JET INJECTION," *PROCEEDINGS OF THE ROMANIAN ACADEMY SERIES A-MATHEMATICS PHYSICS TECHNICAL SCIENCES INFORMATION SCIENCE,* vol. 11, no. 3, pp. 245-252, 2010.

[32] A. Bosioc, C. Tanasa, S. Muntean and R. Susan-Resiga, "Unsteady pressure measurements and numerical investigation of the jet control method in a conical diffuser with swirling flow," in *25TH IAHR SYMPOSIUM ON HYDRAULIC MACHINERY AND SYSTEMS*, Timisoara, 2010.

[33] B. Mulu, P. Jonsson and M. Cervantes, "Experimental investigation of a Kaplan draft tube - Part I: Best efficiency poin," *Applied Energy,* vol. 93, pp. 695-706, 2012.

[34] P. Martin, G. Pugliese and J. Leishman, "Laser doppler velocimetry uncertainty analysis for rotor blade tip vortex measurements," in *38th Aerospace Sciences Meeting and Exhibit*, 2000.

[35] F. Avellan, "Flow investigations in a Francis draft tube: the FLINDT project," in *Proceedings of the 20th IAHR Symposium on Hydraulic Machinery and Cavitation*, Charlote, U.S, 2000.

[36] A. Bosioc, S. Muntean, C. Tanasa, R. Susan-Resiga and L. Vekas, "Unsteady pressure measurements of decelerated swirling flow in a discharge cone at lower runner speeds," in *27TH IAHR SYMPOSIUM ON HYDRAULIC MACHINERY AND SYSTEMS (IAHR 2014)*, Montreal, 2014.

[37] T. Jacob and J. Prenat, "Francis turbine surge: discussion and data base," in *Proc. of the 18th IAHR Symposium on Hydarulic Machinery and Cavitation*, 1993.

[38] M. Nishi, S. Matsunaga, M. Okamoto, M. Uno and K. Nishitani, "Measurements of three-dimensional periodic flow on a conical draft tube at surging condition," *Flows in Non-Rotating Turbomachinery Components, FED,* vol. 69, pp. 81-88, 1988.

[39] R. Thike, "Practical solutions for draft tube insatbility," *Water Power and Dam Construction,* vol. 33, no. 2, pp. 31-37, 1981.

[40] P. Gogstad and O. Dahlhaug, "Evaluation of runner cone extension to dampen pressure pulsations in a Francis model turbine," in *28th IAHR Symposium on Hydraulic Machinery and Systems, IAHR 2016*, Grenoble, 2016.

[41] M. Nishi, K. Yoshida, Z. Ma and M. Fujii, "Alleviation of the pressure surge observed in a elbow draft tube by installation of fin," in *Proceedings of the 20th IAHR Symposium on Hydraulic machinery and Cavitation*, Charlotte, USA, 2000.

[42] R. Susan-Resiga, S. Muntean, A. Bosioc and A. Stuparu, "Stabilisation of the swirl exiting a Francis runner far from the best efficiency point," in *30TH IAHR SYMPOSIUM ON HYDRAULIC MACHINERY AND SYSTEMS (IAHR 2020)*, 2021.

[43] R. Schiling, G. Schober, M. Hutter and S. Thum, "Development of a radial-axial pump-turbine for decentralized small pumped storage power plants," *WasserWirtschaft,* vol. 105, no. 1, pp. 43-47, 2015.

[44] S. Alekseenko, P. Kuibin, V. Okulov and S. Shtork, "Helical vortices in swirling flow," *Journal af Fluid Mechanics,* vol. 382, pp. 195-243, 1999.

[45] A. Garg and S. Leibovich, "Spectral characteristics of vortex breakdown flow field," *Phys. Fluids,* vol. 22, pp. 2053-2064, 1979.

[46] W. Gyllenram, "Analytical and numerical studies of internal swirling flows," Sweden, 2008.

[47] A. Bosioc, R. Szakal, A. Stuparu and R. Susan-Resiga, "Numerical Analysis of the Flow by Using a Free Runner Downstream the Francis Turbine," *International Journal of Turbomachinery Propulsion and Power,* vol. 8, no. 2, p. 14, 2023.

[48] C. Tanasa, A. Bosioc, A. Stuparu, S. Muntean and R. Susan-Resiga, "A Perspective Review of Passive Techniques Applied to Control the Swirling Flow Instabilities From the Conical Diffuser of Hydraulic Turbines," *Applied Mechanics Reviews,* vol. 76, no. 1, p. 010801, 2024.

[49] C. Tanasa and A. Bosioc, Tehnici de control a curgerii cu rotaţie în difuzoarele conice, Timisoara: Editura Politehnica, 2017.

[50] R. Susan-Resiga, T. Vu, S. Muntean, G. Ciocan and B. Nennemann, "Jet control of the draft tube vortex rope in Francis turbines at partial discharge," in *Proceedings of the 23rd IAHR Symposium on Hydraulic Machinery and Systems*, Yokohama, Japan, 2006.

[51] G. Ciocan, T. Vu, B. Nennemann, E. Demers and R. Susan-Resiga, "Liquid control jet during part load operation in a hydraulic turbine,\". Patent WO/2007/142709, 2007.

[52] M. Mohammadi, E. Hajidavalloo and M. Behbahani-Nejad, "Investigation on Combined Air and Water Injection in Francis Turbine Draft Tube to Reduce Vortex Rope Effects," *JOURNAL OF FLUIDS ENGINEERING-TRANSACTIONS OF THE ASME,* vol. 141, no. 5, p. 051301, 2019.

[53] H. Juposhti, R. Maddahian and M. Cervantes, "Optimization of axial water injection to mitigate the Rotating Vortex Rope in a Francis turbine," *RENEWABLE ENERGY,* vol. 175, pp. 214-231, 2021.

[54] S. Kumar and B. Gandhi, "Axial water jet injection in a low head Francis turbine at part load," *PHYSICS OF FLUIDS,* vol. 35, no. 6, p. 065132, 2023.

[55] I. Litvinov, D. Suslov, M. Tsoy, E. Gorelikov, S. Shtork, S. Alekseenko and K. Oberleithner, "Active Control of the Vortex Induced Pressure Fluctuations in a Hydro Turbine Model via Axial and Radial Jets at the Crown Tip," *International Journal of Fluid Machinery and Systems,* vol. 16, no. 4, pp. 320-331, 2023.

[56] A. Bosioc, C. Tanasa, A. Stuparu and R. Susan-Resiga, "Free runner concept downstream of Francis turbines," in *International Conference of Computational Methods in Sciences and Engineering 2021, ICCMSE 2021*, Heraklion, 2022.

[57] F. Gyulai, Pompe, ventilatoare, compresoare, 1988.

[58] A. Ludke, "Centrifugal process compressors - radial vs. tangential suction nozzles," in *ASME*, 1985.

[59] A. Anton, Imbunatatirea caracteristicilor cavitationale la pompele cu impulsor n- PhD Thesis, Timisoara, 1994.

[60] I. Draghici, S. Muntean, A. Bosioc and L. Anton, "LDV measurements of the velocity field on the inlet section of a pumped storage equipped with a symmetrical suction elbow for variable discharge values," in *27TH IAHR SYMPOSIUM ON HYDRAULIC MACHINERY AND SYSTEMS (IAHR 2014)*, Montreal, 2014.

[61] I. Draghici, S. Muntean, A. Bosioc, G. Ginga and L. Anton, "UNSTEADY PRESSURE FIELD ANALYSIS AT PUMP INLET EQUIPPED WITH A SYMMETRICAL SUCTION ELBOW," *PROCEEDINGS OF THE ROMANIAN ACADEMY SERIES A-MATHEMATICS PHYSICS TECHNICAL SCIENCES INFORMATION SCIENCE,* vol. 17, no. 3, pp. 237-244, 2016.

[62] I. Draghici, C. Atanasoaiei, A. Bosioc, S. Muntean and L. Anton, "Experimental analysis of the global performances for a pump with symmetrical suction elbow at two speeds," in *Sustainable Solutions for Energy and Environment Conference, EENVIRO 2016*, Bucharest, 2017.

[63] S. Muntean, A. Bosioc, I. Draghici and L. Anton, "Hydrodynamic Analysis of the Flow Field Induced by a Symmetrical Suction Elbow at the Pump Inlet," in *28th IAHR Symposium on Hydraulic Machinery and Systems (IAHR)*, Grenoble, 2016.

[64] R. Negru, S. Muntean, N. Pasca and L. Marsavina, "Failure assessment of the shaft of a pumped storage unit," in *Fatigue and Fracture of Engineering Materials and Structures*, 2014.

[65] 6. * Fluent, User Guide, 2001.

[66] G. Ardizzon and G. Pavesi, "Optimum incidence angle in centrifugal pumps and radial inflow turbines," *Proceedings of the Institution of Mechanical Engineers, Part A: Journal of Power and Energy,* vol. 212, no. 2, 1998.

[67] A. Bosioc, S. Muntean, I. Draghici and L. Anton, "Hydrodynamic Analysis of the Flow in an Axial Rotor and Impeller for Large Storage Pump," in *28TH IAHR SYMPOSIUM ON HYDRAULIC MACHINERY AND SYSTEMS (IAHR2016)*, Grenoble, 2016.

[68] A. Bosioc, M. Sebastian and L. Anton, "Numerical Simulation of an Axial Rotor with Variable Speed in a Pump Impeller," in *INTERNATIONAL CONFERENCE OF NUMERICAL ANALYSIS AND APPLIED MATHEMATICS (ICNAAM 2017)*, Thessalonik, 2018.

[69] A. Bosioc, D. Mos, I. Draghici, S. Muntean and L. Anton, "Experimental analysis of a pump equipped with an axial rotor with variable speed," in *29TH IAHR SYMPOSIUM ON HYDRAULIC MACHINERY AND SYSTEMS*, 2019.

[70] N. C. Popa, J. J. Rousseau, A. Siblini and J. Chatelon, "Gas distribution control system using magnetic fluid sensors," *Sensors and Actuators A: Phisical,* pp. 337-349, 2006.

[71] L. Yancheng, L. Jianchun, L. Weihua and D. Haiping, "A state-of-the-art review on magnetorheological elastomer devices," *Smart Materials and Structures,* vol. 23, no. 12, p. 123001, 2014.

[72] S. Dyke, B. F. Spencer, M. K. Sain and J. Carlson, "Modeling and control of magnetorheological dampers for seismic response reduction," *Smart Materials and Structures,* vol. 5, no. 5, pp. 565-575, 1996.

[73] Y. Liang, A. Jose, I. Karl and A. Hosoi, "Dynamic Sealing Using Magnetorheological Fluids," *Physical Review Applied,* vol. 10, p. 064049, 2018.

[74] V. Fabre, A. Duparchy, F. Andre and P. Larroze, "State of the art hydraulic turbine model test," in *28th IAHR Symposium on Hydraulic Machinery and Systems*, Grenoble, 2016.

[75] 6. ****** IEC, Hydraulic Turbines, Storage Pumps and Pump-Turbines, IEC 60193, 1999.

[76] C. Munch-Alligne and A. F, "Exploitation du potentiel de la petite hydraulique : Situation actuelle et exemple de développement," *Bulletin ElectroSuisse,* pp. 41-45, 2013.

[77] V. Hasmatuchi, A. Bosioc and C. Munch-Alligne, "On the Dynamic Measurements of Hydraulic Characteristics," in *28TH IAHR SYMPOSIUM ON HYDRAULIC MACHINERY AND SYSTEMS (IAHR2016)*, Grenoble, 2016.

[78] C. Almquist, P. March and H. Franseen, "Further Development of the Sliding Gate Method for Hydroturbine Efficiency Testing," *Hydro Review,* p. 539152, 1997.

[79] A. Abgottspon and T. Staubli, "INDEX TESTS OF A FRANCIS UNIT USING THE SLIDING GATE METHOD," *Engineering,* p. 113539122, 2008.

[80] D. Biner, V. Hasmatuchi, F. Avellan and C. Munch-Alligne, "Design & performance of a hydraulic micro-turbine with counter-rotating runners," in *5th International Youth Conference on Energy (IYCE)*, Pisa, 2015.

[81] B. Orchard and S. Kloss, "Pumps as turbines for water industry," *World Pumps,* pp. 22-23, 2009.

[82] P. Garay, "Using Pumps as HydroTurbines," *Hydro Review,* pp. 52-61, 1990.

[83] J. Chapallaz, P. Eichenberger and G. Fischer, Manual on Pumps used as Turbines, Vieweg: Braunschweig, 1992.

[84] R. Susan-Resiga, A. Bosioc and S. Muntean, "In-situ updating of the cam surface for double regulated bulb turbine," in *9th Meeting of the IAHR WorkGroup on Cavitation and Dynamic Problems in Hydraulic Machinery and System, IAHRWG 2023*, Timisoara, 2025.

[85] F. Gerini, E. Vagnoni, R. Cherkaoui and M. Paolone, "Optimal CAM Computation of Kaplan Turbines Accounting for Wear and Tear Originated by Frequency Control," in *IEEE Madrid Power Tech*, Madrid, 2021.

[86] D. Albright, "Automatic Index Test Box for Kaplan Turbines," 2020.

[87] L. H. Sheldon, "Method to Develop a Family of Cam Curves from a Single Index Test," *Hydro Review,* 2011.

[88] E. Quaranta, "HYDROPOWER AND PUMPED HYDROPOWER STORAGE IN THE EUROPEAN UNION - Status report on technology development, trends, value chains and markets," European Commission - Joint Research Centre, Luxembourg, 2023.

[89] E. Quaranta, R. M. Boes, J. D. Hunt, S. Szabò, J. Tattini and A. Pistocchi, "Considerations on the existing capacity and future potential for energy storage in the European Union's hydropower reservoirs and pumped-storage hydropower," *JOURNAL OF ENERGY STORAGE,* vol. 104, no. A, p. 114431, 2024.

[90] A. Bosioc, Mecanica Fluidelor și Mașini Hidraulice - Suport de Curs și Aplicații de Calcul, Timisoara: Editura Politehnica, 2017.

[91] A. Stuparu and A. Bosioc, Pompe Centrifuge, Timisoara: Editura Politehnica, 2021.

[92] A. Stuparu, A. Bosioc and T. Ciocan, Proiectarea Maşinilor Hidraulice Axiale, Timisoara: Editura Politehnica, 2024.

[93] S. Muntean, R. Susan-Resiga, A. Bosioc, V. Cimpian, D. Nedelcu and C. Safta, "Vortex Flows in Turbomachines," in *Vortex Dominated Flows*, Timisoara, Romania, Ed. Eurostampa, 2009, pp. 203-233.

[94] S. Muntean, A. Bosioc, R. Szakal, L. Vekas and R. Susan-Resiga, "Hydrodynamic investigations in a swirl generator using a magneto-rheological brake," in *1st International Conference on Materials Design and Applications, MDA 2016*, Porto, 2017.

[95] R. Szakal, A. Bosioc, S. Muntean, D. Susan-Resiga and L. Vekas, "Experimental investigations of a magneto-rheological brake embedded in a swirl generator apparatus," in *Advanced Structured Materials*, vol. 98, Springer Verlag, 2019, pp. 265-279.

[96] R. Susan-Resiga, C. Tanasa, A. Bosioc, T. Ciocan, A. Stuparu and S. Muntean, "METHOD AND EQUIPMENT FOR CONTROLLING THE SWIRLING FLOW THROUGH THE CONICAL DIFFUSER OF HYDRAULIC TURBINES". Romania Patent RO130075-B1, 2017.

[97] R. Susan-Resiga, S. Muntean, C. Tanasa, A. Bosioc, T. Ciocan and C. Popescu, "EQUIPMENT FOR CONTROLLING INSTABILITIES OF SWIRL FLOW FROM THE CONICAL DIFFUSER OF HYDRAULIC TURBINES". Romania Patent RO131408-B1, 2019.

[98] R. Susan-Resiga, A. Bosioc, C. Tanasa, A. Stuparu and R. Szakal, "Equipment for eliminating instabilities generated by whirl flowing from draft tube cone of hydraulic turbine e.g. Francis turbine". Romania Patent RO135938-B1, 2022.

[99] R. Susan-Resiga, C. Tanasa and A. Bosioc, "Device for reducing instabilities of swirl flow in conical diffuser of hydraulic turbines". Romania Patent RO137523-B1, 2023.

[100] R. Szakal, A. Bosioc and M. Sebastian, "Unsteady pressure field analysis in different configurations of decelerated swirling flow with 90° sharp heel elbow," in *9th Meeting of the IAHR WorkGroup on Cavitation and Dynamic Problems in Hydraulic Machinery and System, IAHRWG 2023*, Timisoara, 2025.

[101] C. Tanasa, A. Stuparu, A. Bosioc, C. Terteci, G. Belgiu and S. Nanu, "Innovative Device to Control Self-Induced Instabilities Associated with the Swirling Flow from the Discharge Cone of Hydraulic Turbines," *Actuators,* vol. 14, no. 3, p. 13, 2025.

[102] A. Bosioc, A. Stuparu, C. Tanasa and R. Susan-Resiga, "Flat free runner with outer ring for reducing the hydraulic instabilities developed in the discharge cone of a Francis turbine," in *9th Meeting of the IAHR WorkGroup on Cavitation and Dynamic Problems in Hydraulic Machinery and System, IAHRWG 2023*, Timisoara, 2025.

[103] R. Susan-Resiga, A. Bosioc and A. Stuparu, "Enhanced affinity law for centrifugal pumps at variable speed," in *14th International Conference on Hydroinformatics, HIC 202*, Bucharest, 2023.

[104] A. Bosioc, R. Szakal, C. Tanasa and R. Susan-Resiga, "Experimental Investigation of a Free Runner Concept Downstream of Francis Turbines," in *31st IAHR Symposium on Hydraulic Machinery and Systems, IAHR 2022*, Trondheim, 2022.

[105] S. Muntean, D. Mos, R. Szakal, A. Bosioc and R. Susan-Resiga, "Influence of the elbow shape on the unsteady pressure field in decelerated swirling flows," in *30TH IAHR SYMPOSIUM ON HYDRAULIC MACHINERY AND SYSTEMS (IAHR 2020)*, 2021.

[106] A. Stuparu, R. Susan-Resiga and A. Bosioc, "Improving the Homogenization of the Liquid-Solid Mixture Using a Tandem of Impellers in a Baffled Industrial Reactor," *Applied Sciences-Basel,* vol. 11, no. 12, p. 5492, 2021.

[107] R. Szakal, D. Mecea, A. Bosioc, I. Borbath and S. Muntean, "DESIGN AND TESTING A MAGNETO-RHEOLOGICAL BRAKE WITH CYLINDRICAL CONFIGURATION," *PROCEEDINGS OF THE ROMANIAN ACADEMY SERIES A-MATHEMATICS PHYSICS TECHNICAL SCIENCES INFORMATION SCIENCE,* vol. 22, no. 2, pp. 189-197, 2021.

[108] A. Stuparu, R. Susan-Resiga and A. Bosioc, "CFD Simulation of Solid Suspension for a Liquid-Solid Industrial Stirred Reactor," *Applied Sciences-Basel,* vol. 11, no. 12, p. 5705, 2021.

[109] R. Szakal, S. Muntean, A. Bosioc, R. Susan-Resiga and L. Vekas, "3D numerical investigations of the swirling flow in a straight diffuser for the variable speed values of the rotor obtained with a magneto-rheological brake," in *30TH IAHR SYMPOSIUM ON HYDRAULIC MACHINERY AND SYSTEMS (IAHR 2020)*, 2021.

[110] C. Tanasa, A. Stuparu, A. Bosioc and R. Susan-Resiga, "Numerical Analysis of Pulsating Water Jet Method for Mitigating the Vortex Rope," in *2019 INTERNATIONAL CONFERENCE ON ENERGY AND ENVIRONMENT (CIEM)*, Bucuresti, 2019.

[111] S. Muntean, A. Bosioc, I. Draghici and L. Anton, "INVESTIGATION AND ANALYSIS OF THE FLOW FIELD INDUCED BY A SYMMETRICAL SUCTION ELBOW AT THE PUMP INLET," in *PROCEEDINGS OF THE ASME/JSME/KSME JOINT FLUIDS ENGINEERING CONFERENCE*, San Francisco, 2019.

[112] S. Muntean, A. Bosioc, L. Marsavina, S. Galatanu, I. Draghici and L. Anton, "Failure analysis of the rainwater axial pumps installed in a wastewater pumping station," in *29TH IAHR SYMPOSIUM ON HYDRAULIC MACHINERY AND SYSTEMS*, 2019.

[113] A. Stuparu, A. Baya, A. Bosioc, L. Anton and D. Mos, "Experimental investigation of a pumping station from CET power plant Timisoara," in *29TH IAHR SYMPOSIUM ON HYDRAULIC MACHINERY AND SYSTEMS*, 2019.

[114] C. Tanasa, A. Bosioc, S. Muntean and R. Susan-Resiga, "A Novel Passive Method to Control the Swirling Flow with Vortex Rope from the Conical Diffuser of Hydraulic Turbines with Fixed Blades," *Applied Sciences-Basel,* vol. 9, no. 22, p. 4910, 2019.

[115] A. Stuparu, A. Baya, A. Bosioc, L. Anton and D. Mos, "Modelling the Operation Curves of two Similar High Power Centrifugal Pumps," in *INTERNATIONAL CONFERENCE OF NUMERICAL ANALYSIS AND APPLIED MATHEMATICS (ICNAAM 2017)*, Thessalonik, 2018.

[116] V. Hasmatuchi, A. Bosioc, S. Luisier and C. Munch-Alligne, "A Dynamic Approach for Faster Performance Measurements on Hydraulic Turbomachinery Model Testing," *Applied Sciences-Basel,* vol. 8, no. 9, p. 1426, 2018.

[117] A. Bosioc, A. Stuparu and R. Susan-Resiga, "Numerical Analysis of Temperature and Torque in A Magneto-Rheological Clutch," in *International Conference on Numerical Analysis and Applied Mathematics (ICNAAM)*, Rhodes, 2017.

[118] A. Totorean, C. Hudrea, A. Bosioc and S. Bernad, "FLOW FIELD EVOLUTION IN STENTED VERSUS STENOSED CORONARY ARTERY," *PROCEEDINGS OF THE ROMANIAN ACADEMY SERIES A-MATHEMATICS PHYSICS TECHNICAL SCIENCES INFORMATION SCIENCE,* vol. 18, no. 3, pp. 248-255, 2017.

[119] D. Mos, S. Muntean, A. Bosioc, C. Tanasa and R. Susan-Resiga, "Experimental Investigation of the Unsteady Pressure Field in Decelerated Swirling Flow with 74° Sharp Heel Elbow," in *HYPERBOLE SYMPOSIUM 2017 (HYDROPOWER PLANTS PERFORMANCE AND FLEXIBLE OPERATION TOWARDS LEAN INTEGRATION OF NEW RENEWABLE ENERGIES)*, Porto, 2017.

[120] S. Wagoner, "4 Reasons Why Hydropower is the Guarddian of the Grid," Office of the Energy Efficiency & Renewable Energy, 2017.

[121] S. Muntean, C. Tanasa, A. Bosioc and D. Mos, "Investigation of the Plunging Pressure Pulsation in a Swirling Flow with Precessing Vortex Rope in a Straight Diffuser," in *28TH IAHR SYMPOSIUM ON HYDRAULIC MACHINERY AND SYSTEMS (IAHR2016)*, Grenoble, 2016.

[122] C. Tanasa, S. Muntean, A. Bosioc, R. Susan-Resiga and T. Ciocan, "Influence of the air admission on the unsteady pressure field in a decelerated swirling flow," *UPB Scientific Bulletin, Series D: Mechanical Engineering,* vol. 78, no. 3, pp. 161-170, 2016.

[123] A. Javadi, A. Bosioc, H. Nilsson, S. Muntean and R. Susan-Resiga, "Experimental and Numerical Investigation of the Precessing Helical Vortex in a Conical Diffuser, With Rotor-Stator Interaction," *JOURNAL OF FLUIDS ENGINEERING-TRANSACTIONS OF THE ASME,* vol. 138, no. 8, p. 081106, 2016.

[124] C. Tanasa and A. Bosioc, "Experimental and Numerical Investigation of a Draft Tube Cone at Lower Runner Speeds," in *PROCEEDINGS OF THE INTERNATIONAL CONFERENCE ON NUMERICAL ANALYSIS AND APPLIED MATHEMATICS 2015 (ICNAAM-2015)*, Rhodes, 2016.

[125] R. Susan-Resiga, S. Muntean, A. Stuparu, A. Bosioc, C. Tanasa and C. Ighisan, "A variational model for swirling flow states with stagnant region," *EUROPEAN JOURNAL OF MECHANICS B-FLUIDS,* vol. 55, no. 1, pp. 104-115, 2016.

[126] C. Tanasa, R. Susan-Resiga, S. Muntean, A. Stuparu, A. Bosioc and T. Ciocan, "Numerical Assessment of a Novel Concept for Mitigating the Unsteady Pressure Pulsations Associated to Decelerating Swirling Flow with Precessing Helical Vortex," in *INTERNATIONAL CONFERENCE OF COMPUTATIONAL METHODS IN SCIENCES AND ENGINEERING 2015 (ICCMSE 2015)*, Athens, 2015.

[127] A. Bosioc, S. Muntean, R. Susan-Resiga, I. Borbath and L. Vekas, "Numerical Analysis of the Temperature Field in A Magneto-Rheological Brake," in *INTERNATIONAL CONFERENCE OF COMPUTATIONAL METHODS IN SCIENCES AND ENGINEERING 2015 (ICCMSE 2015)*, Athens, 2015.

[128] A. Javadi, A. Bosioc, H. Nilsson, S. Muntean and R. Susan-Resiga, "Velocity and pressure fluctuations induced by the precessing helical vortex in a conical diffuser," in *27TH IAHR SYMPOSIUM ON HYDRAULIC MACHINERY AND SYSTEMS (IAHR 2014)*, Montreal, 2014.

[129] A. Bosioc and C. Tanasa, "LDA measurements of unsteady velocity field for decelerated swirling flows with vortex rope in a discharge cone," *UPB Scientific Bulletin, Series D: Mechanical Engineering,* vol. 76, no. 2, pp. 243-250, 2014.

[130] I. Draghici, A. Bosioc, S. Muntean and L. Anton, "Experimental investigation of the non-uniform inflow generated by the symmetrical suction elbow of a large pump," *UPB Scientific Bulletin, Series D: Mechanical Engineering,* vol. 76, no. 3, pp. 207-2014, 2014.

[131] A. Bosioc, S. Muntean, R. Susan-Resiga, L. Vekas and S. Bernad, "Numerical Simulation of the Swirl Generator Discharge Cone at Lower Runner Speeds," in *11TH INTERNATIONAL CONFERENCE OF NUMERICAL ANALYSIS AND APPLIED MATHEMATICS 2013, PTS 1 AND 2 (ICNAAM 2013*, Athens, 2013.

[132] C. Tanasa, R. Susan-Resiga, S. Muntean and A. Bosioc, "Flow-Feedback Method for Mitigating the Vortex Rope in Decelerated Swirling Flows," *JOURNAL OF FLUIDS ENGINEERING-TRANSACTIONS OF THE ASME,* vol. 135, no. 6, p. 061304, 2013.

[133] C. Tanasa, A. Bosioc, S. Muntean and R. Susan-Resiga, "FLOW-FEEDBACK CONTROL TECHNIQUE FOR VORTEX ROPE MITIGATION FROM CONICAL DIFFUSER OF HYDRAULIC TURBINES DRAFT TUBE," *PROCEEDINGS OF THE ROMANIAN ACADEMY SERIES A-MATHEMATICS PHYSICS TECHNICAL SCIENCES INFORMATION SCIENCE,* vol. 12, no. 2, pp. 125-132, 2011.

[134] H. Brekke, "Performance and safety of hydraulic turbines," in *25th IAHR Symposium on Hydraulic Machinery and Systems, Online at: IOP Conf. Series: Earth and Environmental Science*, Timisoara, Romania, 2010.

[135] O. Bergman, "Numerical investigation of the flow in a swirl generator, using OpenFoam," Goteborg, Sweden, 2010.

[136] C. Tanasa, R. Susan-Resiga, A. Bosioc and S. Muntean, "Mitigation of pressure fluctuations in the discharge cone of hydraulic turbines using Flow-Feedback," in *25TH IAHR SYMPOSIUM ON HYDRAULIC MACHINERY AND SYSTEMS*, Timisoara, 2010.

[137] A. Zobeiri, "Investigations of time dependent flow phenomena in a turbine and pump-turbine of Francis type: rotor-stator interactions and precessing vortex rope," Ecole Polytehnique de Lausanne, Switzerland, 2009.

[138] M. Iliescu, "Analysis of large scale hydrodynamic phenomena in turbine draft tubes," Switzerland, 2009.

[139] R. Fuchs, "The visible vortex-Interactive analysis and extraction of vortices in large time-dependent flow data sets," Wien, 2008.

[140] S. Muntean, Analiza numerica a curgerii in turbinele hidraulice Francis, Timisoara: Ed. Orizonturi Universitare, 2008.

[141] P. Stein, "Numerical simulation and investigation of drat tube vortex flow," Coventry University in colaboration with Andtritz-Va Tech Hydro, 2007.

[142] M. Kjeldsen, "Water injection for the mitigation of draft tube pressure pulsations," in *International Meeting on Cavitation and Dynamic Problems in Hydraulic Machinery and Systems*, Barcelona, Spain, 2006.

[143] D. Bauer, "Selective visualisationof unsteady 3D flow using scale-space and feature-based technique," Zurich, 2006.

[144] R. C. G. M. S. A. I. &. A. F. Susan-Resiga, "Numerical simulation and analysis of swirling flow in the draft tube of a Francis turbine," in *Proceedings of the 23rd IAHR Symposium on Hydraulic Machinery and Systems*, Yokohama, Japan, 2006.

[145] B. Marjavaara, "CFD Drived optimization of hydraulic turbine draft tubes using surogate models," 2006.

[146] H. Huth, "Fatigue design of hydraulic turbine runners," Trondheim, Norway, 2005.

[147] E. Spirodonov, "Designing an ejector pump for a hydraulic system for discharging water and emptyng tanks," *Chemical and Petroleum Engineering,* vol. 41, no. 1-2, pp. 66-74, 2005.

[148] F. Avellan, "Introduction to cavitation in hydraulic machinery," in *The 6th International Conference on Hydraulic Machinery and Hydrodynamics*, Timisoara, Romania, 2004.

[149] G. Round, Incmpressible flow turbomachines. Design, Selection, Applications, and Theory, Linacre House, Jordan Hill, Oxford, 2004, pp. 67-71.

[150] T. Vekve, "An experimental investigation of draft tube flow," Norway, 2004.

[151] R. Susan-Resiga, Mecanica fluidelor numerica, Timisoara, Romania: Ed. Orizonturi Universitare, 2003.

[152] S. Mauri, "Numerical simulation and flow analysis of an elbow diffuser," Switzerland, 2002.

[153] G. Blommaert, "Etude du comportament dynamique des turbines Francis: controle actif de leur stabilite de functionement," 2000.

[154] M. Roth, "Automatic extraction of vortex core lines and other line-type features for scientific visualization," 2000.

[155] H. Radha Krishna, Hydraulic design of hydraulic machinery, Avebury: ed. Limited Asghate Publishing, 1997, pp. 417-437.

[156] S. Qinghua, "Experimental investigation of frequency characteristics of drat tube pressure pulsations for Francis turbines," in *Proc. of the 18th IAHR Symposium on Hydraulic Machinery and Cavitation*, Valencia, Spain, 1996.

[157] T. Jacob, "Evaluation sur modele reduit et prediction de la stabilite de functionnement des turbines Francis," Switzerland, 1993.

[158] T. Wahl, "Draft tube surging hydraulic model study," 1990.

[159] G. Ionescu, Teoria diferentiala a curbelor si suprafetelor cu aplicatii tehnice, Cluj-Napoca, Romania: Ed. Dacia, 1984.

[160] I. Anton, Turbine hidraulice, Timisoara, Romania: Ed. Facla, 1979.

[161] H. Falvey, "Draft tube surge- a rewiew of present knowledge and an adnoted bibliography," 1971.

[162] J. Harvey, "Some observations of the vortex brekdown phenomenon," *Journal of Fluid Mechanics,* vol. 14, 1962.

[163] H. Falvey and J. Cassidy, "Frequency and amplitude of pressure surges generated by swirling flows," in *Proceedings of 5th Symposium of International Association for Hydraulic Machinery, Equipments and Cavitation*, Stockholm, Sweden, 1970.

[164] M. Nishi, M. Shigenori, K. Takashi and S. Yosutashi, "Flow regimes in a elbow draft tube," in *IAHR Symposium, Operating Problems of Pump Station and Power Plants*, 1982.

[165] G. Angelico, F. Muciaccia and F. Rossi, "Part load behaviour of a turbine - a study on a complete model of hydraulic power plant," in *13th IAHR Symposium on Hydraulic Machinery and Cavitation*, Montreal, Canada, 1986.

[166] T. Wahl and M. F. T. Skinner, "The twin vortex draft tube surge," *Water Power,* 1991.

[167] I. Kougias, G. Aggidis, F. Avellan, S. Deniz, U. Lundin, A. Moro, S. Muntean, D. Novara, J. Perez-Diaz, E. Quaranta, P. Schild and N. Theodossiou, "Analysis of emerging technologies in the hydropower sector," *Renewable and Sustainable Energy Reviews,* vol. 113, p. 109257, 2019.

[168] A. Amini, E. Vagnini, A. Favrel, K. Yamaishi, A. Muller and F. Avellan, "Upper part-load instability in a reduced-scale Francis turbine: an experimental study," *EXPERIMENTS IN FLUIDS,* vol. 64, no. 6, 2023.

[169] D. Stefan, M. Hudec, V. Uruba, P. Prochazka, O. Urban and P. Rudolf, "Experimental investigation of swirl number influence on spiral vortex structure dynamics," in *30TH IAHR SYMPOSIUM ON HYDRAULIC MACHINERY AND SYSTEMS (IAHR 2020)*, 2021.

[170] D. Puga, C. Geng, Z. Wang and X. Luo, "Cavitating vortex rope in a diffuser at different operation conditions," *PHYSICS OF FLUIDS,* vol. 37, no. 1, p. 015220, 2025.

[171] S. Kumar and B. Gandhi, "Combined air and water injection in Francis turbine draft tube at part load," in *32ND IAHR SYMPOSIUM ON HYDRAULIC MACHINERY AND SYSTEMS*, Roorkee, 2024.

[172] A. Bosioc, R. Szakal, C. Tanasa, G. Gherge and R. Susan-Resiga, "The influence of the free runners on the decelerated swirling flow from the draft tube cone of hydraulic turbines," in *32ND IAHR SYMPOSIUM ON HYDRAULIC MACHINERY AND SYSTEMS*, Roorkee, 2024.

[173] A. Luna-Ramirez, A. Campos-Amezcua, O. Dorantes-Gomez, Z. Mazur-Czerwiec and R. Munoz-Quezada, "Failure analysis of runner blades in a Francis hydraulic turbine - Case study," *ENGINEERING FAILURE ANALYSIS,* vol. 59, pp. 314-325, 2016.

[174] H. Foroutan, SIMULATION, ANALYSIS, AND MITIGATION OF VORTEX ROPE FORMATION IN THE DRAFT TUBE OF HYDRAULIC TURBINES, Pennsylvania: The Pennsylvania State University, 2015.

[175] F. Casanova, "Failure analysis of the draft tube connecting bolts of a Francis-type hydroelectric power plant," *ENGINEERING FAILURE ANALYSIS,* vol. 16, no. 7, pp. 2202-2208, 2009.

[176] S. Khullar, K. Singh, M. Cervantes and B. Gandhi, "Influence of runner cone profile and axial water jet injection in a low head Francis turbine at part load," *SUSTAINABLE ENERGY TECHNOLOGIES AND ASSESSMENTS,* vol. 50, p. 101810, 2022.

[177] D. Suslov, S. Skripkin, M. Tsoy, E. Gorelikov and S. Shtork, "Active vortex control downstream the turbine runner in the Francis hydro turbine model," *Thermophysics and Aeromechanics,* vol. 31, no. 4, pp. 819-830, 2024.

[178] D. Sannes, I. Iliev, E. Agnalt and O. Dahlhaug, "Pressure Pulsation in a High Head Francis Turbine Operating at Variable Speed," in *8th Current Research in Hydraulic Turbines, CRHT 2018*, Dhulikhel, 2018.

[179] D. Frunzaverde, S. Muntean, G. Marginean, V. Cimpian, L. Marsavina, R. Terzi and V. Serban, "Failure analysis of a Francis turbine runner," in *25th IAHR Symposium on Hydraulic Machinery and Systems, IOP Conf. Series: Earth and Environmental Science 12 012115*, Timisoara, Romania, 2010.

[180] D. H. Wang and W. H. Liao, "Magnetorheological fluid dampers: A review of parametric modelling," *Smart Materials and Structures,* p. 023001, 2011.

[181] C. Rossa, A. Jaegy, A. Micaelli and J. Lozada, "Development of a multilayered wide-ranged torque magnetorheological brake," *Smart Materials and Structures,* vol. 23, no. 2, p. 025028, 2014.

[182] C. Rossa, A. Jaegy, J. Lozada and A. Micaelli, "Design considerations for magnetorheological brakes," *IEEE/ASME Transactions on Mechatronics,* vol. 19, no. 5, pp. 1669-1680, 2014.

[183] J. Huang, J. Zhang, Y. Yang and Y. Wei, "Analysis and design of a cylindrical magneto-rheological fluid brake," in *10th International Manufacturing Conference in China (IMCC 2002)*, Beijing, 2002.

[184] S. Bernad, A. Bosioc, A. S. R. Totorean and E. Bernad, "Vortices in by-pass graft flow," in *11th International Conference of Numerical Analysis and Applied Mathematics 2013, ICNAAM 2013*, 2013.

[185] S. Bernad, A. Totorean, A. Bosioc, R. Stanciu and E. Bernad, "Numerical investigation of Dean vortices in a curved pipe," in *11th International Conference of Numerical Analysis and Applied Mathematics 2013, ICNAAM 2013*, 2013.

[186] S. Bernad, A. Bosioc, E. Bernad and M. Craina, "Comparison between experimentally measured flow patterns for straigth and helical type graft," in *Bio-Medical Materials and Engineering*, 2014.

[187] A. Totorean, A. Bosioc, S. Bernad and R. Susan-Resiga, "Identification and visualization of vortices in by-pass graft flow," *Proceedings of the Romanian Academy Series A - Mathematics Physics Technical Sciences Information Science,* vol. 15, no. 1, pp. 52-59, 2014.

[188] S. Bernad, A. Bosioc, E. Bernad and M. Craina, "Helical type coronary bypass graft performance: Experimental investigations," *Bio-Medical Materials and Engineering,* vol. 26, pp. S477 - S486, 2015.

[189] A. Totorean, A. Bosioc, S. Bernad and R. Susan-Resiga, "Critical flow regions in the coronary by-pass graft anastomosis," *Proceedings of the Romanian Academy Series A - Mathematics Physics Technical Sciences Information Science,* vol. 16, no. 2, pp. 168-175, 2015.

[190] E. Bernad, S. Bernad, A. Totorean, C. Hudrea, A. Bosioc and N. Crainic, "Fluid dynamics in 45 degrees arterial by-pass model," in *International Conference of Computational Methods in Sciences and Engineering 2015, ICCMSE 2015*, Athens, 2015.

[191] E. Bernad, C. Hudrea, S. Bernad, A. Totorean and A. Bosioc, "Luminal flow alteration in presence of the stent," in *International Conference of Computational Methods in Sciences and Engineering 2015, ICCMSE 2015*, Athens, 2015.

[192] S. Bernad, A. Totorean, A. Bosioc, N. Crainic, C. Hudrea and E. Bernad, "Fluid mechanics in stented arterial model," in *International Conference of Computational Methods in Sciences and Engineering 2015, ICCMSE 2015*, Athens, 2015.

[193] A. Totorean, S. Bernad, A. Bosioc, C. Hudrea, E. Bernad and R. Susan-Resiga, "The influence of number of turns to helicity variations at the outlet sections in helical geometries with applications for by-pass graft," in *International Conference of Computational Methods in Sciences and Engineering 2015, ICCMSE 2015*, Athens, 2015.

[194] S. Bernad, A. Totorean, A. Bosioc, I. Petre and E. Bernad, "Stent implantation influence wall shear stress evolution," in *International Conference of Numerical Analysis and Applied Mathematics 2015, ICNAAM 2015*, Rhodes, 2016.

[195] S. Bernad, A. Bosioc, E. Bernad, I. Petre and A. Totorean, "Flow characteristics in narrowed coronary bypass graft," in *International Conference of Numerical Analysis and Applied Mathematics 2015, ICNAAM 2015*, Rhodes, 2016.

[196] E. Bernad, S. Bernad, A. Totorean, A. Bosioc and I. Sargan, "Flow patterns in helical-type graft: Biomedical applications," *International Journal of Design and Nature and Ecodynamics,* vol. 12, no. 1, pp. 30-43, 2017.

[197] S. Bernad, A. Bosioc, A. Totorean, I. Petre and E. Bernad, "Wall Shear Stress Evolution in Carotid Artery Bifurcation," in *PROCEEDINGS OF THE INTERNATIONAL CONFERENCE ON NUMERICAL ANALYSIS AND APPLIED MATHEMATICS 2016 (ICNAAM-2016)*, Rhodes, 2017.

[198] H. Squire, "Analysis of the vortex brekdown phenomena, part1," Imperial College Aeronautics Departament, 1960.

[199] J. Cassidy, "Experimental study and analysis of draft tube surging," Denver, Colorado, USA, 1969.

[200] J. Keller, W. Egli and R. Althaus, "Vortex brekdown as a fundamental element of vortex dynamics," *Journal of Applied Mathematics and Physics,* vol. 39, pp. 404-440, 1988.

[201] T. Vu and W. Shyy, "Viscous flow analysis as a design tool for hydraulic turbine components," *J. of Fluids Engineering,* vol. 112, no. 5, March 1990.

[202] M. Nishi, S. Matsunga, M. Okamoto and K. Takatsu, "Wall pressure measurements as a diagnosis of draft tube surge," in *Proceedings of the 15th IAHR Symposium on Hydraulic Machinery and Cavitation*, Belgrade, Serbia, 1990.

[203] P. Kuibin and V. Okulov, "Determination of the precession frequency of a helical vortex," *Tech. Phys. Lett.,* vol. 20, pp. 274-278, 1994.

[204] K. Kikuyama, Y. Hasegawa, G. Augusto, K. Nisibori and S. Nakamura, "The swirling inlet flow effects on the pressure recovery of a low head water turbine draft tube," in *Proc of the 18th IAHR Symposium on Hydraulic Machinery and Cavitation*, Valencia, Spain, 1996.

[205] G. Ciocan and J. Kueny, "Tip clearence flow in turbomachines-experimental flow analysis," in *Proceedings of thw 18th IAHR Symposium on Hydraulic Machinery and Cavitation*, Valencia, Spain, 1996.

[206] K. Riley, M. Hobson and S. Bence, Mathematical methods for physics and engineering, Cambrige University Press, 1997.

[207] M. Nishi, K. Yoshida and K. Morimitsu, "Control of separation in a conical diffuser by vortex generators jets," *JSME International Journal,* vol. 41, no. Series B, pp. 233-238, 1998.

[208] G. Blommaert, J. Prenat, F. Avellan and A. Boyer, "Active control of Francis turbine operation stability," in *3rd ASME/JSME Joit Fluids Engineering Conference*, San Francisco, California, USA, 1999.

[209] T. Rus, B. Sirok, M. Hocevar and M. Novak, "Simultaneous analysis of structural and pressure pulsations of cavitated vortex core in a Francis turbine," in *Proceedings of the 4th International Conference on Hydro-Science and Enginnering*, Seoul, South Korea, 2000.

[210] A. Ruprecht, T. Helmrich, T. Aschenbrenner and T. Scherer, "Simulation of pressure surge in a hydro power plant caused by an elbow draft tube," in *10th International Meeting of the Workgroup on the Behaviour of Hydraulic Machinery under Steady Oscilatory Conditions*, Trondheim, Norway, 2001.

[211] A. Skotak, J. Mikulasek and P. Troubil, "Unsteady flow in the draft tube with elbow. Part A - experimental investigation," in *10th International Meeting of the Workgroup on the Behaviour of Hydraulic Machinery under Stedy Oscilatory Conditions*, Trondheim, Norway, 2001.

[212] T. Vu and S. Retieb, "Accuracy assessment of current CFD tools to predict hydraulic turbine efficiency hill chart," in *Proccedings of the 21st IAHR Symposium on Hydraulic Machinery and Systems*, Laussane, Switzerland, 2002.

[213] M. Sick, P. Doerfler, M. Sallaberger, A. Lohmberg and M. Casey, "CFD simulation of the draft tube vortex," in *Proceedings of the 21st IAHR Symposium on Hydraulic Machinery and Systems*, Lausanne, Switzerland, 2002.

[214] Z. Wang and L. Zhou, "Experimental study on pressure surge in draft tube," in *Proc. of the 21st IAHR Symposium on Hydraulic Machinery and Systems*, Lausanne, Switzerland, 2002.

[215] L. Anton and A. Baya, Mecanica fluidelor, masini hidraulice si actionari, Timisoara, Romania: Ed. Orizonturi Universitare, 2002.

[216] B. Papillon, M. Sabourin, M. Couston and C. Deschenes, "Methods for air admission in hydroturbines," in *Proceedings of the 21st IAHR Symposium on Hydraulic Machinery and Systems*, Lausanne, Switzerland, 2002.

[217] P. Lowys, F. Paquet, M. Couston, M. Farhat, S. Natal and F. Avellan, "Onboard measurements of pressure and strain fluctuations in a model of low head Francis turbine - Part 2 measurements and preliminary analysis results," in *Proceedings of the 21st IAHR Symposium on Hydraulic Machinery and Systems*, Lausanne, Switzerland, 2002.

[218] A. Ruprecht, T. Helmrich, T. Aschenbrenner and A. Archerer, "Simulation of vortex rope in a turbine draft tube," in *Proceedings of the 21st IAHR Symposium on Hydraulic Machinery and Systems*, Lausanne, Switzerland, 2002.

[219] M. Kurokasa, M. Kikuchi, K. Hirano, Y. T. and H. Inuoe, "Interchangeability of vortex brekdown types," *Experiments in Fluids,* vol. 34, pp. 77-86, 2003.

[220] P. Doerfler, A. Lohmberg, W. Mishler and M. Sick, "Investigation of pressure pulsation and runner forces in a single-stage reversible pump-turbine model," in *Proceedings of the 11th IAHR International Meeting of the Workgroup on the Behaviour Machinery and Steady Oscillatory Conditions*, Stuttgart, Germany, 2003.

[221] F. R. Menter, R. Langtry and T. Hansen, "CFD simulation of turbomachinery flow-verification, validation and modelling," in *European Congress on Computational Methods in Applied Sciences and Engineering*, 2004.

[222] T. Vu, B. Nennemann, G. Ciocan and M. Iliescu, "Experimental study and unsteady simulation of the FLINDT draft tube rotating vortex rope," in *Proc. of the Hydro 2004 Conference*, Porto, Portugal, 2004.

[223] M. Freitag and M. Klein, "Direct numerical simulation of a recirculating swirling flow," *Flow, Turbulence and Combustion,* vol. 75, pp. 51-66, 2005.

[224] S. Karambirov and V. Chebaevskii, "Possibilites of improving ejector pump characteristics," *Chemical and Petroleum Engineering,* vol. 41, no. 1-2, pp. 75-80, 2005.

[225] R. Zhang, Q. Cai, J. Wu, S. Liu and J. Zhang, "The phisical origin of severe low-frequency pressure fluctuations in giant Francis turbine," *Modern Physical Letter B,* vol. 19, no. 28-29, pp. 99-102, 2005.

[226] R. Susan-Resiga, G. Ciocan, I. Anton and F. Avellan, "Analysis of the swirling flow downstream a Francis runner," *Journal of Fluids Engineering,* vol. 128, pp. 177-189, 2006.

[227] T. Vu, B. Nennemann, E. Demers, R. Susan-Resiga and G. Ciocan, "Control jet for hydraulic turbines". Patent 2549749, 2006.

[228] Z. Wang and L. Zhou, "Simulation and measurements of pressure oscilations caused by vortex ropes," *Journal of Fluids Engineering,* vol. 128, pp. 649-655, 2006.

[229] G. Ciocan, M. Iliescu, T. Vu, B. Nennemann and F. Avellan, "Experimental study and numerical simulation of the FLINDT draft tube rotating vortex," *Journal of Fluids Engineering,* vol. 129, pp. 146-158, 2007.

[230] Z.-D. Qian, J.-D. Yang and W.-X. Huai, "Numerical simulation and analysis of pressure pulsation in Francis turbine with air admission," *J. of Hydrodynamics,* Vols. Ser. B, 19, no. 4, pp. 467-472, 2007.

[231] O. Kirschner and A. Ruphrecht, "Vortex rope measurements in a simplified drat tube," in *2nd IAHR International Meeting of the Workgroup on Cavitation and Dynamic Problems in Hydraulic Machinery and Systems*, Timisoara, Romania, 2007.

[232] G. Ciocan and M. Iliescu, "3D PIV measurements in two phase flow and rope parametrical modeling," in *24th IAHR Symposium on Hydraulic Machinery and Systems*, Foz do Iguassu, 2008.

[233] M. Iliescu, G. Ciocan and F. Avellan, "Analysis of the cavitating draft tube vortex in a Francis turbine using Particle Image Velocimetry measurements in two-phase flow," *Journal of Fluids Engineering,* vol. 130, pp. 021105-021105-10, 2008.

[234] A. Ruprecht, J. Grupp, A. Al-Salaymeh and O. Kirscher, "Experimantal and numerical investigation of vortex control in a simplified straight drat tube model," in *24th IAHR Symposium on Hydraulic Machinery and Systems*, Foz do Iguassu, 2008.

[235] S. Muntean, R. Susan-Resiga, A. Bosioc, A. Stuparu and L. Anton, "Mitigation of pressure fluctuation in a conical diffuser with precessing vortex rope using axial jet control method," in *The 24th IAHR Symposium on Hydraulic Machinery and Systems*, Foz do Iguassu, Brasil, 2008.

[236] A. Lipej, D. Jost, P. Meznar and V. Djelic, "Numerical prediction of pressure pulsation amplitude for different operating regimes of Francis turbine draft tube," in *24th IAHR Symposium on Hydraulic Machinery and Systems*, Foz do Iguassu, Brasil, 2008.

[237] P. Stein, M. Sick, P. Doerfler, P. White and A. Braune, "Numerical simulation of the cavitating draft tube vortex in a Francis turbine," in *Proc. of the 23rd IAHR Symposium on Hydraulic Machinery and Systems*, Yokohama, Japan, 2008.

[238] C. Chen, N. Christophe, M. Farhat, F. Avellan and Y. Tsujimoto, "One-Dimensional analysis of full load draft tube surge," *Journal of Fluids Engineering,* vol. 130, no. 041106-1-041106-6, 2008.

[239] S. Muntean, H. Nilsson and R. Susan-Resiga, "3D numerical analysis of the unsteady turbulent swirling flow in a conical diffuser using Fluent and OpenFoam," in *Proceedings of the 3rd IAHR International Meeting of the Workgroup on Cavitation and Dynamic Problems in Hydraulic Machinery and Systems*, Brno, Czech Republic, 2009.

[240] S. Muntean, R. Susan-Resiga and A. Bosioc, "3D numerical analysis of unsteady pressure fluctuations in a swirling flow without and with axial water jet control," in *The 14th International Conference on Modelling Fluid Flow*, Budapest, Hungary, 2009.

[241] R. Susan-Resiga, S. Muntean, P. Stein and F. Avellan, "Axisymmetric swirling flow simulation of draft tube of vortex in Francis turbines at partial discharge," *Journal of Fluid Machinery and Systems,* vol. 2, no. 4, pp. 295-302, 2009.

[242] S. Liu, L. Zhang, M. Nishi and Y. Wu, "Cavitating turbulent flow simulation in a Francis turbine based on mixture model," *J. of Fluids Engineering,* vol. 131, 2009.

[243] R. Zhang, J. Wu, S. Chen and Z. Wu, "Characteristics and control of the draft tube flow in part-load Francis turbines," *Journal of Fluids Engineering,* vol. 131, no. 1, 2009.

[244] S. Lais, Q. Liang, U. Henggeler, T. Weiss, X. Escaler and E. Equsquiza, "Dynamic analysis of Francis runners-experiment and numerical simulation," *Int. J. of Fluid Machinery and Systems,* vol. 2, no. 4, pp. 303-313, 2009.

[245] O. Kirschner, A. Ruprecht and E. Gode, "Experimental investigation of pressure pulsation in a simplified draft tube," in *Proceedings of the 3rd IAHR International Meeting of the Workgroup on Cavitation and Dynamic Problems in Hydraulic Machinery and Systems*, Brno, Czech Republic, 2009.

[246] R. Susan-Resiga, S. Muntean, V. Hasmatuchi, I. Anton and F. Avellan, "Analysis and prevention of vortex brekdown in the simplified discharge cone of a Francis turbine," *Journal of Fluids Engineering,* vol. 132, 2010.

[247] O. Kirschner, H. Schmitd, A. Ruprecht, R. Mader and P. Mausburger, "Experimental investigation of vortex control with an axial jet in the draft tube of a model pump-turbine," in *25th IAHR Symposium on Hydraulic Machinery and Systems*, Timisoara, Romania, 2010.

[248] C. Nicolet, A. Zobeiri, P. Maruzewski and F. Avellan, "On the upper part load vortex rope in Francis turbine: experimental investigation," in *25th IAHR Symposium on Hydraulic Machinery and Systems, Onlineat: IOP Conf. Series: Earth and Environmental Science*, Timisoara, Romania, 2010.

[249] T. Vu, C. Devals, Y. Zhang, B. Nennemann and F. Guibault, "Steady and unsteady flow computation in a elbow draft tube with experimental validation," in *25th IAHR Symposium on Hydraulic Machinery and Systems, Online at: IOP Conf. Series: Earth and Environmental Science*, Timisoara, Romania, 2010.

[250] P. Kuibin, V. Okulov, R. Susan-Resiga and S. Muntean, "Validation of the mathematical models for predicting the swirling flow and the vortex rope in a Francis turbine operated at partial discharge," in *25th IAHR Symposium on Hydraulic Machinery and Systems, Online at: IOP Conf. Series: Earth and Environmental Science*, Timisoara, Romania, 2010.